UNIVERSIDADE DE LISBOA

Faculdade de Medicina Veterinária

BESNOITIA BESNOITI AND *TOXOPLASMA GONDII* INVASION: THE ROLE OF THE PARASITE´S TUBULIN FOLDING PATHWAY AND MANIPULATION OF HOST CELL ORGANIZATION

Rita Isabel de Amorim Cardoso

CONSTITUIÇÃO DO JÚRI

Doutor Andrew Edward Hemphill

Doutora Isabel Maria Soares Pereira da Fonseca de Sampaio

Doutora Maria Helena Antunes Soares

Doutor José Augusto Farraia e Silva Meireles

Doutor Helder Carola Espiguinha Cortes

Doutor José Alexandre da Costa Perdigão e Cameira Leitão

ORIENTADOR

Doutor José Alexandre da Costa Perdigão e Cameira Leitão

CO-ORIENTADORA

Doutora Maria Helena Antunes Soares

2014

LISBOA

UNIVERSIDADE DE LISBOA

Faculdade de Medicina Veterinária

BESNOITIA BESNOITI AND *TOXOPLASMA GONDII* INVASION: THE ROLE OF THE PARASITE´S TUBULIN FOLDING PATHWAY AND MANIPULATION OF HOST CELL ORGANIZATION

Rita Isabel de Amorim Cardoso

TESE DE DOUTORAMENTO EM CIÊNCIAS VETERINÁRIAS
ESPECIALIDADE DE CIÊNCIAS BIOLÓGICAS E BIOMÉDICAS

CONSTITUIÇÃO DO JÚRI

Doutor Andrew Edward Hemphill

Doutora Isabel Maria Soares Pereira da Fonseca de Sampaio

Doutora Maria Helena Antunes Soares

Doutor José Augusto Farraia e Silva Meireles

Doutor Helder Carola Espiguinha Cortes

Doutor José Alexandre da Costa Perdigão e Cameira Leitão

ORIENTADOR

Doutor José Alexandre da Costa Perdigão e Cameira Leitão

CO-ORIENTADORA

Doutora Maria Helena Antunes Soares

2014

LISBOA

Acknowledgments

I would like to thank my supervisor, Alexandre Leitão, for helping me to overcome all the challenges presented to me during the course of this work, from little to fundamental things you have always supported me, and I am truly thankful. Working with you brought me a great amount of knowledge, and important new perspectives, and I sincerely hope to be able to continue having your support and advice. I cannot end without recognizing your infinite patience when dealing with me and my (sometimes) 'idiosyncratic behavior'.

I would also like to thank my co-supervisor, Helena Soares, for all the support and scientific knowledge, and for always being prepared with new ideas to new problems, which helped me to circumvent many obstacles.

My special thanks to Helder Cortes, for believing in me, in my work, and for being a good friend. Thank you also for all the knowledge about *B. besnoiti*.

Thank you, my colleagues and friends at the bench: Afonso Basto, Alexandra Tavares, Dulce Santos, Eduardo Marcelino, Joana Morais, João Gonçalves, Rúben Ramalho, Rodrigo Cunha, Samuel Francisco, Sara Zúquete and Sofia Nolasco. All of you taught me how to work around the lab, helped me when I needed, and were always available for a conversation. You were able to turn serious work into laughing moments (particularly you, Sara and Samuel). I would like to give special thanks to Sofia Nolasco, for the help and knowledge about cell culture and immunofluorescence.

I am thankful to Silvia Almeida, for the knowledge and help on real time PCR.

To Helga Waap, for being a good colleague and friend, and for defying me to work on other projects.

I would like to thank Doutor Carlos Novo, for the INETI facilities where the anti *B. besnoiti* CCTα antibody was produced, and for the provided help when producing it.

I would also like to thank Professor Doutor Carlos Martins for letting me use the infectious diseases facilities.

A special thank you to Professora Doutora Conceição Peleteiro for allowing me to use the pathological anatomy facilities, and to D. Maria Augusta, D. Rosário, Sandra Carvalho, and Rute Noiva, for their friendly support.

I am also thankful to Faculdade de Medicina Veterinária de Lisboa (FMV) and Centro de Investigação Interdisciplinar em Sanidade Animal (CIISA), in the persons of Professor Doutor Luís Tavares and Professor Doutor Luís Costa, for all the support since I have initiated my work.

Thank you, my close friends, Aldina Almeida, Maria Matos, and Susana Cruz. I truly think you believe more in my success than I do. Thank you for that. I would also like to thanks Maria Matos for the help in editing the images.

Finally, my family that has always supported and provided me in many ways. A special word to my mother, for her generosity, and for making it easier for me to choose my own path.

Financial Support

This study was supported by:

FCT - Fundação para a Ciência e Tecnologia (FCT), through the fellowship SFRH/BD/38122/2007 and project grants PTDC/CVT/71630/2006; PTDC/CVT/105470/2008.

Centro de Investigação Interdisciplinar em Sanidade Animal (CIISA), Faculdade de Medicina Veterinária de Lisboa, Universidade de Lisboa (FMV-UL).

Besnoitia besnoiti and _Toxoplasma gondii_ invasion: the role of the parasite´s tubulin folding pathway and manipulation of host cell organization

Abstract

Besnoitia besnoiti and *Toxoplasma gondii*, the etiological agents of besnoitiosis and toxoplasmosis, respectively, are two apicomplexan parasites unable to replicate outside the host cell. In order to survive inside the host cell, these parasites have developed strategies to subvert the cytoskeleton and the endomembrane system of the host cell. In this work, the strategies used by *B. besnoiti* and *T. gondii* to manipulate the cytoskeleton, remodeling microtubules (MTs), and interfering with the centrosome and Golgi apparatus of the host cell are studied. We observed that the parasitophorous vacuole (PV) of both parasites is surrounded by host MTs, but only *T. gondii* recruits the host cell centrosome towards the PV. However, the host Golgi apparatus is recruited to the PV by both parasites but its organization is affected in different ways. The differences found between these two parasites are most likely a result of two distinct evolutionary mechanisms and might reflect the different tissue tropism and pathogeny.

Since not only the host cell cytoskeleton, but also the cytoskeleton of the parasite, participate in the establishment of infection, this work also addresses the role of the parasite cytoskeleton during entry and development inside the host cell. For this we propose that components of the tubulin folding pathway are good candidates to regulate cytoskeleton dynamics and reorganization during host invasion. Thus, we started the characterization of the gene structure and expression patterns of the components of tubulin folding pathway (CCTα, TBCB, TBCE and α-tubulin). These studies suggest that these proteins have an important role in parasite replication.

Overall, our results contribute to the present knowledge of the mechanisms underlying host cell invasion by these parasites, which might be important for the definition of future therapeutic strategies.

Keywords: *Besnoitia besnoiti*, *Toxoplasma gondii*, microtubule cytoskeleleton, Golgi apparatus, centrosome, tubulin folding pathway.

Estudo da invasão por *Besnoitia besnoiti* e *Toxoplasma gondii*: papel de componentes da via de aquisição da estrutura tridimensional nativa da tubulina do parasita e manipulação da organização da célula hospedeira

Resumo

Besnoitia besnoiti e *Toxoplasma gondii*, agentes etiológicos da besnoitiose e toxoplasmose, respetivamente, são dois parasitas do filo Apicomplexa incapazes de se replicarem fora da célula hospedeira. De forma a sobreviver dentro da célula hospedeira estes parasitas desenvolveram estratégias para subverter o citoesqueleto e sistema endomembranar da célula. Neste trabalho são estudadas as estratégias utilizadas por *B. besnoiti* e *T. gondii* para manipular o citoesqueleto, remodelar microtúbulos (MTs), e interferir com o centrossoma e o aparelho de Golgi da célula hospedeira. Observámos que o vacúolo parasitóforo (VP) dos dois parasitas está rodeado de MTs da célula hospedeira, mas apenas *T.gondii* desloca o centrossoma para o VP. No entanto, o aparelho de Golgi é recrutado para próximo do VP por ambos os parasitas, sendo a sua organização afetada de forma diferente. As diferenças encontradas entre os dois parasitas são provavelmente o resultado de evoluções diferentes, podendo isto refletir o seu diferente tropismo e patogenicidade.

Visto que para além do citoesqueleto da célula hospedeira, também o citoesqueleto do parasita participa no desenvolvimento da infeção, este trabalho também se destina a estudar o papel do citoesqueleto do parasita durante a entrada e multiplicação dentro da célula hospedeira. Desta forma propomos que os componentes da via de aquisição da estrutura tridimensional nativa da tubulina são bons candidatos para regular a dinâmica e reorganização do citoesqueleto durante a invasão. Assim, caracterizámos a estrutura dos genes CCTα, cofator B, cofator E e α-tubulina, e o seu padrão de expressão, obtendo dados que sugerem que estas proteínas poderão ter um importante papel na replicação do parasita.

Globalmente, os nossos resultados contribuem para o conhecimento dos mecanismos subjacentes à invasão da célula hospedeira por estes parasitas, o que poderá ser importante no futuro para a definição de estratégias terapêuticas.

Palavras chave: *Besnoitia besnoiti*, *Toxoplasma gondii*, citoesqueleto de microtúbulos, aparelho de Golgi, centrossoma, via de aquisição da estrutura tridimensional nativa da tubulina.

Table of Contents

Index of Figures

Index of Tables

Abbreviations

ADP - Adenosine diphosphate

AIDS - Acquired immunodeficiency syndrome

AKAP450 - A-kinase anchoring protein 450

Akt - Serine/threonine-protein kinase

Alp – Altered polarity protein

ALS - Amyotrophic lateral sclerosis

AMP - Adenosine monophosphate

ARF - ADP ribosylation factor

ARHGAP10 - Rho GTPase activating protein 10

Arl - ADP-ribosylation factor-like

Arp2/3 - Actin-related protein 2/3

ATP - Adenosine triphosphate

BBS - Bardet–Biedl syndrome

bp – base pair

CAM – Calmodulin

CAMLG - Calcium modulating ligand

CAP - Cyclase-associated proteins

CAP350 – Centrosome associated protein 350

CAP-Gly – Cytoskeletal associated protein glycine rich

CARP - Domain in cyclase-associated proteins

CCT - Chaperonin containing TCP-1

Cdc20p - Cell division cycle protein 20

Cdc42 - Cell division cycle protein 42

Cdk5 – Cyclin dependent kinase 5

CDK5Rap2 - CDK5 regulatory subunit associated protein 2

cDNA - complementary DNA

CGN - *cis*-Golgi network

CIN2 - Chromosome instability 2

CLASP - Cytoplasmic linker associated proteins

CLIP - Cytoplasmic linker protein

CP148 - Centrosomal protein 148

Ct - Threshold cycle

DA3 - Myeloid cell line

DABCO - Diazabicyclo[2.2.2]octane

DAPI - 4', 6-Diamidino-2-Phenylindole

DC – Dendritic cell

DLI-1 - Dynein light intermediate chain 1

DMEM - Dulbecco's modified Eagle's medium

DNA - Deoxyribonucleic acid

DNase - Deoxyribonuclease

dNTPs - deoxynucleotide triphosphates

EB – End binding

EBNA-3 - Epstein–Barr virus nuclear antigen 3

EDTA - Ethylenediaminetetraacetic acid

EFSA - European food safety authority

ELISA - Enzyme linked immunosorbent assay

EMBL-EBI - European molecular biology laboratory - European bioinformatics institute

ENO - Enolase

ER - Endoplasmic reticulum

EuPathDB - Eukaryotic pathogen database resources

FKBP - FK506 binding protein

FRAP – FKBP rapamycin associated protein

FRM – Formin

FTCD - Formiminotransferase cyclodeaminase

g – gram

GAP – Glideosome associated protein

GAP – GTPase activating protein

GAPDH - Glyceraldehyde-3-phosphate dehydrogenase

GCC185 - Golgi coiled coil protein 185

GCP60 - Golgi resident protein 60

GDP - Guanosine diphosphate

GFAP - Glial fibrillary acidic protein

GFP - Green fluorescent protein

GM130 – Golgi matrix protein 130

GMAP210 - Golgi microtubule associated protein 210

GOLPH3 - Golgi phosphoprotein 3

GPI- Glycosylphosphatidyl inositol

GRA - Dense granule protein

GRASP - Golgi reassembly stacking protein

GTP - Guanosine triphosphate

HAART – Highly active anti-retroviral therapy

HEAT – Domain in several cytoplasmic proteins

HFF - Human foreskin fibroblast

HIF1α - Hypoxia inducible factor 1 α

HOST - Host organelle-sequestering tubule

HSP - Heat shock protein

hTERT-RPE-1 - Human telomerase-immortalized retinal pigmented epithelial cells

IF - Intermediate filament

IFAT - Immunofluorescence antibody test

IFNg - Interferon gamma

IFT20 – Intraflagellar transport protein 20

IL-4 – Interleukin 4

IMC - Inner membrane complex

IMP - Intramembranous particle

IPTG - Isopropyl β-D-1-thiogalactopyranoside

ISP – Inner membrane complex sub-compartment protein

ITS1 - Internal transcribed spacer 1

KASH - Klarsicht, ANC-1, Syne Homology

kb – 10^3 base pairs

kDa – 10^3 Dalton

M – molar

Kif9 – Kinesin family member 9

LB - Lysogeny broth medium

LDH - Lactate dehydrogenase

LRR - Leucine-rich repeats

MACF – Microtubule actin cross linking factor

MACF1b – Microtubule actin crosslinking factor 1b

MAP – Microtubule associated protein

MAT - Modified agglutination test

MDCK - Madin-Darby canine kidney cells

mg – milligram

MIC – Microneme protein

MJ - Moving junction

ml – milliliter

mM – milimolar

MOWIOL – A coverslip mounting solution

mRNA – messenger ribonucleic acid

MTOC – Microtubule organizing center

mTORC2 - mTOR complex 2

MTs - Microtubules

NCBI-BLAST - National center for biotechnology information - Basic local alignment search tool

NDPK - Nucleotide diphosphate kinase

NEDD1 - Neural precursor cell expressed developmentally down-regulated protein 1

NF-kB - Nuclear factor kappa B

nm –nanometer

NMIIA - Non-muscle myosin IIA

NTZ - Nitazoxanide

PBS – Phosphate buffered saline

PCM - Pericentriolar material

PCR - Polymerase chain reaction

PDI - Protein disulfide isomerase

PFA - Paraformaldehyde

PFD - Prefoldin

PhLP – Phosducin-like protein

PI3K - Phosphatidylinositol 3 kinase

PKA - Protein kinase A

PKD1 – Protein kinase D1

Plk1 - Polo-like kinase 1

PRF - Profilin

PTM – Post-translational modification

PV - Parasitophorous vacuole

PVM - Parasitophorous vacuole membrane

Rab – Ras related proteins in brain

Rac1 – Ras related C3 botulinum toxin substrate 1

Rbl2 – Rescues β-tubulin lethality

RhoA - Ras homolog gene family, member A

RINT-1 - RAD50 interactor 1

RNA - Ribonucleic acid

RON - Rhoptry neck protein

ROP - Rhoptry bulb protein

RP2 - Retinitis pigmentosa 2

RT-PCR - Reverse transcription polymerase chain reaction

SAC - Spindle assembly checkpoint

SAG – Surface antigen

SAMP1 - Senescence-accelerated mouse prone 1

SAS6L - Spindle assembly abnormal protein 6 - like

SDS - Sodium dodecyl sulfate

SDS-PAGE - SDS-poliacrilamide gel electrophoresis

siRNA – small interfering ribonucleic acid

SOC - Super optimal broth medium with catabolite repression

SOD - Superoxide dismutase

SPM - Protein colocalized with the subpellicular microtubules

STAT - Signal transducer and activator of transcription

SUN-1 - Sad1 and UNC84 domain containing 1

SYBR Green - Fluorescent DNA binding dye

TAE - Tris-acetate-EDTA

TaSE – *Theileria annulata* secretory protein

TBCA - Tubulin folding cofactor A

TBCB - Tubulin folding cofactor B

TBCC - Tubulin folding cofactor C

TBCCD1 - TBCC-domain containing 1

TBCD - Tubulin folding cofactor D

TBCE - Tubulin folding cofactor E

TBS – Tris-buffered saline

TCP-1- Tailess complex polypeptide 1

TEM - Transmission electron microscopy

TEMED - N, N, N, N, - tetramethylethylenediamine

TgAMA1 - *Toxoplasma gondii* apical membrane antigen 1

TgDLC - *Toxoplasma gondii* dynein light chain

TgICMAP1 – *Toxoplasma gondii* intraconoid microtubule associated protein1

TgM2AP - *Toxoplasma gondii* microneme 2 associated protein

TgMORN1 – *Toxoplasma gondii* membrane occupation and recognition nexus 1

TGN - *trans*-Golgi network

TgPLP1 – *Toxoplasma gondii* perforin-like protein 1

TIZ - Tizoxanide

TM - Melting temperature

ToxoDB - *Toxoplasma gondii* genomic resources database

TRAP – Thrombospondin related anonymous protein

TRiC - TCP-1 ring complex

Triton X-100 – Iso-octylphenoxypolyethoxyethanol

TrxL - Thioredoxin-like protein

Tween 20 - Polyoxyethylenesorbitan monolaurate

Ubl - Ubiquitin-like domain

UV - Ultraviolet

WASP - Wiskott–Aldrich syndrome protein

WHAMM - WASP homolog associated protein with actin, membranes and microtubules

X-Gal - 5-bromo-4-chloro-3-indolyl-beta-D-galacto-pyranoside

ZW10 - Zeste White 10

ZYG- 12 - Zygote defective protein 12

ºC – Celsius degrees

µg – microgram

µl – microliter

µm – micrometer

µM – micromolar

γ-TuRC - γ-tubulin ring complex

Chapter 1: Introduction

Obligate intracellular parasites such as the apicomplexan *Besnoitia besnoiti* and *Toxoplasma gondii*, have co-evolved with hosts to be able to invade their cells and flourish. To be successful they need to establish specific parasite–host cell interactions, and then manipulate the host cell structures, mechanisms and pathways in order to replicate and grow. These events are strictly required for the completion of their life cycles and are in the basis of their pathogenesis.

B. besnoiti is the causative agent of bovine besnoitiosis, that affects all cattle breeds, at all ages (seroprevalence increases with age, with the highest rates occurring in animals more than 4 years old (Waap *et al*., 2014)), and both sexes (reviewed in Cortes *et al*., 2014). When a herd is infected, the fatality rate is about 10% (Pols, 1960), and after 3 years of the introduction of the disease, the intra-herd prevalence is frequently higher than 80% (reviewed in Cortes *et al*., 2014). Following this dramatic onset, usually only sporadic clinical cases are observed in a herd, lower than 1% (Cortes *et al*., 2006b). Considering this, the disease may lead to high economic losses, as it affects milk production, causes abortions, transient or permanent infertility of bulls, and severe skin lesions.

The present knowledge on *B. besnoiti* is rather sparse when compared to the closely related parasite *T. gondii*. Only a few genes have been sequenced and proteomic research is at the very beginning (Fernández-García *et al*., 2009a; García-Lunar *et al*., 2012b; Fernández-García *et al*., 2013). A review of GenBank-listed records comprise basically 18S, 5.8S and 28S ribosomal RNA genes, first and second internal transcribed spacers (ITS1 and ITS2), and protein disulfide isomerase (PDI). As for *T. gondii*, mapping of *T. gondii* genes has already been achieved (Khan *et al*., 2005). Thus, in this work we used *T. gondii* as a comparison model organism, adding also, in the process, new data about the mechanisms of infection of this parasite.

Studies on *T. gondii* are important, since the parasite is capable of infecting all warm-blooded animals including humans, and infection can result in a wide spectrum of clinical signs depending on the host animal species. It has a worldwide distribution, and it is currently estimated that approximately one-third of the world's population is infected with the parasite (Jones *et al*., 2007). Most infections generate few or no symptoms, but acute infections are a concern in human medicine, particularly during pregnancy and in immunocompromised individuals, as *T. gondii* can cause encephalitis or systemic infections in individuals with HIV/AIDS. Also, *T. gondii* congenital infection results in one of the main causes of abortion, fetal mummification, stillbirth and neonatal mortality in sheep and goats, with important economic repercussions in a flock, due to both the large number of the aborted fetuses as well as the loss of milk production (reviewed in Innes, 2010). T. *gondii* is indeed of significant

veterinary importance, and the absence of an efficient therapy and prophylactic measures, contributes to the serious impact of an outbreak in the income of an affected farm. The same is true for *B. besnoiti*, where a lack of information concerning the routes of transmission and pathogeny makes it even harder to control the disease and to reduce the economical consequences in an infected herd.

In order to contribute for a better understanding of the mechanisms underlying *B. besnoiti* and *T. gondii* infection, in this work we focused on the ability of the above mentioned parasites to invade host cells, modulate the host microtubule (MT) cytoskeleton, and recruit the host cell centrosome and Golgi apparatus. We also studied the levels of expression of genes participating in the tubulin folding pathway of the microtubular cytoskeleton of the parasites, during invasion and replication inside the host cell. Studying how these two parasites interact with their host cells may contribute for a better understanding of the strategy used by each parasite during infection, which might shed some light on the molecular mechanisms underlying the pathogenesis of the two diseases, providing knowledge that can be useful for the research of efficient therapies.

1.1 - Bovine besnoitiosis

The tissue cyst forming coccidian protozoan *B. besnoiti* is classified in the family Sarcocystidae, subfamily Toxoplasmatinae of the phylum Apicomplexa, and closely related to the genus *Hammondia*, *Neospora* and *Toxoplasma* (reviewed in Olias *et al*., 2011).

1.1.1 History

A disease referred to as «l'elephantiasis et de l'anasarque du boeuf» was described by Cadéac (1884) in cattle from Southern France. From this report it seems that the condition was known in Southern France as early as 1859 (Bigalke, 1968). Subsequent investigations by Besnoit & Robin (1912) revealed the presence of a large number of thick-walled spherical cysts, harboring numerous spores, in the skin and subcutaneous tissues of cattle from the Pyrenees.

Franco & Borges (1916), in a thirty years study, reported that since 1885 the disease was encountered frequently in slaughter cattle at the abattoir in Lisbon, particularly in animals from Alentejo, and named the etiological agent *B. besnoiti*. Since then the disease has been described in several African states as well as in Asia (Krasov *et al*., 1975; Bigalke & Prozesky, 2004; Olias *et al*., 2011).

The occurrence of the disease in Europe received little attention until the last decade of the 20th century, since when its prevalence seems to be increasing, being recognized as emerging in Europe by the EFSA (European Food Safety Authority, 2010). Until now, cases have been reported in France (Besnoit & Robin, 1912; Liénard *et al*., 2011), Italy (Agosti *et al*., 1994; Gentile *et al*., 2012), Spain (Juste *et al*., 1990; Fernández-García *et al*., 2009b), Portugal ((Franco & Borges, 1915; Leitão, 1949; Cortes *et al*., 2003), Germany (Mehlhorn *et al*., 2009; Rostaher *et al*., 2010), Hungary (Hornok *et al*., 2014) and Switzerland (Lesser *et al*., 2012).

1.1.2 - The genus *Besnoitia*

In the genus *Besnoitia* 10 species are currently recognized: *B. akodoni, B. bennetti, B. besnoiti, B. caprae, B. darlingi, B. jellisoni, B. neotomofelis, B. oryctofelisi, B. tarandi, and B. wallacei*. Dubey *et al*., 2004 phylogenetic analysis indicated a close relationship between parasites of cattle, goats, caribou, and equids (*B. besnoiti, B. caprae, B. tarandi*, and *B. bennetti*), and of species that parasitize rodents, lagomorphs, and opossums (*B. jellisoni, B. akodoni, B. oryctofelisi*, and *B. darlingi*). Ellis *et al*., 2000 reported an identical ITS1 (internal transcribed spacer 1) sequence in both *B. besnoiti and B. caprae*, and all published sequences, including the ITS1 region, are not discriminative for large mammalian *Besnoitia* isolates on a species or strain level (reviewed in Olias *et al*., 2011; Fig.1).

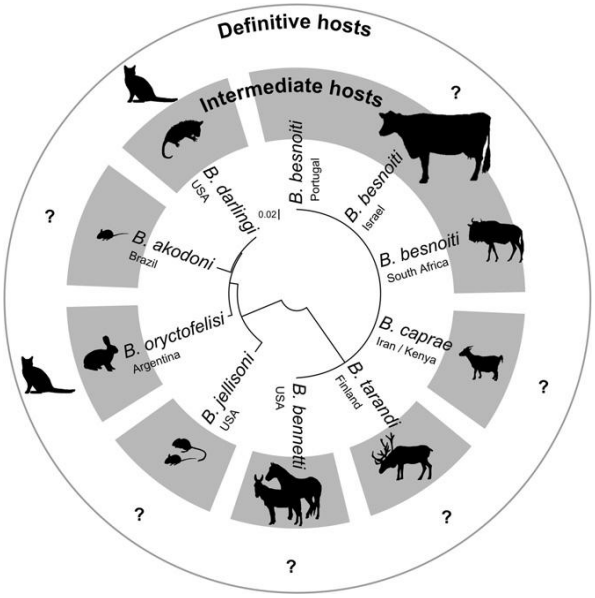

Fig.1: Phylogenetic tree of the ITS1 region of parasite isolates in the genus *Besnoitia*.
Eight out of ten named *Besnoitia* species and their known natural host types are shown. The missing species are *B wallacei* (rodents), *and B. neotomofelis* (woodrat), whose final host is the cat. Adapted from Olias *et al.*, 2011.

1.1.3 - Transmission and Life Cycle

Besnoitia genus is suggested having a two-host (heteroxenous) life cycle with a multiplication in two phases. The first phase is the intestinal sexual stage (oocysts), which has been found in the domestic cat, the final host for *B. darlingi, B. wallacei, B. oryctofelisi and B. neotomofelis* (Nganga *et al*., 1994; Dubey & Lindsay, 2003; Dubey *et al*., 2003a; Dubey *et al*., 2004; Dubey & Yabsley, 2010). No other final host species are known, and a heteroxenous transmission has not yet been identified for *B. jellisoni, B. akodoni* and all large mammalian *Besnoitia* species (*B. besnoiti, B. caprae, B. tarandi,* and *B. bennetti*) (reviewed in Olias *et al*., 2011). The second, asexual phase of the life cycle is in the intermediate host after ingestion of oocysts shed by the definitive host. Oocysts release sporozoites in the digestive tract, which differentiate into tachyzoites that invade multiple cells (Pols, 1954). Finally, in the chronic stage of the disease tissue cysts evolve, and tachyzoites differentiate into bradyzoites that remain within the cysts (Langenmayer *et al*., 2014).

As for *B. besnoiti*, cattle is the intermediate host (Bigalke, 1967), being the definitive host unknown. The hypothesis of cattle infection through ingestion of mature *B. besnoiti* oocysts shed in the feces of an unknown, but possibly carnivorous definitive host, can be contested, since no definitive host was ever identified. No oocysts were found in the feces of domestic cats fed musculature and connective tissues containing numerous cysts using Israelian and South African isolates (Diesting *et al*., 1988). This result was confirmed in a study by Basso *et al*., 2011, where dogs and cats were fed 5×10^6 *B. besnoiti* tachyzoites, or tissue cysts containing at least 2×10^7 *B. besnoiti* bradyzoites. In this study, domestic dogs and cats were not shown to be definitive hosts of *B. besnoiti*, but cats seroconverted after feeding on *B. besnoiti* tissue cysts. In accordance with these results, a large-scale serum survey of *B. besnoiti* in 205 free-living carnivores in Spain (wolves, red foxes, pine martens, stone martens, Eurasian badgers, common genets, Egyptian mongooses, European wildcats and feral cats) was performed, with no evidence to support the idea that wild carnivores are implicated in the life cycle of *B. besnoiti* in the geographical regions analyzed (Millán *et al*., 2012). This could indicate that in *B. besnoiti* transmission another intermediate host is involved, or that an important mechanical transmission between cattle maintains the natural infection cycle.

In fact, there are several evidences in favor of a mechanical transmission: bovine besnoitiosis can be transmitted experimentally by mechanical transfer of either tachyzoites or bradyzoites from an infected animal to a susceptible one; experimentally, tabanids (*Tabanocella denticornis, Atylotus nigromaculatus*), mosquitoes (*Culex* spp.), tse tse flies (*Glossina*

brevipalpis) and stable flies (*Stomoxys calcitrans*) have been proven to mechanically transmit *B. besnoiti* between cattle and also between cattle and rabbits (Bigalke, 1960; Bigalke, 1968); there is a seasonal incidence of the disease; and the cysts are localized in the dermis, where they are easily accessible to the probing proboscis of a wide variety of blood-sucking arthropods (Bigalke, 1968).

In addition, the successful transmission by cohabitation can also indicate that the transmissibility of *B. besnoiti* by various natural openings could be possible. By artificial infection, cattle were susceptible to tachyzoites, but not to bradyzoites, administered by mouth. Nonetheless, bradyzoites and tachyzoites were infective via the nostrils. This could indicate the nasal mucous membrane as a potential source, and route of infection. In fact, in cattle, cysts lie much closer to the surface in the nasal membrane, and there is the possibility of spontaneous or mechanical rupture of cysts by the rough tongue, with the appearance of bradyzoites in the nasal mucus. There are, however, reasons why nasal infection is probably not the usual mode of transmission in nature: the number of bradyzoites ruptured and present in nasal droplets is very low and insufficient for the infection of a bovine; and the seasonal incidence of the disease (Bigalke, 1968).

1.1.4 - Pathogenesis and Clinical Signs

In the acute stage of besnoitiosis, tachyzoites appear in the blood circulation and lymph stream, proliferating in monocytes, macrophages, neutrophils, fibroblasts and endothelial cells in blood vessels (mainly in the papillary layer, with a few scattered in the reticular layer) (Bigalke, 1981; Langenmayer *et al*., 2014). They are about 6–7,5×2,5–3,9 μm (Reis *et al*., 2006), and cause vasculitis and thrombosis, especially of the capillaries and small veins in the dermis, subcutis, fascia, testes and upper respiratory mucosae (Basson *et al*., 1970; Langenmayer *et al*., 2014). After parasitaemia cessation, the parasites disappear from the blood circulation and reappear in growing histiocytes in the fibrous tissue of the dermis, subcutaneous tissue, testis, sclera conjunctiva and mucous membrane of the upper respiratory tract. This is in accordance with previous observations by Pols, 1960, in which proliferation in macrophages ceases after a relatively short period, continuing the parasite to multiply in histiocytes in the tissues, forming cysts containing slow growing bradyzoites (chronic stage).

In the first, acute, initial phase, 4 to 12 days after infection, and lasting 6–10 days, associating with the high parasitaemia, the clinical signs may include increased body temperature, heart and respiratory rates, serous nasal and ocular discharges, anorexia, weight loss, generalized weakness, reluctance to move, swelling of the superficial lymph nodes, generalized oedema of

the skin, acute orchitis with swollen, painful testes anasarca, and dyspnea (inflammation of the upper respiratory mucosae). Other less common manifestations are diarrhea and abortion (Pols, 1960; Mccully *et al*., 1966; Cortes *et al*., 2005).

The second phase of the disease is the chronic stage: formation of large numbers of tissue cysts (of up to 0,5mm in diameter) containing bradyzoites. The fever, anorexia and weight loss continue. Cysts form in the same tissues in which the tachyzoites were present during the acute disease, including the skeletal muscles, tendons, tendon sheaths and the periosteum of the appendicular skeleton, and can remain unaltered for the rest of the animal´s life, forming in approximately six weeks (reviewed in Cortes *et al*., 2014). Small cysts are seen upon visual inspection of the scleral conjunctiva, a feature of considerable value in clinical diagnosis (Pols, 1960; Sannusi, 1991). The overall appearance of the cysts can be observed thought skin scrapings obtained from infected animals: brilliant white cysts, when seen with a naked eye, in clusters of three to four among cross-sectioned basis of hair (Mehlhorn *et al*., 2009). Each tissue cyst is surrounded by a dense secondary cyst wall of about 20µm in diameter, formed by the deposition of connective tissue fibers by fibroblasts, around the host cell (Rostaher *et al*., 2010). These fibrils are rich in collagen and hyaline, forming the homogeneous and thick cyst wall. During cyst development, the nucleus of the host cell is hypertrophied, and undergoes several divisions, resulting in many flattened, large nuclei at the periphery of the cyst (Langenmayer *et al*., 2014), and inside the host cell, there are thousands of single bradyzoites, banana-shaped in longitudinal sections (Mehlhorn *et al*., 2009), reaching a mean size of 6.0–7.5 µm long and 1.9–2.3 µm wide (Dubey *et al*., 2003b).

The presence of dermal lesions is also another important feature of the chronic stage: thickening (up to 2 cm) and folding or wrinkling of the skin, especially around the neck, shoulders, rump, and limbs (locomotion may be difficult and painful) accompanied by hyperpigmentation and alopecia. Bulls that survive a natural infection develop either a temporary (can persist for six months) or permanent infertility (Pols 1960).

In a post-mortem exam, cysts are found in the mucous membrane of the respiratory tract, cutis, subcutis and muscles, but not in the mucous membrane of either the abomasums, or small and large intestine (Pols 1960). In the male, both testicles can be markedly fibrotic and reduced in size, causing the testicles to be retracted up into the inguinal region. Moreover, spermatozoa cannot be demonstrated in the epididymis or vas deferens of both testicles (Cortes *et al*., 2005).

1.1.5 - Diagnosis

As there are other diseases with similar signs (burns; mange; fungus infection), it is necessary to confirm *B. besnoiti* infections using laboratorial diagnostic tests. These include direct detection of the parasite and/or its DNA in tissue samples (skin scrapings, scleral conjunctival scrapings, histopathology, polymerase chain reaction (PCR)) and indirect detection based on serology (reviewed in Cortes *et al*., 2014).

In skin scrapings bradyzoites can be detected in a useful, rapid and cheap diagnosis, particularly when other diagnostic procedures are unavailable. Scleral conjunctival scrapings may reveal bradyzoites, thus enhancing the diagnostic value of conjunctival cysts in more chronic infections. These are simple methods for confirming clinical cases in the field, using simple diagnostic facilities (Sannusi, 1991).

As for histopathology, due to the very high number of cysts on the skin of a sick animal, it is a good method to diagnose the chronic cases, but not suitable for sub-clinically infected animals. A biopsy punch of 8mm diameter is suitable, and should be obtained at a location where the skin exhibits pathological alterations (reviewed in Cortes *et al*., 2014).

In sub-clinically infected animals, a PCR-based diagnosis of *B. besnoiti* infections in bovine skin samples is a good diagnostic method available. The sensitivity of the amplification reactions is extremely high: it consistently allows the detection of DNA equivalent to one *B. besnoiti* cell. As for the specificity of the test, is very high, since *B. besnoiti* DNA was amplified exclusively from a panel of apicomplexan parasites DNAs (*B. besnoiti, Neospora caninum, T. gondii, Sarcocystis neurona, Sarcocystis cruzi, Sarcocystis tenella, Sarcocystis muris, Sarcocystis spellei, Sarcocystis miescheriana, Sarcocystis zamari, Sarcocystis singapurencei, Sarcocystis gigantea, Sarcocystis moulei, Sarcocystis capracanis, Sarcocystis arieticanis, Sarcocystis speeri*) (Cortes *et al*., 2007b). Meanwhile, cross-reactions with other species of the genus *Besnoitia* (*B. darlingi, B. oryctofelisi*, and *B. neotomofelis*) are possible (Schares *et al*., 2011b). However, this is of limited consequences since these species are not considered cattle parasites.

Concerning the serological tests, the immunofluorescence antibody test (IFAT) is the most widely used and is generally considered a robust test. No cross reactions were observed with serum dilution cutoffs of 1:200 for *N. caninum* and 1:256 for *B. besnoiti*. Nonetheless, at 1:64 dilution, anti-*N. caninum* sera reacted with *B. besnoiti* antigen in some samples (Shkap *et al*., 2002). Cross-reactions between *Besnoitia* species have also been reported by IFAT and Western blot, namely between *B. besnoiti* and *B. tarandi*, a species that infects reindeer (Gutiérrez-Expósito *et al*., 2012).

As for ELISA (Enzyme linked immunosorbent assay), it provides a relatively good diagnostic sensitivity, including all the different clinical courses of bovine besnoitiosis. It can be recommended as a fast and inexpensive mass screening test in seroepidemiology of bovine besnoitiosis, for example, to elaborate a seroprevalence status in a herd or a region. Sensitivity being not as high as IFAT or Western blot, the serodiagnosis of individual cases may rather rely upon the latter two tests (Cortes *et al*., 2006a). Several commercial ELISA tests for the specific detection of antibodies against *B. besnoiti* are already available in the market, and are of special interest for serological identification of sub-clinically infected cattle, in order to avoid the introduction of infected animals into naive herds (Schares *et al*., 2011a).

Another serological test for the diagnosis of bovine besnoitiosis that has proved good diagnostic characteristics is the modified agglutination test (B-MAT). Its sensitivity and specificity was determined in relation to the IFAT, showing an almost perfect test agreement with the IFAT, with a relative sensitivity of 97.2%, and a relative specificity of 99.3%. This test is simple and inexpensive, representing a valuable tool for the diagnosis and study of the epidemiology of bovine besnoitiosis (Waap *et al*., 2011).

The large number of serological tests available, with different specificities and sensitivities, led to an attempt to standardize them for the diagnosis of bovine besnoitiosis in Europe. According to this study, all ELISA assays performed very well and could be used in epidemiological studies. However, Western blot tests performed better and could be employed in the case of uncertain results from valuable samples (García-Lunar *et al*., 2012a).

Recently, the differentiation of acute and chronic bovine besnoitiosis cases was made possible by Schares *et al*., 2013, that used serological tests employing affinity purified antigens of *B. besnoiti* tachyzoites in western blots, conventional ELISA and in avidity ELISA.

1.1.6 - Treatment

Several attempts to develop effective drugs to treat bovine besnoitiosis have been made, but until now with no considerable success (reviewed in Cortes *et al*., 2014).

Sulfamides are commonly used to diminish the severity of clinical signs, failing to cure the infected cattle. Tetracyclines have also been used by some veterinarians, but the efficacy has not been clearly demonstrated (Shkap *et al*., 1985; Shkap *et al*., 1987).

Experimental studies using Nitazoxanide (NTZ), its deacetylated metabolite tizoxanide (TIZ) and Rm4822 (a NTZ-derivative) demonstrated considerable *in vitro* activity against *B. besnoiti* tachyzoites grown in Vero cells. Transmission electron microscopy (TEM) showed that treatment of intracellular tachyzoites with NTZ, TIZ and Rm4822 caused massive

vacuolization and membranous vesiculation within the parasite cytoplasm after 12–48 h, all signs of severely impaired metabolic activity (Cortes *et al*., 2007a).

Recently, arylimidamides, as arylimidamide DB811 induced an *in vitro* high degree of ultrastructural alterations on the proliferating tachyzoites of *B. besnoiti*, with a complete growth inhibition observed with a drug concentration of at 1.6 μM (Cortes *et al*., 2011). Despite this, corresponding studies in animals have not yet been undertaken.

1.1.7 - Prophylaxis

Live tissue culture vaccines have been used in South Africa and Israel (Bigalke *et al*., 1973; Pipano, 1997). In South Africa, the vaccine is based on tachyzoites of an isolate from blue wildebeest grown in cell cultures, and a single inoculation has been shown to prevent clinical disease for one to four years, but it does not consistently prevent subclinical infections. In Israel, the vaccine contains live attenuated parasites from cell cultures, and there are no available data in the scientific literature to judge on its efficacy and safety (reviewed in Cortes *et al*., 2014).

As such, the control of bovine besnoitiosis is based on the use of reliable insecticides, which can be a feasible measure of control considering the possibility of an arthropod involved in the transmission (Jacquiet *et al*., (2010). Thus, prevention relies on regular application of insecticides; separation of healthy cattle from infected cows, wild ruminants, and cats; elimination or isolation of infected animals; serological examination before introducing an animal in a herd free from besnoitiosis; an intensive information campaign for veterinarians (especially in the regions of recent emergence) and for cattle breeders.

1.2 - Toxoplasmosis

Toxoplasmosis is a parasitic disease caused by the protozoan *Toxoplasma gondii*. *T. gondii* is classified in the family Sarcocystidae, subfamily Toxoplasmatinae of the phylum Apicomplexa, and is closely related to the genus *Hammondia, Neospora* and *Besnoitia*.

1.2.1 - History

Nicolle & Manceaux, 1908 found a protozoan in tissues of a hamster-like rodent, the gundi, *Ctenodactylus gundi*, and named it *T. gondii* based on the morphology (mod. L. toxo=arc or

bow, plasma=life) and the host. For the next 30 years, *T. gondii*-like organisms were found in several other hosts, and viable *T. gondii* were first isolated by Sabin & Olitsky, 1937.

1.2.2 - Transmission and Life Cycle

T. gondii is a tissue cyst forming coccidian parasite with a heteroxenous life cycle, in which an asexual phase of development, in various tissues of herbivorous or omnivorous intermediate hosts, is linked to a sexual phase of development in the intestine of carnivorous definitive hosts, being the oocyst stage of *T. gondii* shed in the feces, an important source of infection for many intermediate hosts (reviewed in Innes, 2010).

In intermediate hosts, *T. gondii* undergoes two phases of asexual development. In the first phase, tachyzoites multiply rapidly in many different types of cells, where they can differentiate into bradyzoites, forming tissue cysts. Tissue cysts are located predominantly in the central nervous system (CNS), the eye, as well as skeletal and cardiac muscle, and to a lesser extent in lungs, liver, and kidneys. Tissue cysts are the terminal life-cycle stage in the intermediate host and are immediately infectious. Inside the cysts, bradyzoites can transform again into tachyzoites, break the cyst, reinvade new host cells, and again transform to bradyzoites within new tissue cysts (reviewed in Robert-Gangneux & Dardé, 2012). Importantly, tissue cysts containing bradyzoites persist in species such as sheep, goats, and pigs, while in cattle and deer the host may eventually become clear of infection (reviewed in Buxton, 1990).

The sexual cycle is initiated when a cat ingests tissue cysts: the cyst wall is dissolved in the small intestine and the released bradyzoites penetrate the adjacent epithelial cells. In these cells the bradyzoites pass through a schizogonic cycle followed by gametogony which gives rise to oocysts that are then excreted in the feces. Sporogony occurs outside the host and leads to the development of infectious oocysts which contain two sporocysts, each containing four sporozoites (reviewed in Robert-Gangneux & Dardé, 2012).

In the case of *T. gondii*, the existence of three infectious stages (tachyzoites, bradyzoites contained in tissue cysts, and sporozoites contained in sporulated oocysts (Fig. 2)) makes it possible for *T. gondii* to be transmitted from definitive to intermediate hosts, from intermediate to definitive hosts, as well as between intermediate hosts and between definitive hosts (reviewed in Tenter *et al*., 2000). Intermediate and definitive hosts may acquire a *T. gondii* infection mainly via one of the following routes: (A) horizontally by oral ingestion of infectious oocysts from the environment; (B) horizontally by oral ingestion of tissue cysts

contained in raw or undercooked meat or viscera of intermediate hosts; or (C) vertically by transplacental transmission of tachyzoites (reviewed in Dubey *et al*., 1998).

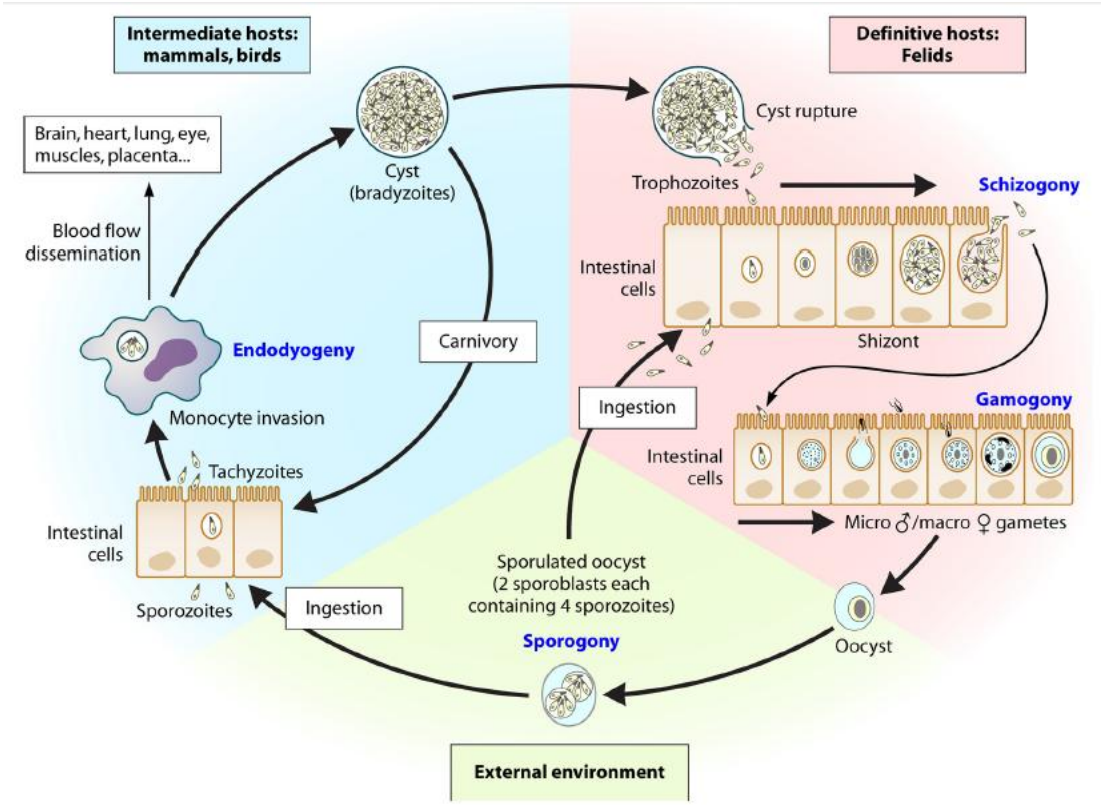

Fig. 2: Life cycle of *T. gondii*.

The biology, infection, and replication of the three infective stages of the parasites in their respective hosts are shown. Adapted from Robert-Gangneux & Dardé, 2012.

1.2.3 - Pathogenesis and Clinical Signs

Cattle, like deer and horses, are susceptible to infection but resistant to disease induced by *T. gondii*, whereas the parasite can cause a lethal infection in the developing fetus of sheep (Esteban-Redondo & Innes, 1997).

Transmission of *T. gondii* to herbivores is either transplacental or by ingestion of fodder or rations contaminated with oocysts. Sporulated *T. gondii* oocysts, ingested by susceptible pregnant sheep, excyst in the digestive tract and release sporozoites that penetrate the intestinal epithelium. In 4 days, organisms can be found in the mesenteric lymph nodes, where they multiply causing marked lymph node enlargement. Around the 5th day tachyzoites are released to cause parasitaemia, which may last until the 12th day. Tachyzoites contained within immune cells (macrophages, dendritic cells (DCs)) can be disseminated throughout the body until an adequate immune response is mounted between 7th and 10th days after infection.

The cessation of the parasitaemia coincides with the onset of an effective immune response and infection then persists as bradyzoites within tissue cysts (Dubey & Sharma, 1980; Dubey, 1984). During the acute phase of infection interferon gamma (IFNg) is produced. Initially, the predominant cells are CD4+ cells, but around 11 days there are mainly CD8+ cells, after which IFNg is no longer detected. Although antibodies start to appear at this time, protective immunity is largely cell-mediated (Innes *et al*., 1995). In sheep seropositive for *T. gondii*, infection persists as bradyzoites within tissue cysts in the eye, brain, lungs, skeletal muscle, and cardiac tissue. Young cysts can be as small as 5 µm in diameter with as few as 2 bradyzoites, while mature cysts can be up to 70 µm with 1000 bradyzoites (reviewed in Dubey *et al*., 1998). Following an infection, sheep develop protective cell-mediated immunity, remaining immune but infected (with bradyzoites in tissue cysts), and they usually do not have further abortions due to the infection. Indeed, clinical signs of toxoplasmosis are seen when a ewe in mid pregnancy becomes infected for the first time. Typical symptoms include stillborn and/or weak lambs that usually have brain damage and a characteristic non-suppurative meningo-encephalitis. Infection in the latter period of gestation may have no clinical consequences, with lambs being born normal and without neurological disease (reviewed in Entrican & Wheelhouse, 2006).

1.2.4 - Zoonotic importance

Toxoplasmosis is one of the more common parasitic zoonoses world-wide. In humans, brain and muscles are the main tissues affected, and the most severe signs are observed in cases of brain parasitism (reviewed in da Silva & Langoni, 2009).

Since tachyzoites only survive for a short period of time outside the host, it has been accepted that postnatal infections in humans are acquired by ingesting tissue cysts contained in meat or viscera of animals, or by ingesting oocysts shed into the environment by domestic cats or wild felines (Fig. 3). The relative importance of these two routes of infection in the epidemiology of *T. gondii* infections remains obscure. If on the one hand, consumption of undercooked meat has been identified as the principle risk factor, on the other hand up to 47% of strict vegetarians have been shown to possess antibodies to *T. gondii* (Hall *et al*., 1999; reviewed in Robert-Gangneux & Dardé, 2012).

Fortunately, while infection with *T. gondii* in humans is very common, clinical disease is largely confined to risk groups, being most cases of infection in immunocompetent humans, asymptomatic, resulting in life-long immunity against toxoplasmosis. Occasionally, various mild symptoms may be observed, of which lymphadenopathy is the most significant clinical

manifestation, but severe manifestations, such as encephalitis, sepsis syndrome/shock, myocarditis, or hepatitis, are very rare in immunocompetent humans (Ho-Yen, 1992). Retinochoroiditis and retinitis are another possible clinical manifestation of the infection, in this case of ocular toxoplasmosis. In the past, this form of the disease was thought to be a result of a prenatal infection, but now it is known that it can be acquired also after birth (Gump & Holden, 1979, Akstein *et al*., 1982). However, if first contracted during pregnancy, *T. gondii* may also be transmitted to the fetus in immunocompetent women. In a pregnant woman, temporary parasitaemia may result in invasion of the placenta by tachyzoites which multiply in the placenta, and enter the fetal circulation or fetal tissues. Congenital toxoplasmosis may cause abortion, neonatal death, or fetal abnormalities with detrimental consequences for the fetus (Remington *et al*., 2006). The effects on the fetus are more severe if transmission occurs at an early stage of pregnancy, usually causing encephalomyelitis with severe consequences (Jacquemard, 2000). If transmission occurs at a late stage of pregnancy the effects on the fetus are less severe, with most infants infected during the third trimester being asymptomatic at birth. Nonetheless, these healthy children may develop symptoms later in life, with the disease affecting the eyes (retinochoroiditis, blindness), the CNS (neurological deficiencies, convulsions, mental retardation), or the ear (deafness) (McLeod & Boyer, 2000).

Clinical signs can be severe in immune compromised individuals, such as those suffering from lymphatic cancers including Hodgkin's disease (Cheever *et al*., 1965), undergoing immunosuppressive treatment (Beauvais *et al*., 1976), or people with acquired immunodeficiency syndrome (AIDS) (Luft *et al*., 1984). Due to the fact that *T. gondii* persists within tissue cysts for the lifetime of the host, when the immune system is compromised, the parasite recrudesces and actively multiplies at the sites of persistent infection. In addition to reactivated toxoplasmosis, immune compromised patients are at risk of severe disease following primary infection, which frequently presents as pulmonary disease or diffuse encephalitis (reviewed in Robert-Gangneux & Dardé, 2012).

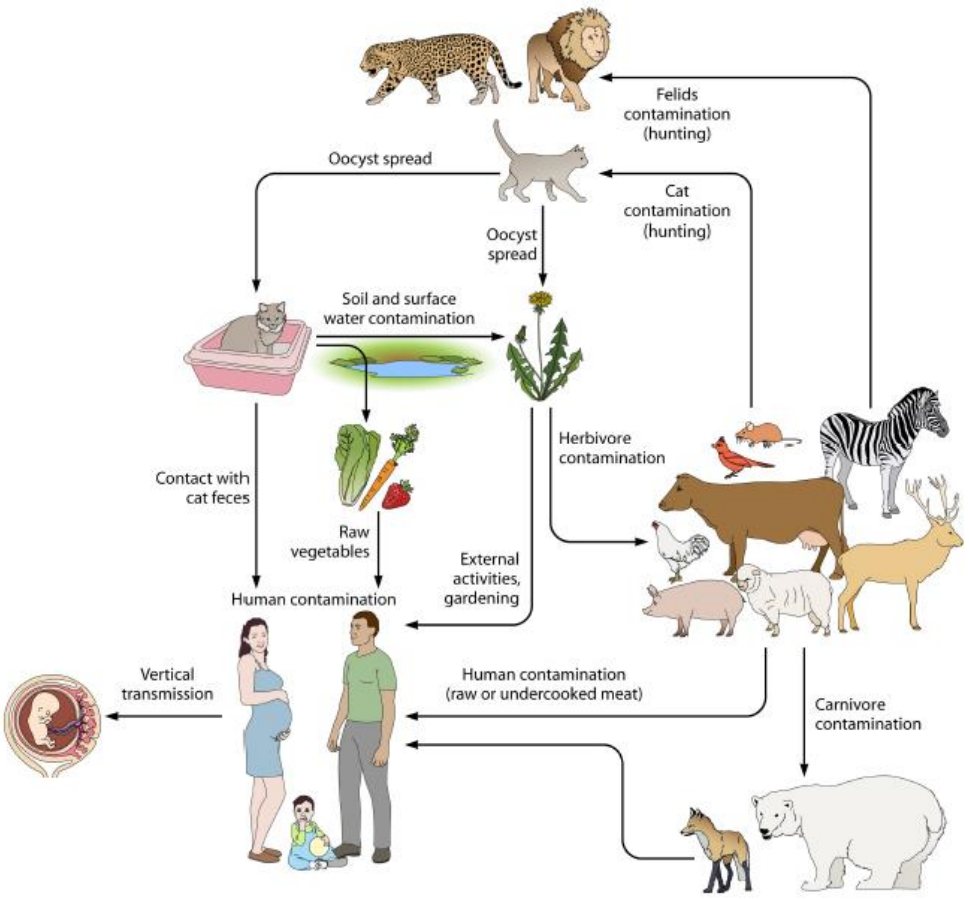

Fig. 3: Sources of *T. gondii* infection in humans.
Adapted from Robert-Gangneux & Dardé, 2012.

1.2.5 - Diagnosis

For the diagnosis of toxoplasmosis, serological tests and tests for the detection of *T. gondii* DNA are used.

The dye test, developed by Sabin & Feldman, 1948, is a serological test highly sensitive and specific with no evidence for false results in humans. A further advantage of the dye test is that since it does not require species-specific reagents, can therefore be used in many different hosts (reviewed in Innes, 2010).

For congenital toxoplasmosis, Remington, 1969 modified the indirect fluorescent antibody test and the ELISA to detect IgM in cord blood, since in humans IgM antibodies do not cross the placenta, whereas IgG antibodies do (Remington *et al*., 1968; Remington, 1969). ELISA tests are widely used today to detect specific antibodies in humans, and there are commercially available IgG avidity tests to diagnose toxoplasmosis in humans (Iqbal & Khalid, 2007).

The modified agglutination test (MAT) is another serological test used extensively for the diagnosis of toxoplasmosis in animals (Fulton & Turk, 1959).
The use of the PCR as a diagnostic tool started when Burg *et al*., 1989 reported the detection of *T. gondii* DNA from a single tachyzoite using the B1 gene. Several subsequent PCR tests have been developed using different gene targets (reviewed in Dubey, 2008).

1.2.6 - Treatment

There are available drugs to treat human toxoplasmosis, but they usually have severe side effects, cannot act against chronic *T. gondii* infections, and some reports of resistance to some of these drugs have been published (Dannemann *et al*., 1992).
The standard therapy for toxoplasmosis in humans is a combined therapy with sulfonamides, pyrimethamine, and spiramycin. These three compounds have provided the mainstay of treatment against the parasite in congenital infection and eye disease: they act against the rapidly dividing tachyzoites, being of most benefit during acute infection. Nonetheless, they have a low efficacy against the tissue cysts. The discovery of clindamycin having anti-toxoplasmal activity provided another drug to treat toxoplasmosis, especially in patients allergic to sulfonamides (Eyles & Coleman, 1953; Garin & Eyles, 1958; Araujo & Remington, 1974; reviewed in Innes, 2010).
In order to treat sheep, experimental studies have been conducted, using monensin (Buxton *et al*., 1988), a combination of sulfadimidine and pyrimethamine (Buxton *et al*., 1993), decoquinate (Buxton *et al*., 1996), and a combination of sulfadimidine and baquiloprim (Buxton & Rodger, 2007). Moreover, under field conditions, the treatment with sulfadimidine seems to be effective, as it reduces the abortion rate and subsequently helps sheep to have a normal length of gestation and subsequently normal milk production (Giadinis *et al*., 2011).

1.2.7 - Prophylaxis

In terms of prophylaxis, as there are no effective vaccines for humans, prevention of zoonotic transmission might be the best way to approach the problem of toxoplasmosis. Recommendations for accomplishing this include: to cook meat thoroughly; to wash hands after handling raw meat; to wash kitchen utensils that have come in contact with raw meat; to wash fruits and vegetables before consumption; to avoid contact with items contaminated with cat feces; to use gloves if cleaning a cat litter box; and to clean all litter boxes with hot water between litter changes. Moreover, freezing of meat overnight in a household freezer (-

12ºC) before human or animal consumption, and/or cooking meat until an internal temperature of 66°C is reached, remain the easiest and most economical method of reducing transmission of *T. gondii* through meat (Verma & Khanna, 2013).

As for ovine toxoplasmosis, the best mean to control the disease is also through prophylactic measures to reduce the incidence of clinical disease, including good management of food and water and vaccination (reviewed in Buxton *et al*., 2007). The use of live vaccines in sheep before the matting period, like the S48 strain Toxovax, reduces tissue cyst development and neonatal mortality in lambs (Buxton & Innes, 1995). The T-263 strain of *T. gondii* is a live mutant designed to reduce or prevent oocyst shedding by cats by developing only partially in the intestinal tract (Verma & Khanna, 2013).

1.3 - *Besnoitia besnoiti* and *Toxoplasma gondii* are closely related apicomplexan parasites

Apicomplexan parasites include, besides *B. besnoiti* and *T. gondii*, several other parasites, for example: *Plasmodium; Eimeria; Theileria*; *Cryptosporidium*; *Babesia* and *N. caninum*. They have complex life cycles, with several developmental stages, but the majority of them are, at one point or another, obligate intracellular parasites. Most apicomplexan parasites grow and replicate inside a host cell within the parasitophorous vacuole (PV), until the cell is lysed by the replicating parasites. Repeated cycles of host cell invasion, parasite replication, host cell lysis, and parasite invasion of new cells account for much of the tissue damage associated with apicomplexan infections.

Apicomplexan parasites share a variety of morphological traits that are considered diagnostic for this phylum (Fig. 4A). One of major importance, that gives name to the phylum, is a specialization of the apical region, named the apical complex, that releases secreted factors essential for attachment, invasion, and subsequent formation of the PV in which the parasite encloses itself (Hakansson *et al*., 2001; Hu *et al*., 2006). The apical complex includes several organelles and structures, like the rhoptries, the micronemes, the apical polar ring, the conoid, the preconoidal rings, and two short MTs (intraconoid MTs, which may be used as tracks for transport of secretory vesicles essential for invasion). Rhoptries and micronemes are secretory organelles that contain products required for motility, adhesion and invasion of host cells, and establishment of the PV (Sinai & Joiner, 2001; Kessler *et al*., 2008). The apical polar ring serves as one of the three microtubule organizing centers (MTOCs) in these parasites; (spindle pole plaques and centrioles/basal bodies are the other MTOCs), nucleating the parasite's subpellicular MTs (Chobotar & Scholtyseck, 1982). The conoid is a small cone-shaped structure thought to play a mechanical role in invasion of host cells. The preconoidal rings, at

the distal tip of the conoid, are the structures from which the conoid fibers originate (Fig. 4B) (Hu *et al*., 2006). Another unique structural feature of parasites belonging to the phylum Apicomplexa is an essential chloroplast-like organelle called the apicoplast (Kohler *et al*., 1997).

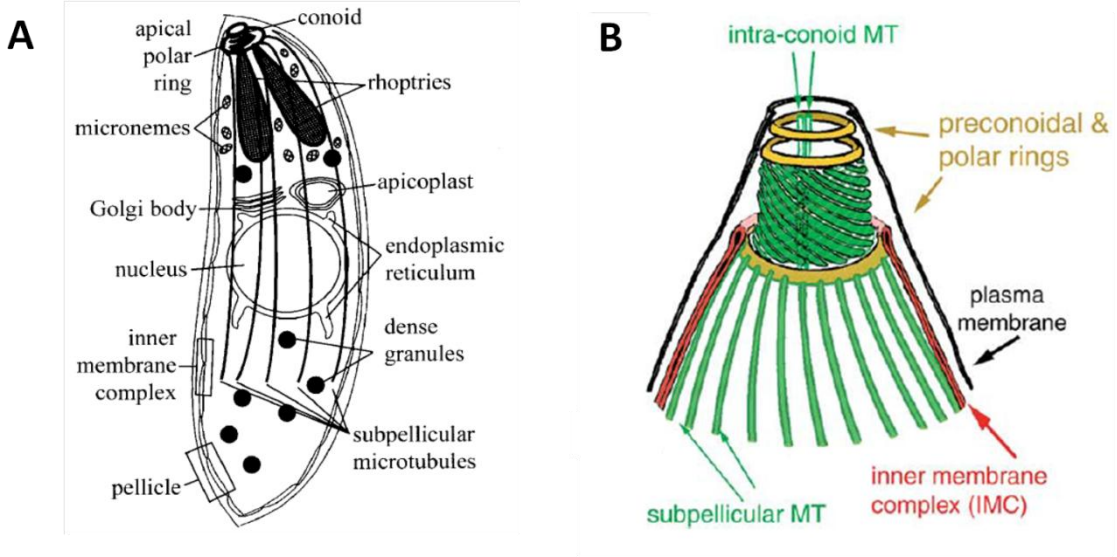

Fig. 4: Apicomplexan parasites morphology.
(A) The morphology of apicomplexan parasite cells. (B) View of the typical apical complex cytoskeleton of some apicomplexan. Adapted from Morrissette & Sibley, 2002b; and Hu *et al*., 2006.

1.4 - Morphological characteristics of *Besnoitia besnoiti* and *Toxoplasma gondii*

As mentioned before, both parasites object of this study (*B. besnoiti* and *T. gondii*) belong to the phylum Apicomplexa, subfamily Toxoplasmatinae, sharing a number of morphological and physiological features. Some of these characteristics are going to be further described, and since *T. gondii* is a well studied parasite, most of the information presented is regarding this parasite, comparing, when possible, to *B. besnoiti*.

1.4.1 - The Pellicle

During the life cycle, *T. gondii* and *B. besnoiti* need to withstand a variety of physically and chemically stressful environments. In addition, the parasites are deformed dramatically during invasion of host cells (Chiappino *et al*., 1984; Nichols & Chiappino, 1987, Reis *et al*., 2006). To maintain structural integrity under these conditions, these parasites need a source of mechanical strength. Mechanical stability of *T. gondii* and *B. besnoiti* is most likely dependent on the pellicle and its underlying cytoskeletal components. The pellicle consists of

the plasma membrane and two tightly apposed membranes of the underlying inner membrane complex (IMC). The membranes of the IMC are characterized by the presence of a two-dimensional particle lattice composed of aligned intramembranous particles (IMPs). The lines of IMPs are organized as single rows interspersed with double rows and the latter are aligned with the underlying subpellicular MTs (D'Haese *et al*., 1977; Morrissette *et al*., 1997). The IMPs likely reflect the transmembrane domains of integral membrane proteins, that are likely to function in signal transduction, interaction with extracellular substrates (such as host cell ligands), force transduction for the actin-myosin motor during invasion, and maintenance of interactions among the pellicle, subpellicular network, and MTs. A few of these proteins have been described in *T. gondii*, but their function is still largely unknown: PhIL1 is detected throughout the IMC but strongly enriched in the apical cap and basal complex (Gilk *et al*., 2006); ISP1 (IMC Sub-compartment Protein1) localizes to a region corresponding to the apical cap; ISP2 (IMC Sub-compartment Protein2) occupies a central IMC region, and plays a role in parasite´s endodyogeny; ISP3 (IMC Sub-compartment Protein3) resides in both the central IMC region and a basal IMC compartment; and ISP4 (IMC Sub-compartment Protein4), that localizes to the central IMC subcompartment, similar to ISP2 (Beck *et al*., 2010). Additionally, only a few proteins are known to directly associate with the IMC membranes. Among them, a number of proteins associated with gliding motility (Gaskins *et al*., 2004; Bullen *et al*., 2009), as well as the heat shock protein Hsp20 (de Miguel *et al*., 2008).

Underlying the pellicle is a filamentous cytoskeletal structure known as the subpellicular network that associates on its outer face with the IMC and on its inner face with the subpellicular MTs (Morrissette *et al*., 1997; Mann & Beckers, 2001; Morrissette & Sibley, 2002b; Gilk *et al*., 2006). This structure is composed of interwoven filaments and extends from the polar ring along the entire length of the parasite. The filaments have a diameter of 8 to 10 nm, and the network has the same general shape as the parasite, suggesting that these filaments may play a role in generating and maintaining cell shape. The thin filaments appear to surround the subpellicular MTs in the anterior region of *T. gondii*, and end in a well-delimited circular structure, ranging from 300-650 nm in diameter, localized at the posterior tip (Mann & Beckers, 2001; Gilk *et al*., 2006; Lemgruber *et al*., 2009). This structure, characterized as a basal complex, contains proteins such as TgMORN1, TgCentrin 2 and a dynein light chain, but no tubulin based structures have been observed (Hu, 2008; Lemgruber *et al*., 2009).

1.4.2 - The Conoid

The conoid is a truncated cone, 280 nm in length and 380 nm in diameter in *T. gondii* (Hu *et al*., 2002), and 600 nm *per* 540 nm in *B. besnoiti* (measured by atomic force microscopy, (Reis *et al*., 2006)), playing a mechanical role in invasion to penetrate robust barriers (Chobotar & Scholtyseck, 1982; Nichols & Chiappino, 1987). This structure can either be recessed in the cell, inside the apical polar ring, or, during invasion, be extruded from the apical polar ring. Protrusion of the conoid is sensitive to parasite cytoplasmic calcium concentration, and can be induced by calcium ionophore treatment (Stommel *et al*., 1997). The structure of the conoid consists of a set of counterclockwise spiraling filaments that create a pointed or coneshaped structure at the extreme apex of these parasites (D'Haese *et al*., 1977; Hu *et al*., 2002). The filamentous subunits of the conoid are curled into an extremely tight coil constructed from tubulin organized into a novel polymer form, consisting of a sheet of nine protofilaments. However, unlike MTs, the protofilaments are not arranged as a closed tube, and instead form ribbons of 9 protofilaments folded into a comma shape. The concave side of the comma always faces the interior of the conoid, and the tail of the comma always points toward the conoid base (Hu *et al*., 2002). Inside the conoid, there are two intraconoid MTs, exhibiting a canonical MT structure (a tube of 13 protofilaments, (Hu *et al*., 2002)).

The specialized arrangement of tubulin in the conoid fibers is probably determined by association with other non-tubulin proteins, probably microtubule associated proteins (MAPs). A few proteins were identified in the conoid of *T. gondii*, such as: TgCentrin3; calcium-binding domain proteins CAM1 and CAM2; and dynein light chain (TgDLC), however the functions of these proteins remain untested (Hu *et al*., 2006; Katris *et al*., 2014). The *T. gondii* preconoidal rings are associated with TgCentrin2 and SAS6L, two proteins typically implicated with centriolar function (Liu *et al*., 2013, de Leon *et al*., 2013). A novel protein, TgICMAP1 (intraconoid microtubule associated protein1) decorates the intraconoidal MTs, and when over-expressed in mammalian cells, coats and stabilizes MTs, suggesting that TgICMAP1 might play a role in stabilizing the intraconoid MTs (Heaslip *et al*., 2009).

1.4.3 - Microtubule Cytoskeleton

In *T. gondii* there are two populations of MTs, nucleated from two different MTOCs: the subpellicular MTs and the spindle MTs, which permit *T. gondii* to control nuclear division independently from cell polarity and cytokinesis. Subpellicular MTs are necessary for host

cell invasion, since they are important for shape and apical polarity of the parasite, and play an important role in segregation of organelles to daughter buds. Conversely, spindle MTs are necessary for chromosome segregation and nuclear scission (Chobotar & Scholtyseck, 1982; Russell & Burns, 1984; Morrissette & Sibley, 2002a).

Subpellicular MTs (22 subpellicular MTs in *T. gondii* (Hu *et al*., 2002) and *B. besnoiti* (Shkap *et al*., 1988)) are organized by lateral association with the apical polar ring (MTOC), being the plus end of the subpellicular MTs distal to this MTOC (Russell & Burns, 1984; Nichols & Chiappino, 1987). Running down the cytosolic face of the pellicle, and ending in the region below the nucleus (approximately two-thirds of the length of the parasite (D'Haese *et al*., 1977; Chobotar & Scholtyseck, 1982; Nichols & Chiappino, 1987; Morrissette & Sibley, 2002b), these spirally arranged MTs closely follow the serpentine body shape of the parasites, conferring an elongated shape and apical polarity, and also contributing to motility by providing tracks that direct the acto-myosin-based activity. The subpellicular MTs are closely associated with the cytosolic face of the IMC, demonstrating a periodicity which suggests that they directly associate with unidentified proteins of the IMC lattice (Morrissette *et al*., 1997; Tran *et al*., 2012), probably MAPs. To support this association, and since MAPs are stabilizing agents, is the fact that subpellicular Mts are highly resistant to conditions that lead to Mts depolymerization (reviewed in Morrissette & Sibley, 2002b). Two novel proteins that colocalize with the subpellicular MTs in *T. gondii* have been identified: SPM1 and SPM2 (Tran *et al*., 2012). *T. gondii* SPM1 is localized along the entire length of the subpellicular MTs but does not localize to the conoid, the intraconoid MTs, or the spindle. SPM2 has a more restricted localization pattern than SPM1: it is associated with the middle third of the subpellicular MTs. These observations indicate that SPM1 is important to MT stability indicating that the SPM2 protein is not required for overall tachyzoite fitness *in vitro*. Neither of these proteins seems essential for tachyzoite viability, but loss of SPM1 decreases overall parasite fitness and eliminates the stability of subpellicular MTs to detergent extraction (Tran *et al*., 2012). In fact, the importance of SPM1 might be related with the recent discovery of a new MAP: TrxL1 (Thioredoxin-Like protein 1), as TrxL1 does not seem to bind to MTs directly, instead it associates with a protein complex containing SPM1. Besides SPM1, several other proteins are found in the TrxL1-containing complex, including TrxL2, a close homolog of TrxL1 (Liu *et al*., 2013).

Another form of subpellicular MTs stabilization in the apicomplexan *T. gondii* is through post-translational modifications (PTM) of tubulin, which is also a mechanism to generate tubulin diversity since the tubulin gene family is quite small (only one α-and two β-tubulin genes). In *T. gondii* the PTMs identified on α-tubulin include acetylation of Lys40, removal of

the last C-terminal amino acid residue Tyr453 (detyrosinated tubulin), and truncation of the last five amino acid residues. Detyrosinated tubulin is diffusely present in subpellicular Mts and apparently accumulates at the posterior end. Polyglutamylation is detected on both α- and β-tubulins. Finally methylation is detected on both tubulins and may be a modification characteristic of the phylum Apicomplexa (Xiao *et al*., 2010).

During mitosis, parasites employ spindle MTs. Spindle MTs are nucleated from electron-dense, amorphous plaques associated with nuclear invaginations and embedded in the nuclear membrane, adjacent to cytoplasmic centrioles/centrosome (Chobotar & Scholtyseck, 1982). This spindle-organizing structure can be referred to as the centrocone, the centriolar plaque, the spindle pole body or spindle pole plaques.

Besides being associated with the spindle pole plaques, responsible for nucleating the assembly of intra-nuclear spindle MTs, the centrosome has also been described as playing a role in the division of membrane-bounded organelles, including the apicoplast (Striepen *et al*., 2000; Hartmann *et al*., 2006); and implicated in the biogenesis of the Golgi apparatus (Stedman *et al*., 2003; Hartmann *et al*., 2006). Another function for the presence of the centrosome in *T. gondii* might be that the centrioles are maintained throughout the asexual life cycle in order to serve as a template for construction of basal bodies that nucleate flagellar axonemes in the male gametes (reviewed in Morrissette & Sibley, 2002b).

1.4.4 - Secretory organelles: rhoptries, micronemes and dense granules

Micronemes, rhoptries and dense granules are secretory organelles that participate in host cell invasion and formation of the PV. Micronemes and rhoptries are located near the apical end, and dense granules are scattered throughout the length of *T. gondii* and *B. besnoiti* (Shkap *et al*., 1988; Paredes-Santos *et al*., 2012).

During *T. gondii* invasion, microneme proteins (MICs) are secreted first, prior to invasion, and coat the parasite with proteins with adhesive domains that are responsible for parasite gliding and adhesion to the host cell, contributing to the formation of an annular moving junction (MJ) with the host cell membrane, through which the parasite enters the host. Microneme secretion is triggered by an increase in intracellular calcium (Carruthers & Sibley, 1999), it always takes place at the level of the polar ring, and requires that the conoid be extruded for the micronemes to dock and fuse with a specific domain at the plasma membrane (Paredes-Santos *et al*., 2012). In *T. gondii* four protein complexes have been functionally characterized, and can be described as the following: micronemal protein 2 (TgMIC2), found in a complex with MIC2-associated protein (TgM2AP) and playing a fundamental role in

gliding motility, host cell attachment and invasion (Huynh & Carruthers, 2006); TgMIC6 forms a complex with two adhesins (TgMIC1 and TgMIC4) and contributes to invasion *in vitro* and virulence *in vivo* (Cérède *et al*., 2005; Sawmynaden *et al*., 2008; Santos & Soldati-Favre, 2011); TgMIC8 assembles with a lectin (TgMIC3) and is essential for rhoptry secretion and invasion (Kessler *et al*., 2008). The fourth complex assembles only at the MJ, bringing together the MIC apical membrane antigen 1 (TgAMA1) and several preassembled rhoptry neck proteins (RONs) (TgRON2-RON4-RON5-RON8) (Alexander *et al*., 2005; Besteiro *et al*., 2009; Straub *et al*., 2009). Indeed, parasites deficient in TgAMA1 can still attach to host cells but fail to form the MJ, and cannot invade host cells (Mital *et al*., 2005).

The second type of organelles to be secreted is the rhoptries. Larger and less abundant (6–14 *per* cell) than micronemes, rhoptries are club-shaped (Paredes-Santos *et al*., 2012). They contain two sets of proteins segregated either in the neck (rhoptry neck proteins or RONs that are often involved in the initial steps of invasion) or in the posterior bulb (rhoptry bulb proteins or ROPs, involved in later stages of invasion and parasite establishment) (Bradley *et al*., 2005). The RON proteins are restricted to the MJ, being responsible for the assembly of the MJ, together with AMA1 (Alexander *et al*., 2005). ROP proteins are delivered either to the PV or into the host cytosol, where they access various compartments and modulate host functions (Paredes-Santos *et al*., 2012; Katris *et al*., 2014). Recent work in *T. gondii* has shown that parasites with dispersed rhoptries are completely unable to invade host cells, but motility, attachment and egress are not impacted, demonstrating that the rhoptries are not required for these processes (Beck *et al*., 2013). In terms of location, rhoptries appear to be docked to a specific region at the apical portion of the tachyzoite to expel its contents – the porosome. This porosome-like structure is seen as a slight depression at the center of the conoid (Paredes-Santos *et al*., 2012).

The dense granules are the third type of secreting organelle. Dense granules secrete their contents (dense granule proteins (GRA)) inside the PV throughout the intracellular cycle, and the secretion takes place preferentially in the lateral, apical portion of the parasite (Chaturvedi *et al*., 1999). The secretory products are used to build the intravacuolar network, a membranous net of tubules that helps to support the PV (Magno *et al*., 2005). Additionally the dense granules also contribute to the discharge of proteins capable of acting as effectors, subverting host functions, for example, TgGRA15 activates the NF-kB pathway (Rosowski *et al*., 2011).

Taken together, microneme secretion is very intense during recognition and adhesion; rhoptry secretion occurs upon entry; and dense granules are constantly secreted after entry and formation of the PV (reviewed in Dubremetz *et al*., 1998).

1.5 - Invasion and replication of *Besnoitia besnoiti* and *Toxoplasma gondii* inside the host cell

1.5.1 - The gliding motility is required for host invasion and based on actin-myosin

Infection of and spread between host cells by *T. gondii,* is critically dependent on actin-myosin based motility systems in the parasite – a unique form of substrate-dependent motion called gliding motility (driving entry to and exit from diverse cell types). The same way as for *T. gondii, B. besnoiti* tachyzoites enter their host cells through gliding motility, with the apical part first, involving actin/myosin motor proteins. The «glideosome», the complex responsible for generation of movement, is composed of actin, myosin, and several associated proteins. This way, an actomyosin motor, located within the pellicle in the space between the plasma membrane and the IMC, drives motility and cell invasion. Supporting this, actin-disrupting or stabilizing drugs (cytochalasin D and jasplakinolide), as well as myosin inhibitors (butanedione monoxime), disrupt *T. gondii* motility and invasion (Dobrowolski & Sibley, 1996; Dobrowolski *et al*., 1997a). Also, cytochalasin inhibition of gliding motility and/or invasion has been demonstrated in *T. gondii* (reviewed in Soldati & Meissner, 2004).

A large fraction of the actin in parasites of the phylum Apicomplexa appears to be in the monomeric G-form rather than the polymerized form (F-form, apicomplexan microfilaments are apparently quite labile under most circumstances). In fact, experiments with *T. gondii* have established that tachyzoites have small amounts of assembled actin, with approximately 98% of *T. gondii* actin in its globular G form ((Dobrowolski *et al*., 1997b). Strikingly, apicomplexans lack the actin-related protein complex Arp2/3, one of the main machineries for actin nucleation in eukaryotes (Gordon & Sibley, 2005).

The actin filaments required for host cell invasion and for general parasite motility are believed to be associated with the cytoplasmic tails of adhesins in the parasite plasma membrane. Specifically, MIC2 of *T. gondii* is believed to interact with F-actin through the glycolytic enzyme aldolase-1 (Jewett & Sibley, 2003). Myosin-A, a type XIV myosin, is also critical for gliding motility (Meissner *et al*., 2002). This protein is found in a complex with an atypical myosin light chain (Herm-Gotz *et al*., 2002) and two accessory proteins, GAP45 and the integral membrane glycoprotein GAP50 (Gaskins *et al*., 2004), of which the latter is responsible for anchoring the motor complex in the parasite's IMC.

1.5.2 - The Moving Junction

Host cell invasion starts with the initial attachment of the parasite with its target cell, followed by intimate association between the apical end of the parasite and the host cell (Fig. 5). The parasite then forces entry into a host cell by forming an electron-dense region, visible as a ring of contact between the parasite and host plasma membrane (reviewed in Tyler *et al*., 2011). Referred to as the moving junction, this is a central structure formed during invasion that starts at the apical pole and moves progressively to the posterior end of the parasite as it enters the cell. It serves as a support to propel the parasite into the PV, but is also thought to be involved in the formation and in defining the biochemical composition of the PV membrane (reviewed in Besteiro *et al*., 2011). After complete entry of the parasite, the MJ disappears, the newly formed PV separates from the host cell plasma membrane and the parasite replicates and divides within it (reviewed in Tyler *et al*., 2011).

Experiments for the molecular characterization of the MJ have started quite recently. In *T. gondii,* a macromolecular complex comprising rhoptry neck proteins RON2, RON4, RON5 and RON8 (Alexander *et al*., 2005, Lebrun *et al*., 2005; Besteiro *et al*., 2009; Straub *et al*., 2009) has been identified. These RON proteins are secreted at the apical tip of the parasite and colocalize with the MJ during invasion, exposed on the cytosolic side of the host cell, which implies that they are secreted inside the host cell by the parasite. The micronemal apical membrane antigen 1 (AMA1) is also part of the MJ macromolecular complex, and has been shown to relocalize from micronemes to the parasite surface. Once secreted at the surface of the parasite, AMA1 is a type I integral membrane protein, with a short cytosolic region and the bulk of the protein forming the ectodomain. Being AMA1 a transmembrane protein on the parasite side and RON2 a transmembrane protein on the host cell side, it has been proposed a model where the parasite would be inserting its own receptor (RON2 and associated RON proteins) for AMA1 to create the MJ. This way, the C terminal region of RON2 binds the ectodomain of AMA1 while the N terminal domain lies within the host cytosol. This suggests that RONs (RON 2, RON4, RON5, and RON8) and MICs, although secreted from different organelles, collaborate to establish the MJ (reviewed in Besteiro *et al*., 2011 and in Tyler *et al*., 2011). Altogether, the requirement for AMA1 in host cell invasion is clear, having a role in apical reorientation (Mitchell *et al*., 2004), intimate attachment, rhoptry secretion (Mital *et al*., 2005), formation of the MJ (Alexander *et al*., 2005, Besteiro *et al*., 2009), and intracellular replication (Santos *et al*., 2011).

The MJ is also believed to actively exclude the incorporation of many of the host transmembrane proteins into the PV, functioning as a filter (Mordue *et al*., 1999; Charron &

Sibley, 2004; Straub *et al*., 2009). In general, type I transmembrane proteins and multimeric protein complexes are barred entry at the MJ, while GPI-anchored, acylated, and lipid raft associated proteins flow freely into the nascent parasitophorous vacuole membrane (PVM). This selective removal of host proteins is likely critical for parasite survival, as it is believed to result in the non-fusogenic nature of the PV and the prevention of targeting to host lysosomes (Straub *et al*., 2009).

After establishing the MJ, the parasite pushes itself forward and the invagination of the plasma membrane around the invading parasite results in the formation of the PV. The pinching off of the PVM separates the PV from the host cell plasma membrane; remaining the intracellular parasite enclosed within the PVM in which it spends its intracellular life (reviewed in Peng *et al*., 2011). After invasion, the parasite modifies the PVM, inserting novel proteins derived from its secretory organelles, the rhoptries and the dense granules (reviewed in Joiner & Roos, 2002).

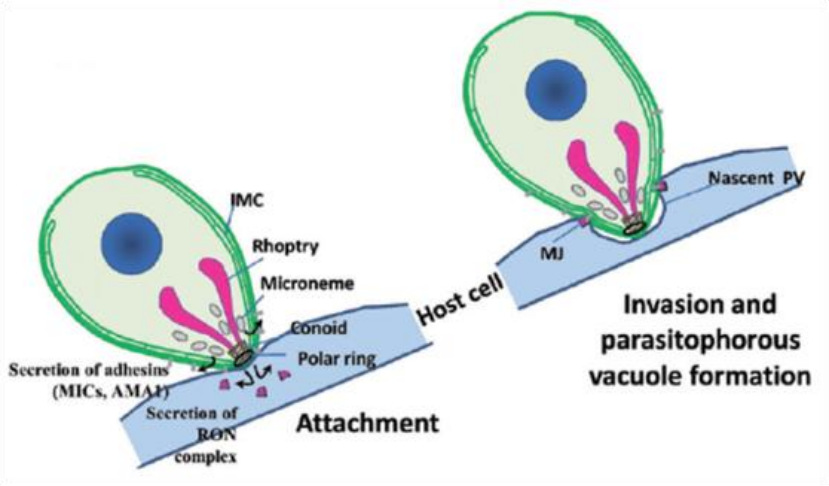

Fig. 5: Initial attachment and invasion steps of an apicomplexan.

The parasite first binds to its host cell using secreted MICs and secretes rhoptry material, including components of the MJ (left). Active penetration of the parasite inside its host cell after MJ formation as the PV forms (right). Adapted from Besteiro *et al*., 2011.

1.5.3 - Cell division

Three distinct replication mechanisms have been described in apicomplexan parasites on the basis of the extent and timing of nuclear division before cytokinesis: these mechanisms are known as endodyogeny (Fig. 6A), schizogony (Fig. 6B) and endopolygeny (Fig. 6D) (reviewed in Francia & Striepen, 2014). Endodyogeny is used by *T. gondii* and *B. besnoiti*. During this mechanism, a single round of DNA replication and nuclear mitosis is followed by the assembly of two daughter cells and cytokinesis. In *T. gondii* endodyogeny there is the

formation of two daughter cells within the mother parasite. These daughter cells are delimited by an inner membrane complex and associated subpellicular MTs, and each contains a complete set of apical organelles (conoid, rhoptries and micronemes), nucleus, mitochondrion, Golgi apparatus, and apicoplast. Once daughter cells are mature, the maternal apical complex is disassembled and the daughter parasites emerge from the maternal plasma membrane (Morrissette & Sibley, 2002a).

The earliest events of cell division in *T. gondii* are extension and fission of the Golgi apparatus and the duplication of the centrosomes (Nishi *et al*., 2008). Also, the pellicle, with the associated subpellicular MTs, is amongst the first structures formed in the new daughter cells, laying down the scaffold for nuclei and organelles to correctly partition into these daughters (reviewed in Anderson-White *et al*., 2012). This way, immediately following centrosome duplication, the first recruitment of molecules associated with the new daughter cell pellicles is seen: Rab11B and IMC15 appear closely associated with the centrosomes shortly after their duplication. Rab11B is implicated in trafficking Golgi-derived vesicles to the developing alveolar sacs of the daughter cell pellicles, and IMC15 is one of the earliest pellicle scaffolding proteins that likely contributes to the coordination of alveolar sac assembly. The assembly of the apical complex is also an early event during cell replication, as a novel *T. gondii* protein, RNG2, located at the apical polar ring, is first recruited to centrosomes immediately after their duplication (reviewed in Anderson-White *et al*., 2012).

It is interesting to refer that in the case of the apicomplexan *Theileria*, replication has unique characteristics, as sporozoites infect leukocytes and reside free in the cytosol, subverting the host division machinery to aid their own propagation, immortalizing these cells and inducing continuous unchecked division (Fig. 6C) (reviewed in Francia & Striepen, 2014).

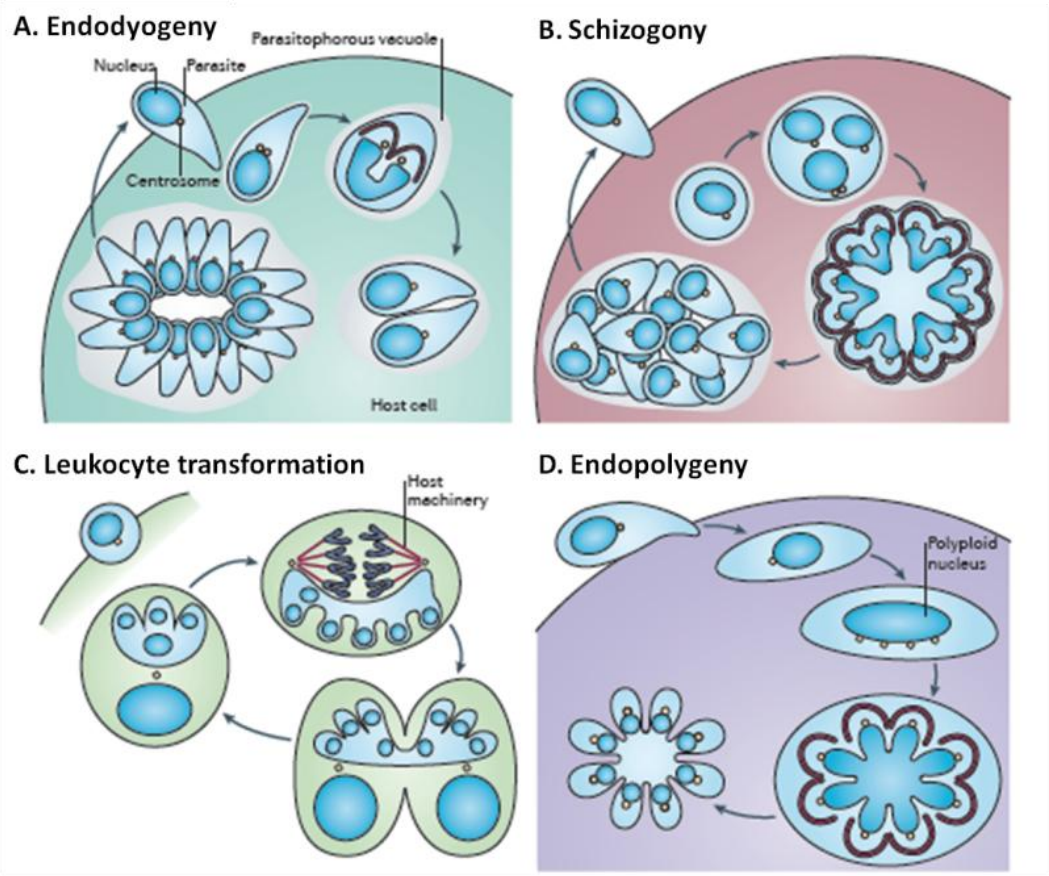

Fig. 6: Replication cycles of different apicomplexan species.

(A) Endodyogeny. Each DNA replication cycle is followed by mitosis and budding. (B) Schizogony. Initially, nuclei multiply by asynchronous rounds of mitosis. The last round is synchronous for all nuclei and coincides with budding at the parasite surface. (C) *Theileria* spp. sporozoites infect leukocytes. The parasite transforms the leukocytes and divides by exploiting the mitotic and cytokinetic machinery of the host. (D) Endopolygeny. DNA replicates without nuclear division, using multiple synchronous mitotic spindles. The final mitotic cycle coincides with budding and the emergence of a new generation of merozoites. Adapted from Francia & Striepen, 2014.

1.5.4 - Egress from the host cell

After tachyzoites multiplication, once the host cell cytoplasm space has been filled with a large PV, and host cell nutrients consumed, the newly formed tachyzoites are programmed to egress and invade neighboring cells to ensure their survival. Egress occurs very quickly, relies on calcium signaling and gliding motility, and it is necessary that the PVM and the host cell plasma membrane to be lysed (reviewed in Frénal & Soldati-Favre, 2009). In *T. gondii*, permeabilization of the PVM has been shown to involve a pore-forming protein named TgPLP1. This perforin-like protein is secreted from the micronemes in a calcium-dependent manner (Kafsack *et al*., 2009). Interestingly, and although to a lesser extent, egress from the

host cell can also occur through a non active mechanism, in which rupture of the host cell membrane would be a consequence of mechanical forces applied on the host cell membrane as the volume of the PV increases upon parasite division (Lavine & Arrizabalaga, 2008).

1.6 - Interaction of *Besnoitia besnoiti* and *Toxoplasma gondii* with their host.

In order to survive inside the host cell, apicomplexan parasites modulate several aspects of the host cell, such as the position of the organelles, metabolism, apoptosis, immune responses, transcription, cell cycle, migration, and the cytoskeleton. Bellow, a resumed description of the main modulations induced by *T. gondii* and *B. besnoiti* is presented. A special importance is given to the modulation of the host cell cytoskeleton, the goal of the present study.

1.6.1 - Nutrient acquisition and recruitment of host cell organelles

All vacuolar pathogens have to scavenge nutrients from their host cells. *T. gondii* modifies PVM permeability by making pores in the PVM, which allows some small molecules (small soluble metabolites (<1300–1900Da) that cannot be synthesized *de novo* by the parasite, to diffuse across the PVM. Examples of these molecules are: glucose, arginine, iron, tryptophan, phospholipids, purine nucleosides, and cofactors that can freely diffuse across the PV and then are presumably pumped into the parasite by membrane transporters (reviewed in Blader & Saeij, 2009).

In contrast to glucose and other small nutrients that passively diffuse across the PV, other nutrients are obtained by more active, parasite-driven mechanisms. For example, *T. gondii* redirects LDL-mediated cholesterol transport to the PV by redirecting host MTs and MT-based transport towards the PV (Coppens *et al*., 2006).

Another strategy to ensure that the parasite has access to host nutrients synthesized in host mitochondria and other organelles, is to relocalize host mitochondria, endoplasmic reticulum (ER), and Golgi apparatus to the PV (Fig. 7). Recruitment of these organelles occurs quickly after a parasite invades a cell (Sinai *et al*., 1997; Coppens *et al*., 2006; Wang *et al*., 2010). It is speculated that host cell mitochondria and ER provide lipids and products of intermediary metabolism to the intracellular parasite, being also a source of new phospholipids that are incorporated into the PVM to ensure the PV enlargement during the process of parasite division (Sinai *et al*., 1997; Coppens *et al*., 2006). In fact, *T. gondii* must acquire serine and choline from the host cell to ensure appropriate synthesis of phosphatidylserine and phosphatidylcholine (Gupta *et al*., 2005). Lipoic acid is used as a cofactor for pyruvate

dehydrogenase in the Kreb's cycle, and is acquired by *T. gondii* by scavenging of the host cell. As lipoic acid exists mainly in the host´s mitochondria, it is tempting to speculate that this at least partly explains the parasite's motivation for anchoring host mitochondria (Crawford *et al*., 2006). Folates and fatty acids can be acquired from the host cells or synthesized *de novo* by *T. gondii* (Quittnat *et al*., 2004; Massimine *et al*., 2005).

The recruitment of these host cell organelles to the PV, seems to be dependent mainly on parasite´s factors, like the rhoptry proteins (ROPs, with ROP 2 acting to recruit mitochondria ((Sinai & Joiner, 2001)) that are injected into the host cell coupled to evacuoles, small vesicles that subsequently fuse with the nascent PV (Hakansson *et al*., 2001). The ROP2 subfamily members ROP4, ROP5, ROP7, ROP8, ROP16 and ROP18 (Fig. 7) have also been shown to associate with the PVM following invasion, suggesting a likely role in host interaction. Furthermore, ROP16 induces STAT3 and STAT6 phosphorylation, required for *T. gondii* successful invasion, since STAT6 is involved in the activation of IL-4 responses such as induction of the expression of anti-apoptotic factors (reviewed in Laliberté & Carruthers, 2008).

In what concerns the ER, the mechanism of ER recruitment is not well understood, but dense granule proteins GRA3 and GRA5 are candidate participants because of their ability to bind an ER integral membrane protein called calcium modulating ligand (CAMLG) (Ahn *et al*., 2006). Supporting this, the dense granule proteins, GRA3, GRA5, GRA7, GRA8 and GRA10, are also localized at the PVM after the invasion of the parasite (Ossorio *et al*., 1994; Lecordier *et al*., 1999; Ahn *et al*., 2005).

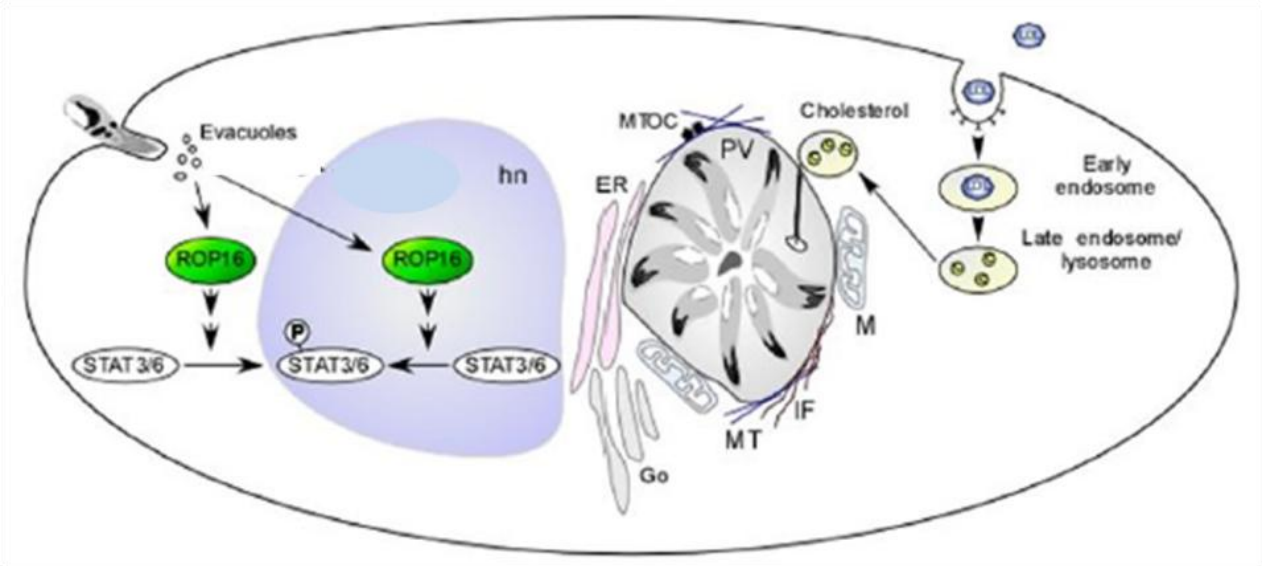

Fig. 7: Reorganization of the host organelles around the PV.

Reorganization of the host mitochondria (M), endoplasmic reticulum (ER), lysosomes, microtubules (MTs), Golgi (Go), microtubule organizing center (MTOC) and intermediate filaments (IF) around the

parasitophorous vacuole (PV) of *T. gondii*. Acquisition of cholesterol via the endocytosis of low density lipoproteins (LDL). Localization of the rhoptry protein ROP16 in the host nucleus (hn) of the host cell soon after invasion. Phosphorylation of the transcription factors STAT3 and STAT6. Adapted from Laliberté & Carruthers, 2008.

1.6.2 - Modulation of the host cell cycle

The most striking example among apicomplexan parasites modulating the host cell cycle is *Theileria*, which transforms its host cells to facilitate replication (reviewed in Dobbelaere & Kuenzi, 2004).

Apparently, *T. gondii* is also able to dysregulate its host's cell cycle: *T. gondii* infection induces human fibroblast monolayers to transit from the G0/G1 to S-phase and remain arrested in the S-phase of the cell cycle (Molestina *et al*., 2008). This transition allows efficient invasion by the parasite, as *T. gondii* has been shown to attach and invade S-phase host cells more readily than cells in other phases of the cell cycle (Lavine & Arrizabalaga, 2009). Interestingly, once inside the host cell, tachyzoites induce the host cell to arrest at the G2/M phase of the cell cycle to enable parasite proliferation (Brunet *et al*., 2008; Molestina *et al*., 2008; reviewed in Peng *et al*., 2011).

Initial characterization of a factor that modulates the host cell cycle during infection indicated that it is a heat-labile factor larger than 10 kDa. This factor was secreted from infected cells and could act on neighboring uninfected cells, which seems like a strategy for *T. gondii* to prepare neighboring cells for infection (Lavine & Arrizabalaga, 2008).

1.6.3 - Modulation of host cell transcription and induction of host cell anti-apoptotic reactions

Experiments indicate that the expression levels of more than 1000 host genes are modulated during *T. gondii* invasion and replication. These genes encode proteins involved in different processes, such as inflammation, apoptosis, metabolism, and cell growth (reviewed in Blader & Saeij, 2009). The migration of the PV towards the nucleus using the host MT network after invasion may facilitate this modulation.

The interference with the host cell apoptosis, extending the life of infected host cells, seems of great importance for *T. gondii* replication and survival until host cell egress. Blocking apoptosis helps the parasite to avoid rapid clearance by macrophages and conserves the integrity of the host cell to obtain nutrients. Interestingly, intracellular bradyzoites also block apoptosis to ensure their survival in the cyst (reviewed in Laliberté & Carruthers, 2008). The

anti-apoptotic mechanisms chosen by *T. gondii*, are mainly through regulating the death receptor (Hippe *et al*., 2008), the nuclear factor kappaB (NF-kB) (Payne *et al*., 2003) and the PI3K pathways (reviewed in Yang *et al*., 2004).

Other apicomplexan parasites, like *Theileria*, also hijack the host NF-kB pathway, dramatically changing the fate of the host cell. This hijacking leads to protection against apoptosis and causes uncontrolled cell proliferation, ensuring a rapid proliferation of the parasitized cells (reviewed in Dobbelaere & Kuenzi, 2004).

Another example of host cell modulation is the fact that following *T. gondii* infection, the host transcription factor hypoxia inducible factor 1 (HIF1α) is induced, as the activity of the HIF1α is important for *T. gondii* growth at physiological oxygen levels (Spear *et al*., 2006).

1.6.4 - Modulation of host cell migration

T. gondii disseminates rapidly from the initial site of infection to secondary lymphoid tissues and then to other tissues (Sumyuen *et al*., 1995). DCs are the key cells that traffic from infected tissues to the spleen and draining lymph nodes, being good candidates for the 'Trojan Horse' that *T. gondii* uses to disseminate. In support of this hypothesis, early *in vitro* studies demonstrated that parasites preferentially infect and replicate inside of monocytes and DCs (Diana *et al*., 2005). Compared to uninfected DCs, infected DCs migrated at higher speeds, for longer distances, and exhibited superior transmigration across endothelial monolayers *in vitro* (Lambert *et al*., 2006). Most importantly, parasitized DCs adoptively transferred to uninfected mice disseminated more quickly than uninfected cells, suggesting an important role of DCs in dissemination of *T. gondii* through the infected animal (Lambert *et al*., 2006). Interestingly, and although induction of cell migration by *T. gondii* is most potent in infected DCs, it is also exhibited by infected macrophages but not by infected lymphocytes. However, it must be considered that it is not certain if an observed transmigration frequency *in vitro* translates to *in vivo* where cytokines, cell-endothelial and cell-matrix interactions will also influence the migration of infected cells (Lambert *et al*., 2010).

Other members of the phylum Apicomplexa closely related to *T. gondii*, for example, *N. caninum*, induce a nearly identical phenotype in DCs (Collantes-Fernandez, *et al*., 2012).

The influence of *T. gondii* in host cell migration has also been address in other cell types, like fibroblasts. In this case a completely different phenotype is observed: parasitized HFFs (human foreskin fibroblasts) were severely impaired in migration in a wound healing assay (Wang *et al*., 2010).

1.6.5 - Modulation of the host cell cytoskeleton during invasion and PV formation

Invasion of *T. gondii* can activate the reorganization of cytoskeleton elements such as actin microfilaments, host IFs and tubulin MTs of the host cell (Coppens *et al*., 2006; da Silva *et al*., 2008; Sweeney *et al*., 2010). In what concerns host actin, *de novo* polymerization is indeed important for the entry of *T. gondii* tachyzoites into host cells. The formation of a host ring-shaped F-actin structure was detected at the MJ, suggesting that a bridge between parasite and host actins is built to provide a solid anchor for pulling the parasite inside the cell. This accumulation of F-actin disappeared within 10 min post entry and up to date there is no evidence of *T. gondii* remodeling host cell actin cytoskeleton post invasion. Besides this, the host Arp2/3 complex was present at the MJ, together with cortactin, a nucleation-promoting factor, which is indicative of a *de novo* polymerization of the host actin induced by the parasite (Gonzalez *et al*., 2009). The same actin accumulation can be seen in *C. parvum* sporozoite invasion, where there is a focal rearrangement and accumulation of host cell actin filaments at the site of infection and initiation of PV formation (Feng *et al*., 2006). It is likely that the changes in the actin microfilaments during *T. gondii* invasion include not only the induction of actin polymerization, but also a local disorganization of the cortical actin network to permit tachyzoite entrance. Considering this, and to overcome the resistance conferred by the host cortical actin, *T. gondii* expresses a protein named toxofilin, which was shown recently to reside in the parasite's rhoptries. Toxofilin caps microfilaments and binds globular actin, making it unavailable for microfilament (re)polymerization (Jan *et al*., 2007). This protein could act as an effector molecule, remodeling the host cytoskeleton, facilitating parasite internalization (reviewed in Frénal & Soldati-Favre, 2009). Moreover, and once again proving the remodeling of the host actin cytoskeleton upon *T. gondii* invasion, it was shown that active parasite invasion of DCs leads to cytoskeletal actin redistribution with loss of adhesive podosome structures and redistribution of integrins (CD18 and CD11c) (Weidner *et al*., 2013).

In *N. caninum* host cell invasion, actin microfilaments were also found consistently associated with the pseudocysts periphery, indicating a physical link between actin filaments and the pseudocyst membrane (reviewed in Hemphill *et al*., 2004).

In *T. gondii*, IF association with the PVM may provide a fortifying scaffold for this organelle and play a role in positioning the PV close to the nucleus. Reorganization from the host nuclear surface to close apposition of the PVM is observed for vimentin IFs during infection (Halonen & Weidner, 1994). Interestingly, in the closely related apicomplexan parasite *N. caninum*, IFs of GFAP (glial fibrillary acidic protein) and actin microfilaments, have been

found in close juxtaposition to the cytoplasmic side of the pseudocyst membrane in rat brain slice cultures (reviewed in Hemphill *et al*., 2004).

In terms of the MT network, upon *T. gondii* invasion, there is a remodeling of the host cell MT cytoskeleton, which is not cell type specific. During parasite attachment and beginning of invasion, host cell MTs localize to the MJ of early invading parasites, shortening the time before parasites initiate host cell invasion (Sweeney *et al*., 2010). After invasion is completed, MTs form a circular basket-like structure that surrounds the PV, where a reorganization of the host MTs is initiated, in close apposition with the PVM and culminating with the PV totally enclosed by a network of host MTs 24 hr post-infection (Melo *et al*., 2001; Coppens *et al*., 2006, da Silva *et al*., 2008; Walker *et al*., 2008; Wang *et al*., 2010).

Such as IFs, MT encasement of the PV could support its structural integrity and juxtanuclear positioning. The stable juxtanuclear positioning of the PV suggests that *T. gondii* uses the microtubular arrays to acquire its defined subcellular position, strategically positioning the PV in proximity to the majority of mammalian organelles, potential reservoirs of nutrients (Coppens *et al*., 2006). In addition, the main host MTOC, the centrosome, is recruited from the nuclear membrane to the PVM (Coppens *et al*., 2006; Wang *et al*., 2010). Functional MTs are necessary for the recruitment of host ER, mitochondria (Sinai *et al*., 1997), and Golgi apparatus, to the PV (Coppens *et al*., 2006; Wang *et al*., 2010). Besides, host MT-based invaginations of the PVM serve as delivery conduits for host lysosomes and endocytic vesicles (Sehgal *et al*., 2005; Coppens *et al*., 2006). These conduits result in a double membrane structure, termed host organelle sequestering tubulo structures or H.O.S.T. The H.O.S.T. delivery system is coated by a dense collar of parasite proteins, including GRA7, which constricts the tubular conduits, thereby sequestering host organelles in the PV lumen, allowing maximal efficient acquisition of nutrients by the intracellular organism (Coppens *et al*., 2006).

The same network has been described in *N. caninum* PV, also containing proteins originating from the dense granule organelles (Hemphill *et al*., 1998; Hemphill *et al*., 2004).

An analog of the H.O.S.T system is present also in erythrocytes infected with *Plasmodium*, with the PVM extending into the host cell cytosol and to the erythrocyte periphery as a network of tubo-vesicular membranes (Haldar *et al*., 2001).

In *B. besnoiti* invasion, there is also a clear interaction with the host cell cytoskeleton, as Mts start to surround the parasite upon the first steps of invasion, originating an Mt web with a cone shape. Adding to this, an Mt ring on the host cell is observable around the parasite entrance site, probably corresponding to the MJ site. On the other hand, *B. besnoiti* invading tachyzoites lose their crescent cell shape and begin to acquire an irregular aspect due to the

appearance of bubble-like small structures on the surface of the parasite. These facts point to an important cross talk of the Mt cytoskeleton of both parasite and host cell in the first steps of invasion (Reis *et al*., 2006).

1.7 - Objectives

B. besnoiti and *T. gondii* are intracellular parasites that have evolved an activate process of host cell entry, an event that requires the reorganization of their cytoskeleton, and that of the host cell. During this process they hijack the host organelles to their advantage. In the last few years, the contributions of host and parasite cytoskeletons during invasion, intracellular replication, and dissemination have been studied for *T. gondii*. Meanwhile, for *B. besnoiti*, studies on the host-parasite interplay, and the manipulation of host cellular mechanisms by the parasite, are at the very beginning.

Therefore, our main goal is to contribute for a better understanding of the processes underlying *B. besnoiti* host cell invasion/infection, using *T. gondii* as a comparison model. Our initial results clearly showed that mammalian cells invasion by *B. besnoiti* involves a cross-talk between the parasite MT cytoskeleton and that of host cell (Reis *et al*., 2006 and present work). To gain new insights about the molecular cellular mechanisms underlying this cross talk we decided to go further, studying the role of the host MT cytoskeleton, centrosome and the intrinsic cell polarity axis in *B. besnoiti* and *T. gondii* host invasion. Moreover, we have put forward the hypothesis that tubulin folding machinery controlling synthesis, degradation, recycling and transport of tubulin, will play a crucial role in MT arrays rearrangement and dynamics, and thus be essential for infection. Our aim was to characterize central components of this via, by cloning the genes and studying their pattern of expression. Specifically we aim to:

- Analyze the host cell MT cytoskeleton remodelling during invasion by *B. besnoiti* and *T. gondii*;

- Investigate the host cell centrosome and Golgi apparatus positioning during invasion by *B. besnoiti* and *T. gondii*;

- Characterize the CCTα-subunit (chaperonin containing TCP-1α) gene, α-tubulin, and TBCB and TBCE genes in *B. besnoiti* and *T. gondii*;

- Determine the intracellular localization of CCTα-subunit in *B. besnoiti* and *T. gondii* in order to see the distribution of the protein inside the parasite;

- Analyze the expression of the CCTα-subunit, α-tubulin, and TBCB and TBCE genes of *B. besnoiti* and *T. gondii* in the course of host cell invasion and parasite replication by real time PCR.

Chapter 2: *Besnoitia besnoiti* and *Toxoplasma gondii*: different strategies to hijack the microtubule cytoskeleleton and Golgi apparatus of the host cell

2.1 - Introduction

As mentioned in the previous chapter, remodeling of the host cell cytoskeleton and recruitment of host cell organelles have already been described during invasion of parasites belonging to the phylum Apicomplexa. Indeed, modulation of the host cell cystoskeleton by apicomplexan parasites is present in *N. caninum* (Hemphill *et al*., 1998; Hemphill *et al*., 2004); *Plasmodium* (Haldar *et al*., 2001); *Theileria* (reviewed in Shaw, 2003); or *E. bovis* (Hermosilla *et al*., 2008) host cell invasion. Also, in *B. besnoiti*, previous results strongly suggest that the Mt cytoskeleton of the host cell has an active role early during invasion, as host Mts surround the parasite in the first moments of invasion (Reis *et al*., 2006). For *T. gondii* infected host cells, the MT cytoskeleton surrounds the PV soon after invasion (Melo *et al*., 2001; Walker *et al*., 2008; Sweeney *et al*., 2010; Wang *et al*., 2010) which is accompanied by the detachment of the centrosome, the major MTOC of mammalian cells, from the nuclear envelope, towards the PV (Coppens *et al*., 2006; Walker *et al*., 2008; Wang *et al*., 2010). Another important feature of *T. gondii* invasion is the strategic positioning of the PV in proximity to the majority of host cell organelles (ER, mitochondrion and Golgi apparatus), potential reservoirs of nutrients (Sinai *et al*., 1997; Coppens *et al*., 2006, Walker *et al*., 2008).

In this context, the following studies were performed to elucidate the role of host MT cytoskeleton, centrosome, and Golgi apparatus during invasion by *B. besnoiti* and *T. gondii*. For this we took profit of our results involving the human TBCC-domain containing 1 (TBCCD1) protein that localizes at the centrosome and is involved in centrosome-nucleus connection. In fact, the knockdown of TBCCD1 causes the dissociation of the centrosome from the nucleus (without affecting Mt-nucleating activity) and disorganization and spreading of the Golgi apparatus throughout the cytoplasm (Gonçalves *et al*., 2010). Therefore, the impact of overexpressing or depleting TBCCD1 from host cells in the ability of *B. besnoiti* to modulate the host MTs, recruit the centrosome, the Golgi apparatus, and invade and replicate in these cells was investigated. The same studies were performed for *T. gondii* to compare the cellular mechanisms used by the two apicomplexan parasites during host cell invasion.

Considering this, an overview of the major features of the MT cytoskeleton and Golgi apparatus of a cell, and their role in cell polarization, is going to be presented, as these components of the host cell were preferentially studied during the course of this work.

2.1.2 - Microtubule Cytoskeleton

The cell cytoskeleton is composed of three different types of fibers: IF, F-actin, and MTs. IFs provide mechanical strength to the cell with many subcellular organelles and macromolecules attached to the network. Actin filaments determine the shape of the cell's surface, their stability, and are involved in cell locomotion. MTs, integrating the MT cytoskeleton, are structures that display enormous plasticity that allows them to intervene in many crucial cellular functions such as cell division, motility, intracellular transport, and various cell signaling pathways.

2.1.2.1 - Microtubules

Microtubules (MTs) are an essential part of the cytoskeleton of the cell, playing a major role in cell migration, intracellular trafficking (serving as tracks for transport of vesicles, organelles, other cytoskeletal elements, protein assemblies and mRNA), control of cell shape, spindle assembly and chromosome motion during mitosis.

They are tubular structures constituted of heterodimers of α-tubulin and β-tubulin, nucleated in organized structures, MTOCs, through interaction with γ-tubulin; with a minus-end capped and anchored at the MTOC, and a plus-end generally localized at the periphery of the cell, forming polarized structures. The α- and β-tubulin heterodimers string together to make long strands – the protofilaments. In general, thirteen protofilaments assemble together forming the hollow, straw-shaped filaments of MTs (Mitchison & Kirschner, 1984).

MTs have a characteristic dynamic behavior, named dynamic instability (Mitchison & Kirschner, 1984): phases of growth, pause and shrinkage, separated by rescue (switch to polymerization) or catastrophe (switch to depolymerization) (reviewed in de Forges *et al.*, 2012). Membrane-bound organelles and trafficking routes use this dynamic instability network to organize and connect intracellular compartments: the nucleus, the ER, the Golgi apparatus and the endosomes/lysosomes. Dynamic instability is also very important to establish and maintain cell polarity during cell migration: inhibition of MT dynamics with nocodazole reduces cell migration into a wound in monolayer cultures (Liao *et al*., 1995). The role of GTP–tubulin in the regulation of MT dynamics has long been known, since the presence of GTP-bound β-tubulin subunits at the MT plus-end (GTP-cap) promotes stabilization of the polymer. Loss of the GTP cap exposes the unstable GDP-bound tubulin core and leads to depolymerization (Mitchison & Kirschner, 1984; Hyman *et al*., 1992). GTP-tubulin was found also in older parts of the polymer, along the MT (GTP-tubulin remnants).

In this case, when depolymerization occurs, they behave as a GTP cap to promote rescue events (Dimitrov *et al*., 2008). Besides this intrinsic regulation (the presence of the GTP-cap and GTP islands), the regulation of MT dynamics depends also of an extrinsic regulation through MAPs that bind to MTs, and through microtubule PTMs.

2.1.2.2 - MAPs: Microtubule-associated proteins

As it was already mentioned, MAPs play a crucial role in extrinsic regulation of MT dynamics. Examples of stabilizing MAPs are *tau*, MAP2 and MAP4. Other MAPs have a destabilizing effect on MTs, either by severing MTs (katanin, spastin and fidgetin (Zhang *et al*., 2007)) or by inducing depolymerization: stathmin binds to free tubulin dimers favoring GTP hydrolysis (Howell *et al*., 1999); the kinesin-13 family triggers catastrophe events (Ems-McClung & Walczak, 2010).

Another important family of MAPs is the plus-end tracking proteins (+TIPs). These +TIPs can mediate interactions with cortical or intracellular structures and have been implicated in signal transduction pathways, regulating MT organization and stability (reviewed in Gundersen *et al*., 2004). Examples of these proteins are:

- CLIP170 (cytoplasmic linker protein), that plays a role in rescue events (Perez *et al*., 1999);
- EB (End-Binding) proteins: dimers of EB1 promote persistent MT growth by suppressing catastrophes *in vitro* (Komarova *et al*., 2009);
- SLAIN2 in mammalian cells and Sentin in *Drosophila* are +TIPs identified as EB-partners (Li *et al*., 2011; van der Vaart *et al*., 2011).

2.1.2.3 - Tubulin post-translational modifications

Tubulin post-translational modifications (PTMs), such as tyrosination, glutamylation, glycylation and acetylation, are also linked to the regulation of MT dynamics. They participate in MT dynamics regulation by recruiting MAPs or by affecting the behavior of motor proteins. These modifications are mostly linked with MT stability (reviewed in de Forges *et al.*, 2012).

Tyrosination of tubulin is carried out by the tubulin-tyrosine ligase that catalyzes the re-addition of a tyrosine at the C-terminal tail of tubulin. The presence of a carboxyterminal tyrosine has a positive effect on MTs by recruiting stabilizing factors and affecting the binding of destabilizing MAPs (reviewed in de Forges *et al.*, 2012).

Glutamylation and glycylation are found in cilia and flagella in mammalian cells; in neurons most MTs are poly-glutamylated (Bonnet *et al*., 2001).
Tubulin acetylation also increases the binding of motors to MTs. This is particularly true for KIF5A, KIF5B/kinesin-1 and dynein in neurons where axonal transport is stimulated (reviewed in de Forges *et al.*, 2012).

2.1.2.4 - The Centrosome

The centrosome has a major role in organizing the MT cytoskeleton in animal cells (MTOC). During interphase, the centrosome organizes an array of MTs that participate in intracellular trafficking, cell motility, cell adhesion and cell polarity. In proliferating mitotic cells, the centrosome duplicates before, or at, the onset of S phase, participating in the assembly and organization of the mitotic spindle (reviewed in Azimzadeh & Bornens, 2007). It is closely associated with the nucleus, and many proteins have been implicated in centrosome perinuclear positioning, such as Zyg-12, Emerin and Samp1 (Malone *et al*., 2003; Salpingidou *et al*., 2007; Buch *et al*., 2009). These are nuclear envelope proteins physically linking the nucleoskeleton and the centrosome. Recently, another centrosomal protein, related with tubulin cofactor C, TBCC-domain containing 1 (TBCCD1), was localized at the centrosome and at the spindle midzone, midbody and basal bodies of primary and motile cilia of human RPE-1 cells (Gonçalves *et al*., 2010). In fact, RPE-1 cells depleted of TBCCD1 did not become confluent, were larger than control cells, and delayed in G1, presenting a lower percentage of assembled primary cilia. It was also observed that TBCCD1 depletion severely affected centrosome localization: instead of the centrosome being located in the cell centre and closely associated with the nucleus, the centrosome was often located at the cell periphery. Interestingly, MTs in TBCCD1-silenced cells were still focused on the misplaced centrosome that was still able to nucleate MTs. In addition, in TBCCD1-silenced cells the Golgi apparatus was disorganized and appeared to follow the centrosome or to be fragmented and spread out in the cytoplasm (Gonçalves *et al*., 2010). Since centrosome and Golgi apparatus positioning are important for cell polarization and directed cell migration (reviewed in Vinogradova *et al*., 2009), live imaging of wound closing shows that human RNAi cells for TBCCD1 are able to close the wound but are delayed compared with the controls. Therefore, all these data suggest that TBCCD1 is a key regulator of centrosome positioning and consequently of internal cell organization (Gonçalves *et al*., 2010).
In terms of structure, the centrosome of animal cells is of a cytoplasmic organelle made of two MT-based cylinders, the centrioles. Each of the two centrioles is oriented perpendicularly

to each other, and is composed of nine MT triplets arranged radially and with a precise symmetry (Piel *et al*., 2000). In animal cells, centrioles can recruit MT nucleating factors, called the pericentriolar material (PCM), which serves as the main MTOC during both interphase and mitosis. Many protein components of the PCM have been identified, but only a subset of these are involved in the function of the centrosome as an MTOC, such as γ-tubulin (Moritz *et al*., 1995; Zheng *et al*., 1995). γ-tubulin forms a complex with members of a conserved protein family, referred to as the γ-tubulin ring complex (γ-TuRC) because of its ring shape (Zheng *et al*., 1995). After nucleation of MTs at the PCM, they are either released into the cytoplasm or recaptured and anchored at the centrosome. The anchoring is associated with only the mother centriole through its sub-distal appendages (Piel *et al*., 2000), and requires ninein (Mogensen *et al*., 2000).

During spindle assembly, MTs are nucleated by the γ-TuRC at the two centrosomes and near the mitotic chromatin, which is in accordance with an increase in the levels of γ-tubulin prior to mitosis. A third nucleation pathway depends on γ-TuRC bound to the sides of existing spindle MTs (reviewed in Lüders & Stearns, 2007).

Centrioles can also move to the cell surface and nucleate the formation of cilia and flagella (transforming into basal bodies), which are important sensory and motile organelles. In post-mitotic cells, the centrosome contains an old, mature centriole called the mother centriole and a young, immature centriole assembled during the previous cell cycle, the daughter centriole, which is about 80% the length of the mother centriole. Only the mature, mother centriole can attach to the plasma membrane and nucleate a cilium or a flagellum behaving as a basal body (reviewed in Azimzadeh & Marshal, 2010).

2.1.2.5 - Non-centrosomal MTOCs

Non centrosomal MTOCs were first identified in higher plants, but are now described in many organisms and cell types. These centers present the same nucleating, anchoring, and stabilization of MTs functions described for the centrosome, with γ-tubulin localizing to all of the noncentrosomal MTOCs. In fact, in the absence of functional γ-tubulin, these MTOCs either do not form or are unable to nucleate and organize MTs (Binarova *et al*., 2006). Several examples of these non centrosomal MTOCs are listed in Table 1.

Structure (organism)	Composition	Properties
Spindle pole body (yeast)	Proteinaceous matrix	γ-tubulin-dependent nucleation of MTs; anchoring of MT minus ends.
Basal bodies (animals)	Proteinaceous matrix	Ends of cytoplasmic MTs bound to electron-dense material at basal foot; presence of γ-tubulin, but nucleation has not been shown.
Cortical membrane (plants)	Membrane	Nucleation of MTs depends on γ-tubulin bound to the sides of existing MTs; anchoring of MTs by lateral interaction.
Cortical basal membrane of polarized epithelial cells (animals)	Membrane	Dynamic MTs; presence of γ-tubulin, but nucleation has not been shown; anchoring of MTs by lateral interaction.
Apical membrane in polarized epithelial cells (animals)	Membrane	γ-tubulin-dependent nucleation of MTs at centrosome; anchoring of MT minus ends at apical membrane.
Nuclear envelope in myotubes (animals); nuclear envelope (plants)	Membrane	γ-tubulin-dependent nucleation of MTs; anchoring of MT minus ends.
Golgi apparatus (animals)	Membrane	Nucleation and anchoring of MTs; presence of γ-tubulin.
Interphase MTOCs at nuclear envelope and along MTs (fission yeast)	Membrane, proteins	γ-tubulin-dependent nucleation of MTs from nuclear envelope or from existing MTs; anchoring of MT minus ends.
Midbody (animals); phragmoplast (plants); equatorial MTOCs (fission yeast)	Proteinaceous matrix	γ-tubulin-dependent nucleation of MTs at cytokinesis; anchoring of MT minus ends.
Mitotic spindle (animals)	Proteinaceous matrix	Non-centrosomal, γ-tubulin-dependent nucleation of MTs; anchoring of MTs by end and lateral interaction.
Mitotic chromosomes (animals)	DNA, proteins	γ-tubulin-dependent nucleation of MTs; capture and anchoring of MT plus ends by kinetochores.

Table 1: Noncentrosomal MTOCs.

Known and potential non centrosomal microtubule organizing centers and their properties. MTOC – microtubule organizing center. Adapted from Lüders & Stearns, 2007.

Considering all these facts, the definition proposed for centrosomal and non centrosomal MTOCs is that they are plastic, often transient, structures that can catalyze γ-tubulin-

dependent MT nucleation and that can anchor MTs by interacting with their minus ends, plus ends or sides (reviewed in Lüders & Stearns, 2007).

An important example of a non centrosomal MTOC is the Golgi apparatus, which nucleates and anchors MTs at its cytoplasmic face, targeting γ-TuRC to *cis* Golgi membranes by interacting with AKAP450, which in turn binds the golgin GM130 (Rivero *et al*., 2009). Involved in this process are also proteins like *trans*-Golgi network (TGN)-associated cytoplasmic linker associated proteins (CLASP), that bind and stabilize the newly assembled MTs (Efimov *et al*., 2007).

2.1.3 - The Golgi apparatus

The Golgi apparatus of mammalian cells is responsible for modification, sorting, and transport of secretory products, lysosomal enzymes, and membrane components. Synthesized proteins are transported from the ER to the Golgi apparatus for posttranslational modifications, sorted into carriers and delivered to the plasma membrane or the endosomal–lysosomal system. During interphase it is composed of stacks of flattened cisterna, tubules, and small vesicles localized around the centrosome. The stacks are linked together by anastomosing branches and a network of tubules and vesicles present on each side of the stacks, usually referred to as the *cis*-Golgi network (CGN - side of materials entry, close to the ER) and the *trans*-Golgi network (TGN - side of materials exit). In mammalian cells, individual Golgi stacks are further linked laterally with equivalent cisternae of different stacks to create a ribbon structure (Tanaka & Fukudome, 1991). During mitosis, the Golgi apparatus breaks down, to reassemble in daughter cells. This change in Golgi apparatus structure is concomitant with a block in secretory trafficking and the reorganization of the MT cytoskeleton. In daughter cells Golgi apparatus membranes fuse and stack into multiple ministacks throughout the cytoplasm that are then transported to the cell center by radial MTs (reviewed in Sütterlin & Colanzi, 2010).

The relation between Golgi apparatus and centrosome is important for specialized functions of mammalian cells, like cell polarization, a prerequisite for cell migration. Cell polarization depends on a reorientation of the Golgi/centrosome in the direction of cell migration, thereby providing membrane and secreted products directly to the most proximate plasma membrane - the leading edge in migrating cells (Bergmann *et al*., 1983). Components of each organelle are able to influence the function of the other organelle (Golgi apparatus and centrosome are functionally linked). There are several proteins identified as functional linkers between the centrosome and Golgi apparatus. For example, centrosome reorientation depends on

phosphorylation of the Golgi apparatus protein GRASP65 (Bisel *et al*., 2008); the Golgi apparatus *cis* protein GM130 affects cell polarization and migration through effects on centrosome organization (Kodani & Sütterlin, 2008); IFT20, required for formation and extension of the cilium, localizes to the Golgi apparatus by binding to the structural Golgi apparatus protein GMAP210 (Follit *et al*., 2006; Follit *et al*., 2008); the putative Golgi apparatus stacking factor GRASP65 (Sütterlin *et al*., 2005), Tankyrase (Chang *et al*., 2005), or the phosphatase Sac1 (Liu *et al*., 2008) are required for correct mitotic spindle formation; AKAP450 (Rivero *et al*., 2009), CAP350 (Hoppeler-Lebel *et al*., 2007), and CDK5Rap2 (Barr *et al*., 2010), are centrosomal proteins associated with the Golgi apparatus whose depletion leads to multipolar spindles and mitotic cell death. AKAP450, whose localization is GM130 dependent, was found to be an essential linker between the centrosome and the Golgi apparatus. This requires the γ-TuRC complex recruited by AKAP450 on Golgi apparatus membranes (Rivero *et al*., 2009).

As for the localization of the Golgi ribbon next to the centrosome, it requires the MT and actin cytoskeleton. Actin fibers detected at the Golgi apparatus are required for the maintenance of its pericentriolar position by providing tracks for actin-based motors myosin-motors moving specifically towards minus or plus ends (reviewed in Brownhill *et al*., 2009). Several myosins, including myosin I/II/V/VI, have been implicated in supporting Golgi apparatus dynamics and vesicle budding from the *trans* Golgi side (reviewed in Allan *et al*., 2002). As for the MT network responsible for pericentriolar Golgi ribbon assembly, it is now known that it contains both centrosomal and Golgi-derived MTs (Vinogradova *et al*., 2012). These two MT arrays present distinct geometries (Efimov *et al*., 2007): the centrosome has a radial MT array; and the Golgi-derived MTs grow tangentially to a stack of origin, usually associated with the *cis* Golgi side, being the direction completely random when stacks are dispersed throughout the cell (Miller *et al*., 2009). In recent work, Vinogradova *et al*, 2012, suggest that the role of the centrosome in Golgi apparatus assembly is to organize a radial array of MTs, bringing Golgi clusters to the cell center; and Golgi-derived MTs are responsible for fusing the ministacks into larger fragments (Hurtado *et al*., 2011). In silico simulations show that lack of either one of the MT arrays leads to the loss of complex polarity associated with integrity disturbance and shape randomization. Neither MT subpopulation alone substitutes the concerted effort of centrosomal and Golgi-derived MTs in the Golgi apparatus assembly: for stack positioning both radial signal and tangential forces are required to bring single stacks together (Vinogradova *et al*., 2012).

The molecular machinery present during Golgi apparatus MTs nucleation has been only partly identified: GM130 - dependent recruitment of the MT nucleation factor AKAP450 to the

Golgi apparatus; GMAP-210 that mediates the interaction between Golgi *cis* side and MTs (Efimov *et al*., 2007; Rivero *et al*., 2009); dynein 1– dynactin activity, that transports the ministacks along the MT network to assemble and form a single complex at the cell center (Vinogradova *et al*., 2012); CLASPs, that are MT plus end–binding proteins essential for the regulation of MT dynamics both in mitotic and interphase cells, and are anchored to the *trans* side via protein GCC185. GCC185 is recruited to the *trans* membranes by two small GTPases, Arl1 and Rab6 (Burguete *et al*., 2008).

The Golgi apparatus is highly asymmetric. While nucleation has been associated with *cis*-Golgi markers (AKAP450), MTs grow from the Golgi apparatus membrane only after being stabilized by *trans*-associated MT regulators (CLASPs), which coat Golgi-derived MTs and thus make them biochemically and dynamically dissimilar from the centrosomal array (Miller *et al*., 2009). Thus, two scenarios are possible during MT nucleation at the Golgi apparatus: 1) concentration of γ-tubulin at the *cis* Golgi membrane provides a pool of MT that later redistribute to *trans* Golgi membrane; or 2) *cis*-Golgi gives rise to multiple unstable MTs, a certain portion of which reaches out the *trans* membrane and is then stabilized by CLASPs (reviewed in Vinogradova *et al*., 2009).

Despite the fact that both Golgi apparatus and centrosome derived MTs are essential for Golgi apparatus assemble and positioning, Vinogradova *et al*., 2012 studies proved that when Golgi apparatus is already positioned in the center of the cell, the centrosome is not needed for Golgi apparatus organization and function. This way, it was proposed that the centrosome supports polarized cell migration indirectly, organizing the Golgi apparatus in a MT-dependent manner; and Golgi apparatus polarity provides asymmetry of the noncentrosomal (Golgi-derived) MT array, which supports trafficking polarity and other asymmetric MT-dependent processes (focal adhesion disassembly, mRNA delivery) (Vinogradova *et al*., 2012).

Interestingly, not all cells need to reorient the Golgi apparatus and the centrosome during cell migration, nonetheless they can move effectively, demonstrating that centrosome behavior depends on cell-substrate adhesion and cell-to-cell interactions (Yvon *et al*., 2002).

2.1.4 - Microtubules and cell polarization during migration

The most important polarity established in «non-polarized» cells is the asymmetry between the center and the periphery of the cell (Fig. 8A). This intracellular asymmetry is established by the MT network. Minus-ends of MTs are in general located at the cell center, bound to a MTOC, and their plus-ends explore the cell periphery. This asymmetry provides an uneven

distribution of signals within a cell, imposing a particular organization of the organelles like the Golgi apparatus, the ER or the endosomes (reviewed in de Forges *et al.*, 2012).

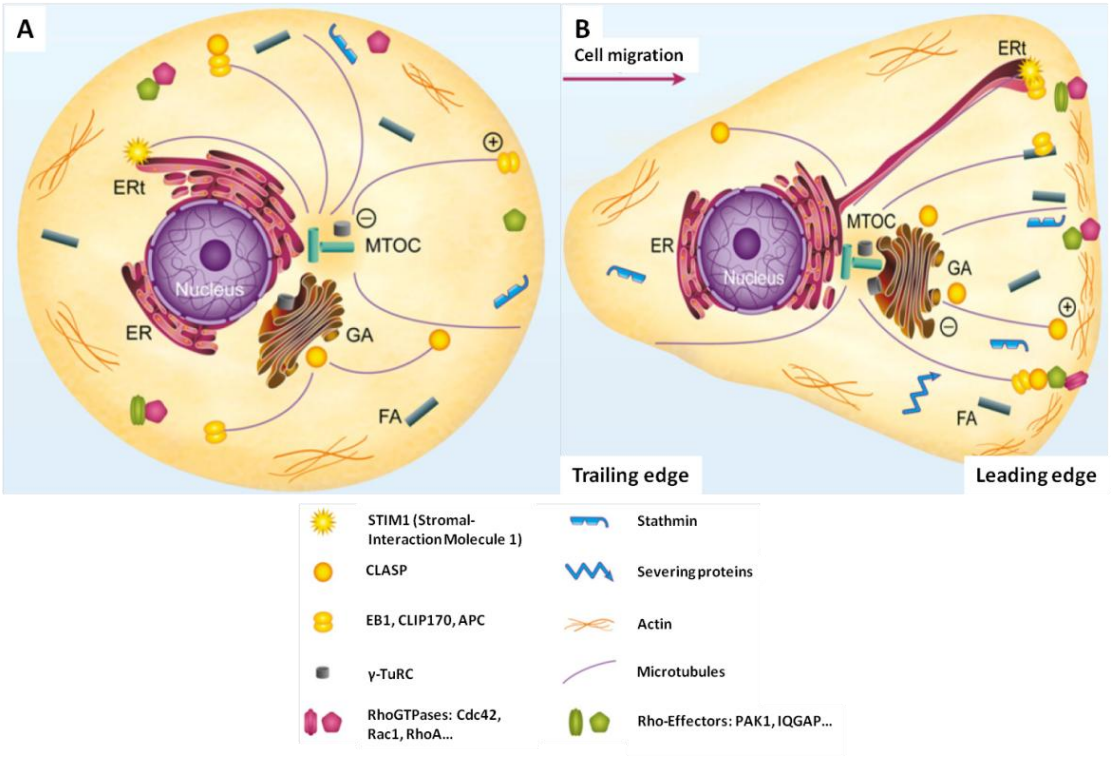

Fig. 8: Intracellular organization of «non-polarized» and polarized cells.
(A) «non-polarized» cell. (B) migrating cell. MTOC, Microtubule Organizing Center; γ-TuRC, γ-tubulin ring complex; ER, endoplasmic reticulum; ERt, endoplasmic reticulum tubule; GA, Golgi apparatus; FA, focal adhesions. Adapted from de Forges *et al.*, 2012.

MT arrays initially produced by the centrosome are radially symmetric. There are four general pathways to break the symmetry of the initial MTs network (Fig. 9) (reviewed in Vinogradova *et al*., 2009):

- Centrosomal MTs array can be modified by differential regulation of MT dynamics at distinct locations: MTs can polymerize at one cell side (rescue) and/or destroyed at the other side (catastrophe);
- MTs can be moved either within the array or after detachment from the array. In this case, the transport of the MTs is driven by molecular motor activity: in many cases motors move MTs that are still attached with their minus ends to the MTOC (in neutrophils, myosin II is capable of bending MTs (Eddy *et al*., 2002)), but they can also relocate MTs that are no longer anchored at their nucleation sites;
- An alternative, non-centrosomal source of MTs can produce an additional asymmetric MT array. An example of this are Golgi apparatus derived MTs;

- Altering the relative positioning of the MTOCs within a cell. For example, during cell migration, the centrosome is relocated to one side of the cell (the leading edge), producing a concentrated MT density at the closest cell edge.

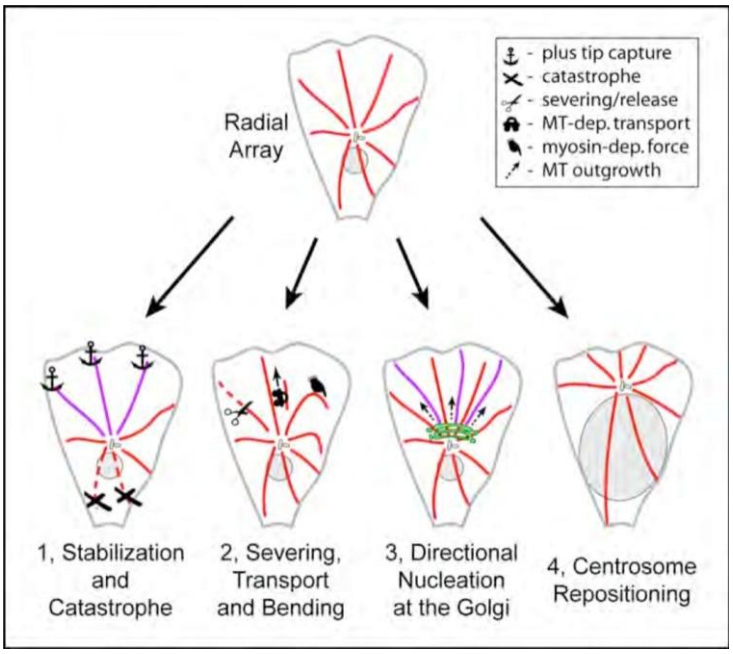

Fig. 9: Principles of MT asymmetry.
Radial array (top) can be transformed into asymmetric network by 1) modulations of MT dynamics, 2) re-positioning of existing MTs, 3) directional MT formation at alternative MT nucleation sites, and 4) repositioning of MTOCs within a cell. Adapted from Vinogradova *et al.*, 2009.

Thus, the polarization of the cell into the leading edge during cell migration imposes an additional axis, a front and a rear of the cell being differentiated, in addition to the center and periphery of «non-polarized» cells (Fig. 8B). Throughout establishment of polarity, the MT network undergoes profound changes and reorientation, along with a whole intracellular reorganization, allowing the formation of a leading edge, with the presence of focal adhesions sites that serve as anchors onto which the cells push or pull themselves in order to migrate. MT dynamics is required to maintain a rapid turnover of focal adhesions, which allows rapid and efficient migration. MTs target focal adhesions that disassemble when MTs depolymerize. This way, a very precise regulation of MT dynamics is necessary at the leading edge, and PTMs of MTs, MAPs and +TIPs play an important role in this regulation (reviewed in de Forges *et al.*, 2012).

MTs have been shown to deliver and control various functional molecules involved in motility, including, integrins to initiate adhesion (Caswell & Norman, 2006), β-actin mRNA (Oleynikov & Singer, 1998) and members of Rho GTPase pathways to organize actin and adhesion rearrangements. Rho-like GTPases are activated by MTs and, in turn, they

participate in the local control of MT dynamics. Three main Rho-like GTPases Rac1, Cdc42 and RhoA, and their effectors, interact with MAPs or +TIPs and participate in MT targeting of focal adhesions (reviewed in Watanabe *et al*., 2005).

Reorientation of the MT array is coupled to the orientation of the Golgi apparatus at the front of the cell. Golgi-derived MTs grow towards the cell leading edge in a polarized manner (Efimov *et al*., 2007). These Golgi-associated MTs have several PTMs, they are highly detyrosinated, acetylated (Thyberg & Moskalewski, 1993) and/or polyglutamylated (Spiliotis *et al*., 2008), properties that can influence MT motors affinity and specificity of these MTs as trafficking routs.

Considering this, during the course of the present work we investigated how *T. gondii* and *B. besnoiti* explore the intrinsic polarity of the host cell, namely trough the manipulation of the host MT cytoskeleton, centrosome, and Golgi apparatus, and the different mechanisms they rely on.

2.2 - Materials and Methods

2.2.1 - Cell culture and parasite culture

In this part of the work the following cell lines were used: Vero (ATCC® CCL81), derived from kidney epithelial cells of an African green monkey; hTERT-RPE-1 (ATCC® CRL-4000), hTERT-RPE-1 centrin-GFP, and hTERT-RPE-1 overexpressing TBCCD1-GFP. The hTERT-RPE-1 is an immortalized cell line of retinal pigment epithelial cells. The cell line hTERT-RPE-1 TBCCD1-GFP stably expresses TBCCD1 protein fused with GFP, whereas hTERT-RPE-1 centrin-GFP stably expresses centrin fused with GFP and it was a kind gift of Dr. Khodjakov, USA.

These cell lines were grown in DMEM/F12 with Glutamax (Invitrogen), supplemented with 10% fetal bovine serum and non-essential amino acids (Invitrogen), maintained in a 37ºC incubator at 5% CO2 in a humid atmosphere, and passaged every 2-3 days, depending on cell confluence.

B. besnoiti Bb1Evora03 strain (Cortes *et al*., 2006b) and *T. gondii* (ME49 strain SAG1-Luciferase-BAG1-GFP, a kind gift from Andrea Crisanti, UK) tachyzoites were grown in Vero cells and maintained in Dulbecco's modified eagle's medium (DMEM) with Glutamax (Invitrogen), supplemented with 10% fetal bovine serum and non-essential amino acids (Invitrogen). Tachyzoites were isolated by collecting the supernatant followed by centrifugation at 770g for 10 min.

2.2.2 - Immunofluorescence

Vero, hTERT-RPE-1, hTERT-RPE-1 centrin-GFP, and hTERT-RPE-1 overexpressing TBCCD1-GFP cells were allowed to adhere to coverslips into the wells of 24-well plates for 12 hours (incubated at 37ºC, 5% CO2). Purified tachyzoites were added at a total amount of 10 parasites for each host cell. Invasion occurred at different time points, depending on the assay, in a 37ºC incubator at 5% CO2.

After incubation, the medium was aspirated from each well, cells were washed with PBS 1x (0,01 M phosphate buffer, 0,0027 M potassium chloride and 0,137 M sodium chloride, pH 7.4), and directly fixed and permeabilized with cold methanol (10 min at -20ºC). Cells were then washed twice with PBS 1x, and once with PBS 1x- Tween 20 0.1% (v/v). Blockage of non-specific background was done with a 3% (m/v) bovine serum albumin solution for 20 min at room temperature. Following blockage, primary antibodies (Table2) were added, and

after 1h of incubation at room temperature, cells were again washed twice with PBS 1x, and once with PBS 1x-Tween 20 0.1% (v/v). We proceeded with the second antibody (Table2) incubation (1h at room temperature) and once more washed the cells twice with PBS 1x, and DNA was stained with DAPI (1 µg/ µl in PBS 1x; Sigma) for 2 min at room temperature. Again, cells were washed with PBS 1x. Finally, coverslips were mounted in mounting medium (MOWIOL 4-88 (Calbiochem) supplemented with 2,5% (m/v) DABCO (Sigma)) and examined under a fluorescence microscope (Leica, DMRA2) equipped with an UV light. Image acquisition was performed with a cooled CCD camera and MetaMorph Imaging Software (Universal Imaging), and images were analyzed with ImageJ software.

Primary antibody	**Host animal in which was produced**	**Dilution used**
anti α-tubulin (Sigma, clone DM1A)	mouse	1:100
anti γ -tubulin (Sigma, clone GTU88)	mouse	1:200
anti-golgin 97 (Molecular Probes, clone CDF4)	mouse	1:200
anti α-tubulin (AbD Serotec, clone YL1/2)	rat	1:250
anti - *B. besnoiti* polyclonal (Marcelino *et al*. 2011)	rabbit	1:5000
anti - *T. gondii* polyclonal (Helga Waap, LNIV)	cat	1:1250
Secondary antibody	**Host animal in which was produced**	**Dilution used**
anti-mouse Alexa 488 (Molecular Probes)	goat	1:500
anti-mouse Alexa 594 (Molecular Probes)	goat	1:500
anti-rabbit Alexa 488 (Molecular Probes)	goat	1:500
anti-rabbit Alexa 594 (Molecular Probes)	goat	1:500
anti-rat Alexa 546 (Molecular Probes)	goat	1:500
anti-cat FITC F-4262 (Sigma)	goat	1:500

Table 2: List of primary and secondary antibodies used in immunofluorescence.

2.2.3 - Transfection of hTERT-RPE-1 and hTERT-RPE-1 centrin-GFP cell lines with small interference RNAs

Cells were transfected using the transfection reagent Oligofectamine 2000 (Invitrogen) and a mixture of four siRNAs (Table3) from Dharmacon (ON-TARGETplus Duplex; Lafayette, CO, USA) and Ambion (Silencer Select siRNAs; Austin, TX, USA) that downregulates the expression of human TBCCD1 gene. Quantities used are detailed in Table 4. The following procedure was used: one day before transfection $2x10^{4}$ cells were plated in 12-well plates; at the time of transfection the transfection reagent was diluted in Optimem (Invitrogen) and incubated for 8min at room temperature; siRNAs were also diluted in Optimem; diluted oligonucleotides were combined with diluted Oligofectamine 2000 and incubated for 20 minutes at room temperature to form stable complexes; growth medium without serum was added to the cells; the mixture Oligofectamine 2000:siRNAs was added to the cells and incubated at 37°C in a CO_2 incubator for 6 hours; after incubation growth medium without serum was replaced with growth medium with 10% serum to stop transfection.
After 54h (for 18h of invasion time), and 66h (for 6h of invasion time) of transfection, purified tachyzoites of *B. besnoiti* and *T. gondii* in the amount of 10 parasites/cell, were added to the transfected cells. The experiment was stopped at 72h of transfection, and coverslips were then processed by immunofluorescence.

siRNA	**Origin**
5’ – GUGGCUUUACUUCGAAAUA - 3’	Dharmacon
5’ – GAGCUAAGAUUGCUUGUAA - 3’	Ambion
5’ – GAUUCAUCGUUGCAACGAA - 3’	Ambion
5’ – CCUUGUGAAUUCUAUGUAU - 3’	Ambion

Table 3: Small interference RNAs sequences.

Number of cells/well (12-well plates)	**Quantity of Oligofectamine**	**Quantity of siRNAs (from stock solution 50µM)**	**Final volume of transfection**
$2x10^{4}$	1,6µl	1µl	500µl

Table 4: Conditions used in transfection.

2.2.4 - Statistical analysis

Statistical analysis was performed using student's t-test and one way ANOVA. The software programs SPSS Statistics version19 and Microsoft Excel 2007 were used.

2.2.5 - Invasion and replication assays

For the replication assay, hTERT-RPE-1 centrin-GFP, hTERT-RPE-1 overexpressing TBCCD1-GFP and hTERT-RPE-1 transfected with siRNA for TBCCD1 cells were allowed to adhere to coverslips into the wells of 24-well plates (incubated at 37ºC, 5% CO2). The quantity of cells in each well was $1,5x10^4$ and purified tachyzoites were added at a total amount of 10 parasites for each host cell ($1,5x10^5$parasite/well). Invasion occurred for 18h in a 37ºC incubator at 5% CO2. After this, all coverslips were processed for immunofluorescence with the polyclonal antibodies against *B. besnoiti* and *T. gondii*. Cells were examined under a fluorescence microscope (Leica, DMRA2), and counted the number of parasites in each vacuole.

For the invasion assay, hTERT-RPE-1 centrin-GFP, hTERT-RPE-1 overexpressing TBCCD1-GFP and hTERT-RPE-1 transfected with siRNA for TBCCD1 cells were allowed to adhere to coverslips into the wells of 24-well plates (incubated at 37ºC, 5% CO2). The quantity of cells in each well was $1,5x10^4$ and purified tachyzoites were added at a total amount of 10 parasites for each host cell ($1,5x10^5$parasite/well). Invasion occurred for 1h in a 37ºC incubator at 5% CO2. After this time each well was washed twice with PBS 1x to eliminate non invaded parasites. Following this procedure, multiplication of the parasites continued for 17h at 37ºC. All coverslips were then processed for immunofluorescence with the polyclonal antibodies against *B. besnoiti* and *T. gondii*. Cells were examined under a fluorescence microscope (Leica, DMRA2), and counted the number of invaded cells *versus* the number of non invaded cells.

2.2.6 - Wound healing assays

hTERT-RPE-1, and hTERT-RPE-1 overexpressing TBCCD1-GFP were grown in glass coverslips ($2,5x10^4$ cells/well in 24 well plates). 12h later these cells were invaded by *B. besnoiti* and *T. gondii*, in the amount of 10parasites/cell, and incubated for 18h at 37 ºC. After 18h of parasite invasion confluent cells were wounded with a 0,1-10µl pipet tip, and live image frames from 120, 360 and 500 min of recovery are shown.

Using the same protocol, live imaging was complemented with data from indirect immunofluorescence. In this case, wound recovery was imaged at 0min, 120min, 240min, and 420min. Cells were stained with the antibodies anti-γ-tubulin (Sigma, clone DM1A), anti-golgin-97 (Molecular Probes, clone CDF4) and the polyclonal antibodies against *B. besnoiti* and *T .gondii*.

2.2.7 - Depolymerization with nocodazole

To address the presence/absence of supranumerary foci of γ-tubulin and other possible nucleation sites for host cell MTs, 1,5x10 ^{4} hTERT-RPE-1 centrin-GFP cells/well were plated in 24-well plates. 12h later, purified tachyzoites of *B. besnoiti* and *T. gondii* in the amount of 10parasites/cell, were added to the cells and incubated for 18h at 37ºC. After 18h of host cell invasion, nocodazole (Sigma) was added to a final concentration of 1µM and incubated for 30 min at 37 ºC. The medium was then aspirated and cells were washed thoroughly with culture medium, and placed in medium without nocodazole at 37 ºC to enable MT repolymerization. Frames were taken at 5min and 15min of MT repolymerization and processed for immunofluorescence in order to see the host cell MTs (α-tubulin) and foci of γ-tubulin.

2.3 - Results

2.3.1 - Host microtubule cytoskeleton is differentially rearranged around the PV of *Besnoitia besnoiti* and *Toxoplasma gondii* during parasite invasion and replication

Previous results strongly suggest that the Mt cytoskeleton of the host cell has an active role during the first steps of *B. besnoiti* host cell invasion, since the host cell Mt cytoskeleton rearranges in order to surround the parasite during cell entrance (Reis *et al*., 2006). Also, for *T. gondii* it was already described that infected host cells form circular, basket-like structures of MTs surrounding the PV as soon as 30min after invasion (Walker *et al*., 2008). To further investigate the involvement of the host MT cytoskeleton during *B. besnoiti* host cell invasion in comparison to what was observed for *T. gondii* invasion, a time course study was performed, by immunofluorescence microscopy. For this, samples of invaded RPE-1 and Vero cells were collected at different time points (15min, 30min, 2h, 6h, 12h, 18h, 24h and 30h post invasion). These invaded cells were then processed for immunofluorescence using a monoclonal antibody against α-tubulin (Fig. 10A, B, C and D), whereas parasites inside the host cells were stained with a polyclonal sera against *B. besnoiti* or *T. gondii*. Host cell MTs around the *B. besnoiti* PV were detected since 15 min of invasion (Fig. 10A and C) suggesting an interaction established early after invasion. As the invasion proceeds and parasites start to replicate, the MTs progressively present a more complex arrangement around the PV (Fig. 10A and C). In fact, as the number of parasites increases inside the PV, the MTs create an alveolus-like structure surrounding each parasite, which finally originates a MT rosette with an organization resembling that of the own parasites inside of the vacuole. These structures are clearly seen at 24 and 30h after invasion (see zoomed detail of 24h and 30h in Fig. 10A and C). The alterations of the host MT cytoskeleton during *B. besnoiti* invasion are slightly different from those observed when host cells are invaded by *T. gondii* (Fig. 10B and D). In fact, and according to what was already described in the literature (Coppens *et al*., 2006; Walker *et al*., 2008), MTs originate a basket-like structure around the PV, but even for longer times of invasion and higher number of parasites inside the PV (see zoomed detail for 24h and 30h in Fig. 10B and D) this MT structure does not show the characteristic alveolar arrangement of the MTs surrounding individual *B. besnoiti* inside the PV. This suggests that throughout invasion, the PV of both apicomplexan parasites interacts with the host MT cytoskeleton, but each of them promote distinct arrangements of these polymers. It is also important to mention that MT rearrangements underlying *B. besnoiti* and *T. gondii* host cell

invasion, and parasite replication, are not a cell-type specific process because they were observed in both Vero (monkey) and RPE-1 (human) cell lines.

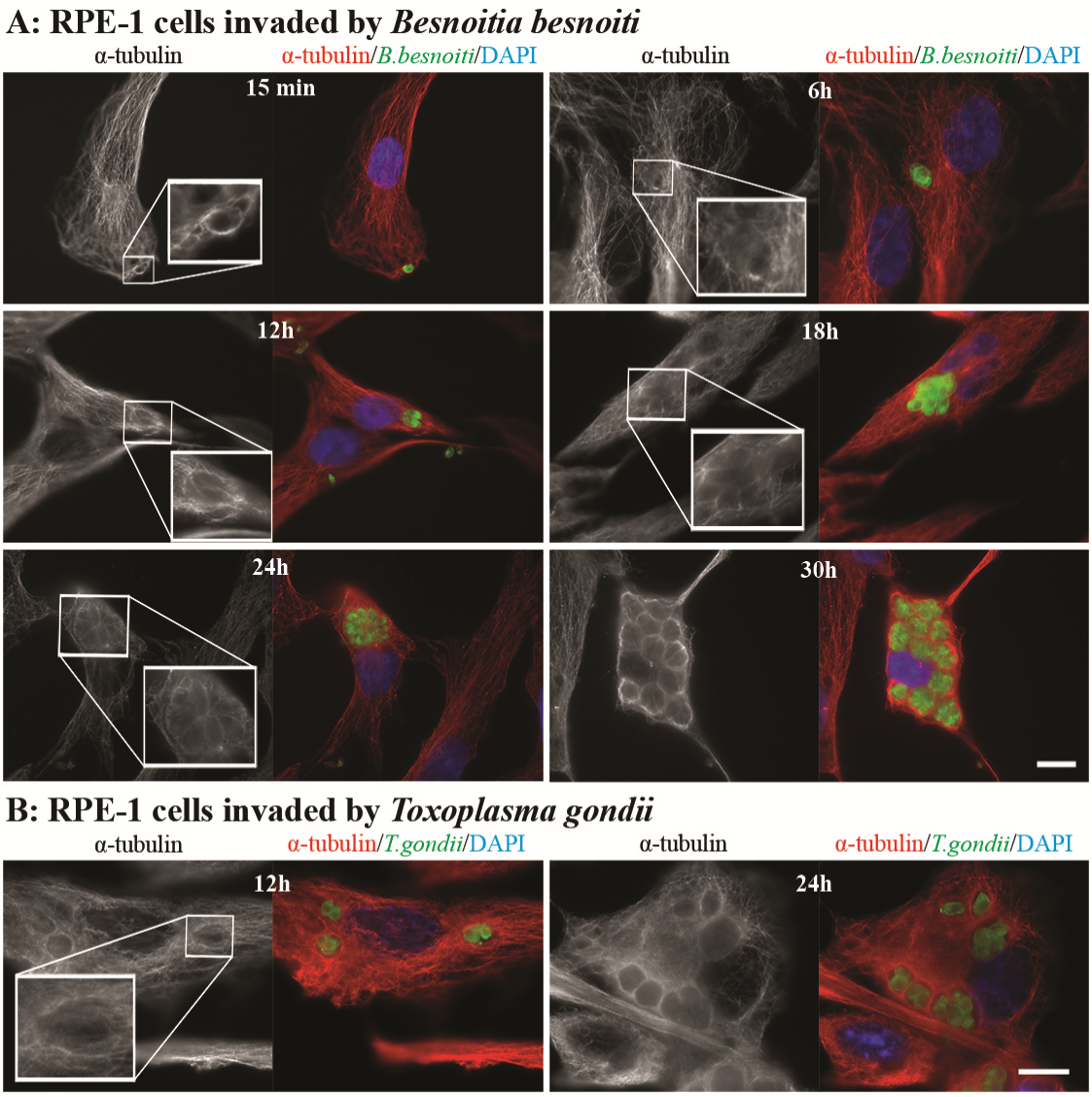

Fig. 10: Host MT cytoskeleton rearrangement around the PV of *B. besnoiti* and *T. gondii*.

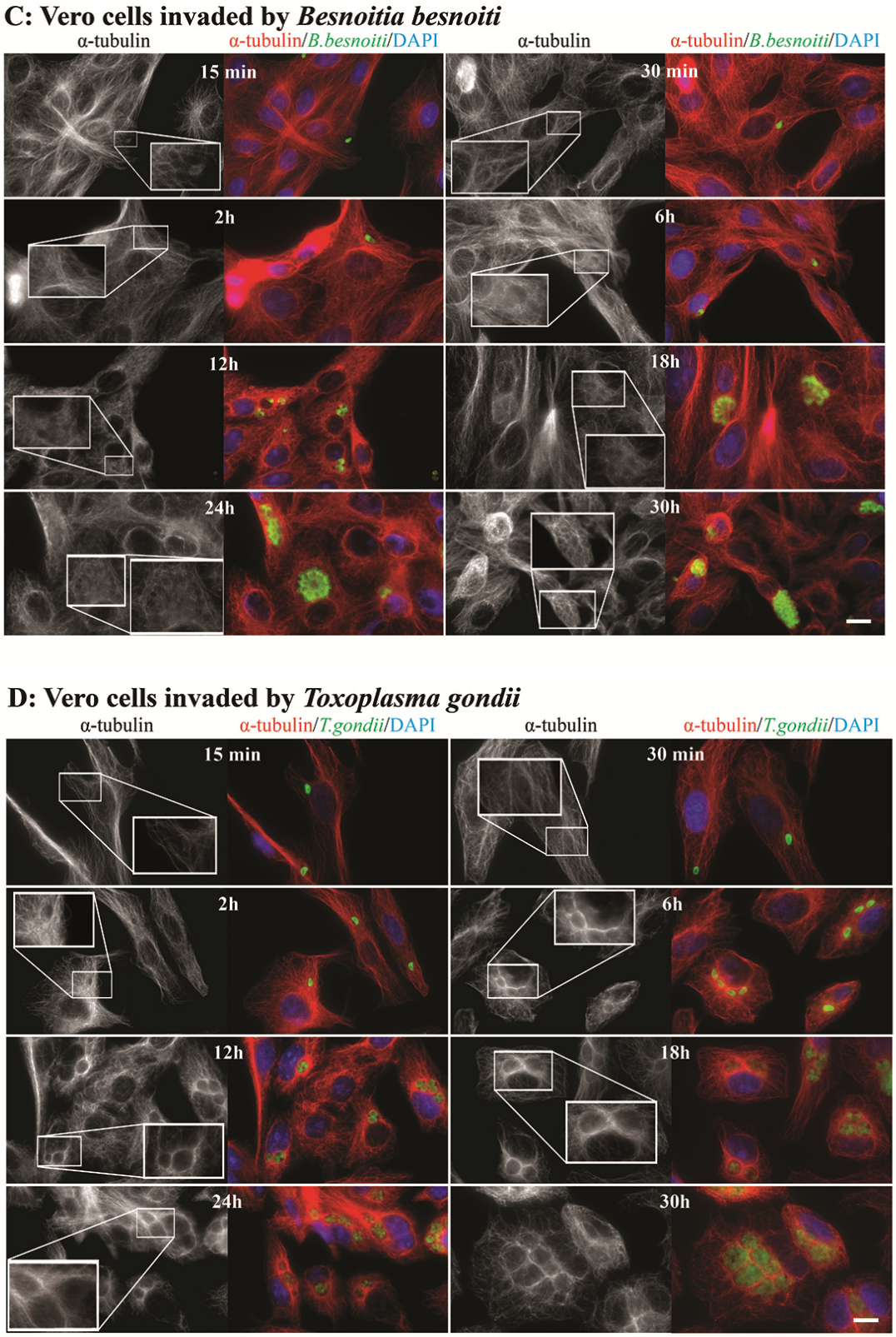

Fig. 10 (continuance). Host MT cytoskeleton rearrangement around the PV of *B. besnoiti* and *T. gondii.*

Indirect immunolocalization of host cell α-tubulin during invasion by *B. besnoiti* and *T. gondii*. Different time points from 15min to 30h of invasion are shown. On the left side, in gray, α-tubulin shows the structure of host cell MTs, and its organization surrounding the PV. Zoomed areas correspond to detailed views of the close interaction between host cell MTs and PVs. On the right side

α-tubulin is shown in red, parasites in green (polyclonal antibodies against *B. besnoiti* and *T. gondii* were used), and blue for DNA staining with DAPI. (A) *B. besnoiti* invading RPE-1 cells. (B) *T. gondii* invading RPE-1 cells. (C) *B. besnoiti* invading Vero cells. (D) *T. gondii* invading Vero cells. Scale bars=7μm.

2.3.2 - Host cell centrosome is recruited by *Toxoplasma gondii* but not by *Besnoitia besnoiti*

The fact that *B. besnoiti* and *T. gondii* host cell invasion and establishment of the PV triggers a response of the host cell MTs surrounding the PV, led to the investigation if the PV membrane has the ability to nucleate/organize MTs, being therefore involved in the remodeling of the host MT cytoskeleton. In fact, previous studies reported that *T. gondii* infection increases the number of γ-tubulin staining foci within the host cell (Walker *et al*., 2008). These foci were described to mainly localize at the PV membrane and were consistent with the normal size of the host MTOC. Due to the differences observed between *T. gondii* and *B. besnoiti* in rearranging the host MT cytoskeleton it was investigated if *B. besnoiti* host cell invasion also originated γ-tubulin foci in the host cell, able to nucleate MTs. For this RPE-1 cells constitutively expressing GFP-centrin, a centriolar marker, were invaded by *B. besnoiti* (Fig. 11A1 and A2) and *T. gondii* (Fig. 11B1 and B2) for 18h, and the host cell MTs were then depolymerized by treating cells with nocodazole (30 μM). After this period, nocodazole was removed by washing the cells with fresh medium and MTs were allowed to recover for 5 min and 15 min in order to localize MT nucleation sites. These cells were processed for IF using a monoclonal antibody against γ-tubulin in order to localize all the sites with ability to nucleate MTs; and with a monoclonal antibody against α-tubulin to label the recovering MT cytoskeleton. Either in the case of *T. gondii* or *B. besnoiti* invaded cells, the described additional foci of γ-tubulin nucleating MTs at the PV membrane (Walker *et al*., 2008), were not observed (Fig. 11).

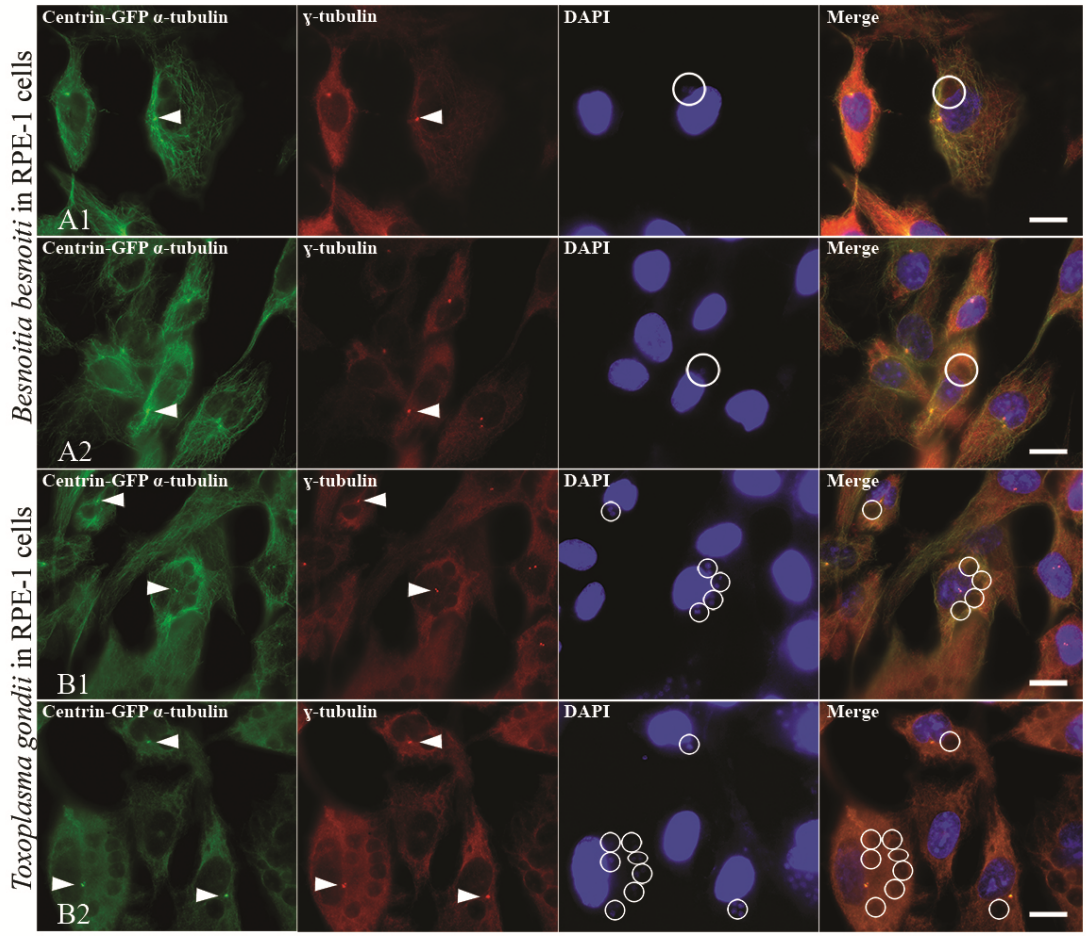

Fig. 11: Investigating the presence of γ-tubulin staining foci additional to the host centrosome in invaded RPE-1 cells by *B. besnoiti* and *T. gondii*.

Indirect immunolocalization of *B. besnoiti* and *T. gondii* in RPE-1 cells at 18h post-invasion and after nocodazole treatment (15min recovery). (A1 and A2) RPE-1 cells invaded with *B. besnoiti*. (B1 and B2) RPE-1 cells invaded with *T. gondii*. Antibodies against γ-tubulin (red) and α-tubulin (green) were used. RPE-1 cells constitutively express centrin-GFP (green). DNA was stained with DAPI (blue). White circles represent the limits of each PV, which can be confirmed by the DAPI staining of the parasites' nuclei. White arrows point to the host cell centrosome, which can be seen either by centrin-GFP (green), or in γ-tubulin staining (red). No other γ-tubulin foci were detected neither in *B. besnoiti* nor in *T. gondii* invaded cells. Scale bars=7µm.

Considering that it was not observed the ability of the PV membrane to recruit γ-tubulin and nucleate/polymerize MTs, but *B. besnoiti* and *T. gondii* invasion caused host MT rearrangements during the first steps of host cell invasion and during PV establishment (Reis *et al.*, 2006; Walker *et al.*, 2008; Sweeney *et al.*, 2010), it was studied the impact of both parasites in the centrosome. In fact, it was conceivable that the manipulation of the centrosome by the parasites could explain the observed MT rearrangements during host invasion. Supporting this hypothesis were the data showing that *T. gondii* invasion promotes

the detachment of the centrosome from the nuclear envelope, which further localizes close to the PV (Coppens *et al*., 2006; Walker *et al*., 2008; Wang *et al*., 2010).

To study the impact of *B. besnoiti* on host cell centrosome, RPE-1 cells were invaded for 6h and 18h and processed by IF using an antibody against γ-tubulin (to allow the identification of the MT nucleating centers, including centrosomes), and the polyclonal antibodies against the parasites. The referred invasion time points were selected due to the fact that they correspond to the stage in which MTs were found to surround a well established PV, but replication of the parasite has not occurred yet (6h, see Fig. 10A and C); and a more advanced stage of MT reorganization, where the MT rosette-like structures start to be evident in *B. besnoiti* invaded cells (18h, see Fig. 10A and C). The obtained results are exemplified in Fig. 12.

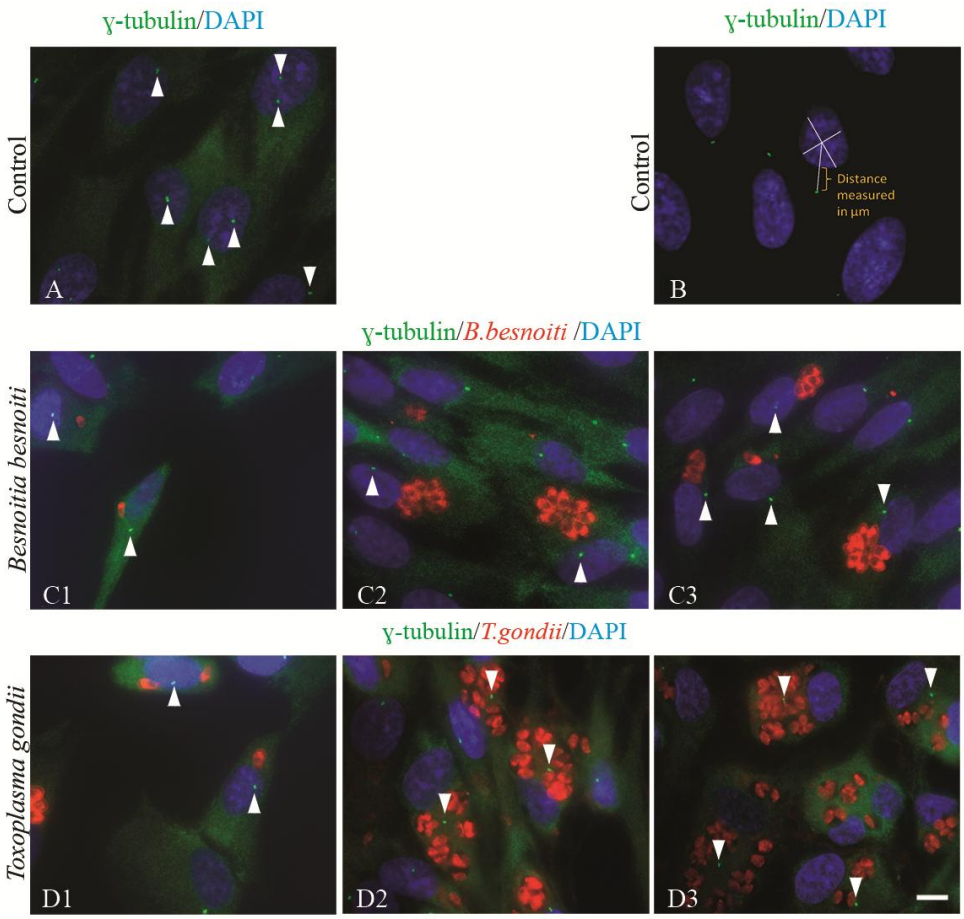

Fig. 12: Host centrosome-nucleus position in RPE-1 host cells invaded with *T. gondii* and *B. besnoiti.* Indirect immunolocalization of *T. gondii* and *B. besnoiti* invading RPE-1 cells. Antibodies against γ-tubulin, *B. besnoiti* (polyclonal antibody), and *T. gondii* (polyclonal antibody) were used. DNA was stained with DAPI. The position of the centrosomes can be seen in green (γ-tubulin staining), in relation to the position of parasites in each PV (red) and host cell nucleus (blue). Arrows indicate the host centrosome positioning. (A) RPE-1 cells, non-invaded control. (B) IF imaging showing how the distance between the host cell nucleus and centrosome was measured using ImageJ software (centrosome-green; nucleus-blue). (C1) *B. besnoiti*, 6h post-invasion. (C2 and C3) *B. besnoiti*, 18h

post-invasion – the position of the centrosome is maintained close to the host cell nucleus. (D1) *T. gondii*, 6h post-invasion. (D2 and D3) *T. gondii*, 18h post-invasion – note the displacement of the centrosomes away from the nuclei and closer to the PVs. Scale bar 7μm.

In comparison with control non invaded RPE-1 cells, RPE-1 cells invaded with *B. besnoiti* for 6h do not present significant alterations, in respect to γ-tubulin staining or altered localization of the centrosomes. In fact, in a series of three independent experiments the number of invaded cells with mislocated centrosomes is similar (about 32±2.6% - Fig. 13A) to the non-invaded RPE-1 cells (30±7.7%). At a later stage (18h post-invasion) there was only a slight increase of mislocated centrosomes (from 30±7.7%, in non-invaded RPE-1 cells, to 40±1.2%, in RPE-1 invaded by *B. besnoiti* - Fig. 13B), and this mislocation represents a slight increase in the average nucleus-centrosome distance, from 2±1.2μm to 2.3±1.7μm, which is not statistically significant (student´s t test; Fig. 13D; measurement exemplified in Fig. 12B). Again γ-tubulin staining was observed only at the centrosomes (Fig. 12). Therefore, and contrary to *T. gondii* (Coppens *et al*., 2006; Walker *et al*., 2008; Wang *et al*., 2010), host cell invasion by *B. besnoiti* does not seem to require any significant alteration of the localization of the host cell centrosome. In this context, and to withdraw any hypothesis that the results obtained for *B. besnoiti* invasion were a consequence of the experimental design, it was investigated if in the same host cell invasion experimental conditions *T. gondii* was able to recruit the centrosome towards the PV. These experiments confirmed that RPE-1 cells at 18h post-invasion with *T. gondii*, present a clear increase of mislocated centrosomes (far from the nucleus - 70±2.8%; Fig.13B), without affecting centrosomal γ-tubulin staining, in comparison to non-invaded RPE-1 cells (control cells; 30±7.7%). Moreover, the distance nucleus-centrosome, increases from 2±1.2μm in RPE-1 non invaded cells to 5±3.2μm (Fig.13D) in invaded cells, being the difference statistically significant (student´s t test $P<0.005$), in agreement with the results described by others (Coppens *et al*., 2006; Walker *et al*., 2008; Wang *et al*., 2010). The analysis of the data obtained for 6h after *T. gondii* host cell invasion (Fig. 13A and C) show that the recruitment of the centrosome by this parasite has not been established yet. In fact, at 6h of invasion, the difference between the nucleus-centrosome distance in non invaded RPE-1 WT cells (1,4±0,8 μm) it is not statistically significant from the distance found in RPE-1 WT cells invaded by *T. gondii* (1,6±1,2μm). This suggests that the phenomenon is more relevant during PV development and parasite replication than in the first steps of invasion. Additionally, the obtained results validate the experimental system for *B. besnoiti*, showing that, despite the fact that both parasites recruit host cell MTs to the PV, only *T. gondii* consistently displaces the centrosome from the host cell nucleus to the PV

membrane. Similar results were observed using Vero cells as host cells (Nolasco, S.; unpublished results)

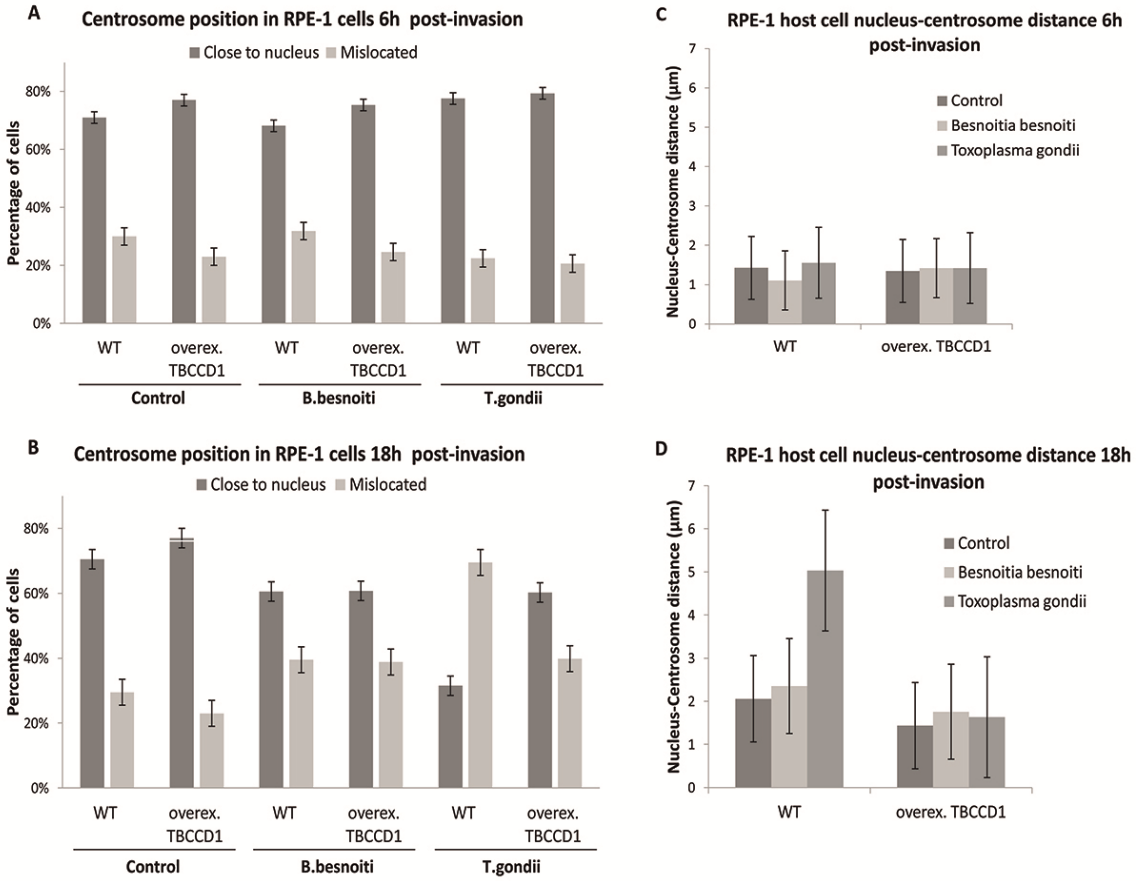

Fig. 13: Centrosome position and nucleus-centrosome distance in RPE-1 cells invaded by *B. besnoiti* and *T. gondii.*

(A and B) Graphics representing the centrosome position in RPE-1 cells invaded by *B. besnoiti* and *T. gondii*. (A) 6h post-invasion. (B) 18h post-invasion. (C and D) Graphics representing the host cell nucleus-centrosome distance in RPE-1 cells and RPE-1 cells overexpressing TBCCD1, invaded by *B. besnoiti* and *T. gondii.* (C) 6h post-invasion. (D) 18h post-invasion. The mean percentage of cells (±sd) with mislocated centrosomes and the mean nucleus-centrosome distance (±sd) in three independent experiments are shown. Total number of cells counted (n): (A) n(control WT) = 354, n(control overexpression TBCCD1) = 314, n(*B. besnoiti* WT) = 230, n(*B. besnoiti* overexpression TBCCD1) = 206, n(*T. gondii* WT) = 285, n(*T. gondii* overexpression TBCCD1) = 248; (B) n(control WT) = 562, n(control overexpression TBCCD1) = 445, n(*B. besnoiti* WT) = 452, n(*B. besnoiti* overexpression TBCCD1) = 350, n(*T. gondii* WT) = 727, n(*T. gondii* overexpression TBCCD1) = 518; (C) n(control WT) = 198, n(control overexpression TBCCD1) = 157, n(*B. besnoiti* WT) = 70, n(*B. besnoiti* overexpression TBCCD1) = 52, n(*T. gondii* WT) = 63, n(*T. gondii* overexpression TBCCD1) = 49; (D) n(control WT) = 307, n(control overexpression TBCCD1) = 199, n(*B. besnoiti* WT) = 87, n(*B. besnoiti* overexpression TBCCD1) = 72, n(*T. gondii* WT) = 270, n(*T. gondii* overexpression TBCCD1) = 95. Statistical significance was calculated using t-test. Scale bar 3µm.

2.3.3 - Golgi apparatus recruitment in RPE-1 cells invaded by *Besnoitia besnoiti* and *Toxoplasma gondii*

It is now well established that centrosome/MTs are involved in the organization and positioning of the pericentrosomal Golgi ribbon (reviewed in Bornens, 2012), and that Golgi apparatus and centrosome are functionally linked (reviewed in Sütterlin & Colanzi, 2010). Also, it was already demonstrated that Golgi membranes are able to nucleate MTs (Efimov *et al*., 2007; Rivero *et al*., 2009).

The fact that only *T. gondii* recruits the centrosome to the PV but both parasites cause the reorganization of the host MT cytoskeleton, gave rise to the hypothesis that this could also be related to different strategies for Golgi apparatus recruitment during host infection. To test this hypothesis RPE-1 and RPE-1 cells constitutively expressing GFP-centrin were invaded for 6h (Fig. 14C1 and D1) and 18h (Fig. 14C2, C3, D2 and D3) by *B. besnoiti* and *T. gondii*. The cells were processed for IF to assess the position and integrity of the Golgi apparatus in relation to the PV. For this it was used a monoclonal antibody against Golgin-97, a Golgi marker, and polyclonal antibodies against *B. besnoiti* and *T. gondii*. The position of the Golgi apparatus in relation to the centrosome was determined through GFP-centrin (Fig 14C1 and D1).

Noteworthy, and contrary to what was observed for the centrosome recruitment, both parasites seem to preferentially establish the PV close to the host cell Golgi apparatus, which was consistently found close/around the PV in invaded RPE-1 cells (Fig. 14). However, a more detailed observation revealed that both parasites differently affect Golgi apparatus organization. *T. gondii* tends to cause fragmentation (the cisternal stacks seem separated from each other) and dispersion of the Golgi apparatus which is in agreement with the data in literature (Coppens *et al*., 2006; Walker *et al*., 2008). On the contrary, the establishment of the PV by *B. besnoiti* parasites close to the Golgi apparatus, in the majority of the cases, does not seem to cause fragmentation/disorganization, but instead to induce Golgi apparatus compaction.

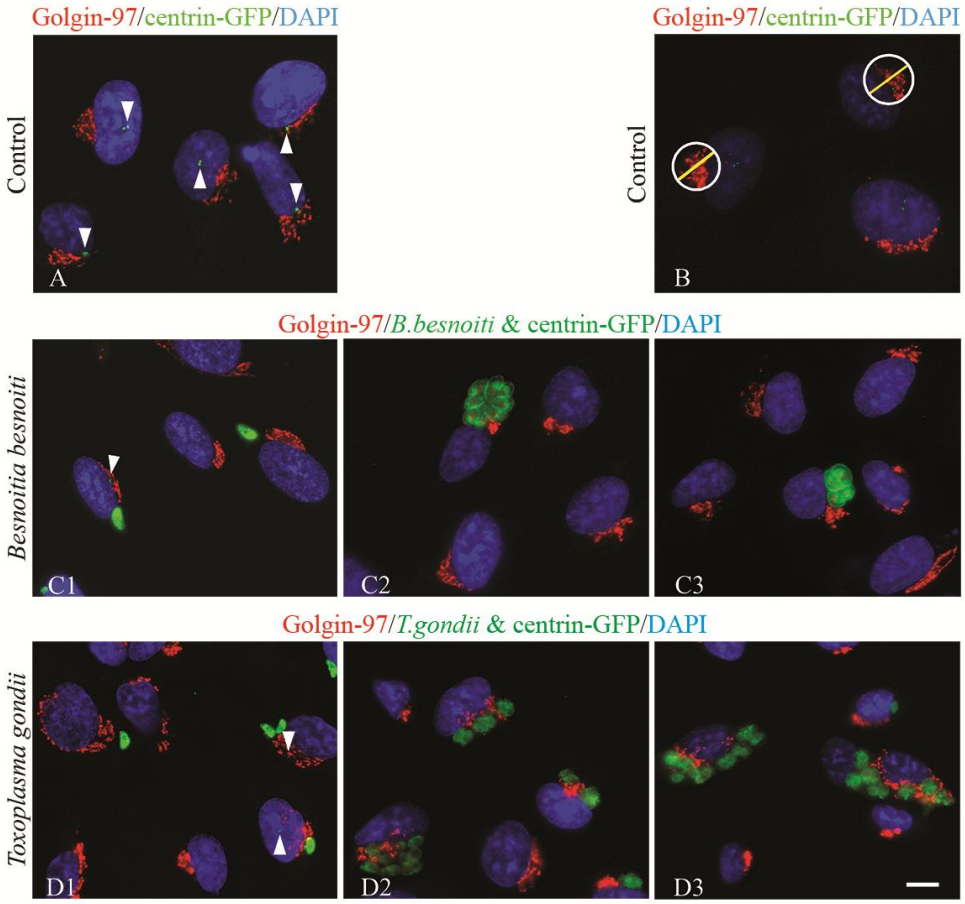

Fig. 14: *B. besnoiti* and *T. gondii* recruit Golgi apparatus in invaded RPE-1 cells.

Indirect immunolocalization of the Golgi apparatus in *B. besnoiti* and *T. gondii* invaded RPE-1 cells. Antibodies used were *B. besnoiti* polyclonal antibody (green), *T. gondii* polyclonal antibody (green) and anti-Golgin 97 (red). DNA was stained with DAPI (blue). (A) RPE-1 cells constitutively expressing centrin-GFP, non-invaded control. (B) IF imaging showing how the measurement of Golgi diameter was performed in non invaded RPE-1 host cells using ImageJ software (Golgi-red; centrosome-green; nucleus-blue). (C1) *B. besnoiti*, 6h post-invasion. (C2 and C3) *B. besnoiti*, 18h post-invasion. (D1) *T. gondii*, 6h post-invasion. (D2 and D3) *T. gondii*, 18h post-invasion. The relative position of the Golgi apparatus to the centrosome can be seen in A, C1, and D1, through centrin-GFP (green-white arrows). In red, Golgi apparatus of the invaded host cells is consistently close and around the PV of both parasites. During *T. gondii* invasion the Golgi ribbon is completely fragmented. Scale bar 7µm.

Indeed, in two independent experiments, at 18h post-invasion by *T. gondii*, 57.1±2.5% of the invaded cells present a fragmented Golgi apparatus (Fig. 15B). On the other hand, only 15.9±4.1% of cells invaded with *B. besnoiti* show a dispersed Golgi (value close to RPE-1 non invaded control cells - 14.8±2.4%; Fig. 15B). To better analyze and quantify these observations the Golgi apparatus diameter was measured as exemplified in Fig. 14B. It was observed that at 18h of invasion the Golgi diameter for cells invaded by *T. gondii*

(11.3±4.9µm; Fig. 15D) was not significantly different from that of non-invaded cells (9.8±4.6µm), while in cells invaded by *B. besnoiti* the Golgi diameter (7.4±3.2µm; Fig. 15D) shows a statistically significant decrease in comparison to the value found in control cells (9.8±4.6µm; one way ANOVA, $P<0.05$).

It is also important to refer that while there is no obvious recruitment of the centrosome by any of the parasites at 6h of invasion (Fig. 12), in what refers to the Golgi apparatus, at 6h of invasion it is already detected in the proximity of the *T. gondii* and *B. besnoiti* PVs (Fig. 14C1 and D1). Also, in the case of *T. gondii*, 33.6±1.6%, of invaded cells already showed a fragmented Golgi apparatus (Fig. 15A).

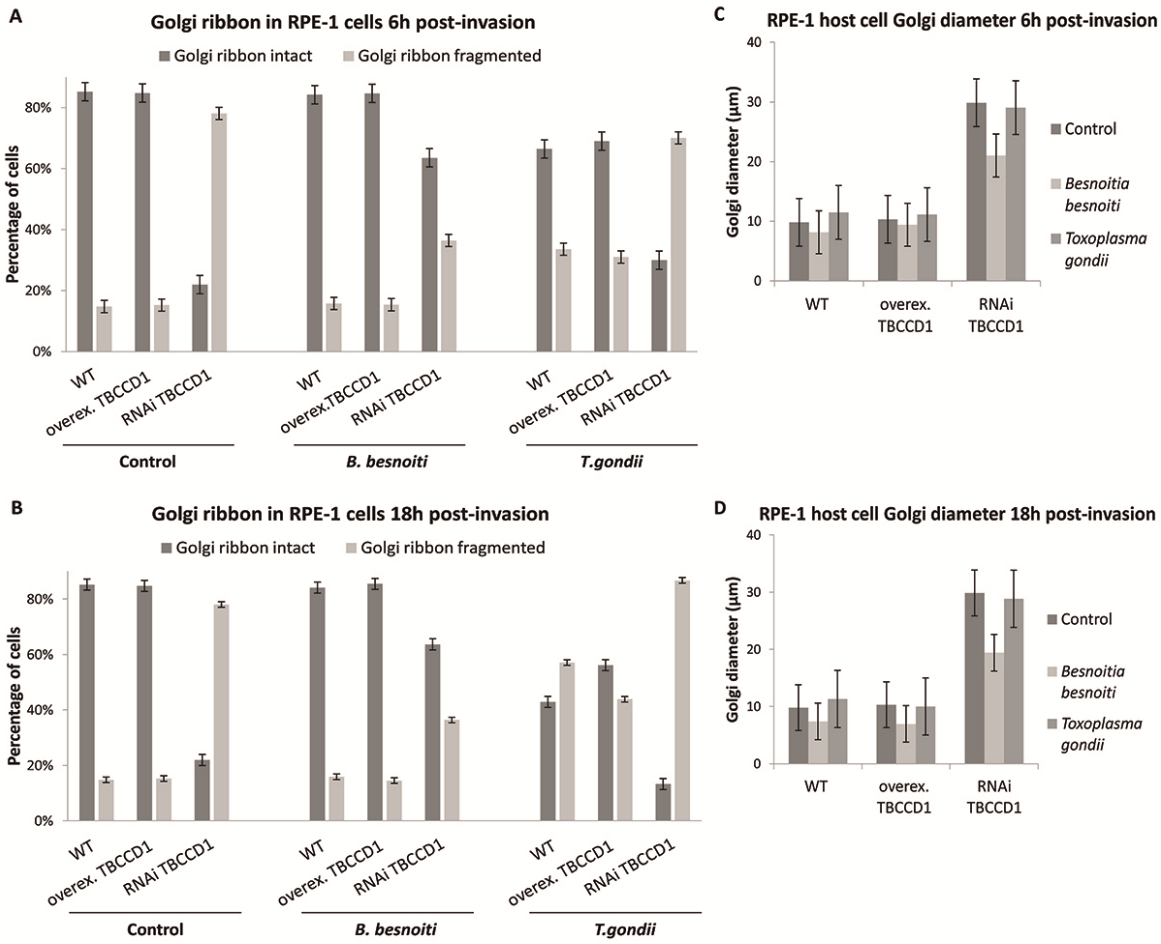

Fig. 15: Golgi ribbon integrity and Golgi diameter in *B. besnoiti* and *T. gondii* invaded RPE-1 cells.
(A and B) Graphics representing Golgi ribbon integrity in *B. besnoiti* and *T. gondii* invaded RPE-1 cells, RPE-1 cells overexpressing TBCCD1-GFP, and RPE-1 cells treated with siRNA TBCCD1. (A) 6h post-invasion. (B) 18h post-invasion. (C and D) Graphics representing Golgi diameter in RPE-1 cells, RPE-1 cells overexpressing TBCCD1-GFP, and RPE-1 cells treated with siRNA TBCCD1 invaded by *B. besnoiti* and *T. gondii*. (C) 6h post-invasion. (D) 18h post-invasion. The mean percentage of cells (±sd) with a fragmented and non-fragmented Golgi, and the mean of Golgi diameter (±sd) in two independent experiments are shown. Total number of cells counted (n): (A)

n(control WT) = 366, n(control overexpression TBCCD1) = 261, n(control RNAi TBCCD1) = 220, n(*B. besnoiti* WT) = 241, n(*B. besnoiti* overexpression TBCCD1) = 196, n(*B. besnoiti* RNAi TBCCD1) = 139, n(*T. gondii* WT) = 283, n(*T. gondii* overexpression TBCCD1) = 278, n(*T. gondii* RNAi TBCCD1) = 163; (B) n(control WT) = 366, n(control overexpression TBCCD1) = 261, n(control RNAi TBCCD1) = 220, n(*B. besnoiti* WT) = 302, n(*B. besnoiti* overexpression TBCCD1) = 257, n(*B. besnoiti* RNAi TBCCD1) = 168, n(*T. gondii* WT) = 298, n(*T. gondii* overexpression TBCCD1) = 253, n(*T. gondii* RNAi TBCCD1) = 233; (C) n(control WT) = 264, n(control overexpression TBCCD1) = 168, n(control RNAi TBCCD1) = 138, n(*B. besnoiti* WT) = 225, n(*B. besnoiti* overexpression TBCCD1) = 144, n(*B. besnoiti* RNAi TBCCD1) = 60, n(*T. gondii* WT) = 250, n(*T. gondii* overexpression TBCCD1) = 205, n(*T. gondii* RNAi TBCCD1) = 68; (D) n(control WT) = 264, n(control overexpression TBCCD1) = 168, n(control RNAi TBCCD1) = 138, n(*B. besnoiti* WT) = 162, n(*B. besnoiti* overexpression TBCCD1) = 149, n(*B. besnoiti* RNAi TBCCD1) = 109, n(*T. gondii* WT) = 168, n(*T. gondii* overexpression TBCCD1) = 153, n(*T. gondii* RNAi TBCCD1) = 117. Statistical significance was calculated using one way ANOVA. Scale bars 5µm.

2.3.4 - The impact of *Besnoitia besnoiti* and *Toxoplasma gondii* invasion on host cell centrosome and Golgi apparatus recruitment in cells depleted of the centrosomal protein TBCCD1

Because both *T. gondii* and *B. besnoiti* parasites recruit the Golgi apparatus during host cell invasion, but only *T. gondii* associates this with the simultaneous recruitment of the centrosome, it was investigated if in this case both events were linked. If this was true, then *B. besnoiti* should have a different mechanism to recruit the Golgi apparatus that does not require the recruitment of the centrosome. For this it was studied the ability of *T. gondii* and *B. besnoiti* to invade and replicate in RPE-1 cells in the background of the depletion of the centrosomal protein TBCCD1. Gonçalves *et al.*, 2010 recently reported that the knockdown of TBCCD1, a protein related to tubulin cofactor C involved in tubulin folding pathway, in RPE-1 cells, causes the displacement of the centrosome from the nucleus and disorganization of the Golgi apparatus. However, the major MT nucleating activity of the centrosome it is not affected by TBCCD1 silencing. Therefore, it was investigated the ability of both parasites to recruit the centrosome and Golgi apparatus in a host cell that already had mispositioned centrosomes and disorganized Golgi apparatus.

As it can be seen in Fig. 16, and despite the misplacement of the centrosome caused by the TBCCD1 siRNA treatment, the PV of *B. besnoiti* is in close association to the nucleus, and continues to be surrounded by host MTs, in a similar way as that observed in invaded RPE-1 WT cells (Fig. 10A).

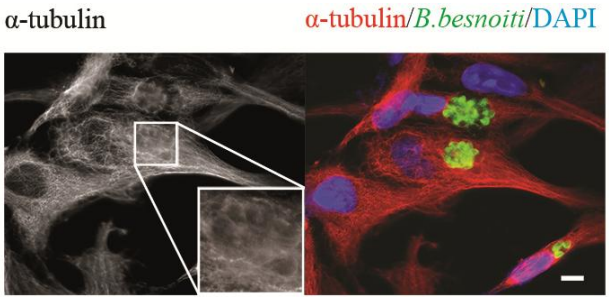

Fig. 16: Indirect immunolocalization of the host cell α-tubulin during invasion by *B. besnoiti* of TBCCD1 depleted RPE-1 cells.

18h post-invasion. On the left side panel, the MTs of an invaded host cell are shown by an antibody against α-tubulin. The zoomed area shows in detail the close interaction of MTs with *B. besnoiti* PV. On the right side panel α-tubulin is shown in red, parasites in green (polyclonal antibody against *B. besnoiti*), and blue for DNA staining with DAPI. Scale bar=7µm.

Additionally no obvious association to the mislocated centrosome was observed (Fig. 17B1, B2 and B3). In the case of *T. gondii* the recruitment of the centrosome is no longer obvious as it was in invaded RPE-1 WT cells (Fig. 17C1, C2 and C3).

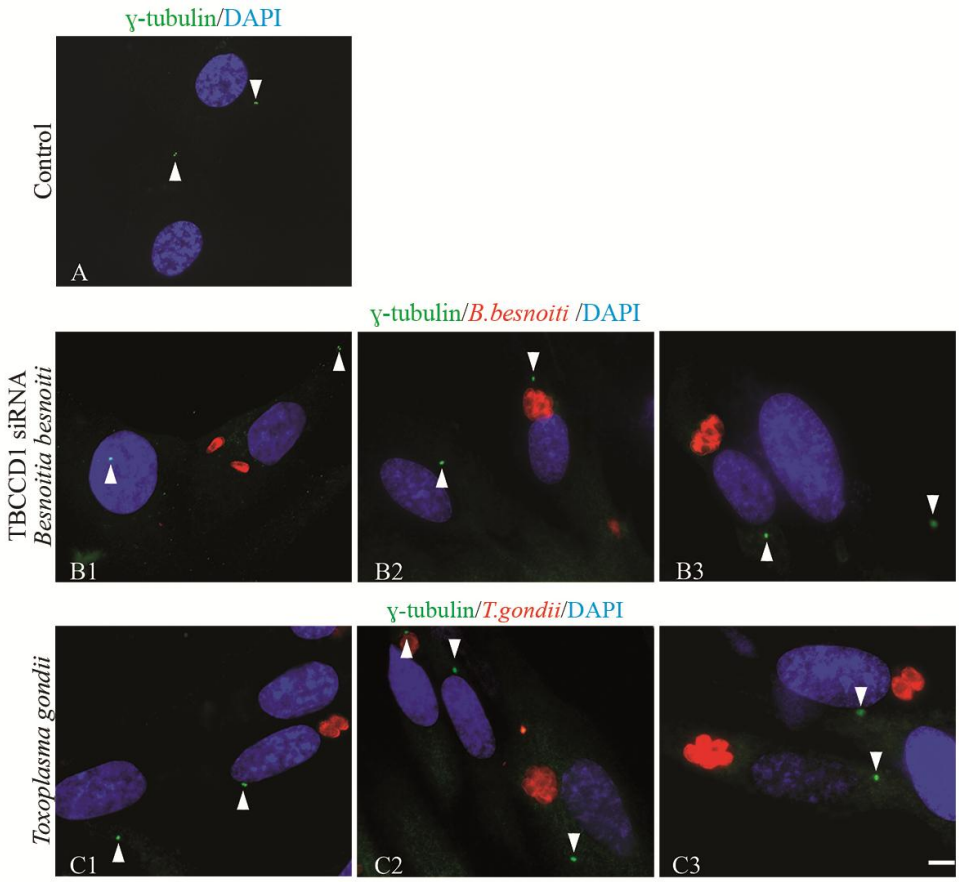

Fig. 17: Mislocated host centrosomes caused by TBCCD1 knockdown are not recruited either by *B. besnoiti* or by *T. gondii*.

Indirect immunolocalization of *T. gondii* and *B. besnoiti* invading TBCCD1 siRNA RPE-1 cells. Antibodies were used against γ-tubulin, *B. besnoiti* (polyclonal antibody), and *T. gondii* (polyclonal

antibody). DNA was stained with DAPI. The position of the centrosomes can be seen in green (γ-tubulin staining – white arrows), in relation to the position of each PV (red) and host cell nucleus (blue). (A) TBCCD1 siRNA RPE-1 cells, non-invaded control. (B1) *B. besnoiti*, 6h post-invasion. (B2 and B3) *B. besnoiti*, 18h post-invasion. (C1) *T. gondii*, 6h post-invasion. (C2 and C3) *T. gondii*, 18h post-invasion. In RPE-1 cells depleted of TBCCD1 the PVs of both parasites are not associated with host cell centrosomes. Scale bar 7µm**.**

Concerning the Golgi apparatus organization and recruitment by the two parasites, it was observed that in TBCCD1 siRNA treated RPE-1 cells invaded for 6h (Fig. 18C and D) and 18h (Fig. 18E, F, G and H) by *B. besnoiti* and *T. gondii*, the PVs are in close association with Golgi elements that sometimes completely surround the PV.

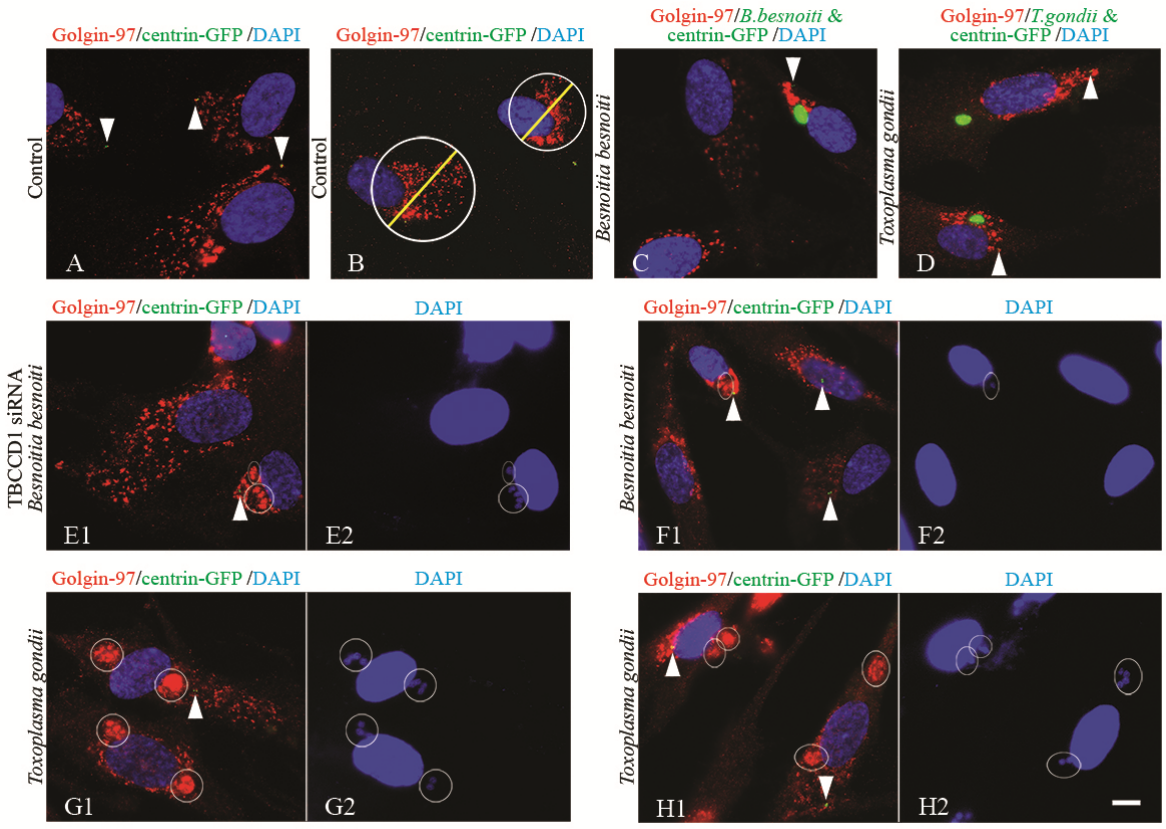

Fig. 18: Golgi apparatus organization in RPE-1 cells depleted of TBCCD1 and invaded by *B. besnoiti* and *T. gondii.*

Indirect immunolocalization of host cell Golgi apparatus in *B. besnoiti* and *T. gondii* invaded TBCCD1 siRNA RPE-1 cells constitutively expressing centrin-GFP. Antibodies used were anti-Golgin 97 (red), *B. besnoiti* polyclonal antibody (in image C-green); and *T. gondii* polyclonal antibody (in image D-green). DNA was stained with DAPI (blue). The relative position of the Golgi apparatus to the centrosome can be determined by centrin-GFP labeling (green – white arrows). In images E1, F1, G1 and H1, white circles represent the limits of each PV, which can be confirmed by the DAPI staining of parasites nuclei on the right image (E2, F2, G2 and H2), and by the red staining of the

parasite Golgi apparatus with anti-Golgin 97. (A) TBCCD1 siRNA RPE-1 cells constitutively expressing GFP-centrin, non-invaded control. In these cells the Golgi ribbon is fragmented and dispersed throughout the cytoplasm. (B) IF imaging showing how the measurement of Golgi diameter was performed in non invaded RPE-1 host cells treated with siRNA TBCCD1 using ImageJ software (Golgi-red; centrosome-green; nucleus-blue). (C) *B. besnoiti*, 6h post-invasion. Golgi apparatus is close to the PV, and shows less fragmentation than in the non-invaded control cells. (D) *T. gondii*, 6h post-invasion. Golgi apparatus is fragmented and close to *T. gondii* PVs. (E and F) *B. besnoiti*, 18h post-invasion. Golgi apparatus of the invaded host cells is consistently more compact (when compared to the control cells, in (A)) and close to the PVs. (G and H) *T. gondii*, 18h post-invasion. Note that Golgi apparatus is completely fragmented throughout the host cell cytoplasm. Scale bar 7μm.

Unexpectedly, in *B. besnoiti* invaded cells, after 18h of invasion, there was an accentuated decrease in the percentage of cells presenting Golgi apparatus fragmentation/dispersion (36.4±1.9%) in comparison to control cells (78.1±4%). These scores were obtained from two independent experiments (Fig. 15B; see Fig. 18B for measurement approach). This is an early phenomenon, as it can already be detected at 6h post-invasion (Fig. 15A). Although in these cells the Golgi diameter is greatly increased since it is dispersed throughout the cytoplasm, at 18h of invasion a statistically significant difference is found (one way ANOVA, $P<0.05$) between Golgi diameter in siRNA non-invaded cells (29.9±7.4μm) and siRNA cells invaded by *B. besnoiti* (19.4±7.3μm). No difference is found in terms of Golgi diameter for TBCCD1 siRNA treated cells invaded by *T. gondii*, neither for 6h of invasion (29±6,8μm; Fig. 15C), nor for 18h of invasion (28.8±7.5μm; Fig. 15D). These results show that, in contrary to what is observed in *T. gondii* invaded cells, *B. besnoiti* invasion causes the compaction of the Golgi apparatus, which is already observable in RPE-1 WT cells (Fig. 14), and becomes more obvious in TBCCD1 siRNA cells. Consequently, *B. besnoiti* invasion seems to rescue Golgi from the disorganization and dispersion provoked by TBCCD1 depletion.

2.3.5 - Host cell centrosome recruitment in RPE-1 cells overexpressing TBCCD1 invaded by *Besnoitia besnoiti* and *Toxoplasma gondii*

Taking into account the role of TBCCD1 in nucleus-centrosome connection, and the results observed during *B. besnoiti and T. gondii* invasion of RPE-1 cells with decreased TBCCD1 levels, it was investigated the ability of the two parasites to recruit the centrosome in RPE-1 overexpressing TBCCD1 at 6h (Fig. 19B1 and C1) and 18h (Fig. 19B2, B3, C2 and C3) of host cell invasion. RPE-1 cells overexpressing TBCCD1 do not present an obvious phenotype

related to centrosome positioning (Fig. 19A). In the case of *B. besnoiti*, in what concerns host centrosome recruitment, the invasion of RPE-1 cells in the background of TBCCD1 overexpression does not significantly differ from that of WT RPE-1 invasion (Fig. 19B1, B2 and B3).

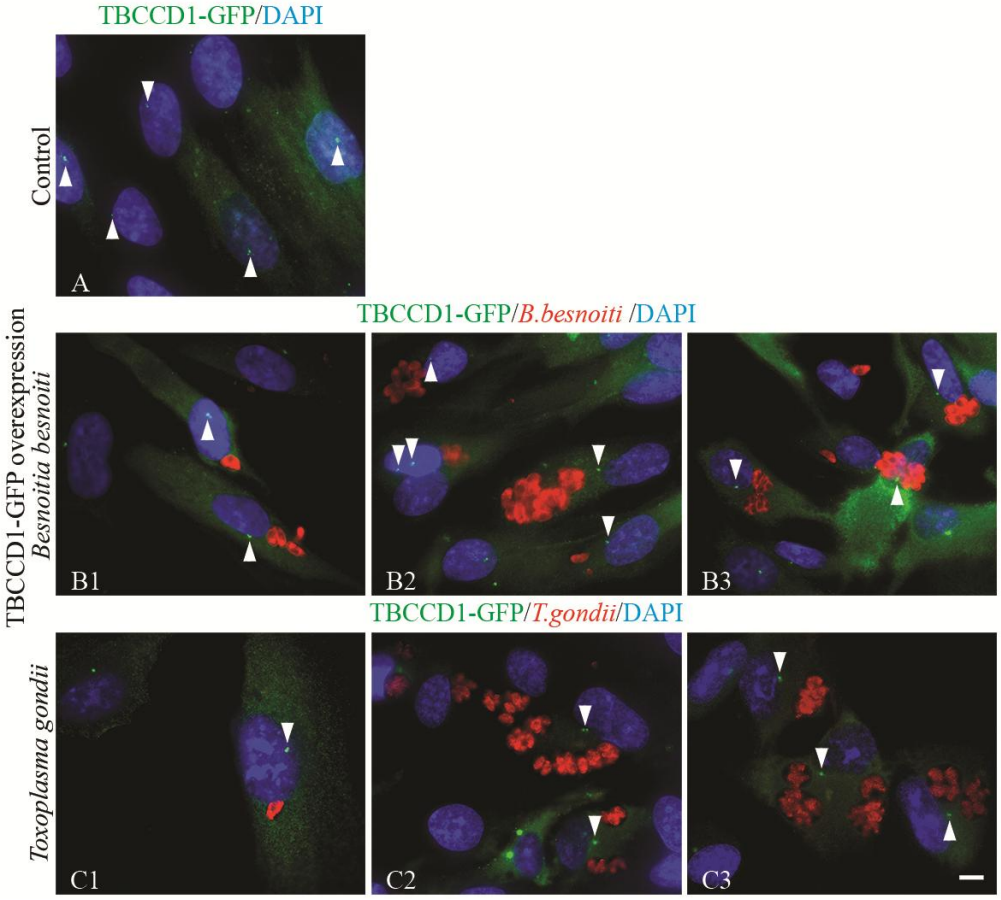

Fig. 19: Host centrosome-nucleus position in RPE-1 host cells overexpressing TBCCD1-GFP invaded with *T. gondii* and *B. besnoiti.*

Indirect immunolocalization of *T. gondii* and *B. besnoiti* invading RPE-1 cells overexpressing TBCCD1-GFP. Antibodies against *B. besnoiti* (polyclonal antibody) and *T. gondii* (polyclonal antibody) were used. DNA was stained with DAPI. The position of the centrosomes is identified by TBCCD1-GFP (green – white arrows), in relation to the position of each PV (red) and host cell nucleus (blue). (A) RPE-1 cells, non-invaded control. (B1) *B. besnoiti*, 6h post-invasion. (B2 and B3) *B. besnoiti*, 18h post-invasion. (C1) *T. gondii*, 6h post-invasion. (C2 and C3) *T. gondii*, 18h post-invasion. Scale bar 7μm.

In fact, in three independent experiments, there is only a small increase of mislocated centrosomes, at 18h of host cell invasion, from 23±12% in non-invaded RPE-1 cells overexpressing TBCCD1, to 39±12% when these cells are invaded by *B. besnoiti* (Fig. 13B). As for the distance between the nucleus and the mislocated centrosomes at 18h of invasion,

the difference is not statistically significant (student´s t test), from 1.4±0.8μm in non-invaded cells to 1.7±1μm in invaded cells (Fig. 13D).

Interestingly, after 18h of invasion, the distance between the nucleus and mislocated centrosomes in *T. gondii* invaded RPE-1 cells overexpressing TBCCD1 (1.6±1.2μm; Fig. 13D), is reduced in comparison to that measured in WT invaded RPE-1 cells (5±3.2μm; Fig. 13D), and the value is much similar to that found in RPE-1 WT non-invaded cells (2.1±1.3μm). Additionally, the proportion of *T. gondii* invaded RPE-1 cells overexpressing TBCCD1 presenting mislocation of the centrosome decreases to 40±8.2% (Fig. 13B), in comparison to the percentage values found in RPE-1 WT cells invaded for the same period of time (70±2.8%; Fig. 13B). These results show that *T. gondii* parasites have a higher difficulty in recruiting the host cell centrosome in RPE-1 cells overexpressing TBCCD1 than in RPE-1 WT cells. This suggests that normally *T. gondii* directly/indirectly manipulates the host cell system of factors involved in centrosome-nucleus connection, as for example TBCCD1.

2.3.6 - Golgi apparatus recruitment and organization in RPE-1 cells overexpressing TBCCD1 invaded by *Besnoitia besnoiti* and *Toxoplasma gondii*

The overall appearance of Golgi apparatus in RPE-1 cells overexpressing TBCCD1 (Fig. 20A) is similar to that of RPE-1 WT cells (Fig. 14A). However, since *T. gondii* has an increased difficulty in recruiting the centrosome in these cells, it was interesting to investigate if this would also reflect any differences in the relationship between the Golgi apparatus organization and localization, and the PV, in comparison to RPE-1 WT invaded cells. Thus, RPE-1 cells overexpressing TBCCD1 were invaded with *T. gondii* and *B. besnoiti*, and the invasion was stopped at 6h (Fig. 20B1 and C1) and 18h (Fig. 20B2, B3, C2 and C3). Comparing Fig. 14 and Fig. 20 it is clear that overexpressing TBCCD1 does not cause any difference in Golgi apparatus recruitment by *T. gondii* or by *B. besnoiti*.

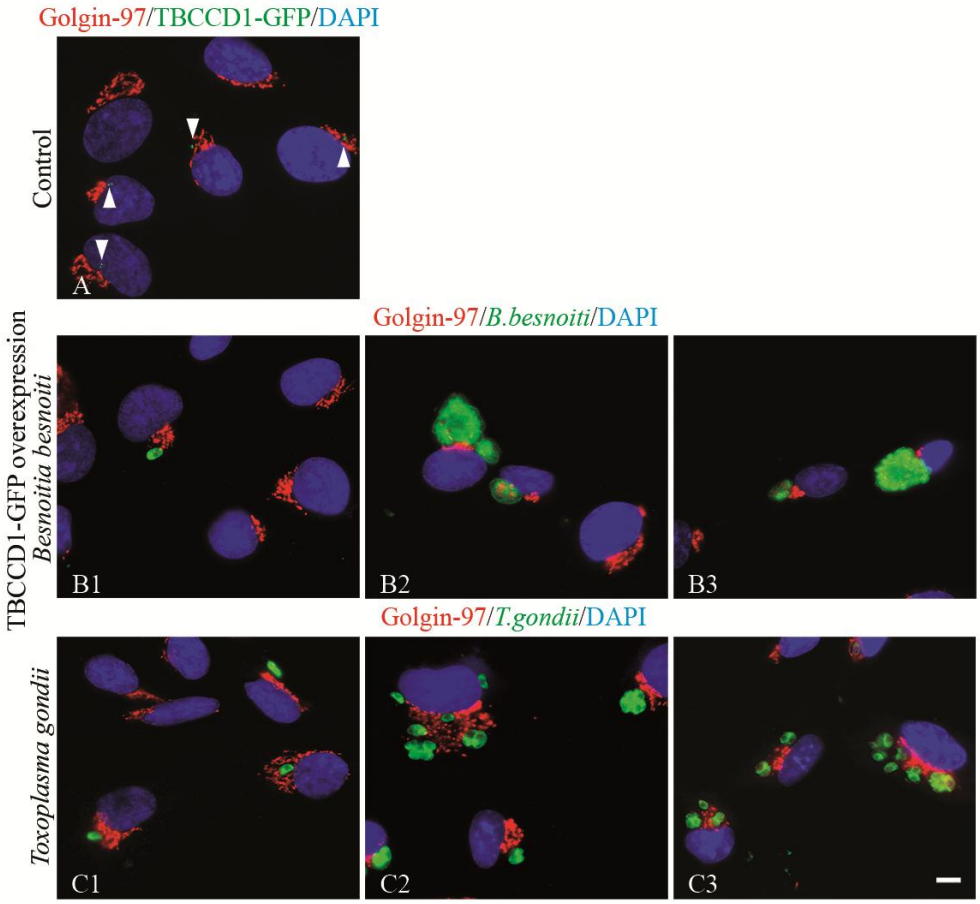

Fig. 20: Golgi apparatus organization in RPE-1 cells overexpressing TBCCD1-GFP and invaded by *B. besnoiti* and *T. gondii*.

Indirect immunolocalization of the Golgi apparatus in *B. besnoiti* and *T. gondii* invaded RPE-1 cells overexpressing TBCCD1-GFP. Antibodies used were *B. besnoiti* polyclonal antibody (green), *T. gondii* polyclonal antibody (green), and anti-Golgin 97 (red). DNA was stained with DAPI (blue). (A) RPE-1 cells overexpressing TBCCD1-GFP (green-white arrows), non-invaded control. (B1) *B. besnoiti*, 6h post-invasion. (B2 and B3) *B. besnoiti*, 18h post-invasion. (C1) *T. gondii*, 6h post-invasion. (C2 and C3) *T. gondii*, 18h post-invasion. In red, Golgi apparatus of the invaded host cells is consistently close and around the PV of both parasites. In *B. besnoiti* invaded cells, the Golgi ribbon seems to be more compact, whereas in *T. gondii* invasion is fragmented, when compared to non-invaded cells. Scale bar 7μm.

In a series of two independent experiments it was noticed that at 18h of invasion by *T. gondii*, RPE-1 cells overexpressing TBCCD1 present 43.9±4.1% (Fig. 15B) of the invaded cells with a fragmented Golgi apparatus, in comparison to the 57.1±2.5% (Fig. 15B) of the invaded cells with a fragmented Golgi apparatus in WT RPE-1 cells, and the non-invaded RPE-1 cells overexpressing TBCCD1 (15 ±2.5%; Fig. 15B). The observed small decrease in the percentage of *T. gondii* invaded RPE-1 cells overexpressing TBCCD1 that contain a fragmented Golgi apparatus, may be related with a more stable pericentrosomal region

provided by higher levels of TBCCD1. In the case of RPE-1 cells overexpressing TBCCD1 invaded by *B. besnoiti*, a percentage of 14.5±3.7%, similar to that in non-invaded RPE-1 cells overexpressing TBCCD1 (15.2±2.5%), and to that in invaded RPE-1 WT (15.9±4.1%), was found (Fig. 15B).

The Golgi diameter parameter was also evaluated in the background of TBCCD1 overexpression during invasion by both parasites. In RPE-1 cells overexpressing TBCCD1, in two independent experiments, at 18h, cells invaded by *B. besnoiti* have a statistically significant decrease in Golgi apparatus diameter (6.9±3μm; Fig. 15D), when compared with non-invaded cells overexpressing TBCCD1 (10.3±4μm; one way ANOVA, $P<0.05$). In the case of cells invaded by *T. gondii* the Golgi apparatus diameter does not differ (10±4μm) from that of non-invaded cells (10.3±4μm; Fig. 15D).

2.3.7 - *Besnoitia besnoiti* and *Toxoplasma gondii* have different outcomes in invasion and replication assays

The results mentioned above for centrosome and Golgi apparatus recruitment show that *B. besnoiti* and *T. gondii* parasites control different host molecular pathways during the establishment of invasion.

Therefore it was investigated if the different strategies of host cell manipulation would be reflected in different outcomes in invasion and replication assays in RPE-1 WT cells, RPE-1 cells depleted of TBCCD1, and RPE-1 cells overexpressing TBCCD1.

Noteworthy, the mispositioning of the centrosome in RPE-1 cells depleted of TBCCD1, doesn´t affect the efficiency of invasion, nor replication, of *B. besnoiti* and *T. gondii*, as showed by the results of a series of two independent invasion and replication assays (Fig. 21A and Fig. 22A and B).

It was also observed that *B. besnoiti* shows similar rates of invasion and replication in WT and overexpressing TBCCD1 RPE-1 cell lines (Fig. 21B and Fig. 22C).

However, differences were detected in the ability of *T. gondii* to replicate in RPE-1 cells overexpressing TBCCD1 (Fig. 22D). In these cells *T. gondii* replication is delayed when compared to WT RPE-1 cells. This observation indicates that *T. gondii* replication requires an efficient recruitment of the host cell centrosome, and that it is able to manipulate the molecular mechanisms involved in the nucleus-centrosome connection. In the case of the invasion assay, no significant differences were found between *T. gondii* invasion of RPE-1 WT cells and RPE-1 cells overexpressing TBCCD1 (Fig. 21B).

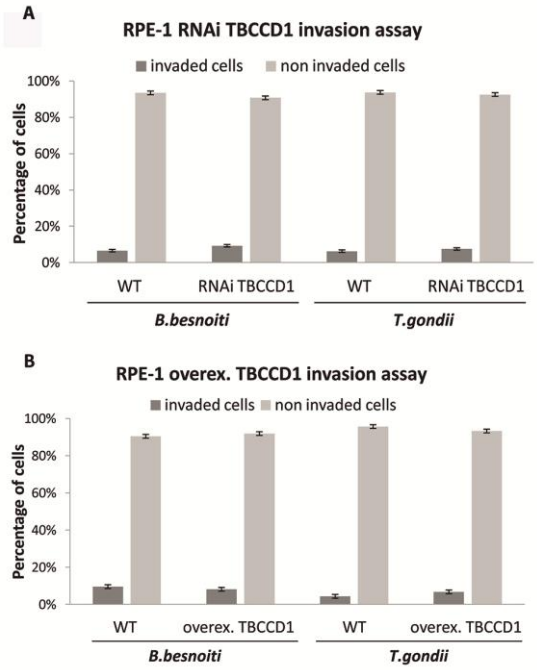

Fig. 21: Invasion assays.

(A) Graphic representing *B. besnoiti* and *T. gondii* invasion assays in cells RPE-1 RNAi for TBCCD1. (B) Graphic representing *B. besnoiti* and *T. gondii* invasion assays in cells RPE-1 overexpressing TBCCD1. The mean percentage of cells (±sd) in two independent experiments is shown. Total number of cells counted (n): (A) n(*B. besnoiti* WT) = 1004, n(*B. besnoiti* RNAi TBCCD1) = 1234, n(*T. gondii* WT) = 1255, n(*T. gondii* RNAi TBCCD1) = 1159; (B) n(*B. besnoiti* WT) = 861, n(*B. besnoiti* overexpression TBCCD1) = 872, n(*T. gondii* WT) = 967, n(*T. gondii* overexpression TBCCD1) = 784.

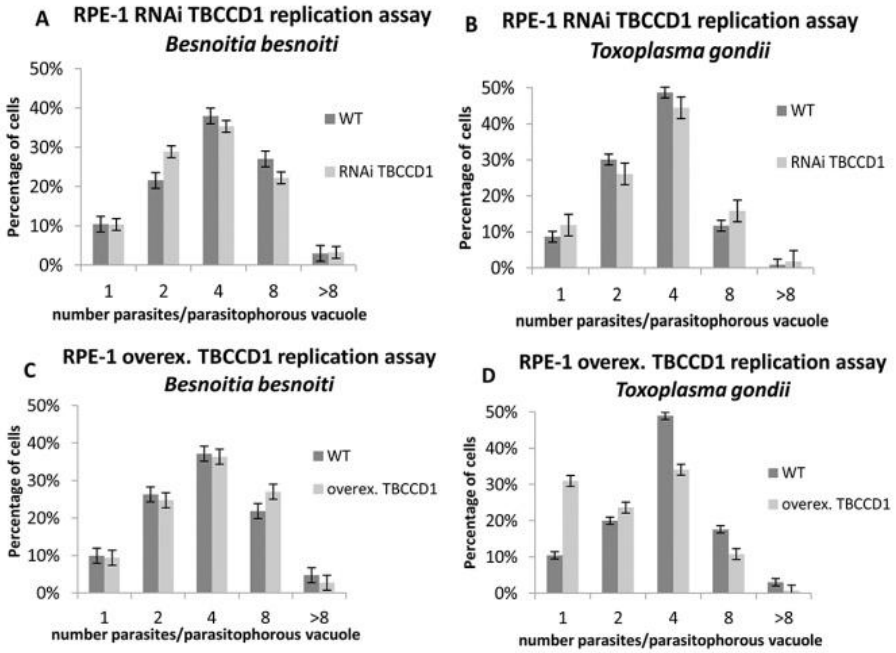

Fig. 22: Replication assays:

(A) Graphic representing *B. besnoiti* replication assays in cells RPE-1 RNAi for TBCCD1. (B) Graphic representing *T. gondii* replication assays in cells RPE-1 RNAi for TBCCD1. (C) Graphic

representing *B. besnoiti* replication assays in cells RPE-1 overexpressing TBCCD1. (D) Graphic representing *T. gondii* replication assays in cells RPE-1 overexpressing TBCCD1. The mean percentage of cells (±sd) in two independent experiments is shown. Total number of cells counted (n): (A) n(*B. besnoiti* WT) = 566, n(*B. besnoiti* RNAi TBCCD1) = 648; (B) n(*T. gondii* WT) = 794, n(*T. gondii* RNAi TBCCD1) = 680; (C) n(*B. besnoiti* WT) = 549, n(*B. besnoiti* overexpression TBCCD1) = 596; (D) n(*T. gondii* WT) = 527, n(*T. gondii* overexpression TBCCD1) = 564.

Apart from the invasion and replication assays already mentioned, it was also performed an assay in which RPE-1 WT cells, RPE-1 cells depleted of TBCCD1, and RPE-1 cells overexpressing TBCCD1 were invaded for 18h by *B. besnoiti* and *T. gondii*. In this assay the number of PVs in each invaded cell was counted. Again, no differences were found for *B. besnoiti* (Fig. 23A); but in *T. gondii*, the total number of PVs in each invaded cell decreases in RPE-1 cells overexpressing TBCCD1-GFP, and RPE-1 cells treated with siRNA TBCCD1, when compared to the WT (Fig. 23B). This suggests that despite the fact that no differences were found in the total number of invaded cells (invasion assay), the number of *T. gondii* tachyzoites able to invade one cell decreases (assuming that each PV counted refers to a successfully invaded tachyzoite) when we interfere with the expression of TBCCD1, a key regulator of centrosome positioning and consequently of internal cell organization.

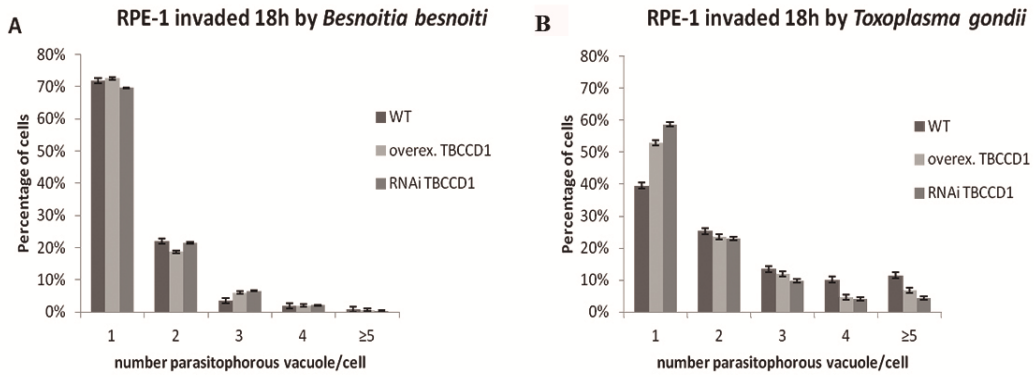

Fig. 23: Number of *B. besnoiti* and *T. gondii* PVs in RPE-1 invaded cells.
(A) Graphic representing the number of counted PVs in each RPE-1 invaded cell (WT, overexpressing TBCCD1, and RNAi TBCCD1) by *B. besnoiti* (18h post-invasion). (B) Graphic representing the number of counted PVs in each RPE-1 invaded cell (WT, overexpressing TBCCD1 and RNAi TBCCD1) by *T. gondii* (18h post-invasion). The mean percentage of cells (±sd) in three independent experiments is shown. Total number of cells counted (n): (A) n(*B. besnoiti* WT) = 457, n(*B. besnoiti* overexpression TBCCD1) = 416, n(*B. besnoiti* RNAi TBCCD1) = 289; (B) n(*T. gondii* WT) = 671, n(*T. gondii* overexpression TBCCD1) = 553; n(*T. gondii* RNAi TBCCD1) = 366.

2.3.8 - The impact of *Besnoitia besnoiti* and *Toxoplasma gondii* invasion in RPE-1 cells migration

Considering the described effects of *T. gondii* and *B. besnoiti* on host cell MTs, centrosome and Golgi apparatus position, as well as the recent description of the capacity of *T. gondii* to modulate the motility of its host cells (Lambert, H. *et al*., 2006; Lambert, H. *et al*., 2010), we decided to compare the effects of the two parasites in migrating cells, by performing wound healing assays.

For this purpose RPE-1 WT cells and RPE-1 overexpressing TBCCD1 cells were grown in glass coverslips and then invaded for 18h by either *T. gondii* or *B. besnoiti*. Confluent RPE-1 WT cells and RPE-1 overexpressing TBCCD1 cells were then wounded with a micropipette tip, and the wound closing was followed. Images were captured at 120, 360, 500 min and 600min of recovery and showed that cells invaded with *T. gondii*, contrary to those invaded with *B. besnoiti*, present a significant delay in wound closing in comparison to control cells. In RPE-1 WT cells, the difference is visible at 500min when control cells almost closed the wound, which in the case of cells invaded by *T. gondii* is still visible (Fig. 24).

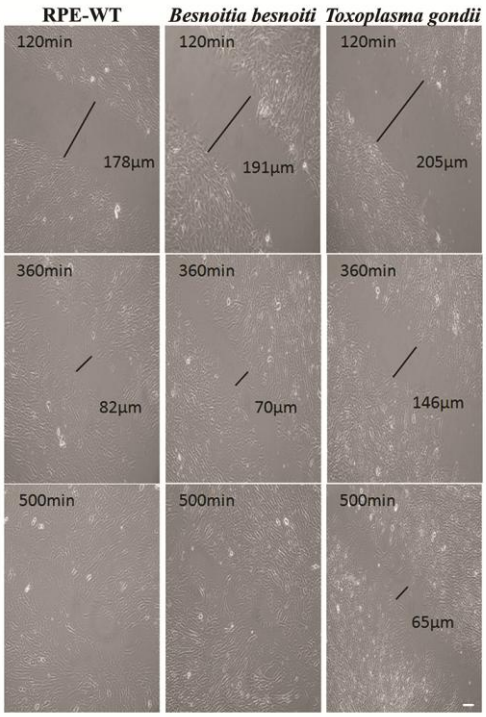

Fig. 24: Wound–healing assay in RPE-1 WT cells invaded by *T. gondii* and *B. besnoiti*.
Non-invaded and invaded RPE-1 were grown to confluence, wounded and imaged for 600min. Frames from 120, 360, and 500min are shown. In this picture we can see that cells invaded with *T. gondii* show a significant delay in wound closing in comparison to control cells. This delay is not observed in cells invaded with *B. besnoiti*. Scale bar 50µm.

In the case of RPE-1 cells overexpressing TBCCD1, there was a delay in closing the wound in all glass coverslips (invaded and non-invaded) when compared to RPE-1 WT cells. Again, it can be seen that cells invaded with *T. gondii* show a significant delay in wound closing in comparison to non-invaded, and *B. besnoiti* invaded cells (Fig. 25).

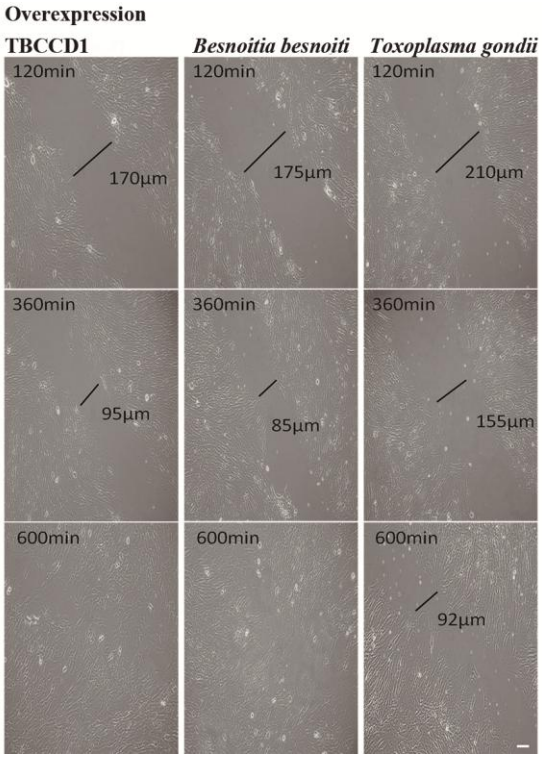

Fig. 25: Wound–healing assay in RPE-1 cells overexpressing TBCCD1 invaded by *T. gondii* and *B. besnoiti*.

Non-invaded and invaded RPE-1 were grown to confluence, wounded and imaged for 600min. Frames from 120, 360, and 600min are shown. In this picture we can see that cells invaded with *T. gondii* show a significant delay in wound closing in comparison to control cells. This delay is not observed in cells invaded with *B. besnoiti*. Scale bar 50µm.

To try to establish a relation between the delay of wound closing in invaded cells and the ability of *T. gondii* to recruit the centrosome and Golgi apparatus to the vicinity of the PV, it was studied the orientation of the centrosome and Golgi apparatus in cells invaded and non-invaded at the leading edge of a closing wound. In fact, it has been described in several different cell types that centrosome reorients towards the leading edge when cells are stimulated to migrate (Gomes *et al*., 2005; Etienne-Manneville, 2008; Schmoranzer *et al*., 2009; Vinogradova *et al.*, 2009). Therefore, it was observed by immunofluorescence microscopy, invaded and non-invaded RPE-1 cells and RPE-1 cells overexpressing TBCCD1 in wound healing assays, stained with antibodies against γ-tubulin (Fig. 26A1, B1, B2, C1,

C2; Fig. 27A1, B1, B2, C1, C2) and Golgin-97 (Fig. 26A2, B3, B4, C3, C4; Fig. 27A2, B3, B4, C3, C4), in order to access the position of both structures during wound closure.

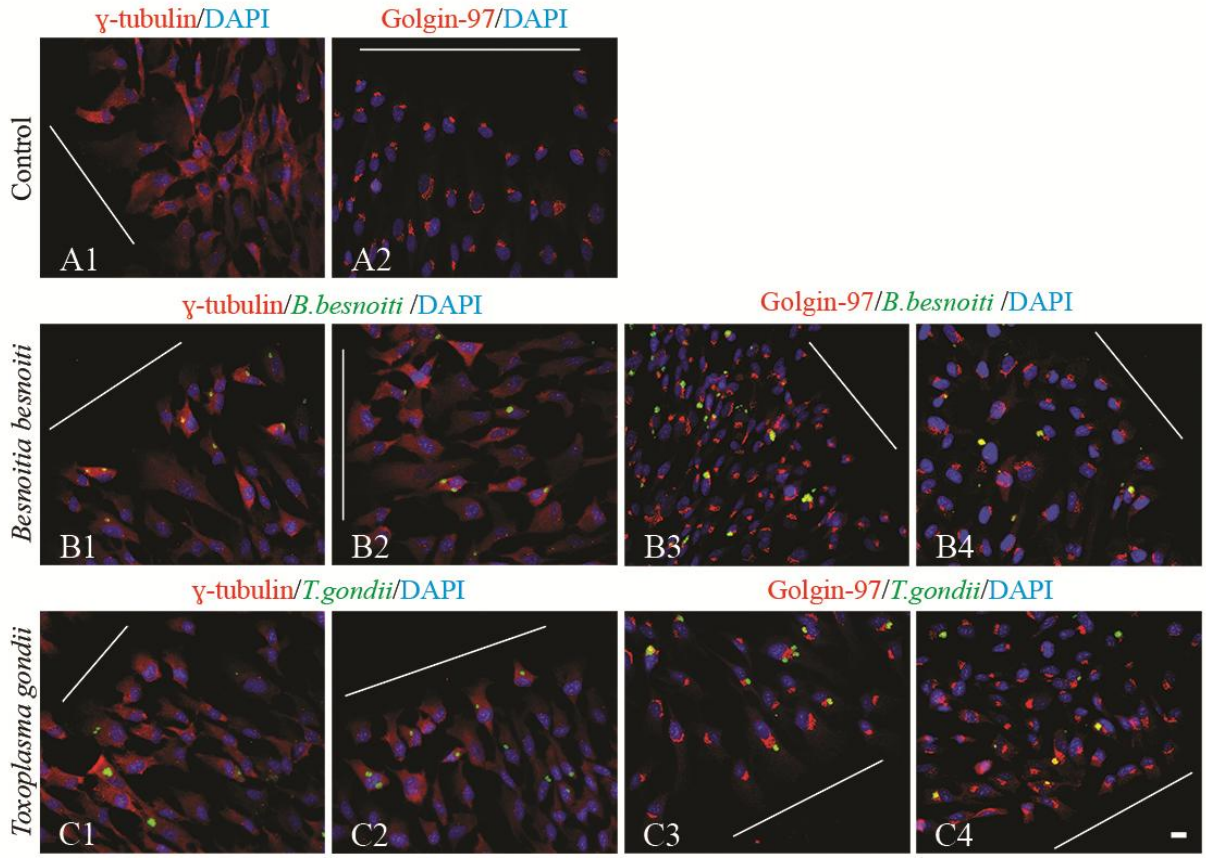

Fig. 26: Indirect immunolocalization of centrosome and Golgi apparatus in *B. besnoiti* and *T. gondii* invaded RPE-1 cells, during wound closure migration.

Antibodies used were *B. besnoiti* polyclonal antibody (green), *T. gondii* polyclonal antibody (green), anti-Golgin 97 (red) and anti-γ-tubulin (red). DNA was stained with DAPI (blue). White lines indicate the position of the wound edge. In A1, B1, B2, C1, and C2, the orientation of the host cell centrosomes towards the wound edge can be seen in red. (A1) RPE-1 cells, non invaded control. (B1 and B2) *B. besnoiti*, 18h post-invasion. (C1 and C2) *T. gondii*, 18h post-invasion. In A2, B3, B4, C3, and C4 the orientation of the host cell Golgi apparatus can be visualized (red). (A2) RPE-1 cells, non invaded control. (B3 and B4) *B. besnoiti*, 18h post-invasion. (C3 and C4) *T. gondii*, 18h post-invasion. Scale bar 20µm.

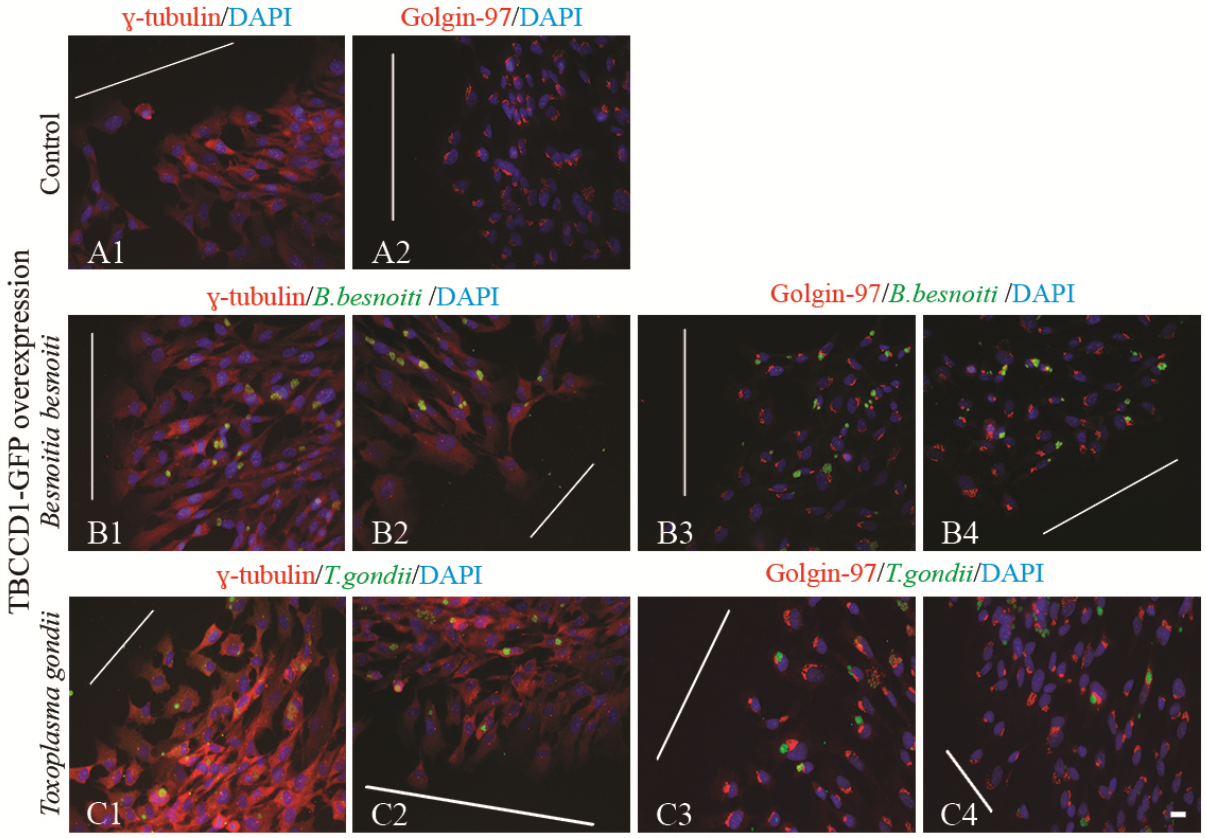

Fig. 27: Indirect immunolocalization of centrosome and Golgi apparatus in *B. besnoiti* and *T. gondii* invaded RPE-1 cells overexpressing TBCCD1, during wound closure migration.

Antibodies used were *B. besnoiti* polyclonal antibody (green), *T. gondii* polyclonal antibody (green), anti-Golgin 97 (red) and anti-γ-tubulin (red). DNA was stained with DAPI (blue). White lines indicate the position of the wound edge. In A1, B1, B2, C1, and C2, the orientation of the host cell centrosomes towards the wound edge can be seen in red. (A1) RPE-1 cells overexpressing TBCCD1, non invaded control. (B1 and B2) *B. besnoiti*, 18h post-invasion. (C1 and C2) *T. gondii*, 18h post-invasion. In A2, B3, B4, C3, and C4 the orientation of the host cell Golgi apparatus can be visualized (red). (A2) RPE-1 cells overexpressing TBCCD1, non invaded control. (B3 and B4) *B. besnoiti*, 18h post-invasion. (C3 and C4) *T. gondii*, 18h post-invasion. Scale bar 20μm.

It was not found any obvious differences between the orientation of the centrosome in invaded and non-invaded cells. Moreover, it was measured the angle between the direction of the wound and the axis connecting the centrosome and nuclear center, in infected and non-infected WT RPE-1 cells and RPE-1 cells overexpressing TBCCD1 (as exemplified in Fig. 28C).

Surprisingly, it was observed that the mean angle of the centrosome towards the wound is quite similar in WT RPE-1 non-invaded cells (68±1.5), invaded by *B. besnoiti* (76.7±2) and invaded by *T. gondii* (70.5±2.5), Fig. 28A. As for RPE-1 overexpressing TBCCD1, it was noticed a slight decrease of the mean angle when compared to RPE-1 WT cells, especially in

those cells invaded by *T. gondii* (50±1,6). These data are supported by Fig. 26 and Fig. 27, where it cannot be seen an obvious difference between the orientation of the centrosome in invaded and non-invaded cells in the leading edge.

In what concerns Golgi apparatus positioning it was counted the number of cells in the leading edge with a Golgi apparatus located within the 90° angle facing the wound (as exemplified in Fig. 28D; Hurtado *et al*., 2011). The results are summarized in Fig. 28B and show that migrating cells invaded by *T. gondii* present a similar localization of Golgi apparatus relatively to the leading-edge in comparison to those non-invaded (which is consistent with the observations in Fig. 26C3 and C4 and Fig. 27C3 and C4). In the case of cells invaded by *B. besnoiti* the values for Golgi reorientation were in RPE-1 WT, 62±1,9% (Fig. 28B), and in RPE-1 overexpressing TBCCD1, 71±1,1%; having non invaded RPE-1 WT cells 74±1,3% and non invaded RPE-1 cells overexpressing TBCCD1 81±0,5% of cells with an oriented Golgi apparatus towards the leading edge. As for *T. gondii* it does not differ much from the non invaded controls, indicating a good reorientation of Golgi ribbon in migrating cells. Curiously, observing Fig. 26C3 and C4 and Fig. 27C3 and C4, the Golgi ribbon is not only reoriented towards the leading edge, as it is also reorganized (non-fragmented) in migrating cells invaded by *T. gondii*.

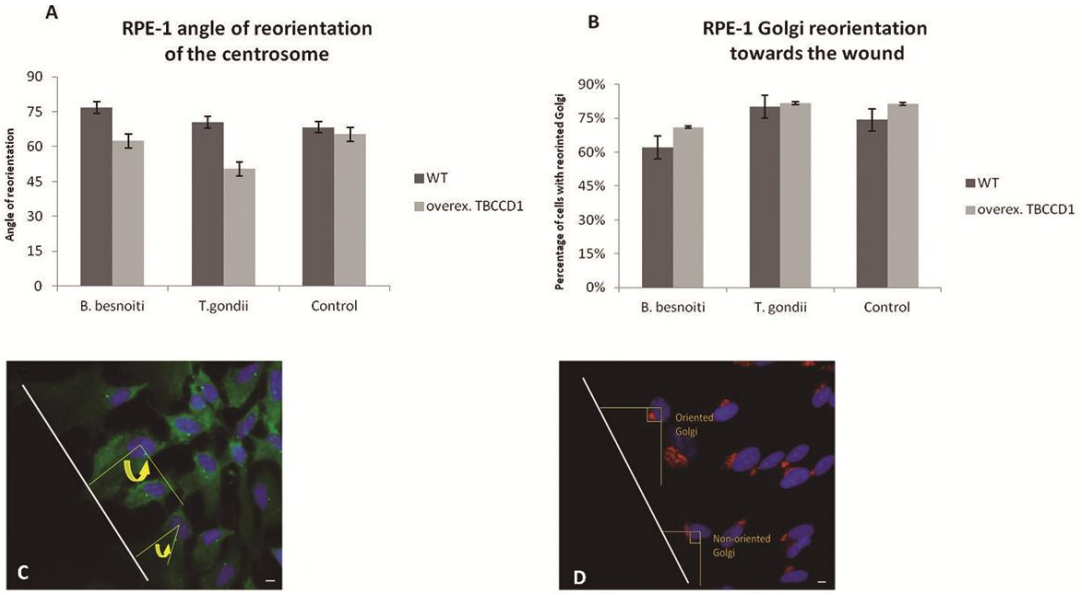

Fig. 28: Centrosome and Golgi reorientation towards the wound.

(A) Graphic representing the angle of centrosome reorientation towards the wound leading edge, in non-invaded RPE-1 WT and RPE-1 cells overexpressing TBCCD1, and in invaded RPE-1 WT and RPE-1 cells overexpressing TBCCD1 by *B. besnoiti* and *T. gondii.* (B) Graphic representing the percentage of cells with a Golgi apparatus reoriented towards the wound leading edge, in non-invaded RPE-1 WT and RPE-1 cells overexpressing TBCCD1, and in invaded RPE-1 WT and RPE-1 cells overexpressing TBCCD1 by *B. besnoiti* and *T. gondii.* (C) IF of how the measurement of the angle of

the centrosome in relation to the leading edge (white line) was performed using ImageJ software (centrosome-green; nucleus-blue). (D) Schematic IF of how the reorientation of the Golgi towards the leading edge (white line) was determined, with an example of a cell with an oriented Golgi, and another with a non-oriented Golgi. ImageJ software was used (Golgi-red; nucleus-blue). The mean angle of reorientation of the centrosome (±sd) and the mean percentage of cells with a reoriented Golgi (±sd) in two independent experiments are shown. Total number of cells counted (n): (A) n(control WT) = 290, n(control overexpression TBCCD1) = 254, n(*B. besnoiti* WT) = 128, n(*B. besnoiti* overexpression TBCCD1) = 174, n(*T. gondii* WT) = 188, n(*T. gondii* overexpression TBCCD1) = 203; (B) n(control WT) = 587, n(control overexpression TBCCD1) = 211, n(*B. besnoiti* WT) = 101, n(*B. besnoiti* overexpression TBCCD1) = 199, n(*T. gondii* WT) = 183, n(*T. gondii* overexpression TBCCD1) = 291. Scale bars3µm.

Overall, this data could suggest that the invasion of RPE-1 cells by *B. besnoiti* and *T. gondii* does not have an obvious effect in directional cell polarization (centrosome or Golgi apparatus positioning); being the delay in wound closure in cells invaded by *T. gondii* related with other factors like interfering with the mechanisms responsible for cell motility.

2.4 - Discussion

2.4.1 - Host microtubule cytoskeleton rearrangement

In the present study we show that the rearrangement of the host Mts is present not only in the initial steps of host cell invasion, but also during PV establishment and parasite replication. In advanced invasion time points, like 30h of invasion, an alveolar like structure of host Mts is present around the PV (Fig. 10), suggesting a clear involvement of the Mt cytoskeleton of the host cell and *B. besnoiti* PV. This interaction between host Mts and parasite´s PV was also seen in *T. gondii* invasion, in accordance to what has been already described by other authors (Sehgal *et al*., 2005; Coppens *et al*., 2006; Walker *et al*., 2008). In fact, a recent screening of a siRNA library targeting individual human genes shows that α and β-tubulin silencing reduces *T. gondii* replication by at least 50% (Moser *et al*., 2013). Interestingly, in the work of Walker *et al*., 2008 it was observed that the host MT rearrangement into ordered circular arrays occurs only in the presence of living *T. gondii* parasites: macrophages containing heat-killed parasites demonstrate no such ordered structures surrounding the vacuole containing the heat-killed parasites. This might be related to the fact that the delivery of parasite secreted effector proteins into the host cell is crucial to rearrange the host MTs. These proteins associate with the PVM and are mostly released from the bulbous part of the rhoptries during invasion and also from secretion of dense granules into the PV after entry. They are probably involved in several processes such as nutrient acquisition; but also the interaction with mitochondria (ROP2 traffics through host MTs to mediate the adhesion of host mitochondria to the PVM) and ER; the restructuring of the IFs and MTs around the PV; and the modulation of certain processes of the host cell (Melo *et al*., 1992; Sinai *et al*., 1997; Sinai & Joiner, 2001; Martin *et al*., 2007). Thus, the importance of host´s MTs during PV establishment could be related to the need of parasites to acquire a juxtanuclear, stable, subcellular position in proximity to the majority of mammalian organelles, like the centrosome (Coppens *et al*., 2006; Wang *et al*., 2010), the host ER (Coppens *et al*., 2006), mitochondria (Sinai *et al*., 1997), and Golgi apparatus (Coppens *et al*., 2006; Wang *et al*., 2010), potential reservoirs of nutrients. This is supported by the observation that MTs beneath the PVM are short, stable MTs, and might serve as scaffoldings to preserve the PV structure and maintain the PV in a stationary position near the host organelles (Coppens *et al*., 2006). Moreover, *T. gondii* alters trafficking within the host cell to deliver host vesicles and organelles to the PVM (Sinai & Joiner, 2001; Coppens *et al*., 2006). In fact, invaginations of the PVM into the lumen of the PV, induced by host MTs have been observed and described as H.O.S.T. (Coppens *et al*., 2006). H. O. S. T is

required for the scavenging of host´s cholesterol and it is reasonable to predict that other essential nutrients are also obtained by the parasite via endocytosis and H.O.S.T. (reviewed in Laliberté & Carruthers, 2008). It is probably this intravacuolar network that is responsible for the rosette arrangement of both parasites, giving an alveolar-like appearance to the PV, more prominent in *B. besnoiti* than in *T. gondii*. In the initial steps of host cell invasion (15min time point), the presence of MTs at the site of the MJ, and surrounding the invading parasite, seem to act by hastening the time that parasites initiate host cell invasion, with no effect on parasite attachment, motility, and penetration rate (Sweeney *et al*., 2010). This finding is also supported by the fact that in the work of Nolasco, S. (unpublished results), cells with depolymerized MTs, after treatment with nocodazole, are less invaded by *T. gondii* and *B. besnoiti*. This could be related to the fact that MTs act as a fulcrum for gliding parasites to use as a pivot to begin to penetrate into the host cell; or that host MTs provide support to help withstand the compressive force induced by a parasite in contact with the host cell; or finally that host MTs may aid in promoting the efficient formation of a functional MJ - when host MTs are disrupted, RON complex delivery to the plasma membrane would be less efficient, causing a lag in the time before parasites could begin to invade (Sweeney *et al*., 2010). Supporting this last hypothesis is the identification of host cellular β-tubulin as a binding partner of TgRON4, as the C-terminal region of β - tubulin interacts with TgRON4 during the invasion step (Takemae *et al*., 2013); and the fact that *Theileria* host cell invasion does not require the formation of a MJ, which coincides with no remodeling on the surface of bovine lymphoid host cells (reviewed in Shaw, 2003).

Several other apicomplexan parasites, apart from *B. besnoiti* and *T. gondii*, show evidence for the modulation of the host cell cytoskeleton:

- the H.O.S.T network has been described in *N. caninum* (reviewed in Hemphill *et al*., 2004), nevertheless, host MT rearrangement around the PV was not detected in this parasite (Coppens *et al*., 2006; Walker *et al*., 2008);
- *Cryptosporidium* induces host cell actin polymerization (Elliott *et al*., 2001). An accumulation of host actin filaments has been observed at the parasite-host interface; and the presence of the actin crosslinking protein α-actin is also detected in the electron-dense plaque formed at the PV-host cell interface early in parasite development but not during parasite replication (Elliott and Clark, 2000);
- an analog of the H.O.S.T system is present also in erythrocytes infected with *Plasmodium*, seeming to function like an intracellular transport system, allowing the import of specific nutrients to *Plasmodium* (Haldar *et al*., 2001). Interestingly, in this

parasite, silencing the host´s α-tubulin, β-tubulin, or co-silencing α and β-tubulin, does not produce significant changes in infection rate (Félix & Silveira, 2011);

- in *Theileria* invasion, and despite the fact this parasite does not form a PV, developing freely in the cytoplasm, there is an interaction with the host MTs that associate with the diffuse material secreted at the surface of the parasite, facilitating the movement of the parasite to the perinuclear region of the host cell (reviewed in Frénal & Soldati-Favre, 2009). Supporting this, *T. annulata* secreted protein TaSE is detected in the host cell cytoplasm, where it colocalizes with α-tubulin (Schneider *et al*., 2007). Additionally, as the host cell enters mitosis, the schizont binds newly forming MTs of the mitotic spindle. This step is independent of Polo-like kinase 1 (Plk1) activity, and it allows the schizont to position itself so that it spans the equatorial region of the mitotic cell, strategically positioned to be included in the plane of cell division at each host cell cytokinesis (von Schubert *et al*., 2010). Finally, in recent work, it was reported a schizont surface protein, p104, that functions as an EB1-binding protein, a protein able to interact with +TIPs in growing MT plus ends of the host cell. So, *Theileria* has the ability to hijack EB1, which regulates host cell MT dynamics, thereby gaining access to the regulatory mechanisms that control the microtubular cytoskeleton dynamics (Woods *et al*., 2013);
- during *E. bovis* invasion of bovine endothelial cells, actin covers the whole macromeront by a thick layer. The same is true for stable, acetylated MTs, which are closely associated with the PV at this phase of development (Hermosilla *et al*., 2008).

Interestingly, the effects on the host cytoskeleton are not exclusive of protozoa: microbial pathogens also manipulate the host cell cytoskeleton for adherence, uptake, exit and dissemination (reviewed in Gruenheid & Finlay, 2003).

2.4.2 - Recruitment of the host cell centrosome

Usually, the centrosome is maintained at the cell centre, closely associated with the nucleus. However, during *T. gondii* invasion, the host cell centrosome is recruited from the nuclear membrane to the PVM (Fig. 12), appearing to be, at least partially, the mechanism by which *T. gondii* effectively remodels host MTs. On the other hand, the mechanism behind the remodeling of host Mt cytoskeleton by *B. besnoiti* remains unclear, since the detachment of the host centrosome from the nucleus to the PV does not occur, and no additional foci of γ-tubulin nucleating MTs at the PV membrane were observed (Fig. 11). Thus, it seems that *B.*

besnoiti remodeling of the host cell cystoskeleton does not depend either of centrosomal MTOC, or of non centrosomal MTOCs (in this case, γ-tubulin foci at the PV). Non centrosomal MTOCs, like centrosomes, are structures that can catalyze γ-tubulin-dependent MT nucleation and anchor MTs (reviewed in Lüders & Stearns, 2007). Interestingly, and despite contradicting the results of Walker *et al*., 2008 (the different results could be due to differences in methodology and/or host cells), no MTs were observed growing from a PV associated focus of γ-tubulin on *T. gondii* invasion either, neither in RPE-1 cells (present work), nor in Vero cells (Nolasco, S., unpublished data), indicating that the rearrangement of host MTs in *T. gondii* invasion/replication is probably dependent mostly on the interaction with the host centrosome, since non centrosomal MTOCs were not detected at the PV membrane. It is interesting to refer that the recruitment of the centrosome by *T. gondii* is not an early phenomenon, since it is only detected at 18h post-invasion, with no significant differences in the nucleus-centrosome distance in invaded RPE-1 WT cells, when compared to non-invaded RPE-1 WT cells at 6h post-invasion (Fig. 13). This suggests that the remodeling of the host MTs is not totally dependent on the centrosome recruitment, at least not in the first stages of PV establishment, since MTs were observed at the PV minutes after invasion, and the centrosome is detached from the nucleus only a few hours later. So, we could hypothesize that the centrosome, as a MTOC, is more crucial in later stages of development of the PV, than in the initial steps of positioning the PV next to the nucleus and host cell organelles. It is important to refer that in infected cells apparently the recruited centrosome maintains its integrity, as it consists of centrioles surrounded by a pericentriolar matrix (at least for NEDD1 and pericentrin (Romano *et al*., 2013)).

Considering that the centrosome is a key player in cell-cycle progression and cellular control, in part because it organizes MTs that participate in intracellular trafficking, cell motility, cell adhesion, cell polarity, and formation of the mitotic spindle (reviewed in Azimzadeh & Bornens, 2007), than the repositioning of the centrosome in the vicinity of *T. gondii* PV is an important strategy to control and modulate host cell functions (distribution of host organelles, modulation of the host cell cycle and cell migration).

The full range of molecular connections involved in the tight coupling between nucleus and centrosome are still largely unknown, constituting an obstacle to the knowledge of the molecular mechanism/(s) behind the recruitment of the centrosome by *T. gondii*. Nevertheless, MTs appear to play a role in the nucleus-centrosome attachment (Aronson *et al*., 1971), with the molecular motor dynein, anchored on the outer nuclear envelope, contributing to attachment with the centrosome by transporting the nuclear cargo towards the minus-end of MTs (Gönczy *et al*., 1999). Although centrosome-nuclear connections remains

poorly understood, genetic and molecular analysis began to reveal a complex framework of proteins that interconnect centrosomes and nuclei, including the KASH/SUN (*K*larsicht/*A*NC-1/*S*yne/*h*omology (KASH)/*S*ad-1/*UN*C-84 (SUN)) families that span the nuclear envelope and serve to establish linkages with dynein and kinesin motors (Starr & Fridolfsson, 2010). In fact, *Caenorhabditis elegans* ZYG-12 and SUN-1 are essential for centrosome–nucleus attachment (Malone *et al*., 2003; Minn *et al*., 2009). ZYG-12 is a type II outer nuclear membrane protein and SUN-1 a type II inner nuclear membrane protein. The proteins interact in the luminal space of the nuclear envelope via the ZYG-12 mini KASH domain and a region of SUN-1 that does not include the SUN domain (Minn *et al*., 2009). Malone *et al*., 2003 also found that ZYG-12 interacts with the dynein light intermediate chain DLI-1, suggesting that ZYG-12 may recruit the dynein complex to the nuclear envelope through its interaction with DLI-1 (reviewed in Gönczy, 2004). In mammalian cells, in addition to the KASH/SUN families, emerin also participates in the linkage of the centrosome, and therefore the tubulin cytoskeleton, with the outer nuclear membrane. Emerin interacts with β-tubulin to anchor the centrosome at the outer nuclear membrane, providing an important cue on how the tubulin cytoskeleton is connected to the nuclear envelop (Salpingidou *et al*., 2007). In *Dictyostelium*, several proteins have been shown to connect the centrosome to nuclei, including the SUN-1 homolog (Xiong *et al*., 2008; Schulz *et al*., 2009), a centrin B homolog (Mana-Capelli *et al*., 2009), and the centrosomal protein, CP148 (Kuhnert, *et al*., 2012). These proteins have structural or regulatory roles in anchoring MT minus ends to the centrosome or in stabilizing components at the nuclear envelope, being also possible that some of these proteins directly bridge the two structures and form primary contacts. Adding to this, recent work in *Dictyostelium* described a kinesin motor protein implicated in maintaining a physical connection between the centrosome and nucleus - Kif9 is anchored to the nuclear envelope and engages MTs to maintain centrosome proximity during interphase (Tikhonenko *et al*., 2013).

It is possible that *T. gondii* plays a regulatory role of one of these molecular components, but the exact mechanism involved in the detachment of the centrosome in cells invaded by *T. gondii* is still unknown.

Despite this, Wang *et al*., 2010 findings seem to provide evidence for the involvement of a host signaling pathway in the structural reorganization of cells invaded by *T. gondii*. It has been demonstrated that *T. gondii* infection of primary fibroblasts results in stable activation of host Akt (Ser/Thr kinase Akt signaling has been implicated in polarization during migratory responses in fibroblasts (Onishi *et al*., 2007; Wang *et al*., 2009)), being the upstream activators of Akt, phosphatidylinositol 3-kinase (PI3K) and mTOR complex 2 (mTORC2)

(reviewed in Franke, 2008). mTORC2 is also able to directly regulate spatial cell growth through actin cytoskeleton remodeling by acting upstream Rho-GTPases (reviewed in Soares *et al*., 2013). Wang *et al*., 2010 showed that host mTORC2-Akt signaling is required for multiple aspects of cell reorganization, including the localization of the host centrosome, the organization of MTs, and the distribution of mitochondria and lysosomes that surround the PV.

Interestingly, in other protozoa parasites, evidence for the migration of the centrosome of the host cell towards the parasite is also seen, as in *Trypanosoma cruzi* invasion of cardiac myoblasts (Tyler *et al*., 2005). This way, *T. cruzi* also remodels and changes the host cell MT cytoskeleton, in this case to develop the necessary infrastructure for transport of lysosomes to the parasite synapse (parasite/ host cell junction during host cell invasion). The fusion of lysosomes is necessary for the construction of the PV (Caler *et al*., 2001). In this parasite, the proposed model of interfering with the host cell MT dynamics initiates with the rapid recruitment of α-tubulin to the parasite´s synapse, and includes the presence of non centrosomal MTOCs, as foci of γ-tubulin are found in nascent PVs. Recruitment of γ-tubulin to the synapse promotes the seeding of MTs as the invagination deepens and the PV is formed. Once formed, this vacuole acts as a secondary MTOC. Interestingly, besides forming a new MTOC, the PV also recruits the cell's MTOC, the centrosome. The existence of two main MTOCs, establishes a bidirectional highway along which vesicles can traffic to and from the parasite immediately after cell invasion (Tyler *et al*., 2005).

In summary, in our experiments during *B. besnoiti* and *T. gondii* invasion there is a rearrangement of the MT cytoskeleton of the host cell. However, in *B. besnoiti* this is not associated with the recruitment of the host cell centrosome to the PV, and in *T. gondii* this association occurs. Meanwhile, the formation of extra foci of γ-tubulin as secondary MTOCs in the host cell cytoplasm does not occur in either parasite.

2.4.3 - Recruitment and morphological rearrangement of the Golgi apparatus

In infected RPE-1 WT cells by *T. gondii* or *B. besnoiti*, the host cell Golgi apparatus was found at the PV surface as soon as 6h after invasion (Fig. 15). This is observed prior to the recruitment of the centrosome by *T. gondii* (not detected at 6h post-invasion), what could suggest that the PV–centrosome association is not a prerequisite for the positioning of the Golgi apparatus by the PV. Interestingly, and supporting this observation, in the work of Wang *et al*., 2010, the loss of PV–MTOC association in cells with defects in the mTORC2-Akt pathway interfered with the distribution of host mitochondria and lysosomes to the PV

but not in the association of these organelles with the PV. Considering the above, it seems that the role of the centrosome is more related with the organization and maintenance of the Golgi apparatus and other host cell organelles around the PV, possibly through the rearrangement of host MTs, than with the initial recruitment of these organelles to the PV. In this work concerning the Golgi apparatus the difference observed between the two parasites was that in *T. gondii* invasion the Golgi ribbon was found fragmented into smaller units (in accordance to what was described by Walker *et al*., 2008; Coppens *et al*., 2006; and Romano *et al*., 2013), and in *B. besnoiti* it was not only apparently intact, as it presented a statistically significant decrease in diameter, pointing to some degree of compaction. Moreover, the breakdown of the host Golgi apparatus is independent of the host cell type, as the event occurred not only in the RPE-1 cells used in our study, but also in infected HFF, MDCK cells, and Vero cells (Romano *et al*., 2013).

Being vacuolar pathogens, *T. gondii* and *B. besnoiti* have to scavenge nutrients from their host cells. Glucose and other small nutrients can cross the PVM passively, but other nutrients are obtained by more active mechanisms (reviewed in Blader & Saeij, 2009). One of these mechanisms is to relocalize host mitochondria, ER, and Golgi apparatus to the PV (Sinai *et al*., 1997; Coppens *et al*., 2006, Wang *et al*., 2010, Romano *et al*., 2013). The Golgi apparatus is involved in several important cellular functions including transport and PTM of proteins and glycosylation of lipids synthesized in the rough endoplasmic reticulum and destined for the secretory pathways (reviewed in van Vliet *et al*., 2003). So, it is reasonable to assume this is an important organelle for the parasite to recruit and control in order to survive and replicate inside the host cell, since this could facilitate the interception of host vesicular trafficking. In fact, despite its ability to synthesize *de novo* sphingolipids (*T. gondii* contains >20 species of sphingolipids consisting of both saturated and unsaturated fatty acids (Bisanz *et al*., 2006; Lige *et al*., 2011)), the parasite also appears to scavenge sphingolipids derived from the host cell via the host Golgi apparatus. In this case, *T. gondii* intercepts Golgi apparatus derived vesicles after destabilizing the structure of the Golgi apparatus, resulting in its breakdown into ministacks; and it sequesters Rab14-, Rab30-, or Rab43-associated vesicles containing sphingolipids, within the PV (Romano *et al*., 2013).

The fragmentation of the Golgi apparatus is characterized by its reorganization in small, round, disconnected, and dispersed elements (reviewed in Cole & Lippincott-Schwartz, 1995) and it occurs under various conditions, such as cell division, stress, malignant transformation or treatment with various inhibitors. It occurs during mitosis (Lucocq & Warren, 1987) and is also noted in apoptotic cells, indicating that a fragmented Golgi apparatus can also be associated with cellular dysfunction (Chiu *et al*., 2002). In fact, the dissociation of the Golgi

apparatus is a classical feature in neurodegenerative diseases, where the fragmentation of the Golgi is even considered to be an early causative step in neural apoptosis. Earlier examinations of human brain tissues and animal models have shown that fragmentation of the Golgi apparatus occurs in Alzheimer's disease (Baloyannis *et al*., 2004), Parkinson's disease (Fujita *et al*., 2006) and amyotrophic lateral sclerosis (ALS) (Stieber *et al*., 1998).

As to what could cause the observed Golgi apparatus fragmentation during *T. gondii* invasion and compaction in *B. besnoiti* invasion, a few hypothesis must be considered: interference with the MT cytoskeleton, with the Golgi structural proteins or with membrane dynamics (through interference with membrane trafficking molecules (reviewed in Wei & Seemann, 2010)).

In what concerns the interaction of the parasites with the host cell cytoskeleton, we assume that the perturbation of the MT network by *T. gondii* and *B. besnoiti* could affect the function and morphology of the Golgi apparatus, since the integrity and location of the Golgi is most likely a result of the interaction of this organelle with the MT cytoskeleton and its motor proteins. Moreover, the Golgi apparatus can provide MT nucleation function in retinal pigment epithelial cells (Efimov *et al*., 2007; Rivero *et al*., 2009), and in multiple other epithelial cell lines (Efimov *et al*., 2007), and it is now known that the MT network responsible for Golgi apparatus assembly are both centrosomal and Golgi derived MTs (Vinogradova *et al*., 2012). Indeed, after mitosis the Golgi apparatus breaks down, to reassemble in daughter cells. In daughter cells Golgi membranes fuse and stack into multiple ministacks throughout the cytoplasm. The molecular motor dynein transports the ministacks along the newly emerging interphase MT network and assemble to form a single complex. One significant function of Golgi-derived MTs in Golgi assembly is the pre-merging of ministacks into larger fragments in the cell periphery. In a second stage, centrosomal MTs provide the tracks along which Golgi elements are transported to the cell center and then tangentially connected into a ribbon (Vinogradova *et al*., 2012). When MT nucleation at the Golgi apparatus is specifically inhibited, only the centrosome-based MT array persists and a fragmented Golgi apparatus collapses around the centrosome, proving that Golgi-based MTs are responsible for Golgi ribbon integrity and morphology, and that centrosomal MTs are required for pericentrosomal positioning of the Golgi apparatus (Miller *et al*., 2009; Vinogradova *et al*., 2012).

Considering all the above, a possible scenario during *B. besnoiti* and *T. gondii* invasion is that Golgi apparatus recruitment by both parasites is mediated by the PV interaction with host MTs. The interaction with these two subsets of MTs (those nucleating from the centrosome, and those nucleating from the Golgi apparatus), seems to differ between *B. besnoiti* and *T.*

gondii, with *T. gondii* causing a Golgi fragmentation phenotype consistent with the persistence of the centrosome nucleated array of Mts, and inhibition of the Golgi Mts. This phenotype is in accordance with the observed requirement for recruitment of the host cell centrosome. *B. besnoiti* has a different effect on Golgi nucleated Mts, since a compaction of this organelle is observed. The repositioning of the Golgi apparatus next to the PV suggests also an effect on the centrosome radial MT distribution in *B. besnoiti* invasion, but this does not depend on the recruitment of the centrosome.

As already mentioned, changes in Golgi apparatus structure during *T. gondii* and *B. besnoiti* host cell invasion can also be related with interference with the Golgi structural proteins and membrane trafficking proteins. Several proteins have been described as being involved in regulation of Golgi apparatus morphology, such as:

- the motor non-muscle myosin IIA (NMIIA). This protein is dynamically associated with *trans*-Golgi network membranes (Ikonen *et al*., 1997), and when phosphorylated modulates the binding and/or release of NMII from the Golgi, which regulates the extension of Golgi membrane tubules and/or the separation of vesicles from the Golgi apparatus (Ikonen *et al*., 1997);
- the regulatory protein Rab1: in cells expressing a mutant of Rab1, which can affect guanine nucleotide exchanges, the Golgi apparatus is dispersed into scattered vesicles (Wilson *et al*., 1994);
- golgins, uniquely expressed in higher eukaryotes. Golgins can link membranes to the cytoskeleton, making them important players for ribbon formation. During mitosis, fragmentation of the Golgi is triggered by the phosphorylation of several proteins, including golgin-84 and GM130 (reviewed in Wei & Seemann, 2010). During apoptosis, fragmentation is induced by caspase-dependent cleavage of golgins, such as giantin, golgin-160 and p115 (Mancini *et al*., 2000; Chiu *et al*., 2002; Lowe *et al*., 2004). Furthermore, the capacity of the Golgi apparatus to nucleate MTs is also dependent on golgins. The formation of MTs at the *trans*-Golgi requires γ-tubulin and CLASPs, which are recruited to the membrane through interaction with the golgin GCC185 (Efimov *et al*., 2007);
- GRASPs (Golgi reassembly stacking proteins). Recent work has begun identifying components necessary for linking cisternal stacks into a contiguous Golgi ribbon, and GRASPs appear to be able to link Golgi membranes, either for stacking or ribbon formation (reviewed in Ji *et al*., 2013). In vertebrates, two GRASPs were found, termed GRASP65 and GRASP55, which localize to *cis* and medial cisternae respectively (Barr *et al*., 1997; Shorter *et al*., 1999). Phosphorylation and

dephosphorylation of GRASPS make important contributions to the Golgi apparatus disassembly and reassembly: phosphorylation leads to GRASP65 deoligomerization and Golgi unstacking, whereas dephosphorylation of GRASP65 leads to reformation of the oligomers and restacking (reviewed in Ji *et al*., 2013). Depletion of GM130 or its binding partner GRASP65, by using RNA interference, disrupts formation of the Golgi ribbon but does not block transport through the secretory pathway (Puthenveedu *et al*., 2006).

Interestingly, in *Chlamydia trachomatis* (also an intracellular pathogen) infected human epithelial cells there is also a fragmentation of the Golgi apparatus into small, albeit intact, Golgi ministacks (similar to *T. gondii* invasion) dependent on golgin-84 cleavage. Remarkably, Golgi apparatus fragmentation is a critical factor for efficient chlamydial growth, since a lack of Golgi fragmentation results in reduction in numbers of infectious bacteria. Moreover, stable knockdown of golgin-84 resulted in fully viable cells showing a fragmented Golgi apparatus, leading to a substantial enhancement of chlamydial development. *C. trachomatis* induced Golgi fragmentation affects the processing of glycoproteins in the Golgi apparatus and enhances transport of sphingolipids to the bacterial inclusion at later time points during the infection (Heuer *et al*., 2009). In the same way, *T. gondii* also hijacks sphingolipid-containing Golgi-derived vesicles to the PV lumen in order to growth and replicate. However, different from *C. trachomatis, T. gondii* mediated Golgi fragmentation does not seem to be dependent on cleavage of host Golgi matrix proteins, at least as documented for golgin160 and golgin97 (Romano *et al*., 2013). In fact, from the alternatives described above for what could cause the fragmentation of the Golgi apparatus host cell during *T. gondii* invasion (interference with the MT cytoskeleton, interference with the Golgi structural proteins or with membrane dynamics), the work of Romano *et al*., 2013 points to an interference with membrane traffic. In these studies, the interception of host Golgi–derived Rab vesicles marked with Rab14, Rab30, or Rab43, followed by the trapping of these vesicles in the PV lumen, would perturb vesicular trafficking, resulting in the breakdown of the Golgi apparatus into dispersed vesicular structures. This also shows that *T. gondii* is capable of hijacking numerous Golgi-derived vesicles originating from different stacks of the Golgi, for example, *cis*-Golgi (Rab43) and *trans*-Golgi (Rab14). Nevertheless, not only it is possible that other mechanisms related with the MT cytoskeleton and Golgi proteins may still also contribute to Golgi fragmentation in *T. gondii* invasion, but also Golgi compaction during *B. besnoiti* remains to be explained.

It is important to refer that despite the alteration in Golgi´s morphology during *T. gondii* and *B. besnoiti* host cell invasion, it is to expect that global secretion remains intact, since published data indicate that neither Golgi ribbon integrity nor positioning are critical for the secretory activity of the Golgi apparatus (Miller *et al*., 2009; Yadav *et al*., 2009; Hurtado *et al*., 2011). In fact, disruption of ribbon continuity by either down regulating Golgi-localized proteins (Puthenveedu *et al*., 2006) or depolymerizing MTs (Cole *et al*., 1996) blocks neither intra-Golgi transport nor overall secretion to the plasma membrane. Thus, the maintenance of the functionality of this organelle during invasion allows the pathogens to rely on its synthetic activities.

Despite the fact that MTs are known to contribute to maintain Golgi apparatus morphology and transport to and from this organelle, there is also evidence showing the involvement of actin cytoskeleton components in Golgi morphology and function. Actin and actin binding proteins have been localized to the Golgi apparatus, and many have been shown to be important for Golgi function (reviewed in De Matteis & Morrow, 2000 and Egea *et al*., 2006), and dynamics, such as the reorientation of the Golgi apparatus during cell migration (Magdalena *et al*., 2003) and transport events (Sahlender *et al*., 2005). A recent example is provided by the Golgi protein GOLPH3 that binds to myosin motor 18A (Dippold *et al*., 2009). The interaction between GOLPH3 and myosin 18A is required for extension of the Golgi ribbon and the formation of transport carriers. Another example is p230/golgin-245, which interacts with microtubule–actin cross-linking factor (MACF)1 that links MTs to the actin cytoskeleton (Kakinuma *et al*., 2004). Moreover, one particular form of spectrin (an actin binding protein), β3 spectrin, has been shown to associate with the Golgi apparatus being involved in maintaining the structure of the Golgi apparatus and orchestrating protein traffic in the secretory pathway (Stankewich *et al*., 1998). Taking in consideration that invasion of *T. gondii* not only activates the reorganization of the MT cytoskeleton of the host cell, but also of actin microfilaments (da Silva *et al*., 2008), and that the interaction with the host cell actin is also present in other apicomplexan, such as *N. caninum* (reviewed in Hemphill *et al*., 2004), *T. annulata* (Baumgartner, 2011), *C. parvum* (Elliott & Clark, 2000) or *E. bovis* (Hermosilla *et al*., 2008), it is possible that the changes in Golgi ribbon morphology can be ascribed also to a manipulation of the host cell actin cytoskeleton by *T. gondii* and *B. besnoiti* during invasion and establishment of the PV.

2.4.4 - The expression levels of TBCCD1: how it reflects on the recruitment of the centrosome and Golgi apparatus, and different outcomes in invasion and replication assays

TBCCD1 is a centrosomal protein important for centrosome–nucleus connection (Gonçalves *et al*., 2010), being required for mother–daughter centriole linkage in *Chlamydomonas reinhardtii* (Feldman & Marshall, 2009). Although the mechanism involved in TBCCD1 centrosome-nuclear association is still not clear, it does not seem to constitute a physical link between the nucleoskeleton and the centrosome (Gonçalves *et al*., 2010), as it is in the case of other proteins related to the centrosome perinuclear positioning, such as ZYG-12 (Malone *et al*., 2003), Kif9 (Tikhonenko *et al*., 2013) Emerin (Salpingidou *et al*., 2007) or Samp1 (Buch *et al*., 2009).

In the case of RPE-1 cells overexpressing TBCCD1, no distinctive phenotype is detected in relation to the centrosome position, or Golgi apparatus organization. However, in RPE-1 cells depleted of TBCCD1, a distinct phenotype is observed: siRNA cells do not become confluent, are larger than control cells, have difficulties in assembling primary cilia, present a cell-cycle delay in G1, the centrosome is often located at the cell periphery distant from the nucleus, and the Golgi apparatus is disorganized, appearing to follow the centrosome or be fragmented and spread out in the cytoplasm. This Golgi apparatus phenotype is probably explained by the displacement of the centrosome and the MT aster that could lead to the displacement of the Golgi to the new centrosomal position. Nevertheless, a direct participation of TBCCD1 in Golgi organization and positioning cannot be excluded (Gonçalves *et al*., 2010).

When siRNA RPE-1 cells are invaded by *T. gondii* or *B. besnoiti*, the centrosome of the host cell is distributed in a random orientation with respect to the PV (Fig. 17). In this case, the loss of constraint in centrosome position was not associated with altered MT distribution, since Mts are still detected surrounding the PV (Fig. 16). It seems that parasites invading cells depleted of TBCCD1 are still able to modulate the MT cytoskeleton of the host cell to their advantage, without displacing the centrosome to the PVM. The non recruitment of the centrosome in invaded siRNA cells by *T. gondii* does not implicate differences in the number of invaded cells and replication of the tachyzoites. Meanwhile, the number of PVs *per* cell is reduced in *T. gondii* invasion of cells depleted of TBCCD1, which might indicate a higher difficulty after the first invaded tachyzoite, of subsequent tachyzoites to invade a host cell (Fig, 23), maybe because of an altered dynamics of the MT cytoskeleton in these cells (despite the fact that in RPE-1 cells depleted of TBCCD1, misplaced centrosomes are still able to nucleate MTs and no changes of MT organization are evident (Gonçalves *et al*., 2010; André *et al*., 2013)). Considering that in the first steps of *T. gondii* invasion there is an

interaction with the host cell cytoskeleton, it is reasonable to consider that any changes in the MT dynamics could reflect on the capacity of these parasites to invade. In terms of the Golgi apparatus, it is interesting to notice that in *B. besnoiti* invaded siRNA cells there is a significant compaction, and possible organization, of the previous fragmented and dispersed Golgi apparatus, that acquires a position close to the PV. On the contrary, in *T. gondii* invaded cells it remains fragmented and dispersed throughout the cytoplasm (Fig. 18).

In RPE-1 cells overexpressing TBCCD1, the recruitment of the centrosome by *T. gondii* at 18h of invasion is inhibited, with a significant decrease in the nucleus-centrosome distance when compared to invaded RPE-1 WT cells (Fig. 13). Moreover, in these cells *T. gondii* replication is delayed when compared to WT RPE-1 cells (Fig. 22), suggesting that *T. gondii* replication requires an efficient recruitment of the host cell centrosome, with the manipulation of the molecular mechanisms involved in the nucleus-centrosome connection. In RPE-1 cells overexpressing TBCCD1 the recruitment and overall morphology of the Golgi apparatus in invaded cells by *B. besnoiti* and *T. gondii* is similar to invaded RPE-WT cells.

The fact that in RPE-1 cells overexpressing TBCCD1, only replication, but not invasion of *T. gondii*, is decreased in these cells supports the hypothesis of the recruitment of the centrosome being important only in later, replicating stages, of the tachyzoite. In the case of invaded siRNA cells by *T. gondii* the non recruitment of the centrosome does not show any alteration in the number of invaded cells and replication of the tachyzoites, perhaps because the loss of centrosome constraint makes it possible for the parasite to explore the MT cytoskeleton without recruiting the centrosome to the PVM. Interestingly, the different manipulation of the host cell cytoskeleton by *B. besnoiti* is also shown in these results, as no changes in invasion and replication are found either in invaded RPE-1 cells overexpressing TBCCD1, or in siRNA cells.

2.4.5 - The impact on host cell migration

For directed cell migration, a dynamic nucleus–centrosome connection is important, and several studies reported centrosome reorientation towards the leading edge in migrating cells. However, the relevance of this reorientation is questionable, since it is not true for all cell types and is also substratum-dependent (Yvon *et al*., 2002). Apart from the centrosome, in migrating cells, the Golgi apparatus is also repositioned to face the cell's leading edge (Kupfer *et al*., 1982). Moreover, recent studies suggest a role for the Golgi ribbon in directed secretion and migration: cells with a fragmented Golgi apparatus by depletion of GMAP210 or Golgin-160, but with an intact MT network, continue to secrete, but fail to target the

leading edge and as a consequence the polarized state is not achieved and cells fail to migrate (Yadav *et al*., 2009). Considering that secretion is required for maintaining cell polarity and it becomes directed to the leading edge, Golgi positioning in the direction of cell migration allows the directional trafficking of cargo to the leading edge. Thus, dispersion of the Golgi ribbon, or inhibition of Golgi-associated MT nucleation, perturbs directional cell migration (Miller *et al*., 2009; Yadav *et al*., 2009). This way, it has been proposed that the centrosome is indirectly responsible for polarized cell migration, via organizing integral Golgi apparatus in an MT-dependent manner (Vinogradova *et al*., 2012).

Having in consideration the importance of Golgi apparatus and centrosome reorientation to the leading edge of a migrating cell, we could suppose this partly explained the wound closing delay in cells invaded by *T. gondii*. Since *T. gondii* recruits the host cell centrosome to the PV, the constraint of the centrosome in these cells could impair the reorientation required for directional migratory responses. The same constraint of the Golgi apparatus, localized next to the PV, could justify the difficulty in closing the wound by parasitized cells. Measuring the angle for centrosome and Golgi reorientation (Fig. 28) this hypothesis is not confirmed, since the mean angles for the reorientation of the Golgi and centrosome in cells invaded by *T. gondii* are close to the mean angles of non invaded cells. The fact that *B. besnoiti* invaded cells are not impaired in migration supports the idea that the positioning of the Golgi apparatus next to the PV, that could difficult Golgi reorientation, is not the cause of the wound healing delay observed in *T. gondii*. As an intact Golgi ribbon is necessary to deliver cargo to specific domains on the cell surface, the fact that *T. gondii* causes a fragmentation of the Golgi apparatus, impairing ribbon integrity, could result in polarization defects and explain the failure in directed cell migration. Despite the fact that in our experiments the Golgi ribbon seems to be, at least partially, reorganized (non-fragmented) in migrating cells invaded by *T. gondii* (Fig. 26 and Fig. 27), it could still be implicated a disturbance in directed secretion of the Golgi apparatus. Nonetheless, the mechanism responsible for the delay in wound healing in cells invaded by *T. gondii* is still to be determined.

It is interesting to notice that *T. gondii* modulation of the migratory response of a host cell is also detected in other cells, as in DCs (Diana *et al*., 2005) or macrophages (Lambert *et al*., 2010). However, in these cells they cause a hypermigratory phenotype, in contrast with the phenotype observed in RPE-1 host cells.

Following oral infection, *T. gondii* crosses epithelial and endothelial cellular barriers, enters the lymphatic system and blood, and disseminates within the organism (reviewed in Blader & Saeij, 2009). DCs are cells that traffic from infected tissues to the spleen and draining lymph nodes, making them good targets for *T. gondii* to disseminate within the host. In fact,

compared to uninfected DCs, early infected DCs migrated at higher speeds, for longer distances, exhibiting superior transmigration across endothelial monolayers *in vitro* (Diana *et al*., 2005; Lambert *et al*., 2006). Interestingly, the induction of cell migration by *T. gondii* is also exhibited by infected macrophages but not by infected monocytes, T-cells, B-cells or NK-cells (Lambert *et al*., 2010). Alternatively, *T. gondii* is also able to actively penetrate epithelial monolayers and extracellular matrix using gliding motility (Dobrowolski & Sibley, 1996; Barragan & Sibley, 2002).

The different migration phenotype when comparing *T. gondii* infected retinal pigment epithelial cells (RPE-1 cells) with DCs could be due to the different characteristics of the cytoskeleton of these cells during migration. The possibility to develop a diverse range of dynamic interactions in different environments, sets migrating leukocytes apart from epithelial cells of slow, integrin-mediated adhesion (Friedl *et al*., 1998; Maaser *et al*., 1999). DCs have a rapid and highly dynamic low-adhesive migration strategy, dominated by shape change and morphological adaptation. Epithelial cells, contrary to DCs, have a well defined apical-basal polarity, and cell-cell interactions (like tight junctions), being cell migration dependent on defined force-generating extracellular matrix-integrin complexes, termed focal adhesions. On the other hand, migrating leukocytes develop a highly polarized morphology: a leading edge, the main cell body, and the trailing edge, consisting of a small cytoplasmic backward projection, the uropod (Haston *et al*., 1982; Friedl & Bröcker, 2000). The main body contains the nucleus followed by a narrowing transition zone, where the MTOC is localized (Ratner *et al*., 1997). When DCs become polarized and begin random translocation over the substratum, they present a well-developed broad and stable leading edge, constantly developing new interactions with the substratum, and a uropod that retracts into the cell body at sporadic intervals, resulting in net cell translocation (Burns *et al*., 2001). This different migration phenotype of DCs (in relation to epithelial cells), based on high morphological adaptation, could be related with a different MT cytoskeleton dynamics. In fact, before polarization, T-cells are spherical, the MTOC is located beneath the plasma membrane, and MTs form a basket-like structure around the nucleus. After polarization, the MTs retract into the uropod, with the MTOC in the posterior tip of this structure, playing no active role in motility. This is a configuration that is likely to permit lymphocytes to assume the flexible form required for passage through narrow intercellular channels and extracellular matrix lattices (Ratner *et al*., 1997). The observation that DCs, but not RPE-1 cells, exhibit enhanced migration could also be related to the fact that in DCs *T. gondii* was shown to remain at the cell periphery, underneath the plasma membrane, without dividing. In fact, in these cells 90% of the parasite-positive cells carried a single tachyzoite, while very few cells contained a

parasite-forming rosette (Courret *et al*., 2006). However, it is unclear if the nearly absent replication inside DCs would cause the hypermigratory phenotype; or if it would be a consequence of the different manipulation of the host cell cytoskeleton inside these cells, indicating that a selective mechanism underlies *T. gondii* induced cell migration, probably depending on the MT cytoskeleton of the host cell (Lambert *et al*., 2010).

The same pathways for dissemination were established in *N. caninum*: migrating across polarized trophoblastic monolayers powered by the parasite's own active gliding motility; and infecting DCs (causing also a hypermotility phenotype) (Collantes-Fernandez, *et al*., 2012). However, in the apicomplexan parasite *T. annulata*, the motility of infected macrophages was reduced *in vitro* (Baumgartner, 2011). Together with the fact that *B. besnoiti* does not cause a delay in wound healing in infected RPE-1 cells, this proves that different apicomplexan target the migratory machinery of host cells via different mechanisms. These differences could be related with the different pathogeny of the parasites.

Chapter 3: The role of components of the tubulin folding pathway in *Besnoitia besnoiti* and *Toxoplasma gondii* host cell invasion

3.1 - Introduction

Apicomplexan parasites have the characteristic cytoskeleton components of eukaryotic cells MTs, actin, and IF-like proteins). However, they present differences potentially relevant for the host cell invasion process. For example, subpellicular Mts are highly resistant to conditions that lead to Mts depolymerization, such as cold, antimitotic agents, detergents, and high pressure (reviewed in Morrissette & Sibley, 2002b); which suggests that they may interact with different stabilizing agents like MAPs and/or be post-translated modified. In fact, polyglutamylated and acetylated tubulin has been detected in *B. besnoiti*, with a pattern of distribution similar to that observed for *T. gondii*, with polyglutamylation of Mts preferentially observed in the subpellicular Mts in the anterior pole of the *B. besnoiti* cells, including the conoid (Nolasco, S., unpublished results). Another difference in the apicomplexan cytoskeleton is shown in *T. gondii* where in the conoid tubulin is arranged into a polymer that is quite different from typical Mts (Hu *et al*., 2002). Furthermore, using indirect immunofluorescence it was observed that isolated *B. besnoiti* possesses a set of subpellicular Mts spirally arranged that extend from the apical end for more than 2/3 of the cell body towards the posterior edge (Reis *et al*., 2006). Noteworthy, upon interaction with the host cell *B. besnoiti* undergoes dramatic modifications of its shape and surface, as revealed by atomic force microscopy. These alterations are accompanied by a re-organization of the protozoa Mt cytoskeleton, characterized by the loss of the subpellicular Mts, giving raise to tubulin globular-like structures: tachyzoites lose their crescent cell shape and begin to acquire an irregular aspect due to the appearance of bubble-like small structures on the surface of the parasite. It was also showed that *B. besnoiti* invasion of the host cell may require a modulation of the host cytoskeleton, as host Mts start to surround the parasite upon the first steps of invasion, originating an Mt web with a cone shape (Reis *et al*., 2006). A similar model for *T. gondii* host cell invasion was proposed by Walker *et al*., 2008 and Sweeney *et al*., 2010. These facts point to an important cross talk of the Mt cytoskeleton of both parasite and host cell in the first steps of invasion and indicate that the specialized Mt cytoskeleton of these parasites is a key player in the invasion process. Thus, we postulate that the tubulin folding machinery of the parasite, controlling synthesis flux and transport of tubulin, will play a crucial role in the Mt arrays rearrangements and dynamics of *B. besnoiti* and *T. gondii* during host cell invasion.

3.1.1 - Tubulin folding pathway

As mentioned in the previous chapter, the MT subunits are heterodimers composed of one α-tubulin and one β-tubulin that undergo a complex folding processing before they achieve a quaternary structure that will allow their incorporation into the MT protofilament. Considering the extremely high protein concentration that exists at the cell cytoplasm, there are proteins that prevent the unwanted interaction of these polypeptides (α- and β-tubulin) with the surrounding protein pool during folding. This way, the CCT (cytosolic chaperonin containing TCP-1) intervenes through tubulin and actin folding (Sternlicht *et al*., 1993). Various other cofactors (tubulin cofactors-TBCA, TBCB, TBCC, TBCD, TBCE) identified along the α- and β-tubulin postchaperonin folding route (Lewis *et al*., 1997) are now known to have additional roles in tubulin biogenesis such as participating in the transport and storage of α- and β-tubulin.

3.1.1.1 - CCT (Chaperonin containing TCP-1)

Chaperonins are a ubiquitous family of proteins that can modulate the oligomerization and polymerization of folded native proteins. Actin and tubulin both require interactions with the CCT, also called TCP-1 ring complex (TRiC), in order to reach their native states (Sternlicht *et al*., 1993). The interactions between CCT are sequence-specific and electrostatic in nature. This results in CCT activity being linked to any cellular process that depends on the integrity of the microfilament and MT-based cytoskeletal systems (reviewed in Brackley & Grantham, 2009).

CCT, found in the cytoplasm of all eukaryotic cells, is a large cylinder (900 kDa) formed from two rings, each ring containing eight distinct subunits, which are the products of individual genes: α, β, γ, δ, ε, ζ, η and θ (corresponding to Cct1p-Cct8p in yeast) (Liou & Willison, 1997). Each subunit occupies a fixed position in the chaperonin ring, with every subunit interacting with only one subunit from the opposite ring (Ditzel *et al*., 1998). The reason for eight different subunits seems to be that certain specific combinations of subunits interact with specific structural features or motifs of the protein substrates and hence eight different subunits give a large number of combinations to accommodate a broad variety of substrates (Llorca *et al*., 2001). In each subunit it is possible to identify an equatorial domain that contains the ATP-binding site and both inter- and intra-ring contact sites, an apical domain that is substrate binding, and an intermediate linker domain which connects the first two domains. A built-in lid is formed from helical protrusions that erupt from the apical

domains of all eight CCT subunits, facilitating the encapsulation of folding substrates within the chaperonin cavity (reviewed in Brackley & Grantham, 2009).

Like other chaperonins, CCT uses its large conformational rearrangements generated upon ATP binding to assist in the folding of other proteins (Schoehn *et al*., 2000). With an active folding mechanism , the movements of the apical domains induced upon ATP binding and hydrolysis seal the chaperonin cavity and force the change of the bound, open conformations of actin and tubulin towards compact, quasi-native (or native) structures that are not liberated into the CCT cavity but remain bound to the chaperonin (Fig. 29A) (Llorca *et al*., 2001).

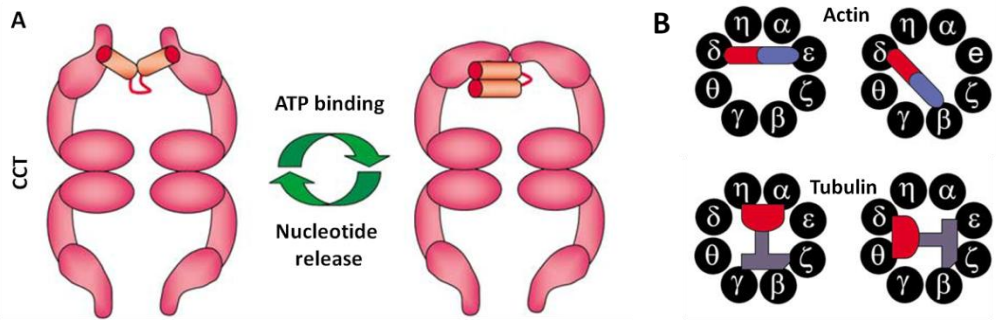

Fig. 29: CCT folding mechanism.

(A) A schematic model of the folding mechanism of CCT. CCT cycles between an open, substrate-receptive conformation and a closed conformation. The apical domains of specific subunits recognize a substrate conformation that has acquired an important degree of secondary and tertiary structure. The sealing of the CCT cavity, carried out by the movements of the apical domains induced upon ATP binding/hydrolysis, is performed by the helical protrusions present at the tip of the apical domains, and the substrate is not liberated in the CCT cavity but remains bound to the apical domains and forced to acquire a more compact, native conformation. (B) The actin and tubulin molecules, already in a quasi-native conformation, interact with the nucleotide-free, open conformation of CCT through specific subunits. The N-terminal domains of actin and tubulin are depicted in red, whereas the C-terminal domains are colored blue. Adapted from Valpuesta *et al.*, 2002.

In the case of the eukaryotic chaperonin, the interaction with its unfolded substrates, actin and tubulin, occurs between specific CCT subunits and the binding determinants of the two cytoskeletal proteins (Fig. 29B) (Rommelaere *et al*., 1999; Llorca *et al*., 2000). Actin and tubulin both bind to CCT in open conformations, binding directly to CCT subunits: actin binds to two subunits (CCTδ and CCTβ or CCTδ and CCTε), and tubulin to five CCT subunits also in two alternative modes of interaction (between CCTα, CCTβ, CCTγ, CCTη and CCTζ; or CCTβ, CCTζ, CCTθ, CCTε and CCTδ) (Llorca *et al*., 1999; Llorca *et al*., 2000).

Other proteins are known to interact with CCT: proteins involved in cell cycle regulation (Cdc20p (Camasses *et al*., 2003)), Cdh1p, Polo-like kinase 1 and cyclin E), Gα-transducin, (involved in retinal phototransduction), the Von Hippel Lindau tumor suppressor protein, luciferase, and members of the WD repeat containing family (reviewed in Brackley & Grantham, 2009). Other proteins that are folded by CCT are certain viral proteins such as the Epstein-Barr virus-encoded nuclear protein (EBNA-3), the hepatitis B virus capsid and the type D retrovirus Gag polyprotein (reviewed in Valpuesta *et al*., 2002).

Being essential in tubulin and actin folding, the effects of reducing CCT levels by siRNA in mammalian cultured cells, reflect in cell cycle progression (cell cycle events are delayed in CCT(RNAi) embryos). Reduction in CCT levels by siRNA also leads to disorganization of the actin-based cytoskeleton in mammalian cells: depletion of CCT does not affect actin polypeptide synthesis but causes a reduction in levels of native actin and perturbation of actin-based cell motility (Grantham *et al*., 2006).

Although it is clear that it is the CCT chaperonin that is essential for the folding activity of actin and tubulin, the CCT subunits themselves may have an important activity in MT organization and dynamics, interacting with forms of assembled MT structures. This way, the CCTθ subunit has been implicated with the Ras signaling pathway during yeast morphogenesis (Rademacher *et al*., 1998). In *Tetrahymena*, the expression of some CCT subunit genes is modified by perturbations in Mt arrays induced by antimitotic agents (Casalou *et al*., 2001). CCT-subunits form a complex with the chaperonin-like BBS6, BBS10 and BBS12 proteins (vertebrate specific BBS genes, Seo *et al*., 2010) required for BBSome assembly - an oligomeric complex of BBS (BBS1-2, BBS4-5, BBS7-9) proteins that have been directly implicated in ciliogenesis by promoting vesicle trafficking to the cilia membrane (Nachury *et al*., 2007). The adrenal medullary form of CCT (chromobindin A) binds efficiently to chromaffin granule membranes (reviewed in Kubota *et al*., 1995). The CCTη subunit of *B. microti* was cloned during a study of immunogenic antigen identification, and passive immunisations using the monoclonal antibody against this protein showed a significant inhibition of parasitaemia caused by *B. microti* (Nishisaka *et al*., 2001). Finally, some CCT subunits (α, γ, ζ and θ) behave as MAPs *in vitro*, with the presence of selected CCT subunits in MAP preparations, pointing to functions other than those undertaken when they are incorporated into the core of the CCT chaperone (Roobol *et al*., 1999).

The activity of CCT is linked to other chaperones: GimC, also known as prefoldin (PFD) is a cochaperone of CCT that exists both in archaea and eukaryotes that binds non-native actin and tubulin and forms a transient ternary complex with CCT, delivering substrates to CCT for folding in a protected compartment (Vainberg *et al*., 1998).

3.1.1.1.1 - CCTα

CCTα gene is highly expressed in testis (Willison *et al*., 1990), and this subunit is more abundant in growing neurites than other CCT-subunits (Roobol *et al*., 1995). Noteworthy, mouse CCTα mRNA is present in high levels in postimplantation embryos and rapidly growing cells in tissue culture (Kubota *et al*., 1992). The fact that CCTα subunit does not always co-localize with the other subunits, is another important observation that suggests other functions for CCTα as a free entity.

The amino acid sequence of CCTα is highly conserved in eukaryotes (animals, plants, yeasts and protozoa). Mouse CCTα shows more than 95% identity to CCTα of other mammalian species and more than 60% identity to those of other animals, plants and yeasts (reviewed in Kubota *et al*., 1995). In terms of localization, granular structures in cytoplasm are seen in addition to diffuse background staining, when antibodies anti-CCTα are used in cultured cells (Lewis *et al*., 1992).

Strengthening the hypothesis that CCT subunits free or as part of oligomeric complexes could have distinct additional roles *in vivo*, is the fact that CCTα has been localized at the centrosome, where incubation with an antibody against CCTα *in vitro* prevents Mt growth, indicating that CCTα may be essential for nucleated MT assembly from this organelle (Brown *et al*., 1996), and at the manchette (MT structure unique to male germ cells) during spermiogenesis (Soues *et al*., 2003). Also, in *Tetrahymena* exponentially growing cells, the CCTα, CCTε, CCTδ, and CCTη-subunits colocalize with tubulin in cilia, basal bodies, oral apparatus, and contractile vacuole pores, indicating a putative association of these subunits with the Mt structures (Seixas *et al*., 2003). CCTα subunit was also detected in the final stages of sea urchin cilia regeneration and rabbit tracheal cilia and progressively appeared in regenerating embryonic cilia as their growth slowed down, suggesting a regulatory role correlated with growth or turnover (Stephens & Lemieux, 1999).

After the release from the cytosolic chaperonin, the quasi-native tubulin intermediates interact with tubulin-specific cofactors A; B; C; D and E. Native tubulin is released from a supercomplex that contains both α- and β-tubulin and cofactors C, D, and E after GTP hydrolysis (reviewed in Fanarraga *et al*., 2001).

3.1.1.2 - Tubulin folding cofactors

In mammals, five proteins have been identified in the folding and association of α- and β-tubulin polypeptides (Lewis *et al*., 1997): TBCA (tubulin folding cofactor A), TBCB (tubulin

folding cofactor B), TBCC (tubulin folding cofactor C), TBCD (tubulin folding cofactor D), and TBCE (tubulin folding cofactor E) (Gao *et al*., 1993, Tian *et al*., 1997). These cofactors have been implicated in tubulin dimer formation, as well as in MT dynamics, through the *in vivo* and *in vitro* regulation of tubulin heterodimer assembly and disassembly. The interaction of the cofactors with the tubulin heterodimer is represented in Fig. 30. There is free exchange of β-tubulin between TBCA and TBCD, and of α-tubulin between TBCB and TBCE, resulting in the formation of TBCD/β and TBCE/α, respectively. The latter two complexes interact, forming a supercomplex (TBCE/α/TBCD/β). Release of the native α/β heterodimer occurs via interaction of the supercomplex with TBCC and through GTP hydrolysis (tubulin cofactors behave as GTPase-activating proteins, stimulating the GTP-binding protein β-tubulin to hydrolyze its GTP). This reaction acts as a switch for the disassembly of the supercomplex and the release of the GDP-bound heterodimer that polymerizes in MTs following spontaneous exchange with GTP (Fontalba *et al*., 1993; Gao *et al*., 1993; Tian *et al*., 1997; Tian & Cowan, 2013).

In other organisms, like *S. cerevisiae* (Feierbach *et al*., 1999), *S. pombe* (Hirata *et al*., 1998; Radcliffe *et al*., 2000), *A. thaliana* (Steinborn *et al*., 2002), *T. brucei* (Fleming *et al*, 2013), *C. reinhardtii*, (Feldman & Marshall, 2009) or *Drosophila* (Baffet *et al*., 2012), the interactions between their cofactors and specific tubulin monomers are consistent with the results found in mammals.

After MTs catastrophe/depolymerization, a large proportion of the tubulin heterodimers are directly recycled into novel polymers. However, in some circumstances, highly modified tubulin polypeptides or specific tubulin isotypes might be targeted for destruction. Because the α- and β-tubulin heterodimer is a very stable complex, which does not dissociate under physiological conditions in the absence of tubulin cofactors (Caplow & Fee, 2002), these proteins seem to also contribute to α- and β-tubulin heterodimer dissociation *in vivo*, assisting in tubulin monomer recycling.

Considering this, the above mentioned reaction of the tubulin α/β-heterodimer assembly, can also be seen in reverse (Fig. 30): incubation *in vitro* of native heterodimers with a molar excess of TBCD or TBCE results in heterodimer disruption and the formation of the TBCD/β complex (the TBCE/α complex does not appear to exist as a stable entity (Tian *et al*., 1997)). This way, TBCD and TBCE participate in MT dynamics through the dissociation of the tubulin heterodimer by sequestering β- and α- tubulin respectively. The fact that during TBCD or TBCE overexpression massive MT depolymerization occurs (Bhamidipati *et al*., 2000; Martín *et al*., 2000; Kortazar *et al*., 2007; Tian *et al*., 2010b), points to this possible dual role for tubulin cofactors in the biogenesis and degradation of the tubulin heterodimer.

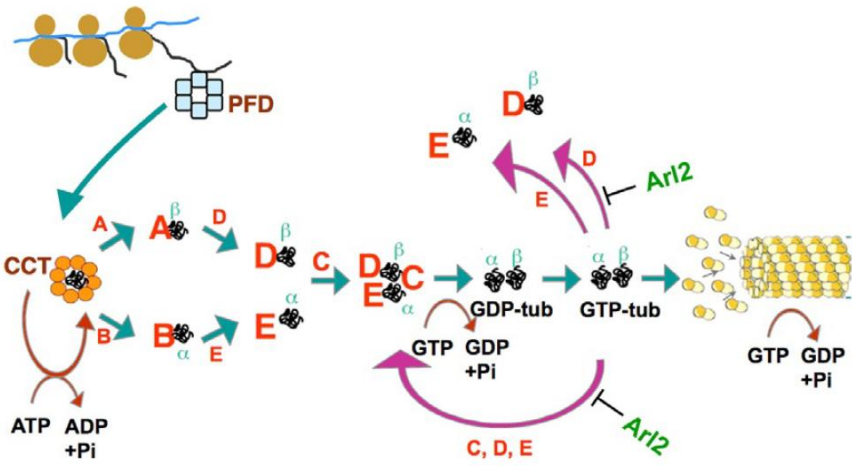

Fig. 30: The chaperone-dependent tubulin folding and heterodimer assembly pathway.
Nascent α- and β-tubulin polypeptides are bound by the chaperone protein prefoldin (blue) and transferred to the cytosolic chaperonin CCT (orange). As a result of multiple rounds of ATP-dependent interaction with the chaperonin, the tubulin target proteins adopt a quasi-native state defined by the acquisition of a native GTP-binding pocket. Quasi-native folding intermediates are captured and stabilized by TBCB (α-tubulin) or TBCA (β-tubulin). The tubulin proteins are transferred by free exchange to TBCD and TBCE, forming TBCD/β and TBCE/α. These complexes associate to form a supercomplex. Entry of TBCC into this supercomplex triggers hydrolysis of GTP, destabilizing and releasing newly formed α/β-tubulin heterodimers. TBCD and TBCE are each capable of disrupting the heterodimer in the back-reaction (shown as purple arrows in this figure); in the presence of TBCC and GTP, resulting in a perpetual cycling of tubulin polypeptides through the supercomplex. The activity of TBCD is modulated via its interaction with the small Ras family GTPase Arl2 (green). Adapted from Tian & Cowan, 2013.

Taking into account the capacity of TBCE to dissociate the heterodimer, Kortazar *et al.*, 2007, propose the existence of a complex in the tubulin dissociation route involving a TBCB–TBCE binary complex. Both cofactors contain two similar domains: an Ubl (ubiquitin-like domain; on the N and C termini of cofactors B and E, respectively) and a CAP-Gly domain (cytoskeletal associated protein glycine rich, characteristic of +TIP proteins) (Lytle *et al.*, 2004; Fleming *et al*, 2013). The CAP-Gly domain is known to be involved in tubulin binding (Riehemann & Sorg, 1993); while proteins with Ubl domain seem to catalyse the formation of ubiquitin–protein conjugates, whereas others appear to target ubiquitinated proteins for degradation or other non-degradative purposes (reviewed in Hartmann-Petersen & Gordon, 2004). TBCE might require its Ubl domain to either be processed by the ubiquitin-proteasome pathway as demonstrated for TBCB, or to send tubulin to the degradative route (Wang *et al.*, 2005). Having in consideration that TBCB and TBCE physically interact in the absence of tubulin, Ubl domains (that are usually involved in protein-protein interactions) of TBCB and

TBCE may contribute to the interaction between the two proteins (Lytle *et al*., 2004). The observation that both TBCB and TBCE do not bind MTs despite containing a CAP-Gly domain might reflect the need for two CAP-Gly domains for MT binding. In fact, a TBCB mutant containing only the CAP-Gly domain of this protein does not localize on MTs and it has no effect on MT depolymerization. After the dissociation of the heterodimer, it is possible that the α-tubulin polypeptide fits better into a single CAP-Gly domain-containing protein, inducing the ternary complex disassembly into either TBCB–α-tubulin and free TBCE; or TBCE–α-tubulin and free TBCB (Kortazar *et al*., 2007). The first option probably results in α-tubulin recycling; the second option could lead tubulin towards destruction because these complexes are unstable, and decay rapidly *in vitro* (Tian *et al*., 1997; Kortazar *et al*., 2006; Kortazar *et al*., 2007). Monomeric β-tubulin will readily be captured by TBCA or TBCD when present in the dissociation reactions (Kortazar *et al*., 2006; Kortazar *et al*., 2007).

While TBCB is not able to interact with, or dissociate, the tubulin heterodimer by itself, TBCE is, *per se*, effective in promoting this dissociation. Nonetheless, this TBCB-TBCE complex displays a more efficient stoichiometric tubulin dissociation activity than TBCE alone (Kortazar *et al*., 2007).

3.1.1.2.1 - TBCA (tubulin cofactor A)

The biochemical function of TBCA was studied in mammalian *in vitro* systems (Tian *et al*., 1996). It was shown that TBCA binds to β-tubulin intermediates derived from CCT, and that, in a next step β-tubulin is transferred to TBCD (Melki *et al*., 1996; Tian *et al*., 1996). TBCA seems to function as a β-tubulin chaperone, capturing and storing β-tubulin monomers after dissociation reactions, serving as a reservoir of still functional β-tubulin polypeptides and thereby as a buffer protecting the cell from an unbalanced α/β-tubulin ratio (Melki *et al*., 1996; Fanarraga *et al*., 1999; Abruzzi *et al*., 2002; Kortazar *et al*., 2006).

This protein is more abundantly expressed in testis, where it is progressively upregulated from the onset of meiosis through spermiogenesis, appearing to be associated with microtubular changes and with β-tubulin processing through spermatogenesis (Fanarraga *et al*., 1999).

The addition of exogenous TBCA protein to *in vitro* transcription–translation reactions of β-tubulin significantly increased the amounts of total tubulin heterodimer and β-tubulin bound to TBCA (Fanarraga *et al*., 1999). Knocking out of TBCA in plants (Kirik *et al*., 2002; Steinborn *et al*., 2002) or by RNAi gene silencing in mammalian cultured cells (HeLa and MCF-7) (Nolasco *et al*., 2005), has a lethal effect, with cells presenting a slightly disturbed Mt cytoskeleton. This may reflect the decrease of β-tubulin steady-state levels detected in this

cell lines upon transfection, that are accompanied also by a decrease of the steady-state levels of α-tubulin. In both mammalian cell lines death is preceded by a G1 cell cycle arrest that is probably due to the alterations of the Mt cytoskeleton. Although it is still not clear how TBCA knockdown affects the Mt cytoskeleton, it is probably a consequence of a decrease in the pool of α/β-tubulin heterodimers competent to polymerize (Nolasco *et al*., 2005).
Overexpression experiments of TBCA and Rbl2p (*S. cerevisiae* TBCA orthologue) have failed to demonstrate a clear phenotype. In contrast, overproduction of Alp31 (*S. pombe* TBCA orthologue) results in the disappearance of intact microtubular structures associated with cell polarity defects (reviewed in Fanarraga *et al*., 2001). Meanwhile, the function of the TBCA gene is dispensable in budding yeast and in fission yeast under normal growth conditions (Radcliffe *et al*., 2000).

3.1.1.2.2 - TBCB (tubulin cofactor B)

In the protozoa *T. brucei* this protein consists of 232 amino acids organized into the N-terminal Ubl domain and a CAP-Gly domain. The Ubl domain is a small globular entity consisting of a mixed four-strand β-sheet that forms a concave groove in which a single α-helix is placed (Fleming *et al*, 2013).
Recently, TBCB was found to associate with the CCT, probably recognizing α-tubulin still bound to CCT (Carranza *et al*., 2013). The proposed mechanism predicts that α-tubulin is released from CCT and bound to TBCB insuring that the α-tubulin monomer would never aggregate. Later, the monomeric tubulin subunit would be transferred to TBCE for dimer assembly and incorporation into growing MTs or would be transferred to the degradative pathway involving the proteasome, if not properly folded (Voloshin *et al*., 2010).
TBCB is a soluble cytoplasmic protein in interphase cells and also localizes at the centrosome and at the base of the primary cilium. As mitosis progresses towards metaphase, TBCB is often localized to spindle MTs. In anaphase most of this cofactor has progressively disappeared from the centrosome and is concentrated on the midbody MTs. By the end of telophase, TBCB is apparently absent from the centrosome, concentrating at the midbody. These localizations show that TBCB can bind to MTs. However this binding is indirect, occurring through the interaction of TBCB with a MT binding protein like EB1. Since EB1 is known to stabilize the plus ends of MTs, its interaction with TBCB explains how TBCB is able to promote a MT catastrophe when overexpressed, by sequestering EB1 from MT plus ends (Carranza *et al*., 2013).

Interestingly, the p21-activated kinase 1 (Pak1) phosphorylates TBCB on Ser-65 and Ser-128, playing an essential role in MT regrowth. TBCB can be also nitrated, mainly on Tyr-64 and Tyr-98, which attenuates the synthesis of new MTs. The fact that nitration of TBCB antagonizes phosphorylation of TBCB, and nitration of TBCB requires the presence of functional Pak1 phosphorylation sites, supports the existence of a regulatory feedback inhibitory role of TBCB nitration on MT biogenesis in eukaryotic cells with stimulated Pak1 signaling (Rayala *et al*., 2007). Moreover, this cofactor shows also a mechanism of autoinhibition by its C-terminus, implying the interaction of the C-terminal tail of this cofactor (by the last three amino acid residues) with its own CAP-Gly domain, which prevents MT depolymerization (Carranza *et al*., 2013).

In humans, TBCB has been implicated in cancer (Vadlamudi *et al*., 2005), neurodevelopment malformations (Tian *et al*., 2010a), schizophrenia (Martins-de-Souza *et al*., 2009) and neurodegenerative processes (Wang *et al*., 2005). Despite this, the function of TBCB *in vivo* is poorly understood: in *S. pombe*, a knockout of TBCB results in a specific decrease of α-tubulin levels that correlates with an affected MT network and defects in cell division (Radcliffe *et al*., 2000). In several mammalian cell types, however, TBCB knockdown does not affect tubulin levels nor does it destabilize the MT network (Vadlamudi *et al*., 2005). Meanwhile, overexpression of TBCB induces MT depolymerization in human cells through its interaction with TBCE (Kortazar *et al*., 2007). Studies in *Drosophila* confirm that TBCB is required for tubulin dimerization and for tubulin heterodimer dissociation, affecting the levels of both α- and β-tubulins and dramatically destabilizing the MT network in different fly tissues. Surprisingly, TBCB is dispensable for the early MT-dependent steps of oogenesis in *Drosophila*, including cell division, not being required for mitosis in several tissues. In contrast, the absence of TBCB during later stages of oogenesis causes major defects in cell polarity. This establishes a developmental function for TBCB in *Drosophila*: essential for viability, MT network integrity, and cell polarity, but not for cell proliferation (Baffet *et al*., 2012).

3.1.1.2.3 - TBCC (tubulin cofactor C)

TBCC is capable of inducing the TBCD/β-tubulin/TBCE/α-tubulin complex to release the native α-/β-heterodimer, since complexes formed between α-tubulin, β-tubulin, TBCD, and TBCE are not sufficient to release tubulin heterodimers (Zabala & Cowan, 1992). This way, the hydrolysis of GTP by tubulin, stimulated by TBCC and TBCD, is part of the heterodimer assembly reaction: hydrolysis of GTP by β-tubulin acts as a switch for the release from the

supercomplex of native, newly made tubulin heterodimers. In fact, TBCC and TBCD in combination have been shown to be GTPase activators (GAP) for native tubulin; with TBCE enhancing this tubulin-GAP activity (Tian *et al*., 1999).

The tubulin chaperone protein TBCC has a profound influence on tubulin pools and MT dynamics: cells with reduced TBCC content displayed increased MT dynamics; cells with increased TBCC content contain less polymerizable tubulin and display reduced MT dynamics (Hage-Sleiman *et al*., 2010; Hage-Sleiman *et al*., 2011).

TBCC is a protein found at the centrosome and is implicated in bipolar spindle formation (Garcia-Mayoral *et al*., 2011). Cells depleted of TBCC proliferate faster and show an altered cell cycle distribution, with a higher percentage in the S-phase of the cell cycle. This demonstrates that TBCC is a crucial protein in the control of the eukaryotic cell cycle, and supports the hypothesis that this tubulin binding cofactor could be implicated in genomic instability and cancer (silencing of TBCC is associated with enhanced tumor growth *in vivo*) (Hage-Sleiman *et al*., 2011).

In humans, TBCC relates with two proteins: retinitis pigmentosa 2 (RP2) and TBCCD1. RP2 acts as a GTPase-activating protein (GAP) for small GTPase Arl3 (Veltel *et al*., 2008) and has functions related to ciliogenesis in photoreceptors, as well as other cilia-related functions in kidney (Schrick *et al*., 2006), Golgi apparatus (Evans *et al*., 2010), and G protein trafficking (Schwarz *et al*., 2012). Noteworthy, all these three proteins (TBCC, RP2, and TBCCD1) have in common a conserved tubulin-folding cofactor C domain (TBCC; Fig. 31) that is responsible for GAP activity; and a CARP domain, which is found in cyclase-associated proteins (CAPs). TBCC interacts with components of the centrosome by its N-terminal domain, which has a coiled coil spectrin-like domain. This segment is highly charged and participates in tubulin interaction (Garcia-Mayoral *et al*., 2011).

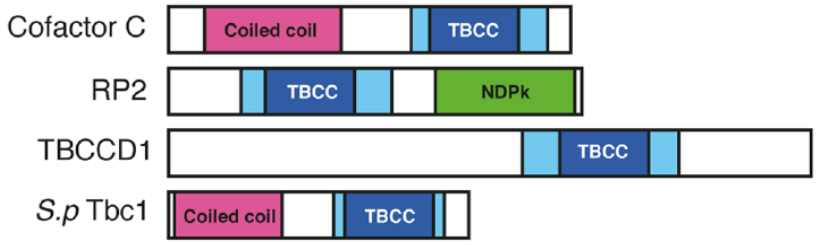

Fig. 31: The conserved domains of the human TBCC domain containing proteins and fission yeast Tbc1.

The TBCC domain is shown in blue, with the light blue indicating two CARP domains usually found in CAP (cyclase-associated proteins). The coiled-coil regions shown in magenta suggest a protein–

protein interaction domain (spectrin-like domain), and the nucleotide diphosphate kinase (NDPK) shown in green is a phosphocarrier domain. Adapted from Mori & Toda, 2013.

3.1.1.2.4 - TBCCD1 (TBCC-domain containing 1)

As previously referred, in humans TBCCD1 is contained within a family of proteins that is divided into three classes: canonical TBCC, retinitis pigmentosa 2 (RP2), and TBCCD1.

C. reinhardtii TBCCD1 localizes to a region sub-proximal to the centrioles, between the centrioles and the nuclear envelope (nucleus-centriole connectors known as rhizoplasts), also being found on the centrioles themselves (Feldman & Marshall, 2009). In human cell lines, TBCCD1 was found in the cytoplasm, the centrosome, the pericentriolar matrix, the basal body of primary cilia, the spindle midzone, and the midbody. André *et al*., 2013 localized TBCCD1 in *T. brucei*: close to the kinetoplast (trypanosome mitochondrial genome); as an elongate structure immediately anterior to the kinetoplast; in the anterior end of the cell body; at the basal and pro-basal body; and at the bilobe (an enigmatic cytoskeletal structure of unclear function and almost completely unknown composition).

A mutant of the green alga *C. reinhardtii* gene that encodes TBCCD1 establishes a bipolar spindle, but cells have defects in spindle orientation. The defects in centriole number control, centriole positioning, and spindle orientation, appear to arise from a primary defect in centriole linkage mediated by TBCCD1, which provides evidence that TBCCD1 in *C. reinhardtii* is required for mother–daughter centriole linkage (Feldman & Marshall, 2009). In the work of Gonçalves *et al.*, 2010, RPE-1 cells depleted of TBCCD1 showed the centrosome distanced from the nucleus, located at the cell periphery, and a disorganized and fragmented Golgi apparatus. In *T. brucei*, following TBCCD1 RNAi induction there is: retardation of the growth rate; loss of normal bilobe architecture, indicating that TBCCD1 plays an important role in organizing the formation of this structure; a flagellum detachment phenotype; cells either lacking kinetoplasts or possessing abnormally large kinetoplasts (loss of centriolar TBCCD1 that causes asymmetric mis-segregation of kinetoplast DNA); and loss of centriole linkage to the single unit-copy mitochondrial genome (or kinetoplast) of the parasite. Despite this, no perturbation of MT organization is evident (André *et al*., 2013).

The mechanism by which TBCCD1 is involved in all these phenomena is still unknown. Since TBCCD1 contains a TBCC domain, it could be a GAP for tubulin. However TBCCD1 lacks the obvious catalytic arginine of TBCC and RP2, although in the alignment of TBCCD1, RP2, and TBCC orthologues, an arginine residue was identified nearby (Feldman & Marshall, 2009). Other amino residues within the TBCC domain, conserved in TBCC and

RP2 (Kühnel *et al*., 2006), are not conserved in TBCCD1. Moreover, whereas TBCC and RP2 partially complement the yeast CIN2 (TBCC) deletion mutant (Bartolini *et al*., 2002), TBCCD1 cannot (Gonçalves *et al*., 2010). Thus the role of TBCCD1 as a GAP is strongly questionable. TBCCD1 also possesses a CARP domain—a characteristic of CAP proteins, which regulate actin polymerization. This way, TBCCD1 could promote a crosstalk between the centrosome, MTs, and actin cytoskeletons, required for centrosome positioning (Gonçalves *et al*., 2010). Another possibility is presented in experiments with *T. brucei*, where it is described that TBCCD1 is involved in filament formation, identifying TBCCD1 as an essential protein associated with filament-based structures in the trypanosome cytoskeleton (André *et al*., 2013). TBCCD1 presence in *Chlamydomonas* rhizoplasts, (striated fibers connecting proximal ends of flagellar basal bodies to the nucleus); and loss of mother–daughter centriole linkage in *C. reinhardtii*, is also consistent with a filament function (Feldman & Marshall, 2009). All these new data point to a TBCC domain with an essential non-tubulin, non-GAP-related function.

3.1.1.2.5 - TBCD (tubulin cofactor D)

TBCD is a large protein that is predicted to fold almost entirely into a series of α-helices with loops that form HEAT or armadillo repeats (Grynberg *et al*., 2003). This protein preferentially binds *in vivo* and *in vitro* to GTP-bound β-tubulin released from TBCA, being part of the formed supercomplex TBCE/α-tubulin/TBCD/β-tubulin (Tian *et al*., 1999).

The gene encoding TBCD is essential for life in higher eukaryotes, as shown by genetic experiments in the model organisms *S. pombe* and *A. thaliana* (Hirata *et al*., 1998; Radcliffe *et al*., 2000; Steinborn *et al*., 2002). The most likely candidate to regulate TBCD is Arl2, a protein that belongs to the Arl family, which represents a group of ARF (ADP ribosylation factors) related proteins, that has been shown to block the dissociating effect of TBCD *in vitro* and *in vivo* (Bhamidipati *et al*., 2000).

The fission yeast orthologue of TBCD is $Alp1^{D}$, and it is demonstrated to have an increased importance in this organism. $Alp1^{D}$ was shown to be toxic to the cell when massively overproduced (cells show severe defects in cell morphology with either short, fragmented MTs, or none at all (Mori & Toda, 2013)), and required not only for the β-tubulin pathway, but also for the α-tubulin pathway, suggesting its unique importance compared with the other cofactors (Hirata *et al*., 1998). Analysis of $Alp1^{D}$ leads to the hypothesis that it has two roles: to fold heterodimers in the tubulin-folding pathway and to depolymerize MTs, which is antagonized by its interaction with GDP-bound Alp41 (the orthologue of human Arl2 (Mori

& Toda, 2013)). Mori & Toda, 2013 propose a model in which Alp41 (that is GDP bound by the action of Tbc1 (the fission yeast orthologue of TBCC)) maintains and regulates MT dynamics by binding and absorbing the free $Alp1^{D}$ within the cell, inhibiting depolymerization of the MTs. Vertebrate TBCD has also MT-depolymerizing activities upon overproduction (Martín *et al*., 2000; Tian *et al*., 2010b).

The work of Cunningham & Kahn, 2008 shows that in mammalian cells TBCD is a centrosomal protein with functions critical to the recruitment of pericentrin and γ-TuRC, initiation of MT growth and organization of the mitotic spindle. It has been shown that TBCD accumulates in immature centrioles (procentrioles) and at the midbody ring during cytokinesis, which suggests that TBCD plays a role in MT retraction during cell abscission, probably by involvement in tubulin heterodimer dissociation (Fanarraga *et al*., 2010a). In fact, TBCD is a centriolar protein implicated in the actual process of centriologenesis and in the assembly and maintenance of the bipolar mitotic spindle (Cunningham & Kahn, 2008; Fanarraga *et al*., 2010a). The accumulation of TBCD in procentrioles is gradually lost during the maturation process, coinciding with MT glutamylation. This might indicate that TBCD participates in the supply of tubulin to procentrioles, while binding and protecting the developing centriolar blades until MT assembly is complete (Fanarraga *et al*., 2010a).

Overexpression of TBCD leads to the loss of anchoring of the γ-TuRC and of nucleation of MT growth at centrosomes (Cunningham & Kahn, 2008); and G1 arrest (Fanarraga *et al*., 2010a). Meanwhile, depletion of TBCD results in mitotic spindle defects (Cunningham & Kahn, 2008) and incomplete MT retraction at the midbody during cytokinesis (Fanarraga *et al*., 2010a). Neither overexpression, knockdown, or expression of mutants of TBCD, leads to any detectable changes in the levels of α-, β-, or γ-tubulins, indicating that the phenotypes observed are not due to changes in tubulin protein levels. These activities each appear to be distinct from the previously described role for TBCD in tubulin heterodimer assembly/disassembly (Cunningham & Kahn, 2008).

3.1.1.2.6 - TBCE (tubulin cofactor E)

TBCE is a protein that associates with α-tubulin after it is released from TBCB. It is mostly a cytoplasmic protein, like all TBCs (in accordance with their tubulin-chaperoning function), but it also accumulates at the Golgi apparatus of motor neurons, where it is essential for axonal tubulin routing (Schaefer *et al*., 2007).

Homologues of TBCE have been identified in several eukaryotic species, such as *S. cerevisiae* (Pac2p (Hoyt *et al*., 1997)), *S. pombe* (Alp21 (Radcliffe *et al*., 1999)) and *A. thaliana* (PFI

(Steinborn *et al*., 2002)). Pac2p, which has 26% identity to human TBCE, is required for normal MT stability and, when overexpressed in *S. cerevisiae*, is detected in a complex with α-tubulin (Hoyt *et al*., 1997). Alp21 is an essential protein in *S. pombe* involved in the generation of normal MTs (Radcliffe *et al*., 1999). Although the exact mechanism involved in the binding of TBCE to α-tubulin is still unknown, several TBCE homologs contain a N-terminal CAP–Gly domain, an Ubl domain, and leucine-rich repeats (LRR - frequently involved in protein–protein interactions) (Grynberg *et al*., 2003). TBCE might require its Ubl domain to the interaction with the 26S proteasome, thereby linking tubulin destabilization to its degradation *in vivo*. In fact, a TBCE paralogue in mammals, which lacks the CAP-Gly domain (E-like protein, with ~ 30% sequence identity with TBCE) but has an Ubl domain, instead of being involved in tubulin biogenesis, is implicated in degradation (Bartolini *et al*., 2005).

In addition to the *de novo* folding of tubulin dimers, there is evidence that TBCE also influences MT dynamics based on its ability to act both as part of a GTP-activating complex on native tubulin (in combination with TBCC and TBCD, Tian *et al*., 1999) and to sequester α-tubulin subunits from native heterodimers *in vitro*. In the latter reaction, the heterodimer is disrupted and the free subunit decays to a non-native state (Bartolini *et al*., 2005). Consistent with TBCE predicted multifunctional role in the biogenesis and regulation of the tubulin heterodimer, are the following findings: mutations in the *A. thaliana* TBCE gene (PFI) result in microtubular defects (Steinborn *et al*., 2002); an amino acid deletion in murine TBCE results in a progressive motor neuropathy in mice that causes premature death in homozygotes (Martín *et al*., 2002); human mutations of the TBCE gene lead to both Kenny–Caffey and Sanjad–Sakati syndromes - microtubular defects consistent with alterations in the tubulin folding and dimerization pathways have been shown in cells cultured from patients with Kenny–Caffey and Sanjad–Sakati syndromes (Parvari *et al*., 2002).

Considering the facts described above for all tubulin cofactors, and despite the role in heterodimer assembly/disassembly, it seems that these cofactors can also directly modulate MT behavior, being key participants in the reorganization of the cell cytoskeleton. For example: TBCB plays a role in determining MT behavior in the neuronal growth cone (Fanarraga *et al*., 2007), and regulates MT density in microglia during their transition to reactive states (Fanarraga *et al*., 2009); TBCC is involved in tumor cell regulation (Hage-Sleiman *et al*., 2010); TBCD localizes at the Fleming bodies, ring-like structures localized at the midbody during cytokinesis, where it is implicated in cell abscission (Fanarraga *et al*., 2010a, 724). TBCD also participates in basal body assembly in differentiating ciliated cells

where there is a recruitment of this cofactor into round structures that surround a γ-tubulin central spot, which are called «centriolar rosettes» (Fanarraga *et al*., 2010a; Fanarraga *et al*., 2010b), and is detectable at the base of the mammalian spermatozoa flagellum, where highly sophisticated MTs are also assembled and maintained (Fanarraga *et al*., 2010b).

Taking into account the remodeling of the parasite and host cytoskeleton during *B. besnoiti* and *T. gondii* cell entry, we proceeded with the characterization and analysis of the pattern of expression of the CCTα-subunit gene of *B. besnoiti* and *T. gondii*; and of α-tubulin, TBCB and TBCE in *T. gondii*, at different steps of host cell invasion/infection. It was also addressed the intracellular localization of CCTα-subunit in *B. besnoiti* and *T. gondii* cells in order to try to establish a functional relation between Mt cytoskeleton re-arrangements and protein localization in the first steps of host cell invasion.

3.2 - Materials and Methods

3.2.1 - Cell culture and parasite culture

In this part of the work the following cell lines were used: Vero (ATCC® CCL8), and hTERT-RPE-1 (ATCC® CRL-4000). These cell lines were grown in DMEM/F12 with Glutamax (Invitrogen), supplemented with 10% fetal bovine serum and non-essencial amino acids (Invitrogen), maintained in a 37ºC incubator at 5% CO2 in a humid atmosphere, and passaged every 2-3 days, depending on cell confluence.

B. besnoiti Bb1Evora03 strain (Cortes *et al*., 2006b) and *T. gondii* (ME49 strain SAG1-Luciferase-BAG1-GFP, a kind gift from Andrea Crisanti, UK) tachyzoites were grown in Vero cells and maintained in DMEM with Glutamax (Invitrogen), supplemented with 10% fetal bovine serum and non-essential amino acids (Invitrogen). Tachyzoites were isolated by collecting the supernatant followed by centrifugation at 770g for 10 min.

3.2.2 - Characterization of genes involved in the tubulin folding of *Besnoitia besnoiti*

Relatively little is known about the molecular biology of *B. besnoiti*, so the first step to achieve the characterization of *B. besnoiti* genes, was to design primers that could amplify part of its coding sequence from cDNA. To do this, we took advantage of the sequences for the genes in study already sequenced and annotated for the closely related parasites *T. gondii* and *N. caninum*. The coding sequences from *N. caninum* (strain Liverpool) and *T. gondii* (strain ME49) were retrieved from the Eukaryotic Pathogen Database Resources (EuPathDB) and the *Toxoplasma gondii* Genomic Resources Database (ToxoDB), and aligned using ClustalW2 run on the European Molecular Biology Laboratory - European Bioinformatics Institute (EMBL-EBI). These alignments are presented in annex I, Fig 54. They were analyzed for regions of greater homology, and primer pairs were designed in order to try to amplify a PCR product of cDNA from *B. besnoiti* of each intended gene (CCTα, TBCB, TBCE and α-tubulin). In most cases, more than one primer pair was designed for each gene (Table 5).

Primer name	Oligonucleotide sequence
CCTα	
TCP1 alpha Left	5´-ATGGCACTCGCAATCTTCG-3’
TCP1 alpha Right	5´-CTTGATGATGTTGATCGAGCTGA-3’
CCTaReverse	5'- CTAGTCATCCTGTTGGCCC -3'
PR2CCTatoxo	5´- CCTTCGTCTTGCTCACAGC – 3´
TBCB	
TBCB Left	5’-CAAATTCACTCCAGAGGACCC -3’
TBCB Right	5’- CGGACCCACATAGGCAAC-3´
TBCB F	5’-GTCAAAGACAAGCTGTACAG-3’
TBCB R	5’- CCAGAGCCACGCCAATCC – 3’
TBCE	
TBCE Left	5´-TCCGATACATCGGTCCTGTC-3’
TBCE Right	5´-CGAGGAGCATGGAGTCTATTTG-3’
TBCE Forward	5’ – GACGCAGAGTTGTGGATAG – 3’
TBCE Reverse	5’ – CCTTGCGTCCGACGAATTC – 3’
α-tubulin	
PFATUBULINA	5´-ATGAGAGAGGTTATCAGCATC – 3’
PRATUBULINA	5’- TTAGTACTCGTCACCATAGCC – 3´

Table 5: List of used primers for each gene.

3.2.2.1 - cDNA synthesis

For cDNA synthesis, *B. besnoiti* tachyzoites were purified from *in vitro* cultures and total RNA was extracted with a commercial kit (High Pure RNA Isolation Kit - Roche). RNA was treated with the enzyme DNase I (Invitrogen) to eliminate genomic DNA. An RNA sample was reverse transcribed in two-step RT-PCR (Reverse transcription polymerase chain reaction) procedure with First Strand cDNA Synthesis Kit (Thermo Scientific Fermentas) for the production of cDNA.

3.2.2.2 - Thermocycling conditions for gene amplification

Since *B. besnoiti* genes were not yet characterized, the primers used were not homologous, so several PCR conditions were performed in order to try to amplify each gene from the pool of *B. besnoiti* tachyzoites cDNA. The main variation in terms of components (Table 6) was in $MgCl_2$ concentration, and all the reagents used were from Thermo Scientific Fermentas, with the exception of the primers that were synthesized by Sigma. In what concerns cycle conditions, several annealing temperatures were used (Table 7).

Component	Final concentration
10x Buffer	1x
$MgCl_2$	0,5 – 8,0mM (gradient of 0,5mM increments)
Primers	0,1-0,5 µM
dNTP	0,4–1,0 mM
Taq DNA Polymerase	1-2,5 units/25 µl of reaction
Template	≈50ng
Final Volume=25µl	

Table 6: Concentration of PCR components.

Cycle conditions	Guidelines
Denaturation	95°C. 5 min in the initial cycle; 30 seconds in the rest of the cycles.
Annealing	Temperature gradient: from 50ºC to 65ºC (with increments of 1ºC). 30 seconds.
Extension	72°C.~1 min/kb of expected product; 10 min in the last cycle.
Number of Cycles	40 cycles

Table 7: Cycle conditions used in PCR.

3.2.3 - Cloning of genes involved in tubulin folding of *Besnoitia besnoiti* and *Toxoplasma gondii*

For *B. besnoiti*, the only gene cloned was the 600bp of CCTα, since it was the only gene characterized. It was also cloned the ITS1 to serve as a housekeeping gene for real time PCR.
In the case of *T. gondii*, all genome is already sequenced and annotated. This way, we used the ToxoDB and EuPathDB in order to retrieve the sequences of the cloned genes: CCTα, TBCB, TBCE and α-tubulin. ITS1 was also cloned to use as a housekeeping gene in real time PCR.
Primer pairs were designed to amplify each intended gene from the cDNA of *B. besnoiti* and *T. gondii* tachyzoites (Table 8 and Table 9).

Primer name	Oligonucleotide sequence
CCTα	
PFCCTAToxo	5’ – CGCGGATCCCATATGGCACTCGCAATCTTCG - 3’
PRCCTAToxo	5’ – CCCAAGCTTCTAGTCATCCTGTTGGCCC - 3’
TBCB	
PFTBCBToxo	5’ – CGCGGATCCCATATGTCGGGCTTGTCTATCAAC - 3’
PRTBCBToxo	5’ – CCCAAGCTTTTAGATTTCGTCCAGCAAATC - 3’
TBCE	
TBCE Forward	5’ – GACGCAGAGTTGTGGATAG – 3’
TBCE Reverse	5’ – CCTTGCGTCCGACGAATTC – 3’
α-tubulin	
PFATUBULINA	5’ - ATGAGAGAGGTTATCAGCATC – 3’
PRATUBULINA	5’ - TTAGTACTCGTCACCATAGCC – 3’
ITS1	
PFITS1toxo	5’ - TATCGAAAGGTATTATTGC – 3’
PRITS1toxo	5’ – AGTATCCCAACAGAGACA – 3’

Table 8: List of primers for *T. gondii* cloning.

Primer name	Oligonucleotide sequence
CCTα	
PFCCTaResBb	5’ - CGCGGATCCCATATGGACCGCCAAAGTGGTCAG– 3´
PRCCTaResBb	5’- CCGGAATTCCGGGGTACTTGATGTCGC – 3´
ITS1	
Primer ITS1 Forward	5’ - TGACATTTAATAACAATCAACCCTT - 3’
Primer ITS1 Reverse	5’ - GGTTTGTATTAACCAATCCGTGA – 3’

Table 9: List of primers for *B. besnoiti* cloning.

3.2.3.1 - Thermocycling conditions for gene amplification

As it was mentioned, before cloning the genes listed above, they were amplified by PCR from the pool of *B. besnoiti* and *T. gondii* tachyzoites cDNA. The concentration of the reagents and the conditions used were equal for all genes and are listed in Table 10 and Table 11. All the reagents used were from Thermo Scientific Fermentas, with the exception of the primers that were synthesized by Sigma.

Component	Final concentration
10x Buffer	1x
$MgCl_2$	1,5mM
Primers	0,4 µM
dNTP	0,4mM
Taq DNA Polymerase	2,5 units / 25 µl of reaction
Template	~50ng
Final Volume=25µl	

Table 10: Concentration of PCR components.

Cycle conditions	Guidelines
Denaturation	95°C. 5 min in the initial cycle; 30 seconds in the rest of the cycles.
Annealing	Temperature: 60ºC. 30 seconds.
Extension	72°C.~1 min/kb of expected product; 10 min in the last cycle.
Number of Cycles	40 cycles

Table 11: Cycle conditions used in PCR.

3.2.3.2 - DNA electrophoresis analysis and gel extraction

After amplification, cDNA samples were run in an agarose gel. The concentration of agarose of the gel used was 1-2% (m/v), depending on the expected size of the cDNA. Gel electrophoresis was conducted with TAE buffer (Tris-Acetate-EDTA, 0,4M Tris acetate, containing 0,01M EDTA, pH 8,3). Upon completion of electrophoresis, the band of interest was excised with a sterile scalpel, and the DNA extracted with QIAquick Gel extraction kit from QIAGEN.

3.2.3.3 - pGEM®-T Easy vector and ligation reaction

DNA inserts were cloned in pGEM®-T Easy Vector from Promega. This is a linearized vector with a single 3'-terminal thymidine at both ends. The T-overhangs at the insertion site greatly improve the efficiency of ligation of PCR products by preventing recircularization of the vector and providing a compatible overhang for PCR products generated by thermostable polymerases. The ligation insert:vector was performed with a 2X Rapid Ligation Buffer and T4 DNA Ligase (both provided with the T Easy vector kit). Ligation reactions using this buffer were incubated for 1 hour at room temperature, or overnight at 4°C (the extended incubation period increases the number of colonies after transformation). The pGEM®-T Easy Vector is approximately 3kb and supplied at 50ng/µl. To calculate the appropriate amount of PCR product (insert) to include in the ligation reaction, the following equation was used:

$$\frac{\text{ng of vector} \times \text{kb size of insert}}{\text{kb size of vector}} \times \text{insert:vector molar ratio} = \text{ng of insert}$$

3.2.3.4 - Transformations using the pGEM®-T Easy vector ligation reactions

E. coli JM109 high efficiency competent cells (≥1 × 10^8 cfu/µg DNA) were used for transformations. These cells were provided with the pGEM®-T Easy Vector Systems II from Promega.

Briefly, the protocol used started with the preparation of LB (lysogeny broth medium, 10g/L tryptone, 5g/L yeast extract, 5g/L NaCl)/ampicillin/IPTG/X-Gal plates. 2µl of each ligation reaction was added to a sterile 1.5ml microcentrifuge tube on ice. Meanwhile, frozen JM109 competent cells were removed from storage at -80ºC and placed in an ice bath until just thawed (about 5 minutes). Carefully, 50µl of cells were transferred into each tube with the ligation reaction, and placed on ice for 20 minutes. After this, the cells were heat-shocked for 45–50 seconds in a water bath at exactly 42°C, and immediately returned to ice for 2 minutes. 950µl room-temperature SOC medium (super optimal broth medium with catabolite repression, 20 g/L tryptone, 5 g/L yeast extract, 4.8 g/L $MgSO_4$, 3.6 g/L dextrose, 0.5g/L NaCl, 0.19 g/L KCl) was added to the tubes containing cells transformed with ligation reactions, and incubated for 1,5 hours at 37°C with shaking. 100µl of each transformation culture was plated in LB/ampicillin/IPTG/X-Gal plates and incubated overnight (16–24 hours) at 37°C.

3.2.3.5 - Colony screening and isolation of plasmid DNA

After screening (by colony PCR) the colonies that grew overnight, positive colonies that contained the recombinant plasmid with the insert were further multiplied in liquid LB containing ampicilin (100µg/ml), overnight at 37ºC with shaking.

From these colonies, recombinant plasmid DNA was isolated and purified using a commercial kit - Plasmid Midi Kit from QIAGEN.

3.2.3.6 - DNA sequencing

Following isolation and purification of DNA from recombinant plasmids, the DNA was sequenced to confirm the identity of the cloned DNA fragment. Sequencing reactions were performed using the Big Dye Terminator v1.1 Cycle Sequencing kit from Applied Biosystems, according with manufacturer guidelines. The sequencing machine used was ABI Prism 377 DNA Sequencer (Applied Biosystems), and the software used was «377 DNA Sequencer», «filter set E» and «377 BigDye Terminator v1.1 Matrix Standards».

3.2.4 - Polyclonal antibody production against *Besnoitia besnoiti* CCTα

The polyclonal antibody was produced in INETI (Instituto Nacional de Engenharia, Tecnologia e Inovação), in the group of Doctor Carlos Novo, with the collaboration of Alexandra Tavares.

3.2.4.1 - Induction and purification of the protein

In order to produce a polyclonal antibody against *B. besnoiti* CCTα truncated protein, the corresponding region of the protein was cloned in the bacteria expression vector pET28a. Competent cells *E. coli* Rosetta(DE3)pLysS were transformed with the expression vector, and grown to an optical density of 0,4 to 0,5. The production of the protein was induced by the addition of IPTG (isopropyl β-D-1-thiogalactopyranoside) 1mM. To determine the best time of induction, an analysis of different time points was done after the addition of IPTG. Cells were harvested by centrifugation at 800 g for 10 min. Bacterial pellets were resuspended in 10 ml of 50 mM (pH 8) TrisHCl and Lysozyme (1,25 mg) was added. The cells were lysed by several cycles of sonication, and centrifuged, and proteins were purified using an affinity column containing nickel (Ni Sepharose 6 Fast Flow - GE Healthcare) to trap the histidine tag of CCTα. Since the soluble fraction gave low amounts of the purified *B. besnoiti* CCTα, which was not enough to immunize animals, it was decided to analyze soluble and insoluble protein extracts. The fractions were eluted using concentrations of imidazole in the range of 80-300mM. After protein purification, a sample was applied into a SDS-PAGE (sodium dodecyl sulfate - polyacrylamide gel electrophoresis) 12% (v/v), and the protein was transferred to a nitrocellulose membrane (Bio-Rad Laboratories). The immunoblots were blocked overnight at 4 ºC with 0,05M TBS (Tris-buffered saline: 0,138 M NaCl; 0,0027 M, pH 8.0) + Tween 20 0,05% (v/v) containing 5% (m/v) non-fat milk and probed with an antibody against the histidine tag of CCTα to identify the correct band corresponding to the CCTα protein. Afterwards, a large-scale bacteria culture in the same induction conditions was performed and analyzed in a preparative SDS-PAGE 12% (v/v) gel. This gel was then stained with cupper chloride (CuCl2 0,3M) for 5 minutes (Lee *et al*., 1987). The band corresponding to the *B. besnoiti* CCTα identified by comparison with the extracts from not induced bacteria, was excised and electroeluted.

3.2.4.2 - Electroelution of the CCTα protein from pieces of polyacrylamide gel

For performing electroelution, protein-containing gel pieces were placed in an electroelution chamber. The proteins were then eluted from the gel matrix into a buffer solution (Tris/Glycine/SDS: 0.25 M Tris, 1.92 M glycine and 0.1% SDS, pH 8.6) using an electrical field (105V during 100 min) the eluted protein was recovered and analyzed in a SDS-PAGE.

3.2.4.3 - Production of the polyclonal antibody in Balb/c mice

The purified *B. besnoiti* recombinant His-CCTα was used to immunize 3 Balb/c mice. The immunizations were intraperitoneally, three times at two weeks intervals, with approximately 10 μg of His-CCTα with incomplete Freund's adjuvant (Sigma). Two mice were inoculated only with the adjuvant and from each of the 5 mice a pre-immune serum sample was kept to be used as control. The serological response of the mice was followed by western blot, and three days after the last immunization the mice were sacrificed.

3.2.5 - Immunofluorescence microscopy using the polyclonal sera against *Besnoitia besnoiti* and *Toxoplasma gondii* CCTα

Subsequent to producing the anti *B. besnoiti* CCTα antibody, we performed immunofluorescence assays in isolated and invading tachyzoites of *B. besnoiti* and *T. gondii* (the antibody cross-reacts with *T. gondii* CCTα). For experiments with isolated, extracellular parasites (*T. gondii* and *B. besnoiti*), the supernatant of invaded cell cultures was collected and centrifuged at 770g for 10minutes. Then it was washed three times with PBS 1x (0,01 M phosphate buffer, 0,0027 M potassium chloride and 0,137 M sodium chloride, pH 7.4), and parasites in suspension were allowed to adhere to a coverslip and directly fixed and permeabilized.

In invasion experiments, hTERT-RPE-1 and Vero cells in the amount of $1x10^4$cells/well were allowed to adhere to coverslips in 24-well plates for 12 hours (incubated at 37ºC, 5% CO2). Purified tachyzoites (*T. gondii* and *B. besnoiti*) were added at a total amount of 10 parasites for each host cell. Invasion was allowed to occur during 5 and 15 minutes, in a 37ºC incubator at 5% CO2. After incubation, the medium was aspirated from each well and cells were washed with PBS 1x and directly fixed and permeabilized.

Two protocols for fixation and permeabilization were used in both extracellular and invading parasites: the protocol with methanol and the protocol using paraformaldehyde (PFA).

Fixation and permeabilization with methanol was done by the incubation of cells with cold methanol for 10min at -20ºC (the methanol has to be previously maintained at -20ºC). The protocol with PFA consisted of a first step fixation with a 3,7% solution of paraformaldehyde, 10minutes at room temperature; and a second step where cells were permeabilized with Triton-X 100 0.1% (v/v), 2 minutes at room temperature. In both protocols cells were then washed twice with PBS 1x, and once with PBS 1x- Tween 20 0.1% (v/v). Blockage of non-specific background was done with a 3% bovine serum albumin solution for 20 min at room temperature. After blockage, primary antibodies (Table 12) were added, and after 1h of incubation at room temperature, cells were again washed twice with PBS 1x, and once with PBS 1x- Tween 20 0.1% (v/v). We then proceeded with the second antibody (Table 12) incubation (1h at room temperature). Cells were washed twice with PBS 1x, and DNA was stained with DAPI (1 µg/ µl in PBS 1x; Sigma) for 2 min at room temperature. Finally, coverslips were mounted in mounting medium (MOWIOL 4-88 (Calbiochem) supplemented with 2,5% (m/v) DABCO (Sigma). Cells were examined under a fluorescence microscope *(*Leica, DMRA2) equipped with an UV light. Image acquisition was performed with a cooled CCD camera and MetaMorph Imaging Software (Universal Imaging), and images were analyzed with ImageJ software.

Primary antibody	**Host animal in which was produced**	**Dilution used**
anti CCTα (polyclonal)	mouse	1:200
anti - *B. besnoiti* polyclonal (Marcelino *et al*., 2011)	rabbit	1:5000
anti - *T. gondii* polyclonal (Helga Waap, LNIV)	cat	1:1250
Secondary antibody	**Host animal in which was produced**	**Dilution used**
anti-mouse Alexa 594 (Molecular Probes)	goat	1:500
anti-rabbit Alexa 488 (Molecular Probes)	goat	1:500
anti-cat FITC F-4262 (Sigma)	goat	1:500

Table 12: List of primary and secondary antibodies used in immunofluorescence.

3.2.6 - Real time PCR

3.2.6.1 - RNA isolation and Reverse Transcription

The expression at the transcriptional level of CCT*α* gene in *B. besnoiti*, and of CCTα, α-tubulin, TBCB and TBCE in *T. gondii* was assessed by real time PCR during host cell

invasion. Besides genes involved in the tubulin folding pathway, it was also analyzed ITS1 for *T. gondii*, and ITS1 for *B. besnoiti*, to serve as housekeeping genes for real time PCR.
With this purpose, the amount of mRNA of these genes was analyzed at different moments of host cell invasion, namely: 15min, 30min, 2h, 6h, 12h, 18h, 24h, 30h; and in non-invading free tachyzoites. Vero cells were grown in eight T75 flasks ($9x10^5$/flask) and after 12h at 37ºC, $9x10^6$ tachyzoites were inoculated in each flask. After 15min of invasion the medium of all flasks was changed, so that no further invasion was allowed. For each time point, Vero cells with invaded tachyzoites were trypsinized and total RNA was extracted (Qiagen-RNeasy Mini Kit). Before cDNA synthesis, RNA samples were treated with RNase-free DNaseI (Invitrogen). The same amount of RNA (1µg) in all samples was then reverse-transcribed with SuperScript III Reverse Transcriptase (Invitrogen), according to the manufacturer's protocols. For reverse transcription of the RNA, and because the housekeeping gene used was ITS1, random primers (Roche Applied Science) were used.

3.2.6.2 - Real-time PCR primer design

For primer design the program Primer 3 was used. The primary objective of this program is to design sets of primers that can be run under universal thermal cycling conditions (15 s at 95ºC and 1 min at 60ºC). Thus, the default parameters of the software are set to be very narrow. Most important is the melting temperature (TM) of the primers, and the amplicon length. The TM of the primers was established between 58–60ºC; and default parameters for amplicon lengths were set between 50 and 150 bp. The optimal amplicon length for real-time PCR is around 100 bp, as shorter amplicons amplify more efficiently than longer ones and are more tolerant of reaction conditions. This is because they are more likely to be denatured during the 95 ºC step of the PCR, allowing the primers to compete more effectively for binding to their complementary targets (reviewed in Bustin, 2000). This way, primers chosen were 15-20 bases, with a low probability to form primer dimers, and amplified cDNA fragments with approximately 120 bp in length. Primers were also designed to bind to the junction of sequential exons, avoiding false positive results from amplification of contaminating genomic DNA. The specificity of individual primers was tested using NCBI-BLAST (National Center for Biotechnology Information - Basic Local Alignment Search Tool). All primers used in real time PCR were synthesized by Stab Vida and are listed in Table 13 and Table 14.

Primer name	Oligonucleotide sequence
CCTα	
PFOR3CCTATOXORT	5’ - CATTGGCGACTGGGATCAC – 3’
PREV2CCTATOXORT	5’ - TACTCCAGAGCTCGAGATAC – 3’
TBCB	
TBCB F	5’ - GTCAAAGACAAGCTGTACAG - 3’
RTTBCBTOXOREV	5’ - CAACCACGTGGAGAATGCAA – 3’
TBCE	
PFORTBCETOXORT	5’ - CACGGCCGGTTCTTTCGTC – 3’
PREVTBCETOXORT	5’ - TGTGAGAGGGTTGACGAGG – 3’
α-tubulin	
PFORALPHATUBTOXORT	5’ - GCTCTTCTGCCTGGAACATG – 3’
PREVALPHATUBTOXORT	5’ - GCTCCAAATCCAAGAAGACG – 3’
ITS1	
PFITS1toxo	5’ – TATCGAAAGGTATTATTGC – 3’
PRITS1toxo	5’ – AGTATCCCAACAGAGACA – 3’

Table 13: List of primers for *T. gondii* real time PCR.

Primer name	Oligonucleotide sequence
CCTα	
PFCCTaBb	5’ - GACCGCCAAAGTGGTCAG – 3’
PREVCCTABBRT1	5’ – GTCTACCAGCATCTTGTCC – 3’
ITS1	
PFORITS1BB	5’ - GTGTGCTGCCCTCTTGTTG – 3’
PREVITS1BB	5’ – CAGAGTGAGGAGGTGGATC – 3’

Table 14: List of primers for *B. besnoiti* real time PCR.

3.2.6.3 - Real-time PCR amplification conditions

The concentration of the reagents (Table15) and the conditions for amplification were equal for all genes.

Component	Final concentration
SYBR Green Fastmix Rox (VWR)	10µl
Primer	2,5µl of a 4µM solution
Template cDNA	5µl of ≈ 150ng/µl
H_2O	5µl
Final Volume=25µl	

Table 15: Concentration of PCR components.

To detect PCR products, SYBR Green was used. It is a fluorescent DNA binding dye that binds all double–stranded DNA. The unbound dye exhibits little fluorescence in solution, but during elongation increasing amounts of dye bind to the nascent double-stranded DNA. Consequently, fluorescence measurements at the end of the elongation step of every PCR cycle are performed to monitor the increasing amount of amplified DNA. As the presence of

any double-stranded DNA generates fluorescence, this assay is not very specific. In order to verify specificity dissociation curves were designed, which consists in plotting fluorescence as a function of temperature to generate a melting curve of the amplicon (Ririe *et al*., 1997). The dissociation curve measures the temperature at which the cDNA strands separate into single strands (TM, the point at which 50% of the double stranded DNA molecules are dissociated). As the TM of the amplicon depends markedly on its nucleotide composition, it is possible to identify the signal obtained from the correct product (reviewed in Bustin, 2000).
PCR amplifications were always performed in duplicated wells, using the universal temperature cycles: 10 min at 95ºC, followed by 35 two-temperature cycles (15 s at 95°C and 1 min at 60°C). As the extension rate of Taq polymerase is between 30 and 70 bases/ second, polymerization times as short as 15 s are sufficient to replicate the amplicon, making amplification of genomic DNA contaminants less likely and reducing the time it takes to complete the assay. This was followed by the thermal denaturing step to generate the dissociation curves for verifying amplification specificity. PCR product sizes were validated by electrophoresis using a 2% (m/v) agarose gel.

3.2.6.4 - Data analysis for real-time PCR

In this study, the software used to collect and analyze data was Applied Biosystems 7300 Fast system.
To ensure a thorough and even coverage of the quantification range, 10 fold serial dilutions of the known samples containing the gene of interest cloned in pGEM T-easy vector were prepared. This way, it was covered the expected range of expression within the unknown samples. The software uses the standard curve (from serial dilutions of known samples) to determine the concentration of the unknown samples. The standard curve is automatically generated by the software, and consists of a linear regression of the Ct (threshold cycle) values versus the log of the cDNA quantities, that permits to extract quantification data from Real-Time PCR amplification curves.

3.3 - Results

3.3.1 - Characterization of genes involved in the tubulin folding of *Besnoitia besnoiti*

As it is was described in the section «Material and Methods», several PCR conditions and different combinations of primer pairs were used to amplify *B. besnoiti* genes involved in tubulin folding. Unfortunately, after innumerous reactions it was only possible to amplify part of the CCTα *B. besnoiti* gene using the primer pair TCP1alphaLEFT and TCP1alphaRIGHT. The PCR reaction using these primers amplified more than one product from *B. besnoiti* cDNA. The electrophoresis analysis in a 1,5% agarose gel of the products obtained from the PCR reaction showed the presence of multiple bands, one of which was approximately 600 bp (Fig. 32), the expected size considering the alignments done for the gene CCTα of *T. gondii* ME49_229990, and *N. caninum* LIV_030660.

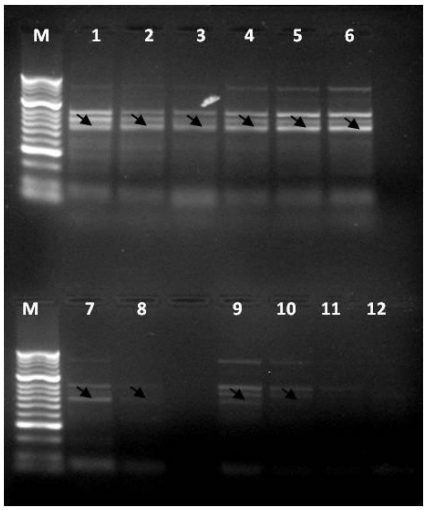

Fig. 32: Analysis by agarose gel electrophoresis of PCR products obtained using primers TCP1alphaLEFT and TCP1alphaRIGHT.
These primers were designed to amplify part of the coding region of the CCTα gene. Different annealing temperatures were tested in order to obtain products of the expected size: 1) 49,9ºC; 2) 50,1ºC; 3) 50,9ºC; 4) 52,2ºC; 5) 53,8ºC; 6) 55,6ºC; 7) 57,6ºC; 8) 59,5ºC; 9) 61,3ºC; 10) 62,8ºC; 11) 63,9ºC; 12) 64,5ºC; M) DNA molecular mass marker Bioline HyperLadder™ II. Arrows indicate the expected 600bp products.

This band was subsequently gel purified, cloned into pGEM-Teasy and transformed into *E. coli* competent cells. The recombinant plasmids containing the correct inserts were identified by colony PCR. Then the selected positive recombinant plasmids were sequenced in both strands using pGEM-Teasy primers T7 and SP6. Analysis of sequence data was done using

databases and tools from NCBI (National Center for Biotechnology Information); EuPathDB; ToxoDB; Expasy-Prosite; and ClustalW2 from EMBL-EBI.

Sequence analysis revealed significant identity between the obtained *B. besnoiti* sequence and those of CCTα gene of *T. gondii* (82%) and *N. caninum* (84%) (Fig. 33A and Table 16). As for other apicomplexan parasites of cattle, such as *B. bovis*, *T. parva* and *T. annulata*, values ranged from 57% to 62% at gene level (Fig. 33B and Table 16). The CCTα *B. besnoiti* nucleotide sequence was also compared with the corresponding sequence of the human malaria parasite *P. vivax* – 61%.

(A)

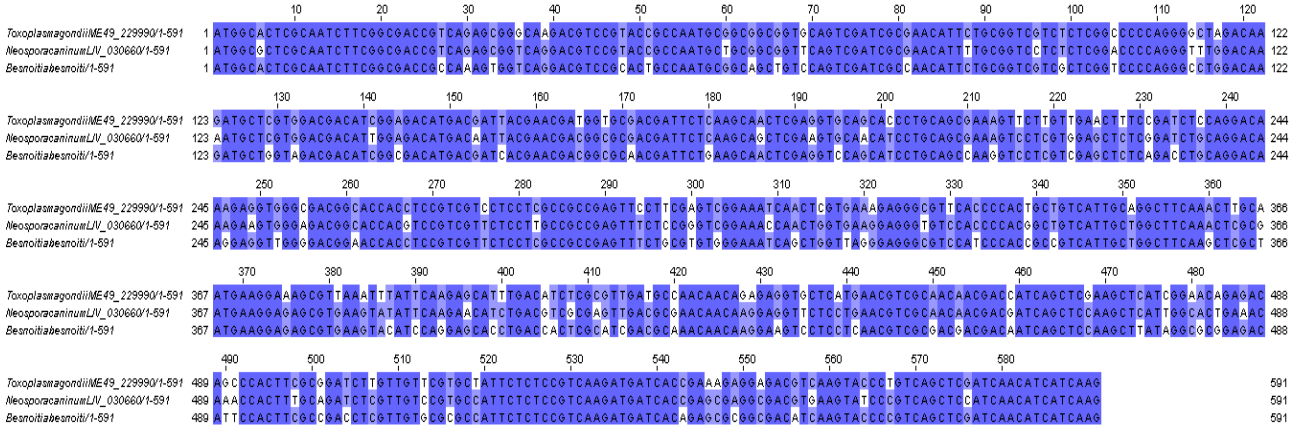

(B)

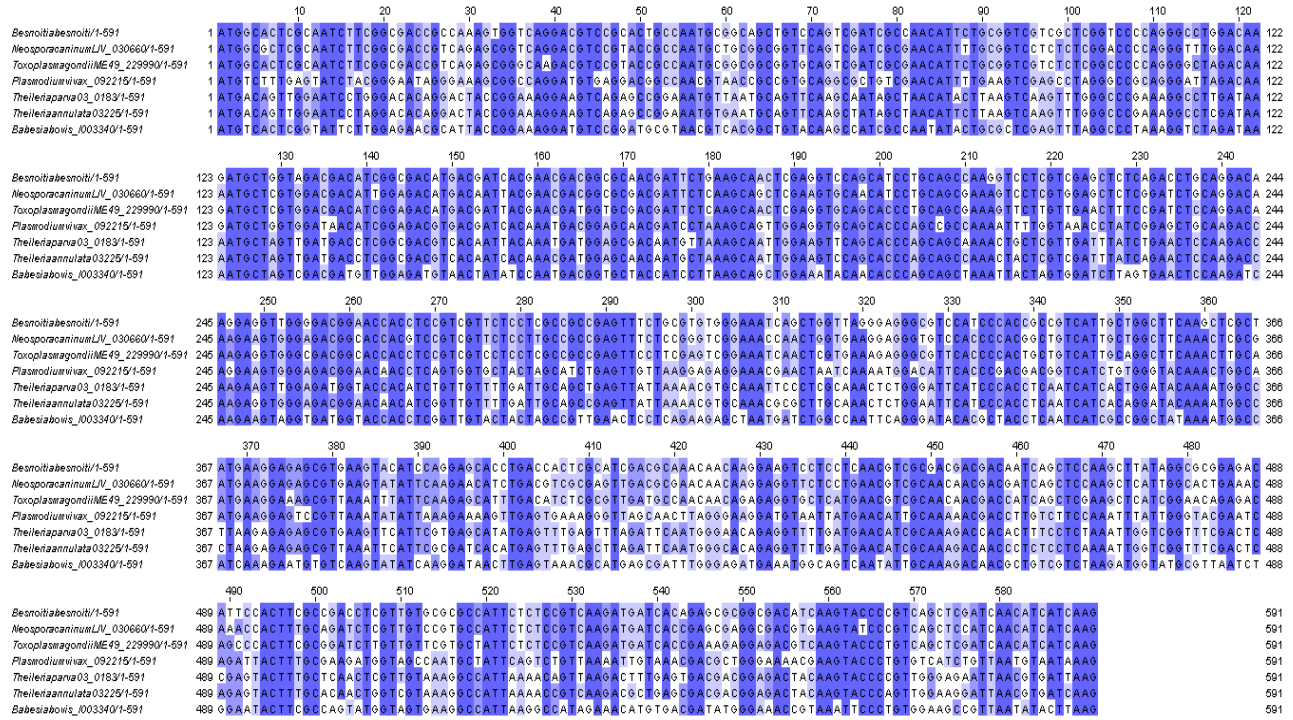

Fig. 33: Nucleotide coding sequence alignments for CCTα.

(A) Nucleotide coding sequence alignment for CCTα of *B. besnoiti*, *T. gondii* (TGME49_229990) and *N. caninum* (NCLIV_030660). (B) Nucleotide coding sequence alignment for CCTα of *B. besnoiti*, *T. gondii* (TGME49_229990), *N. caninum* (NCLIV_030660), *P. vivax* (PVX_092215), *T. parva*

(TP03_0183), *T. annulata* (TA03225) and *B. bovis* (BBOV_I003340). The accession numbers for sequences were retrieved from the EuPathDB database. Alignments were performed using ClustalW2 from EMBL-EBI.

Origin of analyzed nucleotide coding sequences of CCTα	***Besnoitia besnoiti* coding sequence identity (%)**
Toxoplasma gondii (TGME49_229990)	82
Neospora caninum (NCLIV_030660)	84
Babesia bovis (BBOV_I003340)	57
Plasmodium vivax (PVX_092215)	61
Theileria parva (TP03_0183)	60
Theileria annulata (TA03225)	62

Table 16: Nucleotide coding sequence identity between CCTα from apicomplexan and the partial sequence for the gene CCTα of *B. besnoiti*.

The accession numbers for sequences were retrieved from the EuPathDB database. Alignments were performed using ClustalW2 from EMBL-EBI.

The same sequence analysis was performed with the encoded proteins. The identity between *B. besnoiti* CCTα and those of *T. gondii* and *N. caninum*, increased at the aminoacid sequence level, to 95% and 96%, respectively (Fig. 34A and Table17). For the other apicomplexan parasites analyzed, values from 58% to 68% were obtained (Fig. 34B and Table17).

(A)

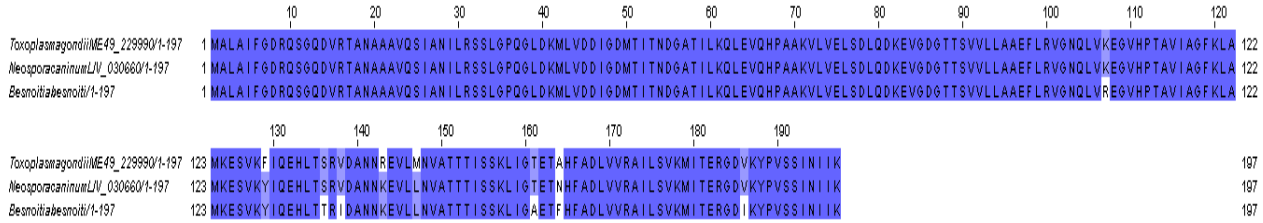

(B)

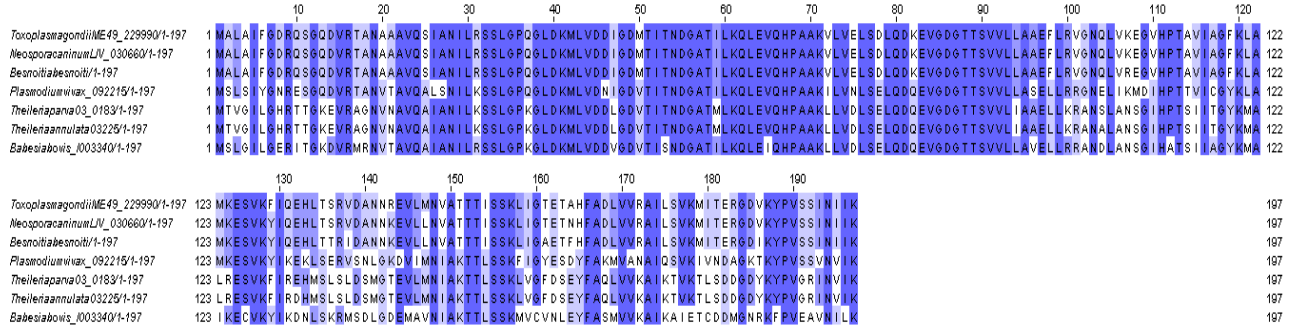

Fig. 34: Aminoacid sequence alignments for CCTα.

(A) Aminoacid sequence alignment for CCTα of *B. besnoiti*, *T. gondii* (TGME49_229990) and *N. caninum* (NCLIV_030660). (B) Aminoacid sequence alignment for CCTα of *B. besnoiti*, *T. gondii* (TGME49_229990), *N. caninum* (NCLIV_030660), *P. vivax* (PVX_092215), *T. parva* (TP03_0183), *T. annulata* (TA03225) and *B. bovis* (BBOV_I003340). The accession numbers for sequences were

retrieved from the EuPathDB database. Alignments were performed using ClustalW2 from EMBL-EBI.

Origin of analyzed aminoacid sequences of CCTα protein	***Besnoitia besnoiti* aminoacid sequence identity (%)**
Toxoplasma gondii (TGME49_229990)	95
Neospora caninum (NCLIV_030660)	96
Babesia bovis (BBOV_I003340)	58
Plasmodium vivax (PVX_092215)	68
Theileria parva (TP03_0183)	62
Theileria annulata (TA03225)	61

Table 17: Aminoacid sequence identity between CCTα from apicomplexan parasites and the partial sequence of *B. besnoiti* CCTα.

The accession numbers for sequences were retrieved from the EuPathDB database. Alignments were performed using ClustalW2 from EMBL-EBI.

In order to confirm the data retrieved from the multiple alignments of CCTα sequences in what respects the evolutionary distances between the parasites in study, genetic phylograms were used (Fig. 35). In the phylogenetic tree it is clear that the three apicomplexan parasites *B. besnoiti*, *N. caninum*, and *T. gondii*; form a closely related group, distant from other apicomplexan parasites (*T. parva*, *T. annulata*, *B. bovis* and *P. vivax*).

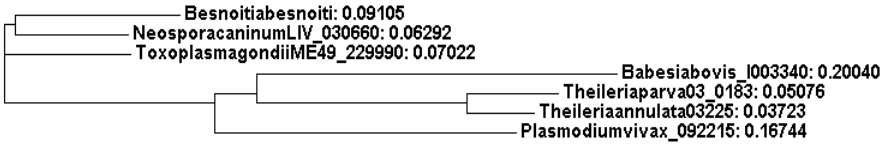

Fig. 35: Phylogenetic tree for the partial nucleotide coding sequence of CCTα.

Accession numbers are for sequences obtained from the EuPath database. Phylograms were obtained in ClustalW2 from EMBL-EBI.

Using the bioinformatic programs and databases Expasy-Prosite (database of protein domains, families and functional sites) and NCBI, the 197 aminoacid sequence of CCTα from *B. besnoiti* was analyzed for conserved domains. As signature patterns of the family of TCP-1 (Tailless Complex Polypeptide 1) chaperonins, three conserved regions located in the N-terminal domain were identified (Fig. 36), once again supporting that the partial sequence corresponded to the *B. besnoiti* CCTα. The first two conserved features (RSSLGPQGLDKML; ITNDGATILKQLEVQHP) are probably polypeptide binding sites (ring oligomerization interfaces on the conserved domain TCP-1α), with the second region (ITNDGATILKQLEVQHP) showing similarity to a domain that has been associated with

actin binding (amino acids 516-530 of Myo4p) (Haarer *et al*., 1994). The third conserved pattern, GDGTTSV, is closely related to a nucleotide phosphate-binding domain of the cAMP-dependent kinase as recognized by Lewis *et al*., 1992.

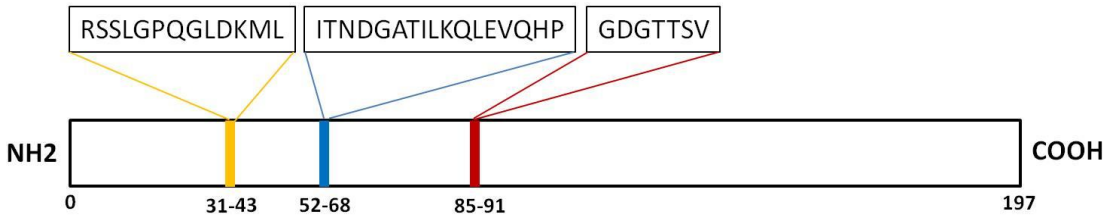

Fig. 36: Diagram of distinct phylogenetic conserved patterns of the family of TCP-1 chaperonins of the aminoacid sequence of part of the *B. besnoiti* CCTα.
The yellow and blue are polypeptide binding sites; the red is a nucleotide phosphate-binding domain. These domains were identified by using Expasy-Prosite (database of protein domains, families and functional sites) and NCBI.

Similar approaches were done for the other genes (α-tubulin, TBCB and TBCE), using different primer combinations, and several annealing temperatures. Multiple bands were extracted from the agarose gel, and sequenced. However, the sequences retrieved never corresponded to α-tubulin, TBCB or TBCE of *B. besnoiti*, as the results from sequence analysis did not reveal any similarity between the obtained *B. besnoiti* sequences and those of *T. gondii* and *N. caninum.*

3.3.2 - Characterization of genes involved in the tubulin folding of *Toxoplasma gondii*

Considering that it was not possible to amplify *B. besnoiti* genes participating in the tubulin folding pathway (only a partial sequence of CCTα was obtained), and that *B. besnoiti* is phylogenetically close to *T. gondii* (with an already sequenced an annotated genome), CCTα, α-tubulin, TBCB and TBCE *T. gondii* genes were amplified from genomic DNA of the parasite and cloned into the pGEM-Teasy vector.
Analysis of sequence data was obtained using databases and tools from NCBI; EuPathDB; ToxoDB, Expasy-Prosite, and ClustalW2 from EMBL-EBI.

3.3.2.1 - CCT (Chaperonin containing TCP-1)

In EuPathDB, the CCTα gene is identified as TGME49_229990, T-complex protein 1 subunit alpha, putative. The coding sequence of CCTα has 1657bp, and is highly conserved in phylum

Apicomplexa (Table 18). *T. gondii* CCTα shows 85% identity to CCTα of *N. caninum*, and more than 60% identity to those of other apicomplexan parasites (*P. vivax, T. annulata, B. bovis, T. parva*-Table 18).

Origin of analyzed nucleotide coding sequences of CCTα	***Toxoplasma gondii* coding sequence identity (%)**
Neospora caninum (NCLIV_030660)	85
Plasmodium vivax (PVX_092215)	63
Theileria annulata (TA_03225)	63
Babesia bovis (BBOV_I003340)	62
Theileria parva (TP03_0183)	61

Table 18: Nucleotide coding sequence identity between CCTα from apicomplexan parasites and the sequence of CCTα of *T. gondii*.

The accession numbers for sequences were retrieved from the EuPathDB database. Alignments were performed using ClustalW2 from EMBL-EBI.

As for the similarity of the aminoacid sequence of *T. gondii* CCTα, a protein with 59kDa and a pI of 6,17, values range from 60 to 97%, as it can be seen in Table 19.

Origin of analyzed aminoacid sequences of CCTα protein	***Toxoplasma gondii* aminoacid identity (%)**
Neospora caninum (NCLIV_030660)	97
Plasmodium vivax (PVX_092215)	65
Babesia bovis (BBOV_I003340)	60
Theileria parva (TP03_0183)	60
Theileria annulata (TA_03225)	60

Table 19: Aminoacid sequence identity between CCTα from apicomplexan parasites and the sequence of CCTα of *T. gondii*.

The accession numbers for sequences were retrieved from the EuPathDB database. Alignments were performed using ClustalW2 from EMBL-EBI.

As expected, using Expasy-Prosite and NCBI to search for conserved domains in *T. gondii* CCTα, there is a hit for the chaperonin-like super family, with a conserved domain for TCP-1 α (7-539 aa). Moreover, in the N-terminal and C-terminal there are several ATP/Mg binding conserved features (for example, GDGTTSV), as well as conserved sites of ring oligomerization interface (polypeptide binding sites, as RSSLGPQGLDKML and ITNDGATILKQLEVQHP) (Fig. 37). In the C-terminal, the motif VCPGGG could be involved in protein-protein interactions expected to occur between CCTα and their substrates (Soares *et al*., 1994). Finally, the C-terminal contains also conserved features for the stacking interactions between one subunit to subunits of the second ring.

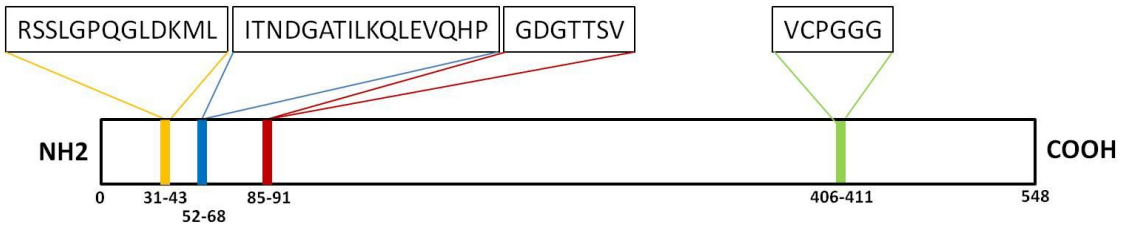

Fig. 37: Diagram of distinct phylogenetic conserved patterns of the family of TCP-1 chaperonins of the aminoacid sequence of *T. gondii* CCTα.

The yellow, blue, and green are polypeptide binding sites; the red is a nucleotide phosphate-binding domain. These domains were identified by using Expasy-Prosite (database of protein domains, families and functional sites) and NCBI.

3.3.2.2 - α-tubulin

The only α-tubulin gene for *T. gondii* is completely sequenced and annotated in the ToxoDB or the EuPath database. The gene is identified as TGME49_316400, alpha tubulin TUBA1 (TUBA1) and the coding sequence is 1362bp long. The nucleotide sequence of the α-tubulin gene is highly conserved between apicomplexan, as for other eukaryotes, showing the highest identity of the genes in study, with a percentage of 92% when compared to *N. caninum*, 79% in relation to *B. bovis*, 77% in comparison with *P. vivax*, and the lowest identity, 71%, with *T. parva* (Table 20).

Origin of analyzed nucleotide coding sequences of α-tubulin	***Toxoplasma gondii* coding sequence identity (%)**
Neospora caninum (NCLIV_058890)	92
Babesia bovis (BBOV_III002820)	79
Plasmodium vivax (PVX_090155)	77
Theileria parva (TP04_0093)	71

Table 20: Nucleotide coding sequence identity between α-tubulin from apicomplexan parasites and the sequence of α-tubulin of *T. gondii*.

The accession numbers for sequences were retrieved from the EuPathDB database. Alignments were performed using ClustalW2 from EMBL-EBI.

In terms of the α-tubulin protein (50kDa; pI:4,74), it is also highly conserved, with the lowest value of identity being 88%, in relation to *T. parva*. Interestingly, the alignment of α-tubulin of *T. gondii and N. caninum* presents a complete identity of 100% (Table 21).

Origin of analyzed aminoacid sequences of α-tubulin protein	*Toxoplasma gondii* aminoacid identity (%)
Neospora caninum (NCLIV_058890)	100
Plasmodium vivax (PVX_090155)	96
Babesia bovis (BBOV_III002820)	93
Theileria parva (TP04_0093)	88

Table 21: Aminoacid sequence identity between α-tubulin from apicomplexan parasites and the sequence of α-tubulin of *T. gondii*.

The accession numbers for sequences were retrieved from the EuPathDB database. Alignments were performed using ClustalW2 from EMBL-EBI.

Running the *T. gondii* α-tubulin protein through the NCBI conserved domains, one conserved domain for α-tubulin (1-435 aa) of the tubulin superfamily was found. Several conserved features were found in the N-terminal, namely (Fig. 38):

- sites for the nucleotide binding site (10-248 aa). In α-tubulin, the nucleotide binding site (non-exchangeable) is buried at the monomer-monomer interface within the dimer;
- sites for the oligomerization interface with the following β subunit (polypeptide binding site 72-224 aa);
- sites for the oligomerization interface with the preceding β-tubulin (2-352 aa).

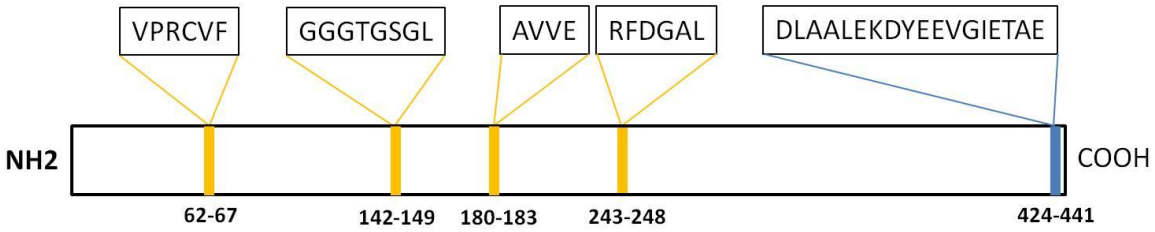

Fig. 38: Diagram of distinct phylogenetic conserved patterns of the aminoacid sequence of the *T. gondii* α-tubulin.

The nucleotide binding sites for GTP, in yellow; the MAP binding region of the tubulin protein, in blue. These features were based in the NCBI search and in Siverajah *et al*., 2003.

3.3.2.3 - TBCB (tubulin cofactor B)

The gene for the TBCB of *T. gondii* is sequenced and annotated as a CAP-Gly domain-containing protein in ToxoDB (Gene ID: TGME49_305060). Its coding sequence is 822bp long, and has a sequence identity of 81% with *N. caninum* (Table 22). The homology decreases when we compare the sequence of *T. gondii* with other apicomplexan (Table 22): *E. acervulina* (59%), *P. vivax* (53%), and *B. bovis* (53%).

Origin of analyzed nucleotide coding sequences of TBCB	*Toxoplasma gondii* coding sequence identity (%)
Neospora caninum (NCLIV_001310)	81
Eimeria acervulina (EAH_00008110)	59
Plasmodium vivax (PVX_098786)	53
Babesia bovis (BBOV_IV005610)	53

Table 22: Nucleotide coding sequence identity between TBCB from apicomplexan parasites and the sequence of TBCB of *T. gondii*.

The accession numbers for sequences were retrieved from the EuPathDB database. Alignments were performed using ClustalW2 from EMBL-EBI.

At a protein level, the percentage of identity for *T. gondii* TBCB (≈31kDa; pI:4,92) decreases to 77% in relation to *N. caninum*, to 38% when compared to *E. acervulina*, to 28% with *B. bovis*, and 26% with *P.vivax* (Table 23).

Origin of analyzed aminoacid sequences of TBCB protein	*Toxoplasma gondii* aminoacid identity (%)
Neospora caninum (NCLIV_001310)	77
Eimeria acervulina (EAH_00008110)	38
Babesia bovis (BBOV_IV005610)	28
Plasmodium vivax (PVX_098786)	26

Table 23: Aminoacid sequence identity between TBCB from apicomplexan parasites and the sequence of TBCB of *T. gondii*.

The accession numbers for sequences were retrieved from the EuPathDB database. Alignments were performed using ClustalW2 from EMBL-EBI.

The search for the conserved domains of *T. gondii* TBCB resulted in two characteristic domains of this protein (Fig. 39):

- an UBQ super family domain, in the N-terminal;
- a CAP-GLY super family domain, in the C-terminal. The CAP-Gly domain is known to be involved in tubulin binding (Riehemann & Sorg, 1993).

Fig. 39: Diagram of the aminoacid sequence of the *T. gondii* TBCB.

Two phylogenetic conserved domains: the Ubl domain (25-107 aa), in yellow; and the CAP-Gly domain (181-257 aa), in blue. These domains were identified by using Expasy-Prosite (database of protein domains, families and functional sites) and NCBI.

3.3.2.4 - TBCE (tubulin cofactor E)

T. gondii TBCE is identified in ToxoDB as TGME49_285220, a CAP-Gly domain-containing protein. The TBCE gene coding sequence has 2122bp, and of the genes studied, is the one with the lowest identity to *N. caninum* (68%). In relation to other apicomplexan, the values are close to those found for CCTα and TBCB (Table 24).

Origin of analyzed nucleotide coding sequences of TBCE	***Toxoplasma gondii* coding sequence identity (%)**
Neospora caninum (NCLIV_014970)	68
Babesia bovis (BBOV_II006350)	53
Plasmodium vivax (PVX_087925)	53
Eimeria acervulina (EAH_00011070)	51

Table 24: Nucleotide coding sequence identity between TBCE from apicomplexan parasites and the sequence of TBCE of *T. gondii*.

The accession numbers for sequences were retrieved from the EuPathDB database. Alignments were performed using ClustalW2 from EMBL-EBI.

The values for protein identity of *T. gondii* TBCE (85kDa; pI:5,58), in relation with other apicomplexan parasites decrease abruptly, with the highest value corresponding to the comparison with the sequence of *N. caninum* (62%), and the lowest value in relation to *E. acervulina*, 16% (Table 25). In fact, TBCE is without a doubt, the component of the tubulin folding pathway, of those in study, with the highest divergence between the apicomplexan parasites aligned.

Origin of analyzed aminoacid sequences of TBCE protein	***Toxoplasma gondii* aminoacid identity (%)**
Neospora caninum (NCLIV_014970)	62
Babesia bovis (BBOV_II006350)	24
Plasmodium vivax (PVX_087925)	20
Eimeria acervulina (EAH_00011070)	16

Table 25: Aminoacid sequence identity between TBCE from apicomplexan parasites and the sequence of TBCE of *T. gondii*.

The accession numbers for sequences were retrieved from the EuPathDB database. Alignments were performed using ClustalW2 from EMBL-EBI.

Analyzing the TBCE sequence for *T. gondii*, two conserved domains were found: an Ubl domain, and a CAP-Gly domain. These domains occur in the TBCE sequence in a reverse order, when compared to TBCB, with the Cap-Gly domain in the N-terminal, and the Ubl domain in the C-terminal of the protein (Fig. 40).

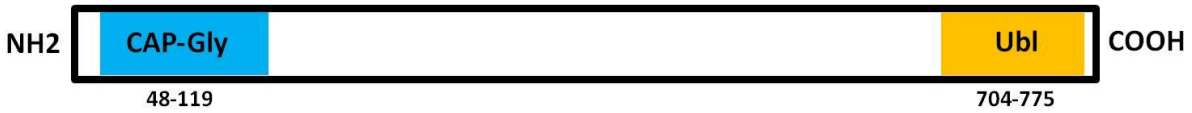

Fig. 40: Diagram of the aminoacid sequence of the *T. gondii* TBCE.
Two phylogenetic conserved domains: the CAP-Gly domain (48-119 aa), in blue; and the Ubl domain (704-775 aa), in yellow. These domains were identified by using Expasy-Prosite (database of protein domains, families and functional sites) and NCBI.

3.3.3 - Polyclonal antibody production against *Besnoitia besnoiti* CCTα protein

The cloning of the partial sequence of *B. besnoiti* CCTα allowed producing a specific polyclonal antibody against CCTα. In order to do this, the corresponding region of the protein was cloned in the bacteria expression vector pET28a under the operon *Lac* promoter. Rosetta(DE3)pLysS bacteria cells were transformed and grown to an optical density of 0,4 to 0,5. To determine the best time of induction of the CCTα gene, an analysis of different time points after the addition of 1mM of the inducer IPTG was done. A sample from the culture (immediately after the addition of IPTG (time 0), and 1, 2, 3 and 4 hours after IPTG addition) was collected, and total cell extracts were prepared. The analysis of the different protein extracts obtained from different time points was done by a SDS-PAGE 12% gel, and the gel was stained with Coomassie to visualize the protein bands. This analysis allowed concluding that the best induction time was 3h (Fig. 41 - arrow).

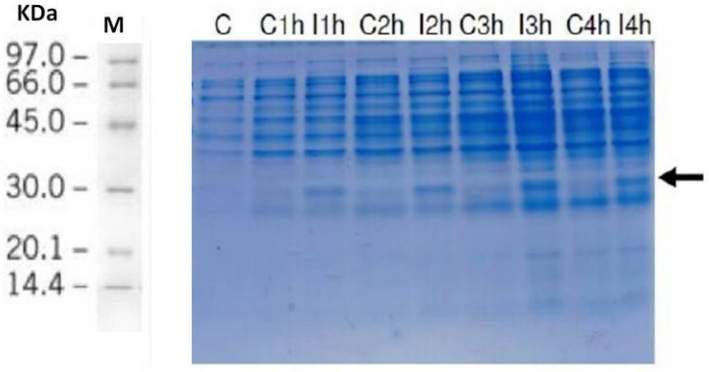

Fig. 41: SDS-PAGE 12% gel of the induction of the truncated *B. besnoiti* CCTα.
Partial *B. besnoiti* CCTα (arrow) at different time points of induction (1h; 2h; 3h and 4h). M – molecular mass marker; C – control cells without IPTG; I – induced cells with 1mM IPTG.

In order to obtain a great yield of the protein to purify and immunize mice, the production was scaled up using the same protocol: Rosetta(DE3)pLysS bacteria cells transformed with the pET28a – *B. besnoiti* truncated CCTα, in frame with a tag of histidines (His), were induced

during 3 hours. Cells were recovered and lysed, and soluble proteins were purified using an affinity column containing nickel. The eluted fractions, using imidazole concentrations in the range of 80-300mM, were analyzed in a SDS-PAGE 12% gel. The gel was then silver stained (Fig. 42) showing the sequential elution of a band corresponding to a protein of about 25 kDa that has the expected molecular mass for truncated His tagged-CCTα. The identity of this band was then confirmed by mass spectrometry showing that this was in fact the truncated CCTα protein.

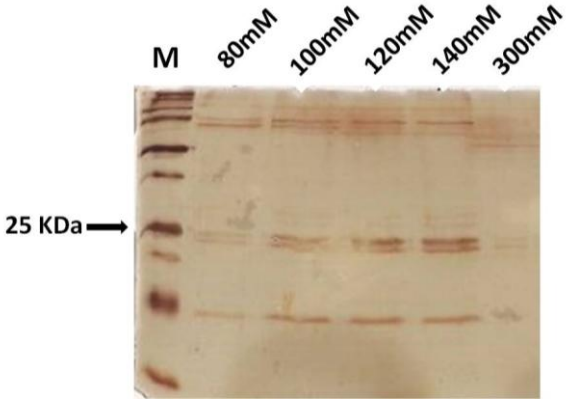

Fig. 42: Eluted fractions from the induction of *B. besnoiti* CCTα.
Analysis of the different affinity purified fractions from the induction of *B. besnoiti* CCTα for 3h with 1mM IPTG. Sequential elution was performed using concentrations of imidazole in the range of 80-300mM. M – molecular mass marker.

Because it was not possible to recover *B. besnoiti* truncated CCTα purified from the soluble fraction in sufficient quantity to immunize animals, a different approach was followed: both soluble and insoluble protein extracts obtained after 3h of induction were analyzed in a SDS-PAGE 12% gel. The gel was then transferred to a nitrocellulose membrane and stained with Ponceau (Fig. 43A), followed by a western blot using an antibody against the histidine tag of CCTα (Fig. 43B).

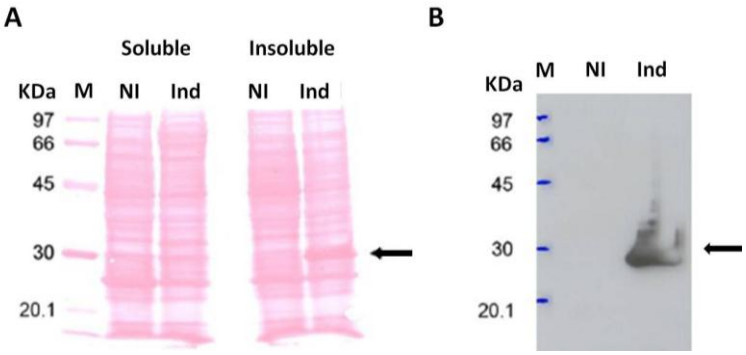

Fig. 43: Ponceau staining and western blot of the *B. besnoiti* truncated CCTα protein.
(A) Analysis of the soluble and insoluble protein fractions of cells induced to produce *B. besnoiti* truncated CCTα (arrow). (B) – Western blot with an anti-histidine antibody, to confirm that the

observed protein corresponds to *B. besnoiti* truncated CCTα (arrow). M – molecular mass marker; NI - Non induced; I - Induced.

After determining which band corresponded to CCTα, a large-scale bacteria culture in the same induction conditions was performed. The band corresponding to *B. besnoiti* truncated CCTα, identified by comparison with the extracts from non induced bacteria, was excised and electroeluted. The obtained protein was again analyzed using a SDS-PAGE 12% and transferred to nitrocellulose (Fig. 44).

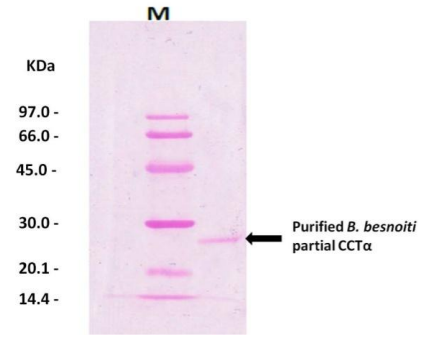

Fig. 44: Analysis by SDS-PAGE 12% electrophoresis of purified truncated *B. besnoiti* CCTα followed by transfer to a nitrocellulose membrane and staining with Ponceau.
A band corresponding to the *B. besnoiti* truncated CCTα purified by electroelution is clearly visible (arrow). M – molecular mass marker.

The purified *B. besnoiti* truncated His tagged-CCTα was used to immunize 3 Balb/c mice. The serological response of the mice was followed by western blot, and three days after the last immunization the mice were sacrificed.
In Fig. 45, is showed the Western blot analysis of the serum of the three immunized Balb/c mice. In all three sera a band corresponding to a protein of approximately 55KDa, the expected size of the CCTα, was observed. This polyclonal antibody was used to obtain the CCTα protein localization inside isolated and invading tachyzoites of *B. besnoiti* and *T. gondii* (the polyclonal antibody produced against the CCTα truncated protein of *B. besnoiti* cross-reacts with the *T. gondii* CCTα protein).

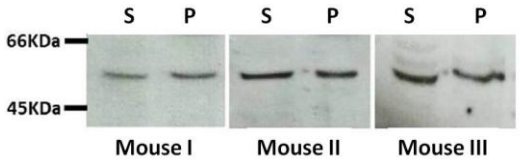

Fig. 45: Western blot analysis of the mice sera.
Analysis of the three sera obtained from the three mice immunized with the *B. besnoiti* truncated His tagged-CCTα. As it can be observed in the figure, in all the cases, the polyclonal serum identified a ~55KDa protein, the expected size of the endogenous CCTα. S-soluble extract; P-pellets.

3.3.4 - Cellular localization of CCTα in *Besnoitia besnoiti* and *Toxoplasma gondii* tachyzoites

The polyclonal antibody against *B. besnoiti* CCTα allowed investigating the localization of the protein in isolated and invading tachyzoites of *B. besnoiti* and *T. gondii*. As it can be seen in Fig. 46 and Fig. 47, CCTα is spread throughout the cytoplasm of the tachyzoites, but the labeling is not homogenous, since the detection of globular like structures occurs mainly at the anterior pole. Interestingly, this is similar to what was observed in the ciliate *T. pyriformis* (Seixas *et al*., 2003) and resembles the occurrence of CCTα-subunit in mammalian cells and in budding yeast (Lewis *et al*., 1992; Ursic *et al*., 1994). In fact, some images (Fig. 46C and D; and Fig 47B and C) suggest that the localization of CCTα accompanies the spiral distribution of the subpellicular MTs, nucleated at the apical polar ring, in the conoid.

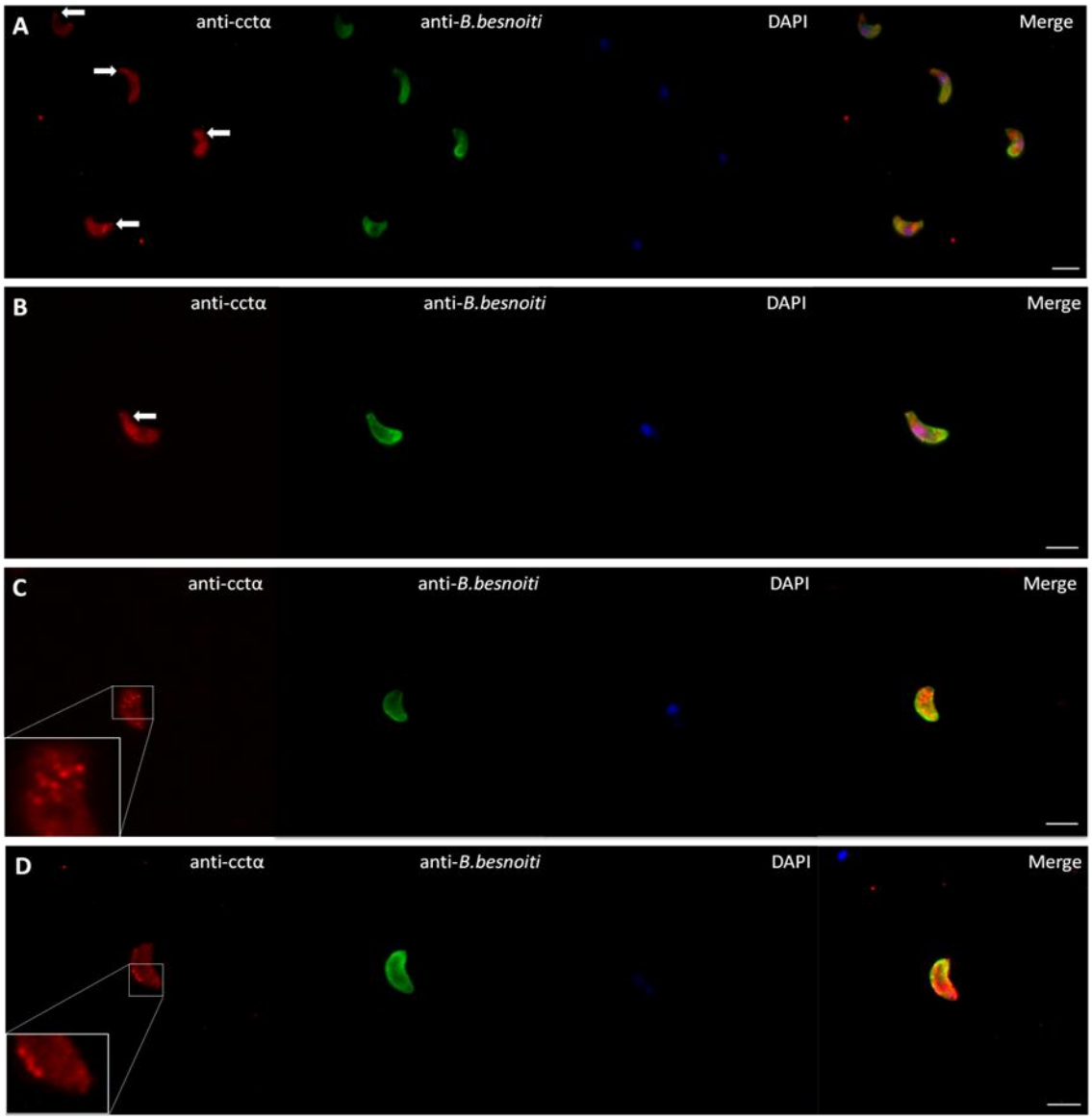

Fig. 46: Indirect immunolocalization of CCTα in tachyzoites of *B. besnoiti*.

Free tachyzoites of *B. besnoiti* were processed for immunofluorescence analysis using the polyclonal antibody against *B. besnoiti* CCTα (red) and anti-*B. besnoiti* polyclonal antibody (green). DNA was

stained with DAPI (blue). (A and B) Arrows show the preferential signal at the anterior pole of the globular like structures. (C and D) Zoomed areas correspond to detailed views of the anterior pole of *B. besnoiti*, showing the cellular localization of CCTα in free tachyzoites. Scale bar represents 7µm in (A) and 5 µm in (B, C and D).

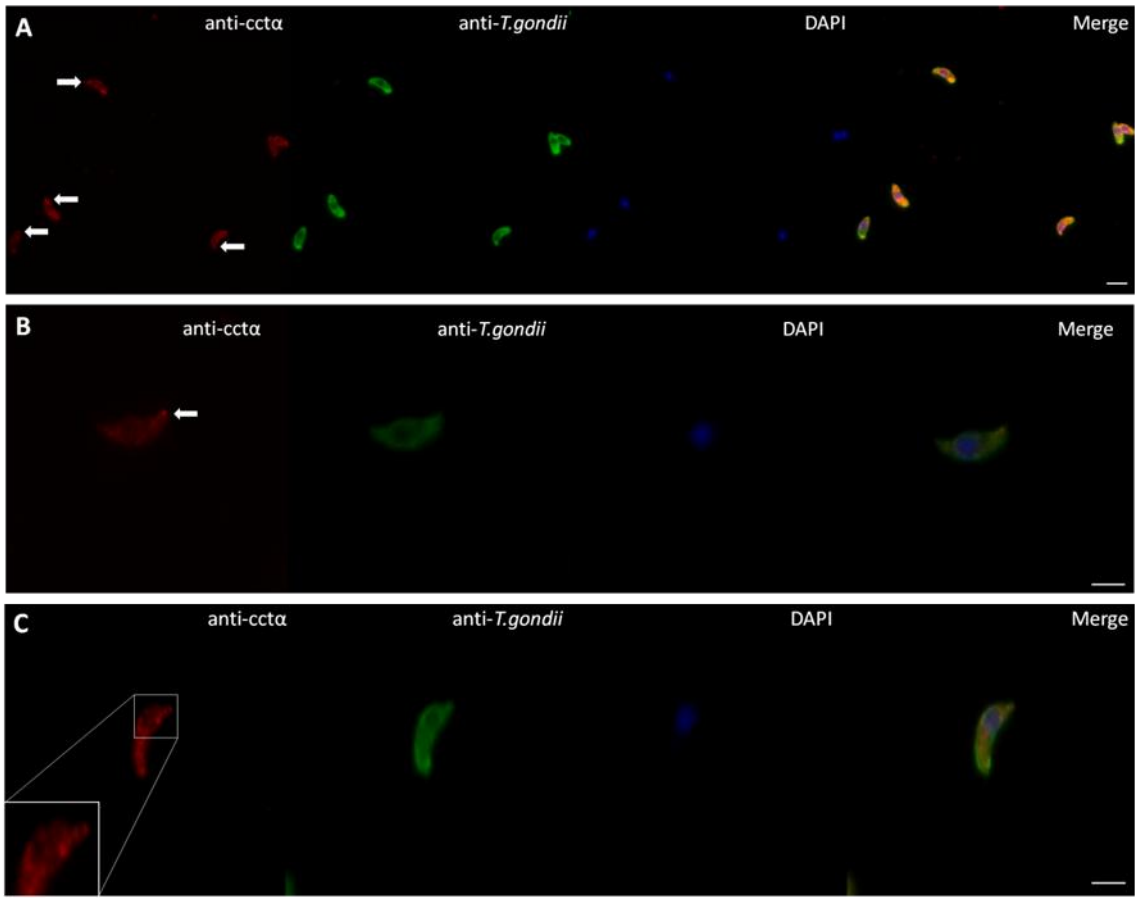

Fig. 47: Indirect immunolocalization of CCTα in tachyzoites of *T. gondii*.
Free tachyzoites of *T. gondii* were processed for immunofluorescence analysis using the polyclonal antibody against *B. besnoiti* CCTα (cross reaction, red) and anti-*T. gondii* polyclonal antibody (green). DNA was stained with DAPI (blue). (A and B) Arrows show the preferential signal at the anterior pole of the globular like structures. (C) Zoomed area corresponds to a detailed view of the anterior pole of *T. gondii*, showing the cellular localization of CCTα in free tachyzoites, which seems to localize with the conoid structure. Scale bar represents 7µm in (A) and 3 µm in (B and C).

To investigate the role of CCTα during the first steps of invasion, Vero and RPE-1 cells invaded for 5 and 15 minutes with *B. besnoiti* or *T. gondii* were processed for indirect immunolocalization (Fig. 48, 49, 50 and 51). Although in these figures the CCTα staining is now more spread over the cytoplasm of *B. besnoiti* and *T. gondii*, there are no dramatic alterations in comparison to what was observed in non invaded tachyzoites (Fig. 46 and 47). In some images the staining seems to be concentrated around the nucleus (Fig. 48A and 51A).

An interesting observation is that in Fig. 48B, Fig. 50A, and Fig. 51B an accumulation of CCTα seems to be present at the site of anchorage to the host cell - the MJ. However, it is not clear if the CCTα present in the MJ belongs to the parasite or if it is recruited from the host cell´s cytoplasm, since the antibody produced also cross reacts with the host cell (the CCTα truncated protein of *B. besnoiti* has a ≈60% identity in terms of the aminoacid sequence with the human CCTα (in the case of RPE-1 cells) and the green monkey CCTα (in the case of Vero cells).

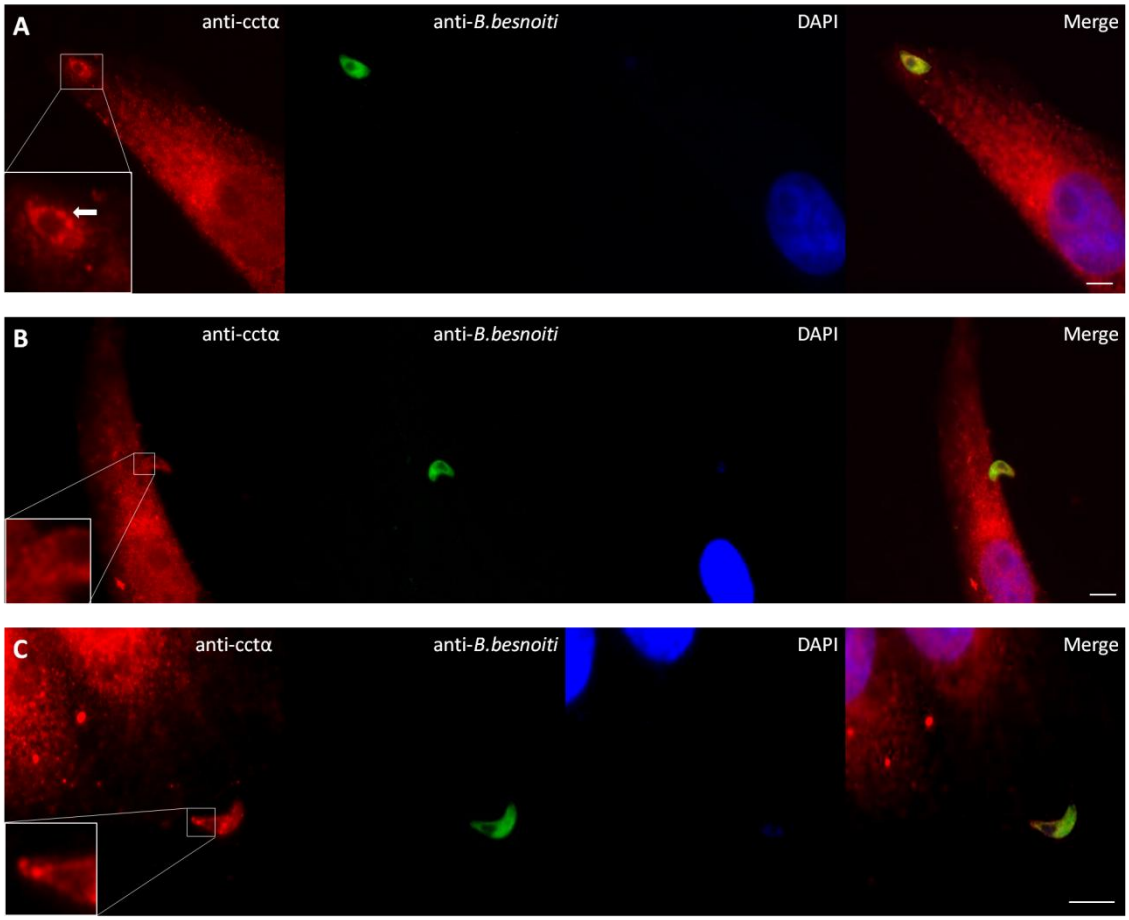

Fig. 48: Indirect immunolocalization of CCTα in tachyzoites of *B. besnoiti* in the first steps of host cell invasion (Vero cells).

Tachyzoites of *B. besnoiti* were processed for immunofluorescence analysis using the polyclonal antibody against *B. besnoiti* CCTα (red) and anti-*B. besnoiti* polyclonal antibody (green). DNA was stained with DAPI (blue). (A) Zoomed area corresponds to a detailed view of a *B. besnoiti* tachyzoite inside a PV, 15min of host cell invasion, showing the cellular localization of CCTα. Arrow indicates CCTα distribution in a ring structure at the apical pole of *B. besnoiti*. (B) Zoomed area corresponds to a detailed view of the anterior pole of *B. besnoiti* tachyzoite entering the host cell, 5min of host cell invasion, showing the cellular localization of CCTα. In this image an accumulation of the globular structures of CCTα seems to be present in the MJ. (C) Zoomed area corresponds to a detailed view of

the anterior pole of an extended *B. besnoiti* conoid (5min of host cell invasion). The globular structures of CCTα seem to localize with the conoid structure. Scale bar represents 7µm.

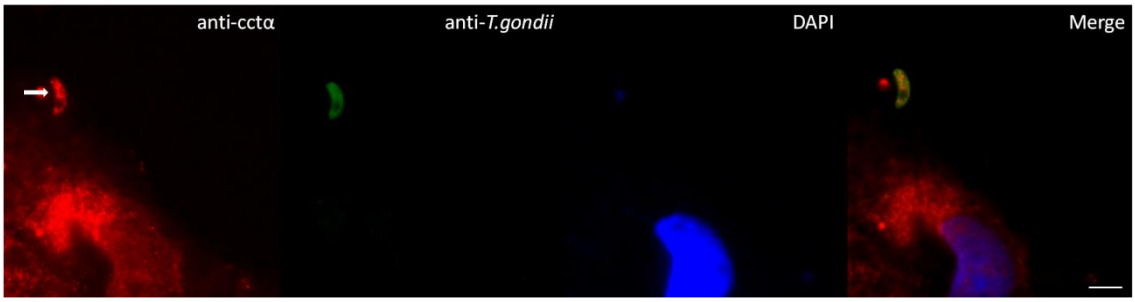

Fig. 49: Indirect immunolocalization of CCTα in a tachyzoite of *T. gondii* in the first steps of host cell invasion (Vero cells).

5min of host cell invasion. *T. gondii* tachyzoites were processed for immunofluorescence analysis using the polyclonal antibody against *B. besnoiti* CCTα (cross reaction, red) and anti-*T. gondii* polyclonal antibody (green). DNA was stained with DAPI (blue). Arrow indicates CCTα distribution in globular structures throughout *T. gondii* cytoplasm. Scale bar represents 7µm.

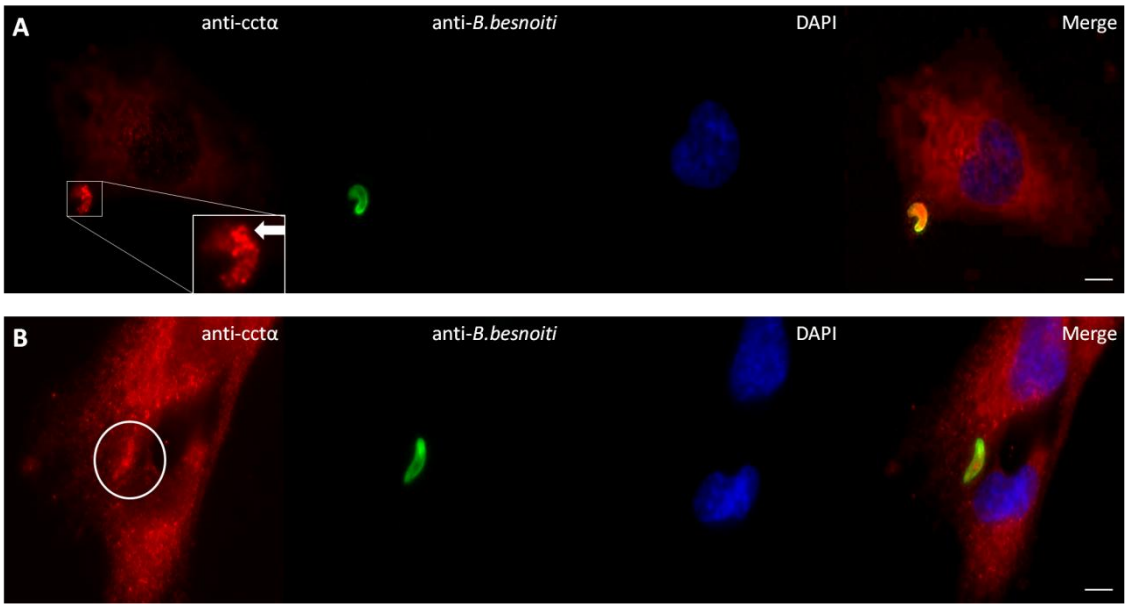

Fig. 50: Indirect immunolocalization of CCTα in tachyzoites of *B. besnoiti* in the first steps of host cell invasion (RPE-1 cells).

Tachyzoites of *B. besnoiti* were processed for immunofluorescence analysis using the polyclonal antibody against *B. besnoiti* CCTα (red) and anti-*B. besnoiti* polyclonal antibody (green). DNA was stained with DAPI (blue). (A) Zoomed area corresponds to a detailed view of a *B. besnoiti* tachyzoite entering a host cell, 5min of host cell invasion. The anterior pole of *B. besnoiti* is already inside the host cell. Arrow indicates CCTα distribution in globular structures at the MJ. (B) Circular area corresponds to a *B. besnoiti* tachyzoite inside the host cell, in a PV (15min of host cell invasion). In

this image the distribution of the globular structures of CCTα inside the PV seems to be similar to the distribution of CCTα in free tachyzoites. Scale bar represents 5µm.

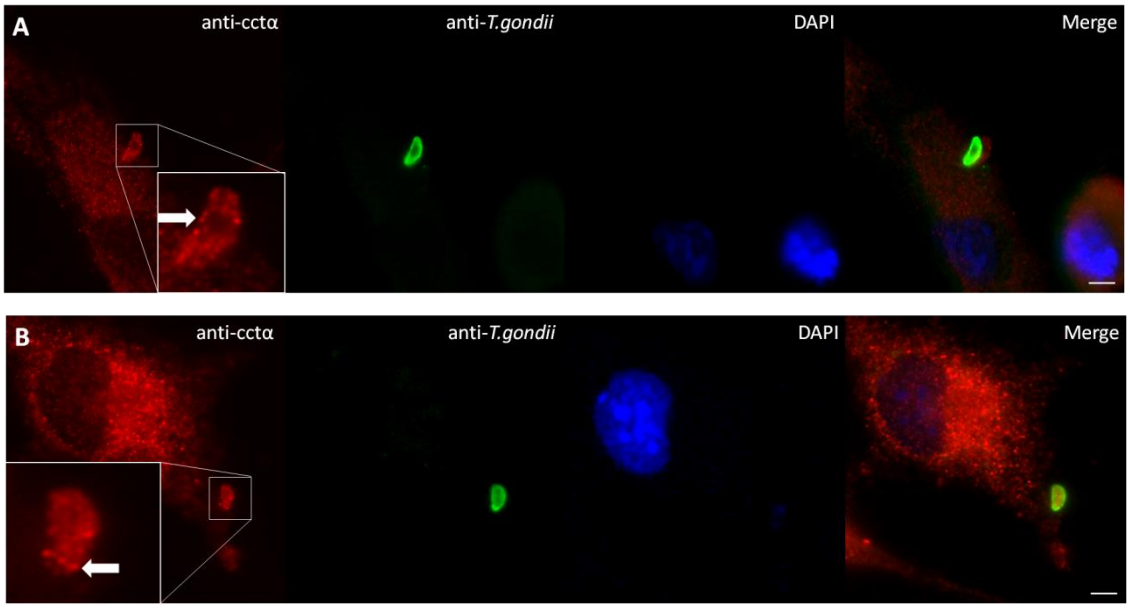

Fig. 51: Indirect immunolocalization of CCTα in tachyzoites of *T. gondii* in the first steps of host cell invasion (RPE-1 cells).

Tachyzoites of *T. gondii* were processed for immunofluorescence analysis using the polyclonal antibody against *B. besnoiti* CCTα (cross reaction, red) and anti-*T. gondii* polyclonal antibody (green). DNA was stained with DAPI (blue). (A) Zoomed area corresponds to a detailed view of a *T. gondii* tachyzoite entering a host cell, 5min of host cell invasion. The anterior pole of *T. gondii* is already inside the host cell. Arrow indicates CCTα distribution in a granular pattern around the nucleus of *T. gondii*. (B) Zoomed area corresponds to a detailed view of a *T. gondii* tachyzoite entering a host cell, with the anterior pole of *T. gondii* already inside the host cell (5min of host cell invasion). Arrow indicates CCTα distribution in globular structures at the MJ. Scale bar represents 7µm.

3.3.5 - Steady-state levels of *Besnoitia besnoiti* CCTα and *Toxoplasma gondii* CCTα, α-tubulin, TBCB, and TBCE mRNAs, during host cell invasion

The characterization of the *B. besnoiti* CCTα partial sequence also allowed the design of homologous primers to start studying the expression of this gene during different steps of host cell invasion by real time PCR. Again, using *T. gondii* as a comparison model to *B. besnoiti*, the CCTα, α-tubulin, TBCB, and TBCE of this parasite were also analyzed, in order to shed a light on how these parasites remodel their cytoskeleton when entering and multiplying inside a host cell. This way, PCR real time absolute quantification assay was used to quantify the expression of *B. besnoiti* CCTα and *T. gondii* CCTα, α-tubulin, TBCB, and TBCE mRNA at

different times of host cell invasion (free tachyzoites; 15 min; 30min; 2h; 6h; 12h; 18h; 24h and 30h). In this method, unknown samples are quantified by interpolating their quantity from a standard curve. The standard curve method for absolute quantification requires the preparation of samples of known template concentration (gene of interest cloned in the pGEM T-easy vector) that can be used by the Applied Biosystems 7300 Fast system software to determine the concentration of the unknown samples. The concentration of any unknown sample can then be determined by simple interpolation of its PCR signal (Ct- threshold cycle) into the standard curve. This way, the quantification of each gene in relation to the used housekeeping gene ITS1 is going to be presented in this section of results.

Analyzing the data obtained from two independent experiments for *B. besnoiti* (Fig. 52A) and three independent experiments for *T. gondii* (Fig. 52B), the variation of the expression levels was similar for the gene CCTα in both parasites. It was observed a decrease in the expression levels during the first minutes of host cell invasion (15 min), in comparison with the levels observed in free, non-invading, tachyzoites. It is important to refer that for *B. besnoiti* the decrease in expression is more pronounced than for *T. gondii*, having also higher values in relation to ITS1. Analyzing the following time points a recovery occurs around 6h and again at 18-24h, for *B. besnoiti*; and in *T. gondii* a first recovery of the expression levels of CCTα is detected at 2h post-invasion, and again at 12 and 24h.

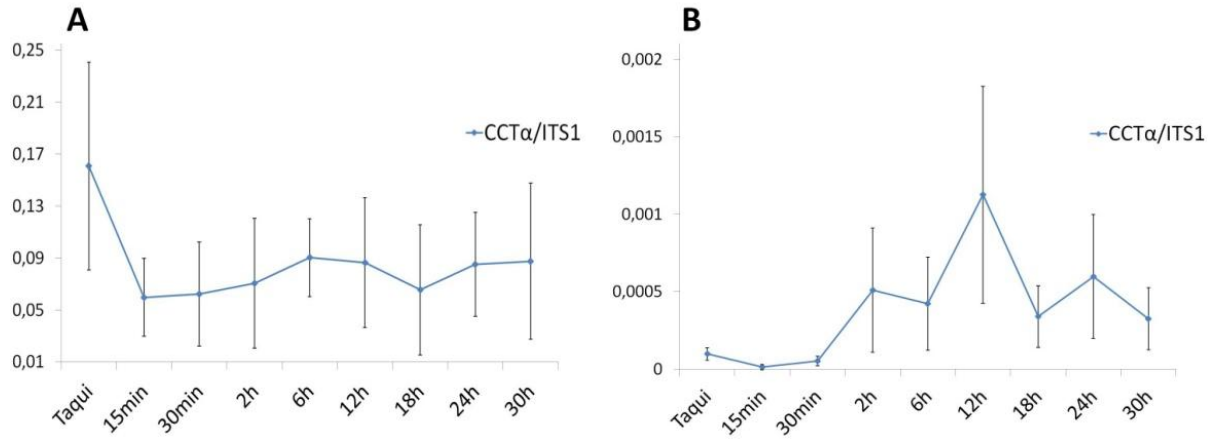

Fig. 52: Quantification of the levels of the CCTα mRNAs, in non-invaded and invaded tachyzoites. Different times of host cell invasion: 15min; 30min; 2h; 6h; 12h; 18h; 24h, and 30h. (A) In *B. besnoiti* results from two independent experiments are shown as the mean quantity values (±sd) of CCTα in relation to the mean quantity values (±sd) of the housekeeping gene ITS1 (CCTα/ITS1). (B) In *T. gondii* results from three independent experiments are shown as the mean quantity values (±sd) of CCTα in relation to the mean quantity values (±sd) of the housekeeping gene ITS1 (CCTα/ITS1).

As for the genes α-tubulin (Fig. 53A) and TBCB (Fig. 53B) of *T. gondii*, the same decrease in the expression levels is seen in the first minutes (15min) of host cell invasion, with a maximum expression levels at 2h, 12h, and 24h of invasion, identical to what was detected for CCTα, suggesting a cyclic behavior. Due to a temporal deviation in one of the experiments, there is a considerable variation in each time point. However, the cyclic behavior is confirmed when analyzing the three experiments individually (data not shown).

The gene TBCE was only possible to amplify in one experiment, represented in Fig. 53C. Even thought we were not able to amplify the gene at all time points, it is clear that the expression of this gene presents a similar behavior observed for the other cytoskeleton genes, with a decrease in the first minutes of invasion (from 15min to 30min).

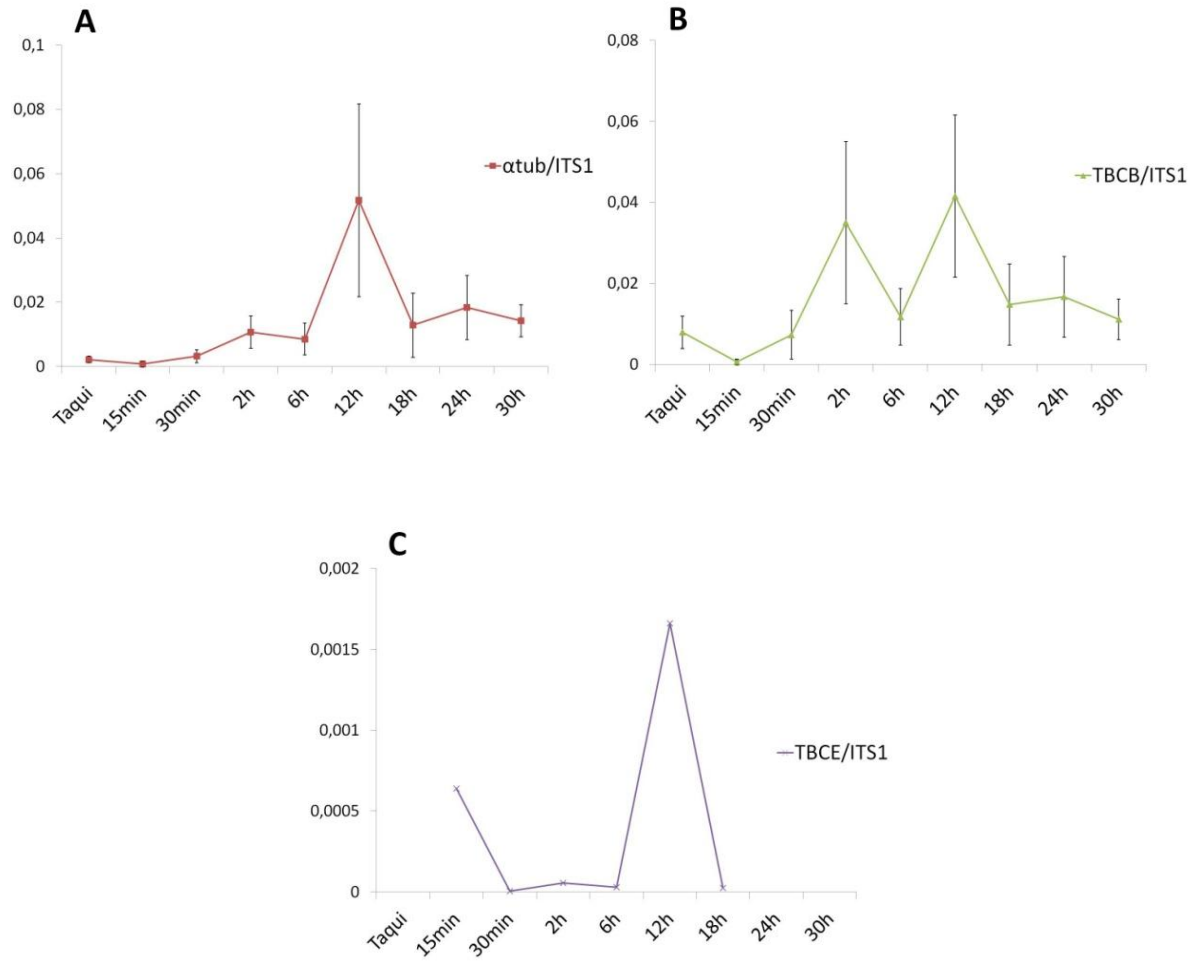

Fig. 53: Quantification of the levels of the α-tubulin, TBCB, and TBCE mRNAs of *T. gondii*, in non-invaded and invaded tachyzoites.

Different times of host cell invasion: 15min; 30min; 2h; 6h; 12h; 18h; 24h, and 30h. Results from three independent experiments are shown. (A) α-tubulin expression: shown as the mean quantity values (±sd) of α-tubulin in relation to the mean quantity values (±sd) of the housekeeping gene ITS1 (α-tubulin/ITS1). (B) TBCB expression: shown as the mean quantity values (±sd) of TBCB in relation

to the mean quantity values (±sd) of the housekeeping gene ITS1 (TBCB/ITS1). (C) TBCE expression: shown as the quantity values of TBCE in relation to the quantity values of the housekeeping gene ITS1 (TBCE/ITS1) in one experiment.

Taking into account the data described above for the two parasites *B. besnoiti* and *T. gondii*, it can be concluded that all the cytoskeletal genes studied showed reduced levels of transcription during the first 15min of host cell invasion, when compared to non invaded tachyzoites. Moreover, 2h-6h after invasion the expression levels of these genes begin to increase, behaving in what might be a cyclic pattern throughout the rest of the time period studied, suggesting the requirement of these proteins for cyclic events most probably related with *T. gondii* and *B. besnoiti* replication and growth inside the PV. In fact, we can relate the 12h and 24h increase with the doubling time (daughter cell formation) for *T. gondii* ME49 strain (11,8hours (Song *et al*., 2013)); and in the case of *B. besnoiti*, the 18-24h increase could also be related with the formation of daughter cells, since *B. besnoiti* has a longer replication time (confirmed in our laboratory experiences). Supporting this is the fact that it was already demonstrated that the expression levels of CCT subunits show a close relation with growth rates in mouse cell lines, where the expression is up-regulated in G1/S transition to early S phase (Yobota *et al*., 1999), indicating that full CCT activity is required for normal cell growth and division. In fact, taking in consideration that CCT is essential for tubulin folding, and that TBCB and TBCE have an important role in heterodimer assembly/disassembly (being key participants in the reorganization of the cell cytoskeleton), the variation of these proteins during *B. besnoiti* and *T. gondii* life cycles can be explained, since during replication there is a major reorganization of the apicomplexan cytoskeleton.

It is also interesting to notice that all the cytoskeletal genes studied have the same variations in the expression behavior, functioning has a whole. This might have its justification considering that CCT is a chaperone assisting in the folding of tubulin, and that once released from CCT, α-tubulin interacts with TBCB, being subsequently transferred to TBCE (reviewed in Fanarraga *et al*., 2001). Thus all these genes are functionally linked, which might justify the similarities in the variation of the expression levels.

3.4 - Discussion

3.4.1 - Isolation and characterization of the CCTα gene from *Besnoitia besnoiti* and *Toxoplasma gondii*; and α-tubulin, TBCB, and TBCE from *Toxoplasma gondii*

CCT has eight subunits encoded by independent and highly diverged genes. One of these subunits is CCTα, whose amino acid sequence is highly conserved in eukaryotes (animals, plants, yeasts and protozoa). The partial sequence of *B. besnoiti* CCTα encodes 197 amino acids, and the predicted protein sequence is identical to that predicted for *T. gondii* (95%) and *N. caninum* (96%). A high protein identity with *N. caninum* (97%) was also seen for the total protein sequence of *T. gondii* CCTα. Moreover, *B. besnoiti* and *T. gondii* CCTα have sequence motifs that are conserved in all apicomplexan parasites studied (*N. caninum*, *T. parva*, *T. annulata*, *B. bovis* and *P. vivax*). These include the motifs RSSLGPQGLDKML (positions 31±43), ITNDGATILKQLEVQHP (positions 52±68), GDGTTSV (positions 85±91) and VCPGGG (positions 406±411; not found in *B. besnoiti* as it is only a partial sequence). These motifs probably represent conserved polypeptide binding sites (RSSLGPQGLDKML, ITNDGATILKQLEVQHP, and VCPGGG); and the GDGTTSV motif is closely related to a nucleotide phosphate-binding domain of the cAMP-dependent kinase (Lewis *et al*., 1992) The presence of these motifs is related to the CCT folding functions, since CCT interacts with proteins (actin and tubulin) in order to reach their native states (Sternlicht *et al*., 1993). Moreover, the ATP-binding site in the equatorial domain allows for the large conformational rearrangements generated upon ATP binding to assist in the folding of these proteins (Schoehn *et al*., 2000).

α-tubulin is a highly conserved protein, which is shown by the amino acid sequence identity between *T. gondii* and *N. caninum* (100%) and the high similarity between *T. gondii* and the other apicomplexan parasites in study (*P. vivax, T. parva,* and *B. bovis*). Analyzing *T. gondii* α-tubulin for conserved motifs, several nucleotide binding sites were found; as well as sites for the oligomerization interface with the following and preceding β subunit of the MT protofilaments; and MAP binding regions.

Compared to CCTα and α-tubulin, the amino acid sequence identity between the different apicomplexan species of TBCB and TBCE is significantly lower. Similar to its human orthologue, TBCB and TBCE have two conserved domains: an ubiquitin-like domain (Ubl), and a cytoskeleton-associated protein (CAP)-glycine rich (Gly) domain (Fig. 39 and Fig. 40). The reverse position of the CAP-Gly domain (on the C- and N-termini of TBCB and TBCE, respectively), and the Ubl domain (on the N- and C-termini of TBCB and TBCE,

respectively) in *T. gondii* TBCB and TBCE is in accordance to the tubulin dissociation route involving a TBCB–TBCE binary complex proposed by Kortazar *et al*, 2007. In this hypothesis, Ubl domains (that are usually involved in protein-protein interactions) of TBCB and TBCE may contribute to the interaction between these two proteins, and the two resulting CAP-Gly domains are where the tubulin heterodimer fits for tubulin processing. After the dissociation of the heterodimer, the ternary complex disassembles into either TBCB/α-tubulin and free TBCE; or TBCE/α-tubulin and free TBCB (Kortazar *et al*., 2007).

In summary, after analyzing the sequences retrieved for the genes in study, *B. besnoiti, T. gondii* and *N. caninum* are closely related, distanced from other studied apicomplexan parasites (*Theileria, Eimeria, Plasmodium* and *Babesia*). However, and despite the morphological, structural and molecular similarity between these parasites, the amplification of *B. besnoiti* with primer sequences for *T. gondii* was not possible, which might indicate some divergence in the course of genome evolution.

3.4.2 - Immunolocalization of CCTα in *Besnoitia besnoiti* and *Toxoplasma gondii* tachyzoites

After characterizing *B. besnoiti* CCTα partial sequence, we addressed the immunolocalization of the protein in invading and non invading (free) tachyzoites. As it can be observed in Fig. 46 and Fig. 47, in free tachyzoites CCTα is spread throughout the cytoplasm, with the detection of globular like structures mainly at the anterior pole. This pattern is consistent to what was observed for the *S. cerevisiae* CCTα, localized in the cortex and the cell cytoplasm with a noticeable granular distribution and an unstained nuclear region (Somer *et al*., 2002). The granular distribution of CCTα is also common to *Tetrahymena*, where CCTα was found between the cilia rows of the protozoa, and in the cytoplasm as small granular/globular like structures (Seixas *et al*., 2003). In agreement with the fact that ribosomes have been found physically associated with the cytoskeleton, existing a close interaction of CCT with ribosome-bound nascent polypeptides (McCallum *et al*., 2000), in *Tetrahymena* cells it is suggested that these globular structures containing TpCCT-subunits are sites of translation and protein folding, closely associated with Mts. In fact, in *Tetrahymena,* evidence points to the existence of oligomeric structures containing CCT subunits that are able to directly bind to tubulin playing a role during cilia biogenesis, tubulin transport, and/or axoneme assembly (Seixas *et al*., 2003). Recently, it has been proved that in *Tetrahymena* CCTα is indeed a ciliary protein that is important for the maintenance of cilia tip integrity, being present in both membrane/matrix and axonemal fractions of cilia, suggesting that the protein is interacting with the axonemal MTs while circulating in the ciliary compartment, which leads into

thinking that the CCT subunits found in the ciliary compartment might have other functions (Seixas *et al*., 2010). Furthermore, CCTα and CCTε subunits appear in the insoluble fraction that contains parts of the cortex structure, including basal bodies and cilia, of *Tetrahymena*, indicating a possible association of these subunits with the Mt structures (Casalou *et al*., 2001).

The fact that in some images of extracellular tachyzoites (Fig. 46C and D; Fig. 47B and C) the localization of CCTα seems to follow the basket-weave pattern of the conoid fibers, accompanying the spiral distribution of the subpellicular MTs along the tachyzoite, seems to support the hypothesis of CCTα being a MAP. It has been described that the conoid fibers have a protofilament structure, but, unlike MTs, the protofilaments are not arranged as a closed tube, and instead form ribbons of nine protofilaments folded into a comma shape. In addition to the protofilaments, small structures with lower contrast are consistently seen in the conoid, likely representing MAPs attached to the tubulin protofilaments. This is in accordance with the fact that although the conoid fibers are composed of the same tubulin isoforms as those of MTs, they do not have a structure of MTs, probably because of their association with other non tubulin proteins: MAPs (Hu *et al*., 2002). We propose that one of these proteins could be CCTα, associating not only to the protofilaments in the conoid fibers, but also accompanying the MT subpellicular structure along the whole length of the parasites. Therefore, the CCTα monomers by themselves may have an important activity in MT organization and dynamics, interacting with forms of assembled MT structures, perhaps facilitating tubulin polymerization in the intracellular environment (Roobol *et al*., 1999). Supporting this hypothesis, CCTα has been localized at the centrosome, indicating that CCTα may be essential for nucleated MT assembly from this organelle (Brown *et al*., 1996) and at the manchette (MT structure unique to male germ cells) during spermiogenesis (Soues *et al*., 2003).

Meanwhile, in order to prove its role as a MAP in these parasites, several other conditions should be addressed: not being quantitatively removed from cell extracts by assembling MTs; not stimulating tubulin assembly *in vitro*; and finally, being dissociated from MTs by ATP (Roobol *et al*., 1999).

In invading tachyzoites (Fig. 48, Fig. 49, Fig. 50, and Fig. 51), there are no dramatic alterations in comparison to what was observed in non invaded tachyzoites, with granular structures in the cytoplasm, sometimes concentrated around the nucleus (which might correspond to a transverse plane of the 22 subpellicular MTs that distribute along the parasite´s body, going around the nucleus, and nucleated at the apical polar ring). Interestingly, an accumulation of CCTα seems to be present at the MJ. However, the

difficulty is to distinguish whether this CCTα belongs to the parasite or if it is recruited from the host cell cytoplasm to the MJ, since the produced antibody against the *B. besnoiti* anti-CCTα cross reacts with the CCTα of the mammalian host cell. Despite the fact that molecular characterization of the MJ in *T. gondii* is incomplete, micronemal and rhoptry proteins have been identified, with AMA1 relocalizing from micronemes to the parasite surface, and RON proteins being secreted inside the host cell by the parasite (Besteiro *et al*., 2009). Since both *B. besnoiti* (Reis *et al*., 2006) and *T. gondii* (Sweeney *et al*., 2010) have host cell MTs localized to the MJ, it can be speculated that by using host MTs, the secreted RON complex is delivered to the host plasma membrane where it binds AMA1 and forms the MJ. Our hypothesis is that CCTα may be involved in interactions between MTs and the MJ that is partially incorporated in the biochemical composition of the PVM, upon invasion of the tachyzoite. This is supported by the fact that a putative member of the TCP-1/chaperonin family MAL13P has been found in the PV of *P. falciparum* (Nyalwidhe & Lingelbach, 2006). Adding to this, there are other evidences that CCT subunits interact with membranes: the adrenal medullary form of CCT efficiently binds to chromaffin granule membranes (reviewed in Kubota *et al*., 1995) and in human erythrocytes, 20–30% of the total CCTα reservoir translocates from the cytoplasm to the plasma membrane following a heat-shock, being actin a strong candidate protein for the specific interaction (Wagner *et al*., 2004). This translocation is thought to have a protective role in cell stabilization during stress. Having this in consideration, we could suppose that the same stabilizing, protective mechanism is present when *B. besnoiti* and *T. gondii* tachyzoites invade the host cell, mobilizing CCTα to the MJ in response to a cellular insult, which in this case could be the compressive forces induced by the tachyzoites when in contact with the host cell.

Thus, we propose that CCTα is a MAP, colocalizing with the subpellicular MTs and fibers of the conoid in *T. gondii* and *B. besnoiti*. Upon invasion, it partially translocates to the MJ, possibly playing a role in the interaction of the host MTs with the molecular components that will later be incorporated at the PV membrane. On the other hand, the presence of CCTα at the MJ could be also a response to the stress generated during cell invasion, due to the all the cytoskeleton remodeling occurring during the protrusion of the conoid, and the recruitment of the host cell cytoskeleton. Therefore, the CCTα could be mobilized from the parasite, the host cell, or both, since the remodeling occurs in both cytoskeletons. Assuming that this remodeling depends on the tubulin folding pathway, it justifies the whole CCT complex (including CCTα) being present at the MJ.

3.4.3 - Gene expression of *Besnoitia besnoiti* CCTα and *Toxoplasma gondii* CCTα, α-tubulin, TBCB, and TBCE, during host cell invasion

Many cellular functions are regulated by changes in gene expression. In order to understand how genes participating in the tubulin folding pathway are regulated during host cell invasion, we quantified the steady-state levels of *B. besnoiti* CCTα and *T. gondii* CCTα, α-tubulin, TBCB, and TBCE mRNAs in free tachyzoites and at different times of host cell invasion (15 min; 30min; 2h; 6h; 12h; 18h; 24hand 30h). Nevertheless, the amplification of TBCE was only possible in one experiment, and this could be due to a lower efficiency of RNA to cDNA conversion, that is dependent on template abundance: it is significantly lower when target templates are rare (Karrer *et al*., 1995); and is negatively affected by non-specific or background nucleic acid present in the reverse transcription reaction (Curry *et al*., 2002). The alternative for amplifying TBCE could be the use of target-specific primers, resulting in the synthesis of the most specific cDNA, therefore providing the greatest sensitivity for quantitative assays (Lekanne Deprez *et al*., 2002). The main disadvantage of this method is that it requires separate priming reactions for each target gene; hence it would not be possible to return to the same preparation to amplify other genes. While it is possible to amplify more than one target in a single reaction tube (multiplex), this is not trivial and requires careful experimental design and optimization of reaction conditions to prevent for the amplification of non specific sequences (reviewed in Wittwer *et al*., 2001).

Although real-time PCR is widely used to quantify biologically relevant changes in mRNA levels, a number of problems remain associated with its use. These include the inherent variability of RNA, variability of extraction, and different reverse transcription and PCR efficiencies. Consequently, it is important that an accurate method of normalization is chosen to control for this error (reviewed in Huggett *et al*., 2005). This way, in our experiments a housekeeping gene (ITS1, a ribosomal RNA) was used as an internal reference against which the gene expression values for the target genes was normalized (reviewed in Karge *et al*., 1998). The ideal housekeeping gene should be expressed at a constant level among different tissues of an organism, at all stages of development, and should be unaffected by the experimental treatment. Thus, rRNAs (ribosomal RNAs), which constitute 85–90% of total cellular RNA, are useful internal controls, as the various rRNA transcripts are generated by a distinct polymerase (reviewed in Paule & White, 2000) and their levels are less likely to vary under conditions that affect the expression of mRNAs (Barbu & Dautry, 1989).

Analyzing the results shown in Fig. 52 and Fig. 53 for *T. gondii* and *B. besnoiti* gene expression it can be concluded that there is a decrease in the levels of the tubulin folding

pathway gene transcripts upon the first minutes of host cell invasion, followed by what could be a cyclic behavior of expression, until the end of the studied time course.

Tachyzoite host cell invasion is dependent on a unique form of gliding motility powered by the parasite actomyosin system. This way, gliding motility and invasion events involve the active participation of the actin cytoskeleton of the parasites and associated proteins (reviewed in Frénal & Soldati-Favre, 2009). Supporting this, actin-disrupting or stabilizing drugs (cytochalasin D and jasplakinolide), as well as myosin inhibitors (butanedione monoxime), disrupt *T. gondii* motility and invasion (Dobrowolski & Sibley, 1996; Dobrowolski *et al*., 1997a), but do not prevent parasite growth and replication (Shaw *et al*., 2000). Therefore, it seems that the actin cytoskeleton is fundamental when entering the host cell, being the MT cytoskeleton of great importance mainly in later events of the tachyzoite cell cycle, more precisely during replication inside the PV. This correlates with a decrease in the expression in the first steps of host cell invasion of all the genes studied that participate in the tubulin folding pathway (CCTα, α-tubulin, TBCB and TBCE); followed by a enhanced expression once the parasite starts to replicate. Also supporting this is the fact that treatment of *T. gondii* with the destabilizing drug oryzalin or the stabilizing drug taxol blocked replication and led to the formation of abnormal parasites (Shaw *et al*., 2000).

B. besnoiti and *T. gondii* tachyzoites replicate inside the PV by means of internal budding, termed endodyogeny, where the nuclear division is followed by formation of two daughter cells within the mother parasite. The daughter cells are delimited by an inner membrane complex and associated subpellicular MTs, and each contains a set of apical organelles (conoid, rhoptries and micronemes) and a nucleus, mitochondrion, Golgi apparatus, ER and apicoplast (Morrissette & Sibley, 2002a). All the processes of organelle migration and segregation during daughter cell budding are likely related with cytoskeletal elements. Indeed, daughter cell budding does not involve a dynamic actin cytoskeleton, but is dependent on the parasite MT system, requiring the polymerization of MTs (Shaw *et al*., 2000; Nishi *et al*., 2008). The two populations of MTs in tachyzoites are spindle MTs and subpellicular MTs. Subpellicular MTs are important for shape and apical polarity, and are not required for scission of the nucleus during mitosis, but play an important role in segregation of organelles to daughter buds (Shaw *et al*., 2000). The spindle MTs form an intra-nuclear spindle (a closed mitosis) to coordinate chromosome segregation during tachyzoite replication (Morrissette & Sibley, 2002a). Both the mitotic spindle and subpellicular MTs formed in the daughter cells are synthesized *de novo* since the subpellicular MTs in the mother cell do not disappear until near the end of the budding process. This way, there is the formation of new, dynamic MTs, without the disassembly of the previous mother MTs (Shaw *et al*., 2000). This probably

coincides with the enhanced expression of the α-tubulin and the folding pathway genes of *B. besnoiti* and *T. gondii* around 2h-6h, and again at 12h-24h, which might correspond with the assembly of new, highly dynamic MTs in daughter cells, in opposition to the non-dynamic, highly stable subpellicular MTs of the mother cell, once the parasites are inside the PV and start to replicate (reviewed in Morrissette & Sibley, 2002b).

The importance of CCT subunits in growing cells has already been demonstrated: in mouse and human cells, faster growing cells express CCT subunits at higher levels (Yobota *et al*., 1999). In fact, mouse tissues abundant in growing cells (testis, spleen, thymus, and bone marrow) express much higher levels of CCT subunits and their mRNAs than those poor in growing cells (heart, kidney, and lung) (Kubota *et al*., 1992; Xie & Palacios, 1994). Moreover, CCT subunits start to be synthesized at an early cleavage stage in mouse preimplantation embryos (Sevigny *et al*., 1995). As expected, in growing cells, one of the CCT roles seems to be assisting in the folding of tubulin and actin (Yobota *et al*., 1999). However, the contribution of the abundant CCT in rapidly growing cells could be extended to other suggested targets: α-transducin (Farr *et al*., 1997); firefly luciferase (Frydman & Hartl, 1996; Gebauer *et al*., 1998); cofilin (Melki *et al*., 1997), the 22-kDa peroxisomal membrane protein (Pause *et al*., 1997) and cyclin E (Won *et al*., 1998). Importantly, the increase in synthesis of CCT subunits occurs at almost the same time as an increase in CCT level, and is controlled at the mRNA level, with a maximum CCT protein and mRNA levels occurring at the G1/S transition through early S phase, in mouse DA3 myeloid cells (Yobota *et al*., 1999). In *T. gondii* tachyzoites, the daughter cells scaffold begins to form just before the end of DNA replication, which, in the case of the RH strain is around 2 to 3h post-invasion (Nishi *et al*., 2008). This can coincide with the CCTα increase in mRNA levels, which would begin at DNA replication and formation of the intranuclear spindle, extending through the formation of the conoid, IMC and associated subpellicular MTs.

Considering the role of TBCB and TBCE in the *de novo* folding of tubulin dimers, it is not surprising that their expression would be increased during the assembly of the daughter cell conoid and other cytoskeletal elements. This is supported by the fact that increasing amounts of TBCB and TBCE mRNA overlaps with increasing α-tubulin mRNA levels (Fig. 53). Since they also seem to participate in the tubulin dissociation route involving a TBCB–TBCE binary complex (Kortazar *et al*., 2007), their enhanced mRNA levels could coincide with the disassemble of the apical conoid complex and the subpellicular cytoskeleton of the mother cell, which are presumably broken down and recycled by the parasite (Nishi *et al*., 2008), assuming that in this case, an increase in the mRNA levels translates into a rise in protein levels.

Summarizing, while the expression of the genes of the tubulin folding pathway decreases in the first steps of host cell invasion, suggesting a not so active role of the MT cytoskeleton at this stage, it increases during parasite replication. Thus, it seems reasonable to conclude that a dynamic MT cytoskeleton in the parasite is essential for parasite growth and daughter cell budding.

Chapter 4: Final Considerations

There are many morphological and ultrastructural similarities between *B. besnoiti* and *T. gondii* infective stages, and research on *B. besnoiti* has benefited from this fact, since *T. gondii* is one of the best characterized protozoan parasites to date. Thus, in this work, *T. gondii* was studied as a comparative model for the observations in *B. besnoiti*, and this allowed to conclude about what seems to be different evolutionary paths, related with different strategies for interacting with the invaded host at a cellular level.

In fact, both parasites remodel the host MTs cytoskeleton during invasion and replication inside the host cell. This remodeling, in *T. gondii* is related with the host cell centrosome recruitment to the PV in more advanced stages of PV development; in *B. besnoiti* this interaction with the host cell centrosome does not seem to occur, so another mechanism independent of the host centrosome must be present during MT reorganization. Meanwhile, both parasites relocate the Golgi apparatus to the PV in the first moments of PV establishment, but have completely different effects on Golgi morphology: *T. gondii* fragments the Golgi ribbon and *B. besnoiti* compacts its structure. The positioning of the Golgi next to the PV is probably dependant on the MT cytoskeleton rearrangements of the host cell occurring both during *B. besnoiti* and *T. gondii* invasion. However, the completely different effect on Golgi´s morphology and structure by the parasites suggests a different mechanism of Golgi manipulation. It seems that *T. gondii* influences the traffic of vesicles inside the Golgi apparatus, sequestering Rab14-, Rab30-, or Rab43-associated vesicles containing sphingolipids, within the PV, which causes fragmentation (Romano *et al*. 2013). Nonetheless, other causative mechanisms of Golgi apparatus fragmentation and compaction can exist, such as those related with the interference with the MT cytoskeleton and Golgi stacking proteins (GRASPs). Further molecular studies on how these two parasites differently affect Golgi´s morphology, would be of great importance in order to shed a light on the different pathogenesis of these two parasites.

We have studied not only the role of host components in *B. besnoiti* and *T. gondii* cell invasion, but also parasite molecules important for biogenesis and dynamics of the microtubule cytoskeleton that are good candidates to be involved in host cell invasion and replication inside the PV. In fact, during invasion, an accumulation of CCTα is detected at the MJ, perhaps having an important role mediating the interaction of the parasite with the host microtubules. Meanwhile, the levels of expression of genes involved in the tubulin folding pathway of the parasites (CCTα, TBCB, TBCE and α-tubulin), behave in an apparent cyclic manner throughout the parasite replication inside the host cell, probably coinciding with the formation of the intranuclear spindle and elongation of the daughter cell scaffold (IMC, conoid and subpellicular MTs). This way, a dynamic MT cytoskeleton in the parasite is

essential in later events of the tachyzoite cell cycle, more precisely during replication inside the PV.

Finally, it is important to refer that there are currently available drugs to treat toxoplasmosis, but they usually have severe side effects, cannot act against chronic *T.gondii* infections, and some reports of resistance to some of these drugs have appeared (Dannemann *et al*., 1992). Moreover, several attempts to develop effective drugs to treat bovine besnoitiosis have also been made, but until now with no considerable success (Shkap *et al*., 1985; Shkap *et al*., 1987). Considering this, elucidation of the molecular effector mechanisms and host cell targets of how *T. gondii* and *B. besnoiti* manipulate host cells to establish infection and propagate in their host, could reveal new vulnerabilities for the parasites that might be useful for an efficient therapeutic and prophylactic research.

References

Abruzzi, K. C., Smith, A., Chen, W., Solomon, F. (2002). Protection from free beta-tubulin by the beta-tubulin binding protein Rbl2p. Molecular and Cellular Biology, 22, 138–147.

Agosti, M., Belloli, A., Morini, M., Vacirca, G. (1994). Segnalazione di un focolaio di Besnoitiosi in bovini da carne importati. Praxis 15, 5–6.

Ahn, H. J., Kim, S., Kim, H. E., Nam, H. W. (2006). Interactions between secreted GRA proteins and host cell proteins across the paratitophorous vacuolar membrane in the parasitism of *Toxoplasma gondii*. *The Korean Journal of Parasitology*, 44, 303–312.

Ahn, H. J., Kim, S., Nam, H. W. (2005). Host cell binding of GRA10, a novel, constitutively secreted dense granular protein from *Toxoplasma gondii*. *Biochemical and Biophysical Research Communications*, 331, 614–620.

Akstein, R. B., Wilson, L. A., Teutsch, S. M. (1982). Acquired toxoplasmosis. *Ophthalmology*, 89, 1299– 1302.

Alexander, D. L., Mital, J., Ward, G. E., Bradley, P., Boothroyd, J. C. (2005). Identification of the moving junction complex of *Toxoplasma gondii*: a collaboration between distinct secretory organelles. *PLoS Pathogens*, 1, e17.

Allan, V. J., Thompson, H. M., McNiven, M. A. (2002). Motoring around the Golgi. *Nature Cell Biology*, 4, 236–242.

Anderson-White, B., Beck, J. R., Chen, C-T., Meissner, M., Bradley, P. J., Gubbels, M. J. (2012). Cytoskeleton assembly in *Toxoplasma gondii* cell division. *International Review Of Cell and Molecular Biology*, 298, 1–31.

André, J., Harrison, S., Towers, K., Qi, X., Vaughan, S., McKean, P. G., Ginger, M. L. (2013). The tubulin cofactor C family member TBCCD1 orchestrates cytoskeletal filament formation. *Journal of Cell Science*, 126, 5350–5356.

Araujo, F. G., Remington, J. S. (1974). Effect of clindamycin on acute and chronic toxoplasmosis in mice. *Antimicrobial Agents and Chemotherapy*, 5, 647–651.

Aronson, J. F. (1971). Demonstration of a colcemid-sensitive attractive force acting between the nucleus and a center. *The Journal of Cell Biology*, 51, 579-583.

Azimzadeh, J., Bornens, M. (2007). Structure and duplication of the centrosome. *Journal of Cell Science*, 120, 2139-2142.

Azimzadeh, J., Marshal, W. F. (2010). Building the Centriole. *Current Biology*, 20(18), 816–825.

Baffet, A. D., Benoit, B., Januschkeb, J., Audo, J., Gourhand, V., Roth, S., Guichet, A. (2012). *Drosophila* tubulin-binding cofactor B is required for microtubule network formation and for cell polarity. *Molecular Biology of the Cell*, 23, 3591-3601.

Baloyannis, S. J., Costa, V., Michmizos, D. (2004). Mitochondrial alterations in Alzheimer's disease. *American Journal of Alzheimer´s Disease & Other Dementias*, 19, 89–93.

Bannister, L. H., Mitchell, G. H. (1995). The role of the cytoskeleton in *Plasmodium falciparum* merozoite biology: an electron-microscopic view. *Annals of Tropical Medicine* and *Parasitology*, 89, 105–111.

Barbu, V., Dautry, F. (1989). Northern blot normalization with a 28S rRNA oligonucleotide probe. *Nucleic Acids Research*, 17(17), 7115.

Barr, A. R., Kilmartin, J. V., Gergely, F. (2010). CDK5RAP2 functions in centrosome to spindle pole attachment and DNA damage response. *The Journal of Cell Biology*, 189, 23–39.

Barr, F. A., Puype, M., Vandekerckhove, J., Warren, G. (1997). GRASP65, a protein involved in the stacking of Golgi cisternae. *Cell*, 91, 253-262.

Barragan, A., Sibley, L. D. (2002). Transepithelial migration of *Toxoplasma gondii* is linked to parasite motility and virulence. *The Journal of Experimental Medicine*, 195, 1625–1633.

Bartolini, F., Bhamidipati, A., Thomas, S., Schwahn, U., Lewis, S. A., Cowan, N. J. (2002) Functional overlap between retinitis pigmentosa 2 protein and the tubulin-specific chaperone cofactor C. *The Journal of Biological Chemistry*, 277, 14629–14634.

Bartolini, F., Tian, G., Piehl, M., Cassimeris, L., Lewis, S. A., Cowan, N. J. (2005). Identification of a novel tubulin-destabilizing protein related to the chaperone cofactor E. *Journal of Cell Science*, 118, 1197–1207.

Basso, W., Schares, G., Gollnick, N. S., Rütten, M., Deplazes, P. (2011). Exploring the life cycle of *Besnoitia besnoiti* - experimental infection of putative definitive and intermediate host species. *Veterinary Parasitology*, 178(3-4), 223-234.

Basson, P. A., Mccully, R. M., Bigalke, R. D. (1970). Observations on the pathogenesis of bovine and antelope strains of *Besnoitia besnoiti* (Marotel, 1912) infection in cattle and rabbits. *Onderstepoort Journal of Veterinary Research*, 37, 105-126.

Baumgartner, M. (2011) *Theileria annulata* promotes Src kinase-dependent host cell polarization by manipulating actin dynamics in podosomes and lamellipodia. *Cellular Microbiology*, 13, 538–553.

Beauvais, B., Garin, J. F., Lariviere, M., Languillat, G., Galal, H. (1976). Toxoplasmose et transfusion. *Annales de parasitologie humaine et comparée*, 51, 625–635.

Beck, J. R., Fung, C., Straub, K. W., Coppens, I., Vashisht, A. A., Wohlschlegel, J. A., Bradley, P. J. (2013). A *Toxoplasma* palmitoyl acyl transferase and the palmitoylated armadillo repeat protein TgARO govern apical rhoptry tethering and reveal a critical role for the rhoptries in host cell invasion but not egress. *PLOS Pathogens*, 9(2), e1003162.

Beck, J. R., Rodriguez-Fernandez, I. A., de Leon, J. C., Huynh, M. H., Carruthers, V. B., Morrissette, N. S., Bradley, P. J. (2010). A novel family of *Toxoplasma* IMC proteins displays a hierarchical organization and functions in coordinating parasite division. *PLoS Pathogens*, 6(9), e1001094.

Bejon, P. A., Bannister, L. H., Fowler, R. E., Fookes, R. E., Webb, S. E., Wright, A., Mitchell. G. H. (1997). A role for microtubules in *Plasmodium falciparum* merozoite invasion. *Parasitology*, 114, 1–6.

Bergmann, J. E., Kupfer, A., Singer, S. J. (1983). Membrane insertion at the leading edge of motile fibroblasts. *Proceedings of the National Academy of Sciences*, 80, 1367–1371.

Besnoit, C., Robin, V. (1912). Sarcosporidiose cutanée chez une vache. *Recueil de Médecine Vétérinaire*, 37, 649-651.

Besteiro, S., Dubremetz, J. F., Lebrun, M. (2011). The moving junction of apicomplexan parasites: a key structure for invasion. *Cellular Microbiology*, 13(6), 797-805.

Besteiro, S., Michelin, A., Poncet, J., Dubremetz, J. F., Lebrun, M. (2009). Export of a *Toxoplasma gondii* rhoptry neck protein complex at the host cell membrane to form the moving junction during invasion. *PLoS Pathogens*, 5: e1000309.

Bhamidipati, A., Lewis, S. A., Cowan, N. (2000). ADP ribosylation factor-like protein 2 (Arl2) regulates the interaction of tubulin-folding cofactor D with native tubulin. *Journal Cell Biology*, 149, 1087–1096.

Bigalke, R. D. (1960). Preliminary observation on the mechanicalvtransmission of cyst organisms of *Besnoitia besnoiti* (Marotel 1912) from a chronically infected bull to rabbits by *Glossina brevipalpis Newstead*, 1910. *Journal of the South African Veterinary Association*, 31, 37–44.

Bigalke, R. D. (1968). New concepts on the epidemiological features of bovine besnoitiosis as determined by laboratory and field investigations. *Onderstepoort Journal of Veterinary Research*, 35, 3–138.

Bigalke, R. D. (1981). Besnoitiosis and Globidiosis. In: Ristic, R., McIntyre, I. (Eds.), *Diseases of Cattle in the Tropics*. (pp. 429–442). The Hague, Netherlands: Martinus Nijhoff Publishers.

Bigalke, R. D., Basson, P. A., Mccully, R. M., Bosman, P. P. (1973) Studies in cattle on the development of a live vaccine against bovine besnoitiosis. *Proceedings of the Biennial Scientific Congress of the South African Veterinary Association.* (pp 2-3). Pretoria, South Africa.

Bigalke, R. D., Prozesky, L. (2004). Besnoitiosis. In: Coetzer, J. A.W., Tustin, R. C. (Ed.), *Infectious Diseases of Livestock*, (pp. 331–359). Cape Town, South Africa: Oxford University Press.

Bigalke, R. D., Van Niekerk, J. W., Basson, P. A., Mccully, R. M. (1967). Studies on the relationship between *Besnoitia* of blue wildebeest and impala, and *Besnoitia besnoiti* of cattle. *Onderstepoort Journal of Veterinary Research*, 34, 7-28.

Binarova, P., Cenklová, V., Procházková, J., Doskocilová, A., Volc, J., Vrlík, M., Bögre L. (2006). γ-tubulin is essential for acentrosomal microtubule nucleation and coordination of late mitotic events in *Arabidopsis*. *The Plant Cell*, 18, 1199–1212.

Bisanz, C., Bastien, O., Grando, D., Jouhet, J., Maréchal, E., Cesbron- Delauw, M. F. (2006). *Toxoplasma gondii* acyl-lipid metabolism: *de novo* synthesis from apicoplast-generated fatty acids versus scavenging of host cell precursors. *The Biochemical Journal*, 394, 197–205.

Bisel, B., Wang, Y., Wei, J.H., Xiang, Y., Tang, D., Miron-Mendoza, M., Yoshimura, S., Nakamura, N., Seemann, J. (2008). ERK regulates Golgi and centrosome orientation towards the leading edge through GRASP65. *The Journal of Cell Biology*, 182, 837–843.

Blader, I. J., Saeij, J. P. (2009). Communication between *Toxoplasma gondii* and its host: impact on parasite growth, development, immune evasion, and virulence. *APMIS: Acta Pathologica, Microbiologica, et Immunologica Scandinavica*, 117(5-6), 458-476.

Bonnet, C., Boucher, D., Lazereg, S., Pedrotti, B., Islam, K., Denoulet, P., Larcher, J. C. (2001). Differential binding regulation of microtubule-associated proteins MAP1A, MAP1B, and MAP2 by tubulin polyglutamylation. *The Journal of Biological Chemistry*, 276, 12839–12848.

Bornens, M. (2008). Organelle positioning and cell polarity. *Nature Reviews Molecular Cell Biology*, 9, 874–886.

Bornens, M. (2012).The Centrosome in Cells and Organisms. *Science*, 335(6067), 422-426.

Bouissou, A., Vérollet, C., Sousa, A., Sampaio, P., Wright, M., Sunkel, C. E., Merdes, A., Raynaud-Messina, B. (2009). {gamma} - Tubulin ring complexes regulate microtubule plus end dynamics. *The Journal of Cell Biology*, 187, 327–334.

Brackley, K. I., Grantham, J. (2009). Activities of the chaperonin containing TCP-1 (CCT): implications for cell cycle progression and cytoskeletal organisation. *Cell Stress and Chaperones*, 14, 23–31.

Bradley, P.J., Ward, C., Cheng, S. J., Alexander, D. L., Coller, S., Coombs, G. H., Dunn, J. D., Ferguson, D. J., Sanderson, S. J., Wastling, J. M., Boothroyd, J. C. (2005). Proteomic analysis of rhoptry organelles reveals many novel constituents for host-parasite interactions in *Toxoplasma gondii*. *The Journal of Biological Chemistry*, 280, 34245–34258.

Brown, C. R., Doxsey, S. J., Hong-Brown, L. Q., Martin, R. L., Welch, W. J. (1996). Molecular chaperones and the centrosome: a role for TCP-1 in microtubule nucleation. *The Journal of Biological Chemistry*, 271, 824–832.

Brownhill, K., Wood, L., Allan, V. (2009). Molecular motors and the Golgi complex: staying put and moving through. *Seminars in Cell & Developmental Biology*, 20, 784–792.

Brunet, J., Pfaff, A. W., Abidi, A., Unoki, M., Nakamura, Y., Guinard, M., Klein, J. P., Candolfi, E., Mousli, M. (2008). *Toxoplasma gondii* exploits UHRF1 and induces host cell cycle arrest at G2 to enable its proliferation. *Cellular Microbiology*, 10, 908–920.

Buch, C., Lindberg, R., Figueroa, R., Gudise, S., Onischenko, E., Hallberg, E. (2009). An integral protein of the inner nuclear membrane localizes to the mitotic spindle in mammalian cells. *Journal of Cell Science*, 122, 2100–2107.

Bullen, H. E., Tonkin, C. J., O'Donnell, R. A., Tham, W. H., Papenfuss, A. T., Gould, S., Cowman, A. F., Crabb, B. S., Gilson, P. R. (2009). A novel family of Apicomplexan

glideosome-associated proteins with an inner membrane-anchoring role. *The Journal of Biological Chemistry*, 284, 25353–25363.

Burg, J. L., Grover, C. M., Pouletty, P., Boothroyd, J. C. (1989). Direct and sensitive detection of a pathogenic protozoan, *Toxoplasma gondii*, by polymerase chain-reaction. *Journal of Clinical Microbiology*, 27, 1787–1792.

Burguete, A. S., Fenn, T. D., Brunger, A. T., Pfeffer, S. R. (2008). Rab and Arl GTPase family members cooperate in the localization of the golgin GCC185. *Cell*, 132, 286–298.

Burns, S., Thrasher, A. J., Blundell, M. P., Machesky, L., Jones, G. E. (2001). Configuration of human dendritic cell cytoskeleton by Rho GTPases, the WAS protein, and differentiation. *Blood*, 98(4), 1142-1149.

Buscaglia, C. A., Coppens, I., Hol, W. G. J., Nussenzweig, V. (2003). Sites of interaction between aldolase and thrombospondin-related anonymous protein in *Plasmodium. Molecular Biology of the Cell*, 14, 4947–4957.

Bustin, S. A. (2000). Absolute quantification of mRNA using real-time reverse transcription polymerase chain reaction assays. *Journal of Molecular Endocrinology*, 25, 169–193.

Buxton, D. (1990). Ovine toxoplasmosis: a review. *Journal of the Royal Society of Medicine*, 83(8), 509–511.

Buxton, D., Blewett, D. A., Trees, A. J., McColgan, C., Finlayson, J. (1988). Further studies in the use of monensin in the control of experimental ovine toxoplasmosis. *Journal of Comparative Pathology*, 98, 225-236.

Buxton, D., Innes, E. A. (1995). A commercial vaccine for ovine toxoplasmosis. *Parasitology*, 110, S11–S16.

Buxton, D., Maley, S. W., Wright, S. E., Rodger, S., Bartley, P., Innes, E. A. (2007). *Toxoplasma gondii* and ovine toxoplasmosis: new aspects of an old story. *Veterinary Parasitology*, 149(1-2), 25-28.

Buxton, D., Rodger, S.M. (2007). Toxoplasmosis and neosporosis. In: *Diseases of Sheep*. (pp. 112-119). London: Blackwell Publishing.

Buxton, D., Thomson, K. M., Maley, S. (1993). Treatment of ovine toxoplasmosis with a combination of sulphamezathine and pyrimethamine. *Veterinary Record*, 132, 409-411.

Buxton, D., Wright, S., Maley, S. W., Thomson, K. M., Brebner, J., Millard, K. (1996). Decoquinate and the control of experimental ovine toxoplasmosis. *Veterinary Record*, 138, 434-436.

Caler, E. V., Chakrabarti, S., Fowler, K. T., Rao, S., Andrews, N. W. (2001) The exocytosis-regulatory protein synaptotagmin VII mediates cell invasion by *Trypanosoma cruzi*. *The Journal of Experimental Medicine*, 193, 1097–1104.

Camasses, A., Bogdanova, A., Shevchenko, A., Zachariae, W. (2003). The CCT chaperonin promotes activation of the anaphase-promoting complex through the generation of functional Cdc20. *Molecular Cell*, 12, 87–100.

Cao, J., Kaneko, O., Thongkukiatkul, A., Tachibana, M., Otsuki, H., Gao, Q., Tsuboi, T., Torii, M. (2009). Rhoptry neck protein RON2 forms a complex with microneme protein AMA1 in *Plasmodium falciparum* merozoites. *Parasitology International*, 58, 29–35.

Caplow, M., Fee, L. (2002). Dissociation of the tubulin dimer is extremely slow, thermodynamically very unfavorable, and reversible in the absence of an energy source. *Molecular Biology of the Cell*, 13, 2120–2131.

Carey, K. L., Jongco, A. M., Kim, K., Ward, G. E. (2004). The *Toxoplasma gondii* rhoptry protein ROP4 is secreted into the parasitophorous vacuole and becomes phosphorylated in infected cells. *Eukaryotic Cell*, 3, 1320–1330.

Carranza, G., Castaño, R., Fanarraga, M. L., Villegas, J. C., Gonçalves, J., Soares, H., Avila, J., Marenchino, M., Campos-Olivas, R., Montoya, G., Zabala, J. C. (2013). Autoinhibition of TBCB regulates EB1-mediated microtubule dynamics. *Cellular and Molecular Life Sciences*, 70, 357–371.

Carruthers, V., Boothroyd, J. C. (2007). Pulling together: an integrated model of *Toxoplasma* cell invasion. *Current Opinion in Microbiology*, 10, 83–89.

Carruthers, V.B., Sibley, L.D., (1999). Mobilization of intracellular calcium stimulates microneme discharge in *Toxoplasma gondii*. *Molecular Microbiology*, 31, 421–428.

Casalou, C., Cyrne, L., Rosa, M., Soares, H. (2001). Microtubule cytoskeleton perturbation induced by taxol and colchicine affects chaperonin containing TCP-1 (CCT) subunit gene expression in *Tetrahymena* cells. *Biochimica et Biophysica Acta*, 1522, 9-21.

Caswell, P. T., Norman, J. C. (2006). Integrin trafficking and the control of cell migration. *Traffic*, 7, 14– 21.

Cérède, O., Dubremetz, J. F., Soête, M., Deslée, D., Vial, H., Bout, D., Lebrun, M. (2005). Synergistic role of micronemal proteins in *Toxoplasma gondii* virulence. *The Journal of Experimental Medicine*, 201, 453–463.

Chang, P., Coughlin, M., Mitchison, T. J. (2005). Tankyrase-1 polymerization of poly(ADP-ribose) is required for spindle structure and function. *Nature Cell Biology*, 7, 1133–1139.

Charron, A. J., Sibley, L. D. (2002). Host cells: mobilizable lipid resources for the intracellular parasite *Toxoplasma gondii*. *Journal of Cell Science*, 115, 3049–3059.

Charron, A. J., Sibley, L. D. (2004). Molecular partitioning during host cell penetration by *Toxoplasma gondii*. *Traffic*, 5, 855-867.

Chaturvedi, S., Qi, H., Coleman, D., Rodriguez, A., Hanson, P. I., Striepen, B., Roos, D. S., Joiner, K. A. (1999). Constitutive calcium-independent release of *Toxoplasma gondii* dense granules occurs through the NSF/SNAP/SNARE/Rab machinery. *The Journal of Biological Chemistry*, 274, 2424– 2431.

Cheever, A. W., Valsamis, M. P., Rabson, A. S. (1965). Necrotising toxoplasmic encephalitis and herpetic pneumonia complicating treated Hodgkins disease. *The New England Journal of Medicine*, 272, 26–29.

Chiappino, M. L., Nichols, B. A., O'Connor, G. R. (1984). Scanning electron microscopy of *Toxoplasma gondii*: parasite torsion and host-cell responses during invasion. *Journal of Protozoology*, 31, 288–292.

Chiu, R., Novikov, L., Mukherjee, S., Shields, D. (2002). A caspase cleavage fragment of p115 induces fragmentation of the Golgi apparatus and apoptosis. *The Journal of Cell Biology*, 159, 637–648.

Chobotar, W., Scholtyseck, E. (1982). Ultrastructure. In: Long, P. L. (Ed.), *The biology of the coccidia*. (pp. 101–165). Baltimore: University Park Press.

Choi, J. H., Bertram, P. G., Drenan, R., Carvalho, J., Zhou, H. H., Zheng, X. F. S. (2002). The FKBP12- rapamycin-associated protein (FRAP) is a CLIP-170 kinase. *EMBO Reports*, 3, 988–994.

Chretien, D., Buendia, B., Fuller, S. D., Karsenti, E. (1997). Reconstruction of the centrosome cycle from cryoelectron micrographs. *Journal of Structural Biology*, 120, 117-133.

Cole, N. B., Lippincott-Schwartz, J. (1995). Organization of organelles and membrane traffic by microtubules. *Current Opinion in Cell Biology*, 7(1), 55–64.

Cole, N. B., Sciaky, N., Marotta, A., Song, J., Lippincott-Schwartz, J. (1996). Golgi dispersal during microtubule disruption: regeneration of Golgi stacks at peripheral endoplasmic reticulum exit sites. *Molecular Biology of the Cell*, 7, 631–650.

Collantes-Fernandez, E., Arrighi, R. B. G., Álvarez-Garcıa, G., Weidner, J. M., Regidor-Cerrillo, J., Boothroyd, J. C., Ortega-Mora, L. M., Barragan, A. (2012). Infected dendritic cells facilitate systemic dissemination and transplacental passage of the obligate intracellular parasite *Neospora caninum* in mice. *PLoS ONE*, 7(3), e32123.

Collins, C. R., Withers-Martinez, C., Hackett, F., and Blackman, M. J. (2009). An inhibitory antibody blocks interactions between components of the malarial invasion machinery. *PLoS Pathogens*, 5, e1000273.

Coppens, I., Dunn, J. D., Romano, J. D., Pypaert, M., Zhang, H., Boothroyd, J. C., Joiner K. A. (2006). *Toxoplasma gondii* sequesters lysosomes from mammalian hosts in the vacuolar space. *Cell*, 125, 261–74.

Cortes, H. C., Mueller, N., Esposito, M., Leitão, A., Naguleswaran, A. Hemphill, A. (2007a). *In vitro* efficacy of nitro- and bromo-thiazolyl-salicylamide compounds (thiazolides) against *Besnoitia besnoiti* infection in Vero cells. *Parasitology*, 134, 975–985.

Cortes, H. C., Nunes, S., Reis, Y., Staubli, D., Vidal, R., Sager, H., Leitão, A., Gottstein, B. (2006a). Immunodiagnosis of *Besnoitia besnoiti* infection by ELISA and Western blot. *Veterinary Parasitology*, 141, 216–225.

Cortes, H. C., Reis, Y., Gottstein, B., Hemphill, A., Leitão, A., Muller, N. (2007b). Application of conventional and real-time fluorescent ITS1 rDNA PCR for detection of *Besnoitia besnoiti* infections in bovine skin biopsies. *Veterinary Parasitology*, 146, 352–356.

Cortes, H. C., Reis, Y., Waap, H., Vidal, R., Soares, H., Marques, I., Pereira da Fonseca, I., Fazendeiro, I., Ferreira, M. L., Caeiro, V., Shkap, V., Hemphill, A, Leitão, A. (2006b). Isolation of *Besnoitia besnoiti* from infected cattle in Portugal. *Veterinary Parasitology*, 141, 226–233.

Cortes, H. C., Muller, N., Boykin, D., Stephens, C. E., Hemphill, A. (2011). *In vitro* effects of arylimidamides against *Besnoitia besnoiti* infection in Vero cells. *Parasitology*, 138(5), 583-592.

Cortes, H., Ferreira, M. L., Silva, J. F., Vidal, R., Serra, P., Caeiro, V. (2003). Contribuição para o estudo da besnoitiose bovina em Portugal. *Revista Portuguesa de Ciências Veterinárias*, 98 (545), 43–46.

Cortes, H., Leitão, A., Gottstein, B., Hemphill, A. (2014). A review on bovine besnoitiosis: a disease with economic impact in herd health management, caused by *Besnoitia besnoiti* (Franco and Borges, 1916). *Parasitology*, FirstView, 1-12.

Cortes, H., Leitão, A., Vidal, R., Vila-Vicosa, M. J., Ferreira, M. L., Caeiro, V., Hjerpe, C. A. (2005). Besnoitiosis in bulls in Portugal. *Veterinary Record*, 157, 262–264.

Courret, N., Darche, S., Sonigo, P., Milon, G., Buzoni-Gatel, D., Tardieux, I. (2006). CD11c- and CD11b-expressing mouse leukocytes transport single *Toxoplasma gondii* tachyzoites to the brain. *Blood*, 107(1), 309–316.

Cowan, N. J., Lewis, S. A. (2001). Type II chaperonins, prefoldin and the tubulin-specific chaperones. *Advances in Protein Chemistry*, 59, 73–104.

Crawford, M. J., Thomsen-Zieger, N., Ray, M., Schachtner, J., Roos, D. S., Seeber, F. (2006). *Toxoplasma gondii* scavenges host-derived lipoic acid despite its *de novo* synthesis in the apicoplast. *The EMBO Journal*, 25, 3214–3222.

Cunningham, L. A., Kahn, R. A. (2008). Cofactor D functions as a centrosomal protein and is required for the recruitment of the γ-tubulin ring complex at centrosomes and organization of the mitotic spindle. *The Journal of Biological Chemistry*, 283, 7155–7165.

Curry, J., McHale, C., Smith, M. T. (2002). Low efficiency of the Moloney murine leukemia virus reverse transcriptase during reverse transcription of rare t(8;21) fusion gene transcripts. *Biotechniques*, 32, 768–770.

D'Haese, J., Mehlhorn, H., Peters, W. (1977). Comparative electron microscope study of pellicular structures in Coccidia (*Sarcocystis, Besnoitia* and *Eimeria*). *International Journal for Parasilology*, 7, 505-518.

da Silva, C. V., da Silva, E. A., Cruz, M. C., Chavrier, P., Isberg, R., Mortara, R. A. (2008). ARF6, PI3-kinase and host cell actin cytoskeleton in *Toxoplasma gondii* cell invasion. *Biochemical and Biophysical Research Communications*, 378(3), 656-661

da Silva, R. C., Langoni, H. (2009). *Toxoplasma gondii*: host-parasite interaction and behavior manipulation. *Parasitology Research*, 105(4), 893-898.

Dannemann, B., McCutchan, J. A., Israelski, D., Antoniskis, D., Leport, C., Luft, B., Nussbaum, J., Clumeck, N., Morlat, P., Chiu, J., Vilde, J-L., Orellana, M., Feigal, D., Bartok,

A., Heseltine, P., Leedom, J., Remington, J. (1992). Treatment of toxoplasmic encephalitis in patients with AIDS. A randomized trial comparing pyrimethamine plus clindamycin to pyrimethamine plus sulfadiazine. *Annals of Internal Medicine*, 116, 33–43.

de Forges, H., Bouissou, A., Perez, F. (2012). Interplay between microtubule dynamics and intracellular organization. *The International Journal of Biochemistry & Cell Biology*, 44, 266– 274.

de Leon J. C., Scheumann, N., Beatty, W., Beck, J. R., Tran, J. Q., Yau, C., Bradley, P. J., Gull, K., Wickstead, B., Morrissette, N. S. (2013). A SAS-6- like protein suggests that the *Toxoplasma* conoid complex evolved from flagellar components. *Eukaryotic Cell*, 12, 1009–1019.

De Matteis, M. A., Morrow, J. S. (2000). Spectrin tethers and mesh in the biosynthetic pathway. *Journal of Cell Science*, 113, 2331–2343.

de Miguel, N., Lebrun, M., Heaslip, A., Hu, K., Beckers, C. J., Matrajt, M., Dubremetz, J. F., Angel, S. O. (2008). *Toxoplasma gondii* Hsp20 is a stripe-arranged chaperone-like protein associated with the outer leaflet of the inner membrane complex. *Biology of the Cell*, 100, 479–489.

Delgehyr, N., Sillibourne, J., Bornens, M. (2005). Microtubule nucleation and anchoring at the centrosome are independent processes linked by ninein function. *Journal of Cell Science*, 118, 1565-1575.

Diana, J., Vincent, C., Peyron, F., Picot, S., Schmitt, D., Persat, F. (2005). *Toxoplasma gondii* regulates recruitment and migration of human dendritic cells via different soluble secreted factors. *Clinical & Experimental Immunology*, 141, 475–484.

Diao, A., Rahman, D., Pappin, D. J., Lucocq, J., Lowe, M. (2003). The coiledcoil membrane protein golgin-84 is a novel rab effector required for Golgi ribbon formation. *The Journal of Cell Biology*, 160, 201–212.

Diesting, L., Heydora, A. O., Matuschka, F. R., Bauer, C., Pipano, E., Waal, D. T., Potgieter, F. T. (1988). *Besnoitia besnoiti*: Studies on the definitive host and experimental infections in cattle. *Parasitology Research*, 75, 114-117.

Dimitrov, A., Quesnoit, M., Moutel, S., Cantaloube, I., Poüs, C., Perez, F. (2008). Detection of GTPtubulin conformation *in vivo* reveals a role for GTP remnants in microtubule rescues. *Science*, 322, 1353–1356.

Dippold, H. C, Ng, M. M., Farber-Katz, S. E., Lee, S. K., Kerr, M. L., Peterman, M. C., Sim, R., Wiharto, P. A., Galbraith, K. A., Madhavarapu, S., Fuchs, G. J., Meerloo, T., Farquhar, M. G., Zhou, H., Field, S. J. (2009). GOLPH3 bridges phosphatidylinositol-4-phosphate and actomyosin to stretch and shape the Golgi to promote budding. *Cell*, 139, 337-351.

Ditzel, L., Löwe, J., Stock, D., Stetter, K.O., Huber, H., Huber, R., Steinbacher, S. (1998) Crystal structure of the thermosome, the archaeal chaperonin and homolog of CCT. *Cell*, 93, 125-138.

Dobbelaere, D. A., Kuenzi, P. (2004). The strategies of the *Theileria* parasite: a new twist in host-pathogen interactions. *Current Opinion in Immunology*, 16, 524–530.

Dobbelaere, D. A., Küenzi, P. (2004). The strategies of the *Theileria* parasite: a new twist in host-pathogen interactions. *Current Opinion in Immunology*, 16, 524–530.

Dobrowolski, J. M., Carruthers, V. B., Sibley, L. D. (1997a). Participation of myosin in gliding motility and host cell invasion by *Toxoplasma gondii*. *Molecular Microbiology*, 26, 163–173.

Dobrowolski, J. M., Niesman, I. R., Sibley, L. D. (1997b). Actin in the parasite *Toxoplasma gondii* is encoded by a single copy gene, ACT1 and exists primarily in a globular form. *Cell Motility and the Cytoskeleton*, 37, 253–262.

Dobrowolski, J. M., Sibley, L. D. (1996). *Toxoplasma* invasion of mammalian cells is powered by the actin cytoskeleton of the parasite. *Cell*, 84, 933–939.

Doxsey, S. J. (2005). Molecular links between centrosome and midbody. *Molecular Cell*, 20, 170-172.

Dubey, J. P. (1984). Experimental toxoplasmosis in sheep fed *Toxoplasma gondii* oocysts. *International Goat Sheep Research*, 2, 93-104.

Dubey, J. P. (2008). The history of *Toxoplasma gondii*-the first 100 years. *The Journal of Eukaryotic Microbiology*, 55(6), 467-745.

Dubey, J. P., Desmonts, G. (1987). Serological responses of equids fed *Toxoplasma gondii* oocysts. *Equine Veterinary Journal*, 19, 337–339.

Dubey, J. P., Lindsay, D. S. (2003). Development and ultrastructure of *Besnoitia oryctofelisi* tachyzoites, tissue cysts, bradyzoites, schizonts and merozoites. *International Journal of Parasitology*, 33, 807–819.

Dubey, J. P., Lindsay, D. S., Speer, C. A. (1998), Structures of *Toxoplasma gondii* tachyzoites, bradyzoites, and sporozoites and biology and development of tissue cysts. *Clinical Microbiology Reviews*, 11(2), 267–299.

Dubey, J. P., Sharma, S. P. (1980). Parasitemia and tissue infection in sheep fed *Toxoplasma gondii* oocysts. *Journal of Parasitology*, 66, 111-114.

Dubey, J. P., Sreekumar, C., Donovan, T., Rozmanec, M., Rosenthal, B. M., Vianna, M. C., Davis, W. P., Belden, J. S. (2005). Redescription of *Besnoitia bennetti* (Protozoa: Apicomplexa) from the donkey (*Equus asinus*). *International Journal for Parasitology*, 35(6), 659-672.

Dubey, J. P., Sreekumar, C., Rosenthal, B. M., Vianna, M. C. B., Nylund, M., Nikander, S., Oksanen, A. (2004). Redescription of *Besnoitia tarandi* (Protozoa: Apicomplexa) from the reindeer (*Rangifer tarandus*). *International Journal of Parasitology*, 34, 1273–1287.

Dubey, J.P., Sreekumar, C., Rosenthal, B. M., Lindsay, D. S., Grisard, E. C., Vitor, R. W. A. (2003a). Biological and molecular characterization of *Besnoitia akodoni* n.sp. (Protozoa: Apicomplexa) from the rodent *Akodon montensis* in Brazil. *Parassitologia*, 45(2), 61–70.

Dubey, J. P., Yabsley, M. J. (2010). *Besnoitia neotomofelis* n. sp. (Protozoa: Apicomplexa) from the southern plains woodrat (*Neotoma micropus*). *Parasitology*, 137, 1731–1747.

Dubey. J. P., Shkap, V., Pipano, E., Fish, L., Fritz, D. L. (2003b). Ultrastructure of *Besnoitia besnoiti* tissue cysts and bradyzoites. *Journal of Eukaryotic Microbiology*, 50, 240–424.

Dubremetz, J. F., Elsner, Y. Y. (1979). Ultrastructural study of schizogony of *Eimeria* bovis in cell cultures. *Journal of Protozoology*, 26, 367–376.

Dubremetz, J. F., Garcia-Réguet, N., Conseil, V., Fourmaux, M. N. (1998). Apical organelles and host-cell invasion by Apicomplexa. *International Journal for Parasitology*, 28(7), 1007-1013.

Dupin, I., Camand, E., Etienne-Manneville, S. (2009). Classical cadherins control nucleus and centrosome position and cell polarity. *The Journal of Cell Biology*, 185, 779-786.

Eddy, R. J., Pierini, L. M., Maxfield, F. R. (2002). Microtubule asymmetry during neutrophil polarization and migration. *Molecular Biology of the Cell*, 13, 4470-4483.

Efimov, A., Kharitonov, A., Efimova, N., Loncarek, J., Miller, P. M., Andreyeva, N., Gleeson, P., Galjart, N., Maia, A. R., McLeod, I. X., Yates, JR 3rd, Maiato, H.,Khodjakov, A., Akhmanova, A., Kaverina, I. (2007). Asymmetric CLASP-dependent nucleation of noncentrosomal microtubules at the trans-Golgi network. *Developmental Cell*, 12, 917–930.

Egea, G., Lázaro-Diéguez, F., Vilella, M. (2006). Actin dynamics at the Golgi complex in mammalian cells. *Current Opinion in Cell Biology*, 18, 168-178.

Elliott, D. A., Clark, D. P. (2000). *C. parvum* induces host cell actin accumulation at the host-parasite interface. *Infection and Immunity*, 68, 2315– 2322.

Elliott, D. A., Coleman, D. J., Lane, M. A., May, R. C., Machesky, L. M., Clark, D. P. (2001). *C. parvum* infection requires host cell actin polymerization. *Infection and Immunity*, 69, 5940–5942.

Ellis, J. T., Holmdahl, O. J., Ryce, C., Njenga, J. M., Harper, P. A., Morrison, D.A. (2000). Molecular phylogeny of *Besnoitia* and the genetic relationships among *Besnoitia* of cattle, wildebeest and goats. *Protist*, 151, 329–336.

Ems-McClung, S. C., Walczak, C. E. (2010). Kinesin-13s in mitosis: key players in the spatial and temporal organization of spindle microtubules. *Seminars in Cell & Develpmental Biology*, 21, 276–282.

Entrican, G., Wheelhouse, N. M. (2006). Immunity in the female sheep reproductive tract. *Veterinary Research*, 37, 295–309.

Esteban-Redondo, I., Innes, E. A. (1997). *Toxoplasma gondii* infection in sheep and cattle. *Comparative Immunology Microbiology and Infectious Diseases*, 20(2), 191-196.

Etienne-Manneville, S. (2008). Polarity proteins in migration and invasion. *Oncogene*, 27, 6970–6980.

European Food Safety Authority (2010). Scientific statement on bovine besnoitiosis. *EFSA Journal*, 8(2), 1499-1514.

Evans, R. J., Schwarz, N., Nagel-Wolfrum, K., Wolfrum, U., Hardcastle, A. J., Cheetham, M. E. (2010). The retinitis pigmentosa protein RP2 links pericentriolar vesicle transport between the Golgi and the primary cilium. *Human Molecular Genetics*, 19, 1358–1367.

Eyles, D. E., Coleman, N. (1953). Synergistic effect of sulfadiazine and daraprim against experimental toxoplasmosis in the mouse. *Antibiotics and Chemotherapy*, 3, 483–490.

Fabbro, M., Zhou, B., Takahashi, M., Sarcevic, B., Lal, P., Graham, M. E., Gabrielli, B. G., Robinson, P. J., Nigg, E. A., Ono, Y., Khanna, K. K. (2005). Cdk1/Erk2- and Plk1- dependent phosphorylation of a centrosome protein, Cep55, is required for its recruitment to midbody and cytokinesis developmental. *Cell*, 9, 477-488.

Fanarraga, M. L., Avila, J., Guasch, A., Coll, M., Zabala, J. C. (2001) Review: postchaperonin tubulin folding cofactors and their role in microtubule dynamics. *Journal of Structural Biology*, 135, 219-229.

Fanarraga, M. L., Bellido, J., Jaen, C., Villegas, J. C., Zabala, J. C. (2010a). TBCD links centriogenesis, spindle microtubule dynamics, and midbody abscission in human cells. *PLoS One*, 5(1), e8846.

Fanarraga, M. L., Carranza, G., Bellido, J., Kortazar, D., Villegas, J. C., Zabala, J. C. (2007). Tubulin cofactor B plays a role in the neuronal growth cone. *Journal of Neurochemistry*, 100(6), 1680–1687.

Fanarraga, M. L., Carranza, G., Castaño, R., Jiménez, V., Villegas, J. C., Zabala, J. C. (2010b). Emerging roles for tubulin folding cofactors at the centrosome. *Communicative & integrative Biology*, 3(4), 306-308.

Fanarraga, M. L., Párraga, M., Aloria, K., del Mazo, J., Avila, J., Zabala, J.C. (1999). Regulated expression of p14 (cofactor A) during spermatogenesis. *Cell Motility and the Cytoskeleton*, 43, 243–254.

Fanarraga, M. L., Villegas, J. C., Carranza, G., Castano, R., Zabala, J. C. (2009). Tubulin cofactor B regulates microtubule densities during microglia transition to the reactive states. *Experimental Cell Research*, 315(3), 535–541.

Farr, G. W., Scharl, E. C., Schumacher, R. J., Sondek, S., Horwich, A. L. (1997). Chaperonin-mediated folding in the eukaryotic cytosol proceeds through rounds of release of native and nonnative forms. *Cell*, 89, 927–937.

Fath, K. R. (2005). Characterization of myosin-II binding to Golgi stacks *in vitro*. *Cell Motility and the Cytoskeleton*, 60, 222–235.

Feierbach, B., Nogales, E., Downing, K. H., Stearns, T. (1999). Alf1p, a CLIP-170 domain-containing protein, is functionally and physically associated with alpha-tubulin. *The Journal of Cell Biology*, 144, 113–124.

Feldman, J. L., Marshall, W. F. (2009). ASQ2 encodes a TBCC-like protein required for mother–daughter centriole linkage and mitotic spindle orientation. *Current Biology*, 19, 1238–1243.

Félix, R. C., Silveira, H. (2011). The interplay between tubulins and P450 cytochromes during *Plasmodium berghei* invasion of *Anopheles gambiae* midgut. *PLoS ONE*, 6(8), e24181.

Feng, H., Nie, W., Bonilla, R., Widmer, G., Sheoran, A., Tzipori, S. (2006). Quantitative tracking of *Cryptosporidium* infection in cell culture, *Journal of Parasitology*, 92, 1350–1354.

Fernández-García, A., Alvarez-García, G., Marugán-Hernández, V., García-Lunar, P., Aguado-Martínez, A., Risco-Castillo, V., Ortega-Mora, L. M. (2013). Identification of *Besnoitia besnoiti* proteins that showed differences in abundance between tachyzoite and bradyzoite stages by difference gel electrophoresis. *Parasitology*, 140(8), 999-1008.

Fernández-García, A., Álvarez-García, G., Risco-Castillo, V., Aguado Martínez, A., Marugán-Hernández, V., Ortega-Mora, L. M. (2009a). Pattern of recognition of *Besnoitia besnoiti* tachyzoite and bradyzoite antigens by naturally infected cattle. *Veterinary Parasitology*, 164(2-4), 104-110.

Fernández-García, A., Risco-Castillo, V., Pedraza-Díaz, S., Aguado-Martínez, A., Alvarez-García, G., Gómez-Bautista, M., Collantes-Férnandez, E., Ortega-Mora, L. M. (2009b). First isolation of *Besnoitia besnoiti* from a chronically infected cow in Spain. *Journal of Parasitology*, 95 (2), 474–476.

Fleming, J. R., Morgan, R. E., Fyfe, P. K., Kelly, S. M., Hunter, W. N. (2013). The architecture of *Trypanosoma brucei* tubulin-binding cofactor B and implications for function. *FEBS Journal*, 280, 3270–3280.

Follit, J. A., San Agustin, J. T., Xu, F., Jonassen, J. A., Samtani, R., Lo, C. W., Pazour, G. J. (2008). The Golgin GMAP210/TRIP11 anchors IFT20 to the Golgi complex. *PLoS Genetics*, 4(12), e1000315.

Follit, J. A., Tuft, R. A., Fogarty, K. E., Pazour, G.J. (2006). The intraflagellar transport protein IFT20 is associated with the Golgi complex and is required for cilia assembly. *Molecular Biology of the Cell*, 17, 3781–3792.

Fontalba, A., Paciucci, R., Avila, J., Zabala, J. C. (1993). Incorporation of tubulin subunits into dimers requires GTP hydrolysis. *Journal of Cell Science*, 106, 627–632.

Forney, J. R., Vaughan, D. K., Yang, S., Healey, M. C. (1998). Actin dependent motility in *Cryptosporidium parvum* sporozoites. *Journal of Parasitology*, 84, 908–913.

Fox, B. A., Gigley, J. P., Bzik, D. J. (2004). *Toxoplasma gondii* lacks the enzymes required for *de novo* arginine biosynthesis and arginine starvation triggers cyst formation. *International Journal for Parasitology*, 34, 323–331.

Francia, M. E., Striepen, B. (2014). Cell division in apicomplexan parasites. *Nature Reviews Microbiology*, 12, 125 - 136.

Franco, E. E., Borges, I. (1915). Nota sobre a sarcosporidiose bovina. *Revista de Medicina Veterinária*, 165, 255-299.

Franke, T. F. (2008). PI3K/Akt: getting it right matters. *Oncogene*, 27, 6473–6488.

Frénal, K., Soldati-Favre, D. (2009). Role of the parasite and host cytoskeleton in apicomplexa parasitism. *Cell Host & Microbe*, 5(6), 602-611.

Friedl, P., Bröcker, E. B. (2000). T cell migration in three-dimensional extracellular matrix: guidance by polarity and sensations. *Developmental Immunology*, 7(2-4), 249-266.

Friedl, P., Zänker, K. S., Bröcker, E. B. (1998). Cell migration strategies in 3-D extracellular matrix: differences in morphology, cell matrix interactions, and integrin function. *Microscopy Research and Technique*, 43, 369-378.

Friedman, J. R., Webster, B., Mastronarde, D., Verhey, K., Voeltz, G. (2010). ER sliding dynamics and ER-mitochondrial contacts occur on acetylated microtubules. *The Journal of Cell Biology*, 190(3), 363–375.

Frydman, J., Hartl, F. U. (1996). Principles of chaperone-assisted protein folding: differences between *in vitro* and *in vivo* mechanisms. *Science*, 272, 1497–1502.

Fujita, Y., Ohama, E., Takatama, M., Al-Sarraj, S., Okamoto, K. (2006). Fragmentation of Golgi apparatus of nigral neurons with alpha-synuclein-positive inclusions in patients with Parkinson's disease. *Acta Neuropathologica*, 112(3), 261–265.

Fulton, J. D., Turk, J. L. (1959). Direct agglutination test for *Toxoplasma gondii*. *The Lancet*, 2(7111), 1068–1069.

Gao, Y., Vainberg, I. E., Chow, R. L. Cowan, N. J. (1993). Two cofactors and cytoplasmic chaperonin are required for the folding of alpha and beta-tubulin. *Molecular and Cellular Biology*, 13, 2478-2485.

García-Lunar, P., Ortega-Mora, L. M., Schares, G., Gollnick, N. S., Jacquiet, P., Grisez, C., Prevot, F., Frey, C. F., Gottstein, B., Alvarez-García, G. (2012a). An inter-laboratory comparative study of serological tools employed in the diagnosis of *Besnoitia besnoiti* infection in bovines. *Transboundary and Emerging Diseases*, 60(1), 59-68.

García-Lunar, P., Regidor-Cerrillo, J., Gutiérrez-Expósito, D., Ortega-Mora, L., Alvarez-García, G. (2012b). First 2-DE approach towards characterising the proteome and immunome of *Besnoitia besnoiti* in the tachyzoite stage. *Veterinary Parasitology*, 195(1-2), 24-34.

Garcia-Mayoral, M. F., Castaño, R., Fanarraga, M. L., Zabala, J. C., Rico, M., Bruix, M. (2011). The solution structure of the N-terminal domain of human tubulin binding cofactor C reveals a platform for tubulin interaction. *PLoS ONE*, 6(10), e25912.

Garin, J. P., Eyles, D. E. (1958). Le traitement de la toxoplasmose experimentale de la souris par la spiramycine. *La Presse Médicale*, 66, 957–958.

Gaskins, E., Gilk, S., DeVore, N., Mann, T., Ward, G., Beckers, C. (2004). Identification of the membrane receptor of a class XIV myosin in *Toxoplasma gondii*. *Journal of Cell Biology*, 165, 383–393.

Gebauer, M., Melki, R., Gehring, U. (1998). The chaperone cofactor Hop/p60 interacts with the cytosolic chaperonin-containing TCP-1 and affects its nucleotide exchange and protein folding activities. *The Journal of Biological Chemistry*, 273, 29475–29480.

Gentile, A., Militerno, G., Schares, G., Nanni, A., Testoni, S., Bassi, P., Gollnick, N. S. (2012). Evidence for bovine besnoitiosis being endemic in Italy-first *in vitro* isolation of *Besnoitia besnoiti* from cattle born in Italy. *Veterinary Parasitology*, 184(2-4), 108-115.

Giadinis, N. D., Terpsidis, K., Diakou, A., Siarkou, V., Loukopoulos, P., Osman, R., Karatzias, H., Papazahariadou, M. (2011). Massive *Toxoplasma* abortions in a dairy sheep flock and therapeutic approach with different doses of sulfadimidine. *Turkisk Journal of Veterinary and Animal Sciences*, 35(3), 207-211.

Gilk, S. D., Raviv, Y., Hu, K., Murray, J. M., Beckers, C. J. M., Ward, G. E. (2006). Identification of PhIL1, a novel cytoskeletal protein of the *Toxoplasma gondii* pellicle, through photosensitized labeling with 5-[^{125}I]Iodonaphthalene-1-Azide. *Eukaryotic Cell*, 5, 1622–1634.

Giovannini, D., Späth, S., Lacroix, C., Perazzi, A., Bargieri, D., Lagal, V., Lebugle, C., Combe, A., Thiberge, S., Baldacci, P., Tardieux, I., Ménard, R. (2011). Independent roles of apical membrane antigen 1 and rhoptry neck proteins during host cell invasion by apicomplexa. *Cell Host & Microbe*, 10(6), 591-602.

Gomes, E. R., Jani, S. and Gundersen, G. G. (2005). Nuclear movement regulated by Cdc42, MRCK, myosin, and actin flow establishes MTOC polarization in migrating cells. *Cell*, 121, 451–463.

Gonçalves, J., Nolasco, S., Nascimento, R., Fanarraga, M. L., Zabala, J. C., Soares, H. (2010). TBCCD1, a new centrosomal protein, is required for centrosome and Golgi apparatus positioning. *EMBO reports*, 11(3), 194-200.

Gönczy, P. (2004). Centrosomes: Hooked on the Nucleus. *Current Biology*, 14, 268–270.

Gönczy, P., Pichler, S., Kirkham, M., Hyman, A. A. (1999). Cytoplasmic dynein is required for distinct aspects of MTOC positioning, including centrosome separation, in the one cell stage *Caenorhabditis elegans* embryo. *The Journal of Cell Biology*, 147, 135-150.

Gonzalez, V., Combe, A., David, V., Malmquist, N. A., Delorme, V., Leroy, C., Blazquez, S., Ménard, R., Tardieux, I. (2009). Host cell entry by apicomplexa parasites requires actin polymerization in the host cell. *Cell Host & Microbe*, 5, 259-272.

Gordon, J. L., Sibley, L. D. (2005). Comparative genome analysis reveals a conserved family of actin-like proteins in apicomplexan parasites. *BMC Genomics*, 6, 179.

Grantham, J., Brackley, K. I., Willison, K. R. (2006). Substantial CCT activity is required for cell cycle progression and cytoskeletal organization in mammalian cells. *Experimental Cell Research*, 312, 2309–2324.

Gromley, A., Yeaman, C., Rosa, J., Redick, S., Chen, C., Mirabelle, S., Guha, M., Sillibourne, J., Doxsey, S. J. (2005). Centriolin anchoring of exocyst and SNARE complexes at the midbody is required for secretoryvesicle- mediated abscission. *Cell*, 123, 75-87.

Gruenheid, S., Finlay, B. B. (2003) Microbial pathogenesis and cytoskeletal function. *Nature*, 422, 775–781.

Grynberg, M., Jaroszewski, L., Godzik, A. (2003). Domain analysis of the tubulin cofactor system: a model for tubulin folding and dimerization. *BMC Bioinformatics*, 4, 46.

Gump, D. W., Holden, R. A. (1979). Acquired chorioretinitis due to toxoplasmosis. *Annals of Internal Medicine*, 90, 58–60.

Gundersen, G. G., Gomes, E. R., Wen, Y. (2004). Cortical control of microtubule stability and polarization. *Current Opinion in Cell Biology*, 16, 106-112.

Gupta, N., Zahn, M. M., Coppens, I., Joiner, K. A., Voelker, D. R. (2005). Selective disruption of phosphatidylcholine metabolism of the intracellular parasite *Toxoplasma gondii* arrests its growth. *The Journal of Biological Chemistry*, 280, 16345–16353.

Gutiérrez-Expósito, D., Ortega-Mora, L. M., Gajadhar, A. A., García-Lunar, P., Dubey, J. P., Alvarez-García, G. (2012). Serological evidence of *Besnoitia* spp. infection in Canadian wild ruminants and strong cross-reaction between *Besnoitia besnoiti* and *Besnoitia tarandi*. *Veterinary Parasitology*, 190(1-2), 19-28.

Haarer, B. K., Petzold, A., Lillie, S. H., Brown, S. S. (1994). Identification of MYO4, a second class V myosin gene in yeast. *Journal of Cell Science*, 107(Pt 4), 1055-1064.

Hage-Sleiman, R., Herveau, S., Matera, E-L. (2011). Silencing of tubulin binding cofactor C modifies microtubule dynamics and cell cycle distribution and enhances sensitivity to gemcitabine in breast cancer cells. *Molecular Cancer Therapeutics*, 10, 303-312.

Hage-Sleiman, R., Herveau, S., Matera, E-L., Laurier, J-F., Dumontet, C. (2010). Tubulin binding cofactor C (TBCC) suppresses tumor growth and enhances chemosensitivity in human breast cancer cells. *BMC Cancer*, 10, 135.

Hakansson, S., Charron, A. J., Sibley, L. D. (2001). *Toxoplasma* evacuoles: a two-step process of secretion and fusion forms the parasitophorous vacuole. *Embo Journal*, 20, 3132-3144.

Haldar, K., Samuel, B. U., Mohandas, N., Harrison, T., Hiller, N. L. (2001). Transport mechanisms in *Plasmodium*-infected erythrocytes:lipid rafts and a tubovesicular network. *International Journal for Parasitology*, 31, 1393–1401.

Hall, S. M., Pandit, A., Golwilkar, A., Williams, T. S. (1999). How do Jains get *Toxoplasma* infection? *The Lancet*, 354, 486–487.

Halonen, S. K., Weidner, E. (1994). Overcoating of *Toxoplasma* parasitophorous vacuoles with host cell vimentin type intermediate filaments. *Journal of Eukaryotic Microbiology*, 41, 65–71.

Hartmann, J., Hu, K., He, C. Y., Pelletier, L., Roos, D. S., Warren, G. (2006). Golgi and centrosome cycles in *Toxoplasma gondii*. *Molecular & Biochemical Parasitology*, 145, 125–127.

Hartmann-Petersen, R., Gordon, C. (2004). Integral Ubl domain proteins: a family of proteasome interacting proteins. *Seminars in Cell & Developmemntal Biology*, 15, 247–259.

Haston, W. S., Shields, J. M., Wilkinson, E. C. (1982). Lymphocyte locomotion and attachment on two-dimensional surfaces and in three-dimensional matrices. *The Journal of Cell Biology*, 92, 747-752.

Heaslip, A. T., Ems-Mcclung, S. C., Hu, K. (2009). TgICMAP1 is a novel microtubule binding protein in *Toxoplasma gondii*. *PLOS ONE,* 4, e7406.

Hemphill, A., Gajendran, N., Sonda, S., Fuchs, N., Gottstein, B., Hentrich, B., Jenkins, M. (1998). Identification and characterization of a dense granule-associated protein in *Neospora caninum* tachyzoites. *International Journal for Parasitology*, 28, 429–438.

Hemphill, A., Vonlaufen, N., Naguleswaran, A., Keller, N., Riesen, M., Guetg, N., Srinivasan, S., Alaeddine, F. (2004). Tissue culture and explant approaches to studying and visualizing *Neospora caninum* and its interactions with the host cell. *Microscopy and Microanalysis*, 10(5), 602-620.

Herm-Gotz, A., Weiss, S., Stratmann, R., Fujita-Becker, S., Ruff, C., Meyhöfer, E., Soldati, T., Manstein, D. J., Geeves, M. A., Soldati, D. (2002). *Toxoplasma gondii* myosin A and its light chain: a fast, single-headed, plus-end directed motor. *EMBO Journal*, 21, 2149–2158.

Hermosilla, C., Schröpfer, E., Stowasser, M., Eckstein-Ludwig, U., Behrendt, J., H. Zahner, H. (2008). Cytoskeletal changes in *Eimeria bovis*-infected host endothelial cells during first merogony. *Veterinary Research Communications*, 32, 521–531.

Heuer, D., Rejman Lipinski, A., Machuy, N., Karlas, A., Wehrens, A., Siedler, F., Brinkmann, V., Meyer, T. F. (2009). *Chlamydia* causes fragmentation of the Golgi compartment to ensure reproduction. *Nature*, 457(7230), 731-735.

Hippe, D., Lytovchenko, O., Schmitz, I., Lu Der, C. G. (2008). Fas/CD95-mediated apoptosis of type II cells is blocked by *Toxoplasma gondii* primarily via interference with the mitochondrial amplification loop. *Infection and Immunity*, 76, 2905–2912.

Hirata, D., Masuda, H., Eddison, M., Toda, T. (1998). Essential role of tubulin-folding cofactor D in microtubule assembly and its association with microtubules in fission yeast. *The EMBO Journal*, 17, 658–666.

Hoppeler-Lebel, A., Celati, C., Bellett, G., Mogensen, M. M., Klein-Hitpass, L., Bornens, M., Tassin, A. M. (2007). Centrosomal CAP350 protein stabilizes microtubules associated with the Golgi complex. *Journal of Cell Science*, 120, 3299– 3308.

Hornok, S., Fedák, A., Baska, F., Hofmann-Lehmann, R., Basso, W. (2014). Bovine besnoitiosis emerging in Central-Eastern Europe, Hungary. *Parasites and Vectors*, 7, 20.

Howe, D. K., Sibley, L. D. (1995). *Toxoplasma gondii* comprises three clonal lineages: correlation of parasite genotype with human disease. *The Journal of Infectious Diseases*, 172, 1561–1566.

Howell, B., Deacon, H., Cassimeris, L. (1999). Decreasing oncoprotein 18/stathmin levels reduces microtubule catastrophes and increases microtubule polymer *in vivo*. *Journal of Cell Science*, 112, 3713–3722.

Ho-Yen, D. O. (1992). Clinical features. In: Ho-Yen, DO., Joss, A. W. L. (Eds.). *Human Toxoplasmosis.* (pp. 56-78). Oxford: Oxford University Press.

Hoyt, M. A., Macke, J. P., Roberts, B.T., Geiser, J.R. (1997). *Saccharomyces cerevisiae* PAC2 functions with CIN1, 2 and 4 in a pathway leading to normal microtubule stability, *Genetics*, 146, 849–857.

Hu, K. (2008). Organizational changes of the daughter basal complex during the parasite replication of *Toxoplasma gondii*. *PLoS Pathogens*, 4, e10.

Hu, K., Johnson, J., Florens, L., Fraunholz, M., Suravajjala, S., DiLullo, C., Yates, J., Roos, D. S., Murray, J. M. (2006). Cytoskeletal Components of an Invasion Machine—The Apical Complex of *Toxoplasma gondii*. *PLoS Pathogens*, 2, e13.

Hu, K., Roos, D. S., Murray, J. M. (2002). A novel polymer of tubulin forms the conoid of *Toxoplasma gondii*. *The Journal of Cell Biology*, 156, 1039-1050.

Huggett, J., Dheda, K., Bustin, S., Zumla, A. (2005). Real-time RT-PCR normalisation; strategies and considerations. *Genes and Immunity*, 6, 279–284.

Hurtado, L., Caballero, C., Gavilan, M. P., Cardenas, J., Bornens, M., Rios, R. M. (2011). Disconnecting the Golgi ribbon from the centrosome prevents directional cell migration and ciliogenesis *The Journal of Cell Biology*, 193(5), 917-933.

Huynh, M. H., Carruthers, V. B. (2006). *Toxoplasma* MIC2 is a major determinant of invasion and virulence. *PLoS Pathogens*, 2, e84.

Hyman, A. A., Salser, S., Drechsel, D. N., Unwin, N., Mitchison, T. J. (1992). Role of GTP hydrolysis in microtubule dynamics: Information from a slowly hydrolyzable analogue, GMPCPP. *Molecular Biology of the Cell*, 3, 1155–1167.

Ikonen, E., de Almeid, J. B., Fath, K. R., Burgess, D. R., Ashman, K., Simons, K., Stow, J. L. (1997). Myosin II is associated with Golgi membranes: identification of p200 as nonmuscle myosin II on Golgi-derived vesicles. *Journal of Cell Science*, 110, 2155–2164.

Innes, E. A. (2010). A brief history and overview of *Toxoplasma gondii*. *Zoonoses and Public Health*, 57(1), 1-7.

Innes, E. A., Bartley, P. M., Buxton, D., Katzer, F. (2009). Ovine toxoplasmosis. *Parasitology*, 136(14), 1887-1894.

Innes, E. A., Panton, W. R. M., Sanderson, A., Thomson, K. M., Wastling, J. M., Maley, S., Buxton, D. (1995). Induction of CD4+ and CD8+ T cell responses in efferent lymph responding to *Toxoplasma gondii* infection: analysis of phenotype and function. *Parasite Immunology*, 17, 151–160.

Iqbal, J., Khalid, N. (2007). Detection of acute *Toxoplasma gondii* infection in early pregnancy by IgG avidity and PCR analysis. *Journal of Medical Microbiology*, 56, 1495–1499.

Irigoien, M., Del Cacho, E., Gallego, M., López-Bernad, F., Qúılez, J., Sánchez-Acedo, C. (2000). Immunohistochemical study of the cyst of *Besnoitia besnoiti*. *Veterinary Parasitology*, 91(1-2), 1–6.

Jacquemard, F. (2000). Clinical aspects of infection during pregnancy. In: Ambroise-Thomas, P., Petersen, E. (Eds.). *Congenital toxoplasmosis: scientific background, clinical management and control.* (pp. 111-120). Paris: Springer-Verlag.

Jacquiet, P., Liénard, E., Franc, M. (2010). Bovine besnoitiosis: epidemiological and clinical aspects. *Veterinary Parasitology*, 174, 30-36.

Jan, G., Delorme, V., David, V., Revenu, C., Rebollo, A., Cayla, X., Tardieux, I. (2007). The toxofilin-actin-PP2C complex of *Toxoplasma*: identification of interacting domains. *Biochemical Journal*, 401, 711–719.

Jewett, T. J., Sibley, L. D. (2003). Aldolase forms a bridge between cell surface adhesins and the actin cytoskeleton in apicomplexan parasites. *Molecular Cell*, 11, 885–894.

Ji, G., Ji, H., Mo, X., Li, T., Yu, Y., Hu, Z. (2013). The role of GRASPs in morphological alterations of Golgi apparatus: mechanisms and effects. *Reviews in the Neurosciences*, 24(5), 485–497.

Joiner, K.A., Roos, D.S. (2002). Secretory traffic in the eukaryotic parasite *Toxoplasma gondii*: less is more. *Journal of Cell Biology*, 157, 557–563.

Jones, J. L., Kruszon-Moran, D., Sanders-Lewis, K., Wilson, M. (2007). *Toxoplasma gondii* infection in the United States, 1999-2004, Decline from the prior decade. *The American Journal of Tropical Medicine and Hygiene*, 77(3), 405-410.

Juste, R. A., Cuervo, L. A., Marco, J. C., Oregui, L. M. (1990). La besnoitiosis bovina: desconocida en Espanã? *Medicina Veterinária*, 7, 613–618.

Kafsack, B. F., Pena, J. D., Coppens, I., Ravindran, S., Boothroyd, J. C., Carruthers, V. B. (2009). Rapid membrane disruption by a perforin-like protein facilitates parasite exit from host cells. *Science*, 323, 530-533.

Kakinuma, T., Ichikawa, H., Tsukada, Y., Nakamura, T., Toh, B. H. (2004). Interaction between p230 and MACF1 is associated with transport of a glycosyl phosphatidyl inositol-anchored protein from the Golgi to the cell periphery. *Experimental Cell Research*, 298, 388–398.

Karge, W. H., Schaefer, E. J., Ordovas, J. M. (1998). Quantification of mRNA by polymerase chain reaction (PCR) using an internal standard and a nonradioactive detection method. *Methods in Molecular Biology*, 110, 43–61.

Karrer, E. E., Lincoln, J. E., Hogenhout, S., Bennett, A. B., Bostoek, R. M., Martineau, B., Lucas, W. J., Gilchrist, D. G., Alexander, D. (1995). *In situ* isolation of mRNA from

individual plant cells: creation of cell-specific cDNA libraries. *Proceedings of the National Academy of Sciences*, 92, 3814–3818.

Katris, N. J., van Dooren, G. G., McMillan, P. J., Hanssen, E., Tilley, L., Waller, R. F. (2014). The apical complex provides a regulated gateway for secretion of invasion factors in *Toxoplasma*. *PLOS Pathogens*, 10, e1004074.

Kessler, H., Herm-Gotz, A., Hegge, S., Rauch, M., Soldati- Favre, D., Frischknecht, F., Meissner, M. (2008). Microneme protein 8 - a new essential invasion factor in *Toxoplasma gondii*. *The Journal of Cell Science*, 121, 947–956.

Khan, A., Taylor, S., Su, C., Mackey, A. J., Boyle, J., Cole, R., Glover, D., Tang, K., Paulsen, I. T., Berriman, M., Boothroyd, J. C., Pfefferkorn, E. R., Dubey, J. P., Ajioka, J. W., Roos, D. S., Wootton, J. C., Sibley, L. D. (2005). Composite genome map and recombination parameters derived from three archetypal lineages of *Toxoplasma gondii*. *Nucleic Acids Research*, 33, 2980–2992.

Kim, J. C., Ou, Y. Y., Badano, J. L., Esmail, M. A., Leitch, C. C., Fiedrich, E., Beales, P. L., Archibald, J. M., Katsanis, N., Rattner, J. B., Leroux, M. R. (2005). MKKS/BBS6, a divergent chaperonin-like protein linked to the obesity disorder Bardet-Biedl syndrome, is a novel centrosomal component required for cytokinesis. *Journal of Cell Science*, 118, 1007-1020.

Kim, S., Willison, K. R., Horwich, A. L. (1994). Cystosolic chaperonin subunits have a conserved ATPase domain but diverged polypeptide-binding domains. *Trends in Biochemical Sciences*, 19, 543–548.

Kirik, V., Grini, P. E., Mathur, J., Klinkhammer, I., Adler, K., Bechtold, N., Herzog, M., Bonneville, J. M., Hülskamp, M. (2002). The *Arabidopsis* tubulin-folding cofactor A gene is involved in the control of the alpha/beta-tubulin monomer balance. *The Plant Cell*, 14, 2265–2276.

Kodani, A., Kristensen, I., Huang, L., Sütterlin, C. (2009). GM130-dependent control of Cdc42 activity at the Golgi regulates centrosome organization. *Molecular Biology of the Cell*, 20, 1192–1200.

Kodani, A., Sütterlin, C. (2008). The Golgi protein GM130 regulates centrosome morphology and function. *Molecular Biology of the Cell*, 19, 745–753.

Kohler, S., Delwiche, C. F., Denny, P. W., Tilney, L. G., Webster, P., Wilson, R. J., Palmer, J. D., Roos, D. S. (1997). A plastid of probable green algal origin in Apicomplexan parasites. *Science*, 275, 1485–1489.

Komarova, Y., De Groot, C. O., Grigoriev, I., Gouveia, S. M., Munteanu, E. L., Schober, J. M., Honnappa, S., Buey, R. M., Hoogenraad, C. C., Dogterom, M., Borisy, G. G., Steinmetz, M. O., Akhmanova, A. (2009). Mammalian end binding proteins control persistent microtubule growth. *The Journal of Cell Biology*, 184, 691–706.

Kortazar, D., Carranza, G., Bellido, J., Villegas, J. C., Fanarraga, M. L., Zabala, J.C. (2006). Native tubulin-folding cofactor E purified from baculovirus-infected Sf9 cells dissociates tubulin dimmers. *Protein Expression and Purification*, 49, 196–202.

Kortazar, D., Fanarraga, M. L., Carranza, G., Bellido, J., Villegas, J. C., Avila, J., Zabala, J. C. (2007). Role of cofactors B (TBCB) and E (TBCE) in tubulin heterodimer dissociation. *Experimental Cell Research*, 313, 425-436.

Krasov, V. M., Omarov, Z. K., Uvaliev, I. U., Khvan, M. V. (1975). Besnoitiosis in animals. *Veterinariya*, 2, 65-70.

Kubota, H., Hynes, G., Willison, K. (1995). The chaperonin containing t-complex polypeptide 1 (TCP-1). Multisubunit machinery assisting in protein folding and assembly in the eukaryotic cytosol. *European Journal of Biochemistry*, 230, 3–16.

Kubota, H., Willison, K., Ashworth, A., Nozaki, M., Miyamoto, H., Yamamoto, H., Matsushiro, A., Morita, T. (1992). Structure and expression of the gene encoding t-complex polypeptide 1 (Tcp-1). *Gene*, 120, 207-215.

Kühnel, K., Veltel, S., Schlichting, I., Wittinghofer, A. (2006). Crystal structure of the human retinitis pigmentosa 2 protein and its interaction with Arl3. *Structure*, 14, 367-378.

Kuhnert, O., Baumann, O., Meyer, I., Graf, R. (2012). Functional characterization of CP148 a novel key component for centrosome integrity in *Dictyostelium*. *Cellular and Molecular Life Sciences*, 69, 1875–1888.

Kupfer, A., Louvard, D., Singer, S. J. (1982). Polarization of the Golgi apparatus and the microtubule-organizing center in cultured fibroblasts at the edge of an experimental wound. *Proceedings of the National Academy of Sciences*, 79, 2603–2607.

Laliberté, J., Carruthers, V. B. (2008). Host cell manipulation by the human pathogen *Toxoplasma gondii*. *Cellular and Molecular Life Sciences*, 65(12), 1900-1915.

Lamarque, M., Besteiro, S., Papoin, J., Roques, M., Vulliez-Le Normand, B., Morlon-Guyot, J., Dubremetz, J. F., Fauquenoy, S., Tomavo, S., Faber, B. W., Kocken, C. H., Thomas, A. W., Boulanger, M. J., Bentley, G. A., Lebrun, M. (2011). The RON2-AMA1 interaction is a critical step in moving junction-dependent invasion by Apicomplexan parasites. *PLoS Pathogens*, 7, e1001276.

Lambert, H., Dellacasa-Lindberg, I., Barragan, A. (2010). Migratory responses of leukocytes infected with *Toxoplasma gondii*. *Microbes and Infection*, 13(1), 96-102.

Lambert, H., Hitziger, N., Dellacasa, I., Svensson, M., Barragan, A. (2006). Induction of dendritic cell migration upon *Toxoplasma gondii* infection potentiates parasite dissemination. *Cellular Microbiology*, 8, 1611–1623.

Langenmayer, M. C., Gollnick, N. S., Majzoub-Altweck, M., Scharr, J. C., Schares, G., Hermanns W. (2014). Naturally acquired bovine besnoitiosis: histological and immunohistochemical findings in acute, subacute, and chronic disease. *Veterinary Pathology*, pii: 0300985814541705.

Lavine, M. D., Arrizabalaga, G. (2008). Exit from host cells by the pathogenic parasite *Toxoplasma gondii* does not require motility. *Eukaryotic Cell*, 7, 131–140.

Lavine, M. D., Arrizabalaga, G. (2009). Induction of mitotic S-phase of host and neighboring cells by *Toxoplasma gondii* enhances parasite invasion. *Molecular and Biochemical Parasitology*, 164, 95–99.

Lebrun, M., Michelin, A., El Hajj, H., Poncet, J., Bradley, P. J., Vial, H., Dubremetz, J. F. (2005). The rhoptry neck protein RON4 re-localizes at the moving junction during *Toxoplasma gondii* invasion. *Cellular Microbiology*, 7, 1823-1833.

Lecordier, L., Mercier, C., Sibley, L. D., Cesbron-Delauw, M. F. (1999). Transmembrane insertion of the *Toxoplasma gondii* GRA5 protein occurs after soluble secretion into the host cell. *Molecular Biology of the Cell*, 10, 1277–1287.

Ledizet, M., Piperno, G. (1987). Identification of an acetylation site of *Chlamydomonas* alpha-tubulin. *Proceedings of the National Academy of Sciences*, 84, 5720–5724.

Lee, C., Levtn, A., Branton, D. (1987). Copper staining: a five-minute protein stain for sodium-dodecyl sulfate-polyacrylamide gels. *Analytical Biochemistry*, 166, 308-312.

Lee, H. S., Komarova, Y. A., Nadezhdina, E. S., Anjum, R., Peloquin, J. G., Schober, J. M., Danciu, O., van Haren, J., Galjart, N., Gygi, S. P., Akhmanova, A., Borisy, G. G. (2010). Phosphorylation controls autoinhibition of cytoplasmic linker protein-170. *Molecular Biology of the Cell*, 21, 2661–2673.

Leitão, J. L. S. (1949). Globidiose bovina por *Globidium besnoiti* (Marotel 1912). *Revista de Medicina Veterinária*, 48, 152-158.

Lekanne Deprez, R. H., Fijnvandraat, A. C., Ruijter, J. M., Moorman, A. F. (2002). Sensitivity and accuracy of quantitative real-time polymerase chain reaction using SYBR green I depends on cDNA synthesis conditions. *Analytical Biochemistry*, 307, 63–69.

Lemgruber, L., Kloetzel J, A., Souza, W. d., Vommaro, R. C. (2009). *Toxoplasma gondii*: further studies on the subpellicular network. *Memórias do Instituto Oswaldo Cruz*, 104, 706-709.

Lesser, M., Braun, U., Deplazes, P., Gottstein, B., Hilbe, M., Basso, W. (2012). [First cases of besnoitiosis in cattle in Switzerland]. *Schweizer Archiv fur Tierheilkunde*, 154(11), 469-474.

Levine, N. D. (1985). *Veterinary Protozoology*. (pp. 256–259). Iowa: Iowa State University Press.

Lewis, S. A., Tian, G., Cowan, N. J. (1997) The α- and β-tubulin folding pathways. *Trends in Cell Biology*, 7, 479–484.

Lewis, S. A., Wang, D., Cowan, A. J. (1988). Microtubule-associated protein MAP2 shares a microtubule binding motif with tau protein. *Science*, 242, 936-939.

Lewis, V. A., Hynes, G. M., Dong, Z., Saibil, H., Willison, K. (1992). T-complex polypeptide-1 is a subunit of a heteromeric particle in the eukaryotic cytosol. *Nature*, 358, 249-252.

Li, W., Miki, T., Watanabe, T., Kakeno, M., Sugiyama, I., Kaibuchi, K., Goshima, G. (2011). EB1 promotes microtubule dynamics by recruiting Sentin in *Drosophila* cells. *The Journal of Cell Biology*, 193, 973–83.

Liao, G., Nagasaki, T., Gundersen, G. G. (1995). Low concentrations of nocodazole interfere with fibroblast locomotion without significantly affecting microtubule level: implications for the role of dynamic microtubules in cell locomotion. *Journal of Cell Science*, 108, 3473-3483.

Liénard, E., Salem, A., Grisez, C., Prévot, F., Bergeaud, J. P., Franc, M., Gottstein, B., Alzieu, J. P., Lagalisse, Y., Jacquiet, P. (2011). A longitudinal study of *Besnoitia besnoiti* infections and seasonal abundance of *Stomoxys calcitrans* in a dairy cattle farm of southwest France.*Veterinary Parasitology*, 177(1-2), 20-27.

Liou, A. K. F., Willison, K. R (1997). Elucidation of the subunit orientation in CCT (chaperonin containing TCP1) from the subunit composition of CCT micro-complexes. *The EMBO Journal*, 16, 4311–4316.

Liu, J., Wetzel, L., Zhang, Y., Nagayasu, E., Ems-McClung, S., Florens, L., Hu, K. (2013). Novel thioredoxin-like proteins are components of a protein complex coating the cortical microtubules of *Toxoplasma gondii*. *Eukaryotic Cell*, 12, 1588–1599.

Liu, Y., Boukhelifa, M., Tribble, E., Morin-Kensicki, E., Uetrecht, A., Bear, J. E., Bankaitis, V. A. (2008). The Sac1 phosphoinositide phosphatase regulates Golgi membrane morphology and mitotic spindle organization in mammals. *Molecular Biology of the Cell*, 19, 3080–3096.

Llorca, O., Martín-Benito, J., Grantham, J., Ritco-Vonsovici, M., Willison, K. R., Carrascosa, J. L., Valpuesta, J. M. (2001). The 'sequential allosteric ring' mechanism in the eukaryotic chaperonin-assisted folding of actin and tubulin. *The EMBO Journal*, 20, 4065-4075.

Llorca, O., Martín-Benito, J., Ritco-Vonsovici, M., Grantham, J., Hynes, G. M., Willison, K. R., Carrascosa, J. L., Valpuesta, J. M. (2000). Eukaryotic chaperonin CCT stabilizes actin and tubulin folding intermediates in open quasi-native conformations. *The EMBO Journal*, 19, 5971–5979.

Llorca, O., McCormack, E., Hynes, G., Grantham, J., Cordell, J., Carrascosa, J. L., Willison, K. R., Fernandez, J. J., Valpuesta, J. M. (1999). Eukaryotic type II chaperonin CCT interacts with actin through specific subunits. *Nature*, 402, 693-696.

Lowe, M., Lane, J. D., Woodman, P. G., Allan, V. J. (2004). Caspase-mediated cleavage of syntaxin 5 and giantin accompanies inhibition of secretory traffic during apoptosis. *Journal of Cell Science*, 117, 1139–1150.

Lucocq, J. M., Warren, G. (1987). Fragmentation and partitioning of the Golgi apparatus during mitosis in HeLa cells. *The EMBO Journal*, 6(11), 3239–3246.

Lüders, J., Stearns, T. (2007). Microtubule-organizing centres: a re-evaluation. *Nature Reviews. Molecular Cell Biology*, 8, 161-167.

Luft, B. J., Brooks, R. G., Conley, F. K., McCabe, R. E., Remington, J. S. (1984). Toxoplasmic encephalitis in patients with acquired immune deficiency syndrome. *The Journal of the American Medical Association*, 252, 913–917.

Luxton, G. W., Gundersen, G. G. (2011). Orientation and function of the nuclear-centrosomal axis during cell migration. *Current Opinion in Cell Biology*, 23, 579–588.

Lytle, B. L., Peterson, F. C., Qiu, S. H., Luo, M., Zhao, Q., Markley, J. L., Volkman, B. F. (2004). Solution structure of an ubiquitin-like domain from tubulin-binding cofactor B. *The Journal of Biological Chemistry*, 279, 46787–46793.

Maaser, K., Wolf, K., Klein, C. E., Niggemann, B., Zänker, K. S., Bröcker, E. B., Friedl, P. (1999). Functional hierarchy of simultaneously expressed adhesion receptors: integrin α2βl but not CD44 mediates MV3 melanoma cell migration and matrix reorganization within three-dimensional hyaluronan- containing collagen matrices. *Molecular Biology of the Cell*, 10, 3067–3079.

Magdalena, J., Millard, T. H., Etienne-Manneville, S., Launay, S., Warwick, H. K., Machesky, L. M. (2003). Involvement of the Arp2/3 complex and Scar2 in Golgi polarity in scratch wound models. *Molecular Biology of the Cell*, 14, 670–684.

Magno, R. C., Lemgruber, L., Vommaro, R. C., Souza, W., Attias, M., (2005). Intravacuolar network may act as a mechanical support for *Toxoplasma gondii* inside the parasitophorous vacuole. *Microscopy Research and Technique*, 67, 45–52.

Malone, C. J., Misner, L., Le Bot, N., Tsai, M. C., Campbell, J. M., Ahringer, J., White, J. G. (2003). The *C. elegans* hook protein, ZYG-12, mediates the essential attachment between the centrosome and nucleus. *Cell*, 115, 825–836.

Mana-Capelli, S., Gräf, R., Larochelle, D. A. (2009). *Dictyostelium discoideum* CenB is a bona fide centrin essential for nuclear architecture and centrosome stability. *Eukaryotic Cell*, 8, 1106–1117.

Mancini, M., Machamer, C. E., Roy, S., Nicholson, D. W., Thornberry, N. A., Casciola-Rosen, L. A., Rosen, A. (2000). Caspase-2 is localized at the Golgi complex and cleaves golgin-160 during apoptosis. *The Journal of Cell Biology*, 149, 603–612.

Mann, T., Beckers, C. (2001). Characterization of the subpellicular network, a filamentous membrane skeletal component in the parasite *Toxoplasma gondii*. *Molecular and Biochemical Parasitology*, 115, 257-268.

Marcelino, E., Martins, T. M., Morais, J. B., Nolasco, S., Cortes, H., Hemphill, A., Leitão, A., Novo, C. (2011). *Besnoitia besnoiti* protein disulfide isomerase (BbPDI): molecular characterization, expression and in silico modelling. *Experimental Parasitology*, 129(2), 164-174.

Maresca, B., Carratù, L. (1992). The biology of the heat shock response in parasites. *Parasitology Today*, 8, 260–266.

Martin, A. M., Liu, T., Lynn, B. C., Sinai, A.P. (2007). The *Toxoplasma gondii* parasitophorous vacuole membrane: transactions across the border. *Journal of Eukaryotic Microbiology*, 54, 25–28.

Martín, L., Fanarraga, M. L., Aloria, K., Zabala, J. C. (2000). Tubulin folding cofactor D is a microtubule destabilizing protein. *FEBS Letters*, 470, 93–95.

Martín, N., Jaubert, J., Gounon, P., Salido, E., Haase, G., Szatanik, M., Guénet, J. L. (2002). A missense mutation in Tbce causes progressive motor neuronopathy in mice. *Nature Genetics*, 32, 443–447.

Martins-de-Souza, D., Gattaz, W. F., Schmitt, A., Rewerts, C., Maccarrone, G., Dias-Neto, E., Turck, C. W. (2009). Prefrontal córtex shotgun proteome analysis reveals altered calcium homeostasis and immune system imbalance in schizophrenia. *European Archives of Psychiatry Clinical Neuroscience*, 259,151–163.

Massimine, K. M., Doan, L. T., Atreya, C. A., Stedman, T. T., Anderson, K. S., Joiner, K. A., Coppens, I. (2005). *Toxoplasma gondii* is capable of exogenous folate transport. A likely expansion of the BT1 family of transmembrane proteins. *Molecular and Biochemical Parasitology*, 144, 44–54.

McCallum, C. D., Hung, D. O., Jonhson, A. E., Frydman, J. (2000). The interaction of the chaperonin tailess complex polypeptide 1 (TCP1) ring complex (TRIC) with ribosome-bound nascent chains examined using photo-cross-linking. *The Journal of Cell Biology*, 149, 591–601.

Mccully, R. M., Basson, P. A., Van Niekerk, J. W., BigalkeI, R. D. (1966). Observations on *Besnoitia* cysts in the cardiovascular system of some wild antelopes and domestic cattle. *Onderstepoort Journal of Veterinary Research*, 33, 245-276.

McLeod, R., Boyer, K. (2000). Management of and outcome for the newborn infant with congenital toxoplasmosis. In: Ambroise-Thomas, P., Petersen, E. (Eds.). *Congenital toxoplasmosis: scientific background, clinical management and control*. (pp. 189-213). Paris: Springer-Verlag.

Mehlhorn, H., Klimpel, S., Schein, E., Heydorn, A.O., Al-Quraishy, S., Selmair, J. (2009). Another African disease in Central Europa: besnoitiosis of cattle. I. Light and electron microscopical study. *Parasitology Research*, 140, 861–868.

Meissner, M., Schluter, D., Soldati, D. (2002). Role of *Toxoplasma gondii* myosin A in powering parasite gliding and host cell invasion. *Science*, 298, 837–840.

Melki, R., Batelier, G., Soulié, S., Williams, R. C. Jr. (1997). Cytoplasmic chaperonin containing TCP-1: structural and functional characterization. *Biochemistry*, 36, 5817–5826.

Melki, R., Rommelaere, H., Leguy, R., Vandekerckhove, J., Ampe, C. (1996). Cofactor A is a molecular chaperone required for beta-tubulin folding: functional and structural characterization. *Biochemistry*, 35, 10422–10435.

Melo, E. J., Carvalho, T. M., De Souza, W. (2001). Behaviour of microtubules in cells infected with *Toxoplasma gondii*. *Biocell*, 25, 53–59.

Melo, E. J., de Carvalho, T. U., de Souza, W. (1992). Penetration of *Toxoplasma gondii* into host cells induces changes in the distribution of the mitochondria and the endoplasmic reticulum. *Cell Structure and Function*, 17, 311-317.

Millán, J., Sobrino, R., Rodríguez, A., Oleaga, A., Gortazar, C., Schares, G. (2012). Large-scale serosurvey of *Besnoitia besnoiti* in free-living carnivores in Spain. *Veterinary Parasitology*, 190(1-2), 241-245.

Miller, P. M., Folkmann, A. W., Maia, A. R., Efimova, N., Efimov, A., Kaverina, I. (2009). Golgi-derived CLASP-dependent microtubules control Golgi organization and polarized trafficking in motile cells. *Nature Cell Biology*, 11, 1069–1080.

Minn, I. L., Rolls, M. M., Hanna-Rose, W., Malone, C. J. (2009). SUN-1 and ZYG-12, mediators of centrosome-nucleus attachment, are a functional SUN/KASH pair in *Caenorhabditis elegans*. *Molecular Biology of the Cell*, 20(21), 4586-4595.

Mital, J., Meissner, M., Soldati, D., Ward, G. E. (2005). Conditional expression of *Toxoplasma gondii* apical membrane antigen-1 (TgAMA1) demonstrates that TgAMA1 plays a critical role in host cell invasion. *Molecular Biology of the Cell*, 16(9), 4341-4349.

Mitchell, G. H., Thomas, A. W., Margos, G., Dluzewski, A. R.' Bannister, L. H. (2004). Apical membrane antigen 1, a major malaria vaccine candidate, mediates the close attachment of invasive merozoites to host red blood cells. *Infection and Immunity*, 72, 154–158.

Mitchison, T., Kirschner, M. (1984). Dynamic instability of microtubule growth. *Nature*, 312, 237–242.

Mogensen, M., Malik, A., Piel, M., Bouckson-Castaing, V., Bornens, M. (2000). Microtubule minus-end anchorage at centrosomal and non-centrosomal sites: the role of ninein. *Journal of Cell Science*, 113, 3013-3023.

Molestina, R. E., El-Guendy, N., Sinai, A. P. (2008). Infection with *Toxoplasma gondii* results in dysregulation of the host cell cycle. *Cellular Microbiology*, 10, 1153–1165.

Mordue, D. G., Desai, N, Dustin, M., Sibley, L. D. (1999). Invasion by *Toxoplasma gondii* establishes a moving junction that selectively excludes host cell plasma membrane proteins on the basis of their membrane anchoring. *The Journal of Experimental Medicine*, 190, 1783–1792.

Mori, R., Toda, T. (2013). The dual role of fission yeast Tbc1/cofactor C orchestrates microtubule homeostasis in tubulin folding and acts as a GAP for GTPase Alp41/Arl2. *Molecular Biology of the Cell*, 24, 1713-1724.

Morisaki, J., Heuser, J., Sibley, L. (1995). Invasion of *Toxoplasma gondii* occurs by active penetration of the host cell. *The Journal of Cell Science*, 108, 2457-2464.

Moritz, M., Braunfeld, M. B., Sedat, J. W., Alberts, B., Agard, D. A. (1995). Microtubule nucleation by gamma-tubulin-containing rings in the centrosome. *Nature*, 378, 638–640.

Morrissette, N. S., Sibley, L. D. (2002a). Disruption of microtubules uncouples budding and nuclear division in *Toxoplasma gondii*. *The Journal of Cell Science*, 115, 1017–1025.

Morrissette, N. S., Sibley, L. D. (2002b). Cytoskeleton of apicomplexan parasites. *Microbiology and Molecular Biology Reviews*, 66, 21-38.

Morrissette, N., Murray, J., Roos, D. (1997). Subpellicular microtubules associate with an intramembranous particle lattice in the protozoan parasite *Toxoplasma gondii*. *Journal of Cell Science*, 110, 35– 42.

Moser, L. A., Pollard, A. M., Knoll, L. J. (2013). A genome-wide siRNA screen to identify host factors necessary for growth of the parasite *Toxoplasma gondii*. *PloS One*, 8(6), e68129.

Nachury, M. V., Loktev, A. V., Zhang, Q., Westlake, C. J., Peränen, J., Merdes, A., Slusarski, D. C., Scheller, R. H., Bazan, J. F., Sheffield, V. C., Jackson, P. K. (2007). A core complex of BBS proteins cooperates with the GTPase Rab8 to promote ciliary membrane biogenesis. *Cell*, 129, 1201–1213.

Nakano, A., Kato, H., Watanabe, T., Min, K. D., Yamazaki, S., Asano, Y., Seguchi, O., Higo, S., Shintani, Y., Asanuma, H., Asakura, M., Minamino, T., Kaibuchi, K., Mochizuki, N., Kitakaze, M., Takashima, S. (2010). AMPK controls the speed of microtubule polymerization and directional cell migration through CLIP170 phosphorylation. *Nature Cell Biology*, 12, 583–590.

Neuman, M. (1972). Serological survey of *Besnoitia besnoiti* (Marotel 1912) infection in Israel by immunofluorescence. *Zentralblatt für Veterinärmedizin B*, 19, 391-396.

Nganga, C. J., Kanyari, P. W., Munyua, W. K. (1994). Isolation of *Besnoitia wallacei* in Kenya. *Veterinary Parasitology*, 52, 203–206.

Nichols, B. A., Chiappino, M. L. (1987). Cytoskeleton of *Toxoplasma gondii*. *Journal of Protozoology*, 34, 217-226.

Nicolle, C., Manceaux, L. (1908). Sur une infection a` corps de Leishman (ou organismes voisins) du gondi. *Comptes Rendus Hebdomadaires des Séances de L'Académie des Sciences*, 147, 763–766.

Nishi, M., Hu, K., Murray, J. M., Roos, D. S. (2008). Organellar dynamics during the cell cycle of *Toxoplasma gondii*. *The Journal of Cell Science*, 121(9), 1559-1568.

Nishisaka, M., Yokoyama, N., Xuan, X., Inoue, N., Nagasawa, H., Fujisaki, K., Mikami, T., Igarashi, I. (2001). Characterisation of the gene encoding a protective antigen from *B. microti* identified it as eta subunit of chaperonin containing T-complex protein 1. *International Journal for Parasitology*, 14, 1673-1679.

Nolasco, S., Bellido, J., Gonçalves, J., Zabala, J. C., Soares, H. (2005). Tubulin cofactor A gene silencing in mammalian cells induces changes in microtubule cytoskeleton, cell cycle arrest, and cell death. *FEBS Letters*, 579, 3515–3524.

Nyalwidhe, J., Lingelbach, K. (2006). Proteases and chaperones are the most abundant proteins in the parasitophorous vacuole of *Plasmodium falciparum*-infected erythrocytes. *Proteomics*, 6(5), 1563-1573.

Oleynikov, Y., Singer, R. H. (1998). RNA localization: different zipcodes, same postman? *Trends in Cell Biology*, 8, 381–383.

Olias, P., Schade, B., Mehlhorn, H. (2011). Molecular pathology, taxonomy and epidemiology of *Besnoitia* species (Protozoa: Sarcocystidae). *Infection Genetics and Evolution*, 11(7), 1564-1576.

Onishi, K., Higuchi, M., Asakura, T., Masuyama, N., Gotoh, Y. (2007). The PI3K-Akt pathway promotes microtubule stabilization in migrating fibroblasts. *Genes to Cells*, 12, 535–546.

Ossorio, P. N., Dubremetz, J., Joiner, K. A. (1994). A soluble secretory protein of the intracellular parasite *Toxoplasma gondii* associates with the parasitophorous vacuole membrane through hydrophobic interactions. *The Journal of Biological Chemistry*, 269, 15350–15357.

Pacheco-Soares, C., De Souza, W. (1998). Redistribution of parasite and host cell membrane components during *Toxoplasma gondii* invasion. *Cell Structure and Function*, 23(3), 159–168.

Paredes-Santos, T. C., de Souza, W., Attias, M. (2012). Dynamics and 3D organization of secretory organelles of *Toxoplasma gondii*. *Journal of Structural Biology*, 177(2), 420-430.

Parsons, M., Valentine, M., Carter, V. (1993). Protein kinases in divergent eukaryotes: identification of protein kinase activities regulated during trypanosome development. *Proceedings of the National Academy of Sciences*, 90, 2656–2660.

Parvari, R., Hershkovitz, E., Grossman, N., Gorodischer, R., Loeys, B., Zecic, A., Mortier, G., Gregory, S., Sharony, R., Kambouris, M., Sakati, N., Meyer, B. F., Al Aqeel, A. I., Al Humaidan, A. K., Al Zanhrani, F., Al Swaid, A., Al Othman, J., Diaz, G. A., Weiner, R., Khan, K. T., Gordon, R., Gelb, B. D., HRD/Autosomal Recessive Kenny-Caffey Syndrome Consortium. (2002). Mutation of TBCE causes hypoparathyroidism–retardation–dysmorphism and autosomal recessive Kenny–Caffey syndrome. *Nature Genetics*, 32, 448–452.

Paule, M. R., White, R. J. (2000). Survey and summary: transcription by RNA polymerases I and III. *Nucleic Acids Research*, 28, 1283–1298.

Pause, B., Diestelkötter, P., Heid, H., Just, W. W. (1997). Cytosolic factors mediate protein insertion into the peroxisomal membrane. *FEBS Letters*, 414, 95–98.

Payne, T. M., Molestina, R. E., Sinai, A. P. (2003). Inhibition of caspase activation and a requirement for NF-kB function in the *Toxoplasma gondii*–mediated blockade of host apoptosis. *Journal of Cell Science*, 116, 4345–4358.

Peng, H. J., Chen, X. G., Lindsay, D. S. (2011). A review: Competence, compromise, and concomitance-reaction of the host cell to *Toxoplasma gondii* infection and development. *The Journal of Parasitology*, 97(4), 620-628.

Perez, F., Diamantopoulos, G. S., Stalder, R., Kreis, T. E. (1999). CLIP-170 highlights growing microtubule ends *in vivo*. *Cell*, 96, 517–527.

Perrotto, J., Keister, D. B., Gelderman, A. H. (1971). Incorporation of precursors into *Toxoplasma* DNA. *Journal of Protozoology*, 18, 470–473.

Pfefferkorn, E. R. (1984). Interferon gamma blocks the growth of *Toxoplasma gondii* in human fibroblasts by inducing the host cells to degrade tryptophan. *Proceedings of the National Academy of Sciences*, 81, 908–912.

Pfefferkorn, L. C., Pfefferkorn, E. R. (1980). *Toxoplasma gondii*: genetic recombination between drug resistant mutants. *Experimental Parasitology*, 50, 305–316.

Piel, M., Meyer, P., Khodjakov, A., Rieder, C. L., Bornens, M. (2000). The respective contributions of the mother and daughter centrioles to centrosome activity and behavior in vertebrate cells. *The Journal of Cell Biology*, 149, 317-329.

Pipano, E. (1997). Vaccines against hemoparasitic diseases in Israel with special reference to quality assurance. *Tropical Animal Health and Production*, 29, 86S–90S.

Plattner, F., Yarovinsky, F., Romero, S., Didry, D., Carlier, M. F., Sher, A., Soldati-Favre, D. (2008). *Toxoplasma* profilin is essential for host cell invasion and TLR11-dependent induction of an interleukin-12 response. *Cell Host & Microbe*, 3, 77–87.

Pols, J. W. (1954). The artificial transmission of *Globidium besnoiti* (Marotel, 1912) to cats and rabbits. *Journal of the South African Veterinary Association*, 25, 37–44.

Pols, J. W. (1960). Studies on bovine besnoitiosis with special reference to the aetiology. *The Onderstepoort Journal of Veterinary Research*, 28, 265-356.

Puthenveedu, M. A., Bachert, C., Puri, S., Lanni, F., Linstedt, A. D. (2006). GM130 and GRASP65-dependent lateral cisternal fusion allows uniform Golgi-enzyme distribution. *Nature Cell Biology*, 8, 238–248.

Quittnat, F., Nishikawa, Y., Stedman, T. T., Voelker, D. R., Choi, J. Y., Zahn, M. M., Murphy, R. C., Barkley, R. M., Pypaert, M., Joiner, K. A., Coppens, I. (2004). On the biogenesis of lipid bodies in ancient eukaryotes: synthesis of triacylglycerols by a *Toxoplasma* DGAT1-related enzyme. *Molecular and Biochemical Parasitology*, 138, 107–122.

Radcliffe, P. A., Garcia, M. A., Toda, T. (2000). The cofactor dependent pathways for α- and β-tubulins in microtubule biogenesis are functionally different in fission yeast. *Genetics*, 156, 93–103.

Radcliffe, P. A., Hirata, D., Vardy, L., Toda, T. (1999). Functional dissection and hierarchy of tubulin-folding cofactor homologues in fission yeast. *Molecular Biology of the Cell*, 10, 2987–3001.

Rademacher, F., Kehren, V., Stoldt, V. R., Ernst, J. F. (1998). A *Candida albicans* chaperonin subunit (CaCct8p) as a suppressor of morphogenesis and Ras phenotypes in *C. albicans* and *Saccharomyces cerevisiae*. *Microbiology*, 144, 2951-2960.

Ratner, S., Sherrod, W. S., Lichlyter, D. (1997). Microtubule retraction into the uropod and its role in T cell polarization and motility. *The Journal of Immunology*, 159, 1063-1067.

Rayala, S. K., Martin, E., Sharina, I. G., Molli, P. R., Wang, X., Jacobson, R., Murad, F., Kumar, R. (2007). Dynamic interplay between nitration and phosphorylation of tubulin cofactor B in the control of microtubule dynamics. *Proceedings of the National Academy of Sciences of the U S A*, 104(49), 19470-19475.

Reis, Y., Cortes, H., Viseu Melo, L., Fazendeiro, I., Leitão, A., Soares, H. (2006). Microtubule cytoskeleton behavior in the initial steps of host cell invasion by *Besnoitia besnoiti*. *FEBS Letters*, 580, 4673–4682.

Remington, J. S. (1969). The present status of the IgM fluorescent antibody technique in the diagnosis of congenital toxoplasmosis. *Journal of Pediatrics*, 75, 1116–1124.

Remington, J. S., McLeod, R., Thulliez, P., Desmonts, G. (2006). Toxoplasmosis. In: Remington, J. S., Klein, J. O. (Eds.), *Infectious Diseases of the Fetus and Newborn Infant*. (5th ed.). (pp. 947–1091). Philadelphia: W. B. Saunders.

Remington, J. S., Miller, M. J., Brownlee, I. E. (1968). IgM antibodies in acute toxoplasmosis. II. Prevalence and significance in acquired cases. *Journal of Laboratory and Clinical Medicine*, 71, 855–866.

Riehemann, K., Sorg, C. (1993). Sequence homologies between four cytoskeleton-associated proteins. *Trends in Biochemical Sciences*, 18, 82–83.

Rios, R. M., Sanchís, A., Tassin, A. M., Fedriani, C., Bornens, M. (2004). GMAP-210 recruits gamma-tubulin complexes to cis-Golgi membranes and is required for Golgi ribbon formation. *Cell*, 118, 323–335.

Ririe, K. M., Rasmussen, R. P., Wittwer, C. T. (1997). Product differentiation by analysis of DNA melting curves during the polymerase chain reaction. *Analytical Biochemistry*, 245 154–160.

Rivero, S., Cardenas, J., Bornens, M., Rios, R.M. (2009). Microtubule nucleation at the cis-side of the Golgi apparatus requires AKAP450 and GM130. *The EMBO Journal*, 28, 1016–1028.

Robert-Gangneux, F., Dardé, M. L. (2012). Epidemiology of and diagnostic strategies for toxoplasmosis. *Clinical Microbiology Reviews*, 25(2), 264-296.

Romano, J. D., Sonda, S., Bergbower, E., Smith, M. E., Coppens, I. (2013). *Toxoplasma gondii* salvages sphingolipids from the host Golgi through the rerouting of selected Rab vesicles to the parasitophorous vacuole. *Molecular Biology of the Cell*, 24, 1974–1995.

Rommelaere, H., De Neve, M., Melki, R., Vandekerckhove, J., Ampe, C. (1999). The cytosolic class II chaperonin CCT recognizes delineated hydrophobic sequences in its target proteins. *Biochemistry*, 38(11), 3246–3257.

Roobol, A., Holmes, F. E., Hayes, N. V. L., Baines, A. J., Carden, A. J. (1995). Cytoplasmic chaperonin complexes enter neurites developing *in vitro* and differ in subunit composition within single cells. *Journal of Cell Science*, 108, 1477–1488.

Roobol, A., Sahyoun, Z. P., Carden, M. J. (1999). Selected subunits of the cytosolic chaperonin associate with microtubules assembled *in vitro*. *The Journal of Biological Chemistry*, 274, 2408–2415.

Rosowski, E. E., Lu, D., Julien, L., Rodda, L., Gaiser, R. A., Jensen, K. D., Saeij, J. P. (2011) Strain-specific activation of the NF-kB pathway by GRA15, a novel *Toxoplasma gondii* dense granule protein. *The Journal of Experimental Medicine*, 208, 195–212.

Rostaher, A., Mueller, R. S.; Majzoub, M., Schares, G., Gollnick, N. S. (2010). Bovine besnoitiosis in Germany. *Veterinary Dermatology*, 21(4), 329–334.

Russell, D. G. (1983). Host cell invasion by Apicomplexa: an expression of the parasite's contractile system? *Parasitology*, 87, 199–209.

Russell, D. G., Burns, R. G. (1984). The polar ring of coccidian sporozoites: a unique microtubule-organizing centre. *The Journal of Cell Science*, 65, 193–207.

Sabin, A. B., Feldman, H. A. (1948). Dyes as microchemical indicators of a new immunity phenomenon affecting a protozoon parasite (*Toxoplasma*). *Science*, 108, 660–663.

Sabin, A. B., Olitsky, P. K. (1937). *Toxoplasma* and obligate intracellular parasitism. *Science*, 85, 336–338.

Sahlender, D. A., Roberts, R. C., Arden, S. D., Spudich, G., Taylor, M.J., Luzio, J. P., Kendrick-Jones, J., Buss, F. (2005). Optineurin links myosin VI to the Golgi complex and is involved in Golgi organization and exocytosis. *The Journal of Cell Biology*, 169, 285–295.

Salpingidou, G., Smertenko, A., Hausmanowa-Petrucewicz, I., Hussey, P. J., Hutchison, C. J. (2007). A novel role for the nuclear membrane protein emerin in association of the centrosome to the outer nuclear membrane. *The Journal of Cell Biology*, 178, 897–904.

Sannusi, A. (1991). A simple field diagnostic smear test for bovine besnoitiosis. *Veterinary Parasitology*, 39, 185-188.

Santos, J. M., Ferguson, D. J., Blackman, M. J., Soldati-Favre, D. (2011). Intramembrane cleavage of AMA1 triggers *Toxoplasma* to switch from an invasive to a replicative mode. *Science*, 331, 473–477.

Santos, J. M., Soldati-Favre, D. (2011). Invasion factors are coupled to key signalling events leading to the establishment of infection in apicomplexan parasites. *Cellular Microbiology*, 13(6), 787–796.

Sawmynaden, K., Saouros, S., Friedrich, N., Marchant, J., Simpson, P., Bleijlevens, B., Blackman, M. J., Soldati-Favre, D., Matthews, S. (2008). Structural insights into microneme protein assembly reveal a new mode of EGF domain recognition. *EMBO Reports*, 9, 1149–1155.

Schaefer, M. K., Schmalbruch, H., Buhler, E., Lopez, C., Martin, N., Guénet, J. L., Haase, G. (2007). Progressive motor neuronopathy: a critical role of the tubulin chaperone TBCE in axonal tubulin routing from the Golgi apparatus. *The Journal of Neuroscience*, 27, 8779–8789.

Schares, G., Basso, W., Majzoub, M., Cortes, H. C., Rostaher, A., Selmair, J., Hermanns, W., Conraths, F. J., Gollnick, N. S. (2009). First *in vitro* isolation of *Besnoitia besnoiti* from chronically infected cattle in Germany. *Veterinary Parasitology*, 163(4), 315-322.

Schares, G., Basso, W., Majzoub, M., Rostaher, A., Scharr, J. C., Langenmayer, M. C., Selmair, J., Dubey, J. P., Cortes, H. C., Conraths, F. J., Haupt, T., Pürro, M.,Raeber, A.,

Buholzer, P., Gollnick, N. S. (2011a). Evaluation of a commercial ELISA for the specific detection of antibodies against *Besnoitia besnoiti*. *Veterinary Parasitology*, 175, 52-59.

Schares, G., Langenmayer, M. C., Scharr, J. C., Minke, L., Maksimov, P., Maksimov, A., Schares, S., Bärwald, A., Basso, W., Dubey, J. P., Conraths, F. J., Gollnick, N. S. (2013). Novel tools for the diagnosis and differentiation of acute and chronic bovine besnoitiosis. *International Journal for Parasitology*, 43, 143–154.

Schares, G., Maksimov, A., Basso, W., Moré, G., Dubey, J. P., Rosental, B., Majzoub, M., Rostaher, A., Selmair, J., Langenmayer, M. C., Scharr, J. C., Conraths, F. J., Gollnick, N. S. (2011b). Quantitative real time polymerase chain reaction assays for the sensitive detection of *Besnoitia besnoiti* infection in cattle. *Veterinary Parasitology*, 178(3-4), 208-216.

Schmoranzer, J., Fawcett, J. P., Segura, M., Tan, S., Vallee, R. B., Pawson, T. and Gundersen, G. G. (2009). Par3 and dynein associate to regulate local microtubule dynamics and centrosome orientation during migration. *Current Biology*, 19, 1065–1074.

Schneider, I., Haller, D., Kullmann, B., Beyer, D., Ahmed, J. S., Seitzer, U. (2007). Identification, molecular characterization and subcellular localization of a *Theileria annulata* parasite protein secreted into the host cell cytoplasm. *Parasitology Research*, 101, 1471–1482.

Schoehn, G., Hayes, M., Cliff, M. J., Clarke, A. R., Saibil, H. R. (2000). Domain rotations between open, closed and bullet-shaped forms of the thermosome, and archaeal chaperonin. *Journal of Molecular Biology*, 301, 323-332.

Schrick, J. J., Vogel, P., Abuin, A., Hampton, B., Rice, D. S. (2006). ADP-ribosylation factor-like 3 is involved in kidney and photoreceptor development. *American Journal of Pathology*, 168, 1288–1298.

Schulz, I., Baumann, O., Samereier, M., Zoglmeier, C., Graf, R. (2009). *Dictyostelium* Sun1 is a dynamic membrane protein of both nuclear membranes and required for centrosomal association with clustered centromeres. *European Journal of Cell Biology*, 88, 621–638.

Schwab, J. C., Beckers, C. J. M., Joiner, K. A. (1994). The parasitophorous vacuole membrane surrounding intracellular *Toxoplasma gondii* functions as a molecular sieve. *Proceedings of the National Academy of Sciences*, 91, 509–513.

Schwarz, N., Hardcastle, A. J., Cheetham, M. E. (2012). Arl3 and RP2 mediated assembly and traffic of membrane associated cilia proteins. *Vision Research*, 75, 2–4.

Sehgal, A., Bettiol, S., Pypaert, M., Wenk, M. R., Kaasch, A., Blader, I. J., Joiner, K. A., Coppens, I. (2005). Peculiarities of host cholesterol transport to the unique intracellular vacuole containing *Toxoplasma*. *Traffic*, 6, 1125 - 1141.

Seixas, C., Casalou, C., Melo, L. V., Nolasco, S., Brogueira, P., Soares, H. (2003). Subunits of the chaperonin CCT are associated with *Tetrahymena* microtubule structures and are involved in cilia biogenesis. *Experimental Cell Research*, 290, 303-321.

Seixas, C., Cruto, T., Tavares A., Gaertig J., Soares, H. (2010). CCTα and CCTδ chaperonin subunits are essential and required for cilia assembly and maintenance in *Tetrahymena*. *PLoS ONE*, 5, e10704.

Seo, S., Baye, L. M., Schulz, N. P., Beck, J. S., Zhang, Q., Slusarski, D. C., Sheffield, V. C. (2010). BBS6, BBS10, and BBS12 form a complex with CCT/TRiC family chaperonins and mediate BBSome assembly. *Proceedings of the National Academy of Sciences*, 107, 1488-1493.

Sevigny, G., Kothary, R., Tremblay, E., Derepentigny, Y., Joly, E. C., Biborhardy, V. (1995). The cytosolic chaperonin subunit TRiC-P5 begins to be expressed at the two-cell Stage in mouse embryos. *Biochemical and Biophysical Research Communications*, 216, 279–283.

Shaw, M. K. (2003). Cell invasion by *Theileria* sporozoites. *Trends in Parasitology*, 19, 2–6.

Shaw, M. K., Compton, H. L., Roos, D. S., Tilney, L. G. (2000). Microtubules, but not actin filaments, drive daughter cell budding and cell division in *Toxoplasma gondii*. *Journal of Cell Science*, 113, 1241-1254.

Shkap, V., De Waal, D. T., Potgieter, F. T. (1985). Chemotherapy of experimental *Besnoitia besnotiti* infection in rabbits. *Onderstepoort Journal of Veterinary Research*, 52, 289-264.

Shkap, V., Pipano, E., Marcus, S., Kriegel,Y. (1994). Bovine besnoitiosis: transfer of colostral antibodies with observations possible relating to natural transmission of the infection. *Onderstepoort Journal of Veterinary Research*, 61, 273-275.

Shkap, V., Pipano, E., Ungar-Waron, H. (1987). *Besnoitia besnoiti* : chemotherapeutic trials *in vivo* and *in vitro*. *Revue d'Elevage et de Medecine Vétérinaire des Pays Tropicaux*, 40, 259–264.

Shkap, V., Reske, A., Pipano, E., Fish, L., Baszler, T. (2002). Immunological relationship between *Neospora caninum* and *Besnoitia besnoiti*. *Veterinary Parasitology*, 106, 35–43.

Shkap, V., Yakobson, B., Pipano, E. (1988). Transmission and scanning electron microscopy of *Besnoitia besnoiti*. *International Journal for Parasitology*, 18, 761–766.

Shorter, J., Watson, R., Giannakou, M. E., Clarke, M., Warren, G., Barr, F. A. (1999). GRASP55, a second mammalian GRASP protein involved in the stacking of Golgi cisternae in a cell-free system. *The EMBO Journal*, 18, 4949-4960.

Sibley, L. D., Dobrowolski, J. M., Morisaki, J. H., Heuser, J. E. (1994). Invasion and intracellular survival by *Toxoplasma gondii*. In: Russell, D. G. (Ed.), *Strategies for intracellular survival of microbes* (pp. 245–264). London: Bailliere Tindall.

Sibley, L. D., Leblanc, A. J., Pfefferkorn, E. R., Boothroyd, J. C. (1992). Generation of a restriction-fragment-length-polymorphism linkage map for *Toxoplasma gondii*. *Genetics*, 132, 1003–1015.

Sinai, A. P., Joiner, K. A. (2001). The *Toxoplasma gondii* protein ROP2 mediates host organelle association with the parasitophorous vacuole membrane. *The Journal of Cell Biology*, 154(1), 95-108.

Sinai, A. P., Webster, P., Joiner, K. A. (1997). Association of host cell endoplasmic reticulum and mitochondria with the *Toxoplasma gondii* parasitophorous vacuole membrane: a high affinity interaction. *Journal of Cell Science*, 110, 2117 - 2128.

Sinden, R. E. (1978). Cell biology. In: Killick-Kendrick, R., Jones, W. (Ed.), *Rodent malaria.* (pp. 85–168). New York: Academic Press.

Siverajah, S., Ryce, C., Morrison, D. A., Ellis, J. T. (2003). Characterization of an alpha tubulin gene sequence from *Neospora caninum* and *Hammondia heydorni*, and their comparison to homologous genes from Apicomplexa. *Parasitology*, 126, 561–569.

Soares, H., Marinho, H. S., Real, C., Antunes, F. (2013). Cellular polarity in aging: role of redox regulation and nutrition. *Genes & Nutrition*, 9(1), 371.

Soares, H., Penque, D., Mouta, C., Rodrigues-Pousada, C. (1994). A *Tetrahymena* orthologue of the mouse chaperonin subunit CCT gamma and its coexpression with tubulin during cilia recovery. *The Journal of Biological Chemistry*, 269, 29299–29307.

Soldati, D., Meissner, M. (2004). *Toxoplasma* as a novel system for motility. *Current Opinion in Cell Biology*, 16, 32–40.

Somer, L., Shmulman, O., Dror, T., Hashmueli, S., Kashi Y. (2002). The eukaryote chaperonin CCT is a cold shock protein in *Saccharomyces cerevisiae*. *Cell Stress & Chaperones*, 7 (1), 47–54.

Song, C., Chiasson, M. A., Nursimulu, N., Hung, S. S., Wasmuth, J., Grigg, M. E., Parkinson, J. (2013). Metabolic reconstruction identifies strain-specific regulation of virulence in *Toxoplasma gondii*. *Molecular Systems Biology*, 9, 708.

Soues, S., Kann, M. L., Fouquet, J. P., Melki, R. (2003). The cytosolic chaperonin CCT associates to cytoplasmic microtubular structures during mammalian spermiogenesis and to heterochromatin in germline and somatic cells. *Experimental Cell Research*, 288, 363–373.

Spear, W., Chan, D., Coppens, I., Johnson, R. S, Giaccia, A., Blader, I. J. (2006). The host cell transcription factor hypoxia-inducible factor 1 is required for *Toxoplasma gondii* growth and survival at physiological oxygen levels. *Cellular Microbiology*, 8, 339–352.

Spiliotis, E. T., Hunt, S. J., Hu, Q., Kinoshita, M., Nelson, W. J. (2008). Epithelial polarity requires septin coupling of vesicle transport to polyglutamylated microtubules. *The Journal of Cell Biology*, 180, 295-303.

Stankewich, M. C., Tse, W. T., Peters, L. L., Ch'ng, Y., John, K. M., Stabach, P. R. Devarajan, P., Morrow, J. S., Lux, S. E. (1998). A widely expressed betaIII spectrin associated with Golgi and cytoplasmic vesicles. *Proceedings of the National Academy of Sciences*, 95, 14158– 14163.

Starr, D. A., Fridolfsson, H. N. (2010). Interactions between nuclei and the cytoskeleton are mediated by SUN/KASH nuclear-envelope bridges. *Annual Review of Cell and Developmental Biology*, 26, 421–444.

Stedman, T. T., Sussmann, A. R., Joiner, K. A. (2003). *Toxoplasma gondii* Rab6 mediates a retrograde pathway for sorting of constitutively secreted proteins to the Golgi complex. *The Journal of Biological Chemistry*, 278, 5433–5443.

Steinborn, K., Maulbetsch, C., Priester, B., Trautmann, S., Pacer, T., Geiges, B. (2002). The *Arabidopsis* PILZ group genes encode tubulin-folding cofactor orthologs required for cell division but not cell growth. *Genes & Development*, 16, 959–971.

Stephens, R. E., Lemieux, N. A. (1999). Molecular chaperones in cilia and flagella: implications for protein turnover. *Cell Motilility and the Cytoskeleton*, 44, 274-283.

Sternlicht, H., Farr, G. W., Sternlicht, M. L., Driscoll, J. K.,Willison, K, Yaffe, M. B. (1993). The t-complex polypeptide 1 is a chaperonin for tubulin and actin *in vivo*. *Proceedings of the National Academy of Sciences*, 90, 9422–9426.

Stieber, A., Chen, Y., Wei, S., Mourelatos, Z., Gonatas, J., Okamoto, K., Gonatas, N. K. (1998). The fragmented neuronal Golgi apparatus in amyotrophic lateral sclerosis includes the trans-Golgi-network: functional implications. *Acta Neuropathologica*, 95, 245–253.

Stommel, E. W., Ely, K. H., Schwartzman, J. D., Kasper. L. H. (1997). *T. gondii*: dithiol-induced $Ca2^{+}$ flux causes egress of parasites from the parasitophorous vacuole. *Experimental Parasitology*, 87, 88–97.

Straub, K., Cheng, S., Sohn, C., Bradley, P. (2009). Novel components of the Apicomplexan moving junction reveal conserved and coccidia-restricted elements. *Cellular Microbiology*, 11, 590–603.

Striepen, B., Crawford, M. J., Shaw, M. K., Tilney, L. G., Seeber, F., Roos, D. S. (2000). The plastid of *Toxoplasma gondii* is divided by association with the centrosomes. *The Journal of Cell Biology*, 151, 1423–1434.

Sumyuen, M. H., Garin, Y. J., Derouin, F. (1995). Early kinetics of *Toxoplasma gondii* infection in mice infected orally with cysts of an avirulent strain. *Journal of Parasitology*, 81, 327–329.

Suss-Toby, E., Zimmerberg, J., Ward, G. E. (1996). *Toxoplasma* invasion: the parasitophorous vacuole is formed from host cell plasma membrane and pinches off via a fission pore. *Proceedings of the National Academy of Sciences*, 93, 8413–8418.

Sütterlin, C., Colanzi, A. (2010). The Golgi and the centrosome: building a functional partnership. *The Journal of Cell Biology*, 188, 621–628.

Sütterlin, C., Polishchuk, R., Pecot, M., Malhotra, V. (2005). The Golgi associated protein GRASP65 regulates spindle dynamics and is essential for cell division. *Molecular Biology of the Cell*, 16, 3211–3222.

Sweeney, K. R., Morrissette, N. S., LaChapelle, S., Blader, I. J. (2010). Host cell invasion by *Toxoplasma gondii* is temporally regulated by the host microtubule cytoskeleton. *Eukaryotic Cell*, 9(11), 1680-1689.

Takahashi, M., Shibata, H., Shimakawa, M., Miyamoto, M., Mukai, H., Ono, Y. (1999). Characterization of a novel giant scaffolding protein, CG-NAP, that anchors multiple signaling enzymes to centrosome and the Golgi apparatus. *The Journal of Biological Chemistry*, 274, 17267–17274.

Takemae, H., Sugi, T., Kobayashi, K., Gong, H., Ishiwa, A., Recuenco, F. C., Murakoshi, F., Iwanaga, T., Inomata, A., Horimoto, T., Akashi, H., Kato, K. (2013). Characterization of the interaction between *Toxoplasma gondii* rhoptry neck protein 4 and host cellular β-tubulin. *Scientific Reports*, 3, 3199.

Tanaka, K., Fukudome, H. (1991). Three-dimensional organization of the Golgi complex observed by scanning electron microscopy. *Journal of Electron Microscopy Technique*, 17, 15–23.

Tenter, A. M., Heckeroth, A. R., Weiss, L. M. (2000). *Toxoplasma gondii*: from animals to humans. *International Journal for Parasitology*, 30(12-13), 1217-1258.

Tenter, A. M., Johnson, A. M. (1997). Phylogeny of the tissue cystforming coccidian. *Advances in Parasitology*, 39, 69-139.

Thyberg, J., Moskalewski, S. (1993). Relationship between the Golgi complex and microtubules enriched in detyrosinated or acetylated α-tubulin: studies on cells recovering from nocodazole and cells in the terminal phase of cytokinesis. *Cell and Tissue Research*, 273, 457–466.

Thyberg, J., Moskalewski, S. (1999). Role of microtubules in the organization of the Golgi complex. *Experimental Cell Research*, 246, 263–279.

Tian, G., Bhamidipati, A., Cowan, N. J., Lewis, S. A. (1999). Tubulin folding cofactors as GTPase-activating proteins. GTP hydrolysis and the assembly of the α/β-tubulin heterodimer. *The Journal of Biological Chemistry*, 274, 24054–24058.

Tian, G., Cowan, N. J. (2013). Tubulin-specific chaperones: components of a molecular machine that assembles the α/β heterodimer. *Methods in Cell Biology*, 115, 155-171.

Tian, G., Huang, Y., Rommelaere, H., Vandekerckhove, J., Ampe, C., Cowan, N. J. (1996). Pathway leading to correctly folded β-tubulin. *Cell*, 86, 287–296.

Tian, G., Jaglin, X. H., Keays, D. A., Francis, F., Chelly, J., Cowan, N. J. (2010a). Disease-associated mutations in TUBA1A result in a spectrum of defects in the tubulin folding and heterodimer assembly pathway. *Human Molecular Genetics*, 19, 3599–3613.

Tian, G., Lewis, S. A., Feierbach, B., Stearns, T., Rommelaere, H., Ampe, C., Cowan, N. J. (1997). Tubulin subunits exist in an activated conformational state generated and maintained by protein cofactors. *The Journal of Cell Biology*, 138, 821–832.

Tian, G., Thomas, S., Cowan, N. J. (2010b). Effect of TBCD and its regulatory interactor Arl2 on tubulin and microtubule integrity. *Cytoskeleton*, 67, 706–714.

Tikhonenko, I., Magidson, V., Gräf, R., Khodjakov, A., Koonce, M. P. (2013). A kinesin-mediated mechanism that couples centrosomes to nuclei. *Cellular and Molecular Life Sciences*, 70(7), 1285–1296.

Tran, J. Q., Li, C., Chyan, A., Chung, L., Morrissette, N. S. (2012). SPM1 stabilizes subpellicular microtubules in *Toxoplasma gondii*. *Eukaryotic Cell*, 11 (2), 206–216.

Tsang, W. Y., Spektor, A., Luciano, D. J., Indjeian, V. B., Chen, Z., Salisbury, J. L., Sánchez, I., Dynlacht, B. D. (2006). CP110 cooperates with two calcium-binding proteins to regulate cytokinesis and genome stability. *Molecular Biology of the Cell*, 17, 3423-3434.

Tyler, J. S., Treeck, M., Boothroyd, J. C. (2011). Focus on the ringleader: the role of AMA1 in apicomplexan invasion and replication. *Trends in Parasitology*, 27(9), 410–420.

Tyler, K. M., Luxton, G. W., Applewhite, D. A., Murphy, S. C., Engman, D. M. (2005). Responsive microtubule dynamics promote cell invasion by *Trypanosoma cruzi*. *Cellular Microbiology*, 7(11), 1579-1591.

Ursic, D., Sedbook, J. C., Himmel, K. L., Culbertson, M. R. (1994). The essential yeast Tcp1 protein affects actin and microtubules. *Molecular Biology of the Cell*, 5, 1065-1080.

Vadlamudi, R. K., Barnes, C. J., Rayala, S., Li, F., Balasenthil, S., Marcus, S., Goodson, H. V., Sahin, A. A., Kumar, R. (2005). p21-activated kinase 1 regulates microtubule dynamics by phosphorylating tubulin cofactor B. *Molecular and Cellular Biology*, 25, 3726–3736.

Vainberg, I. E., Lewis, S. A., Rommelaere, H., Ampe, C., Vandekerckhove, J., Klein, H. L., Cowan NJ. (1998). "Prefoldin, a chaperone that delivers unfolded proteins to cytosolic chaperonin." *Cell*, 93(5), 863–873.

Valpuesta, J. M., Martin-Benito, J., Gomez-Puertas, P., Carrascosa, J. L., Willison, K. R. (2002). Structure and function of a protein folding machine: the eukaryotic cytosolic chaperonin CCT. *FEBS Letters*, 529, 11–16.

van der Vaart, B., Manatschal, C., Grigoriev, I., Olieric, V., Gouveia, S. M., Bjelic, S., Demmers, J., Vorobjev, I., Hoogenraad, C. C., Steinmetz, M. O., Akhmanova, A. (2011). SLAIN2 links microtubule plus end-tracking proteins and controls microtubule growth in interphase. *The Journal of Cell Biology*, 193, 1083–1099.

van Vliet, C., Thomas, E. C., Merino-Trigo, A., Teasdale, R. D., Gleeson, P. A. (2003). Intracellular sorting and transport of proteins. *Progress in Biophysics and Molecular Biology*, 83(1), 1–45.

Veltel, S., Gasper, R., Eisenacher, E., Wittinghofer, A. (2008). The retinitis pigmentosa 2 gene product is a GTPase-activating protein for Arf-like 3. *Nature Structural & Molecular Biology*, 15, 373–380.

Verma, R. Khanna, P. (2013). Development of *Toxoplasma gondii* vaccine: A global challenge. *Human Vaccines & Immunotherapeutics*, 9(2), 291–293.

Vicente-Manzanares, M., Zareno, J., Whitmore, L., Choi, C. K., Horwitz, A. F. (2007). Regulation of protrusion, adhesion dynamics, and polarity by myosins IIA and IIB in migrating cells. *The Journal of Cell Biology*, 176, 573–580.

Vinogradova, T., Miller, P. M., Kaverina, I. (2009). Microtubule network asymmetry in motile cells: role of Golgi-derived array. *Cell Cycle*, 8, 2168–2174.

Vinogradova, T., Paul, R., Grimaldi, A. D., Loncarek, J., Miller, P. M., Yampolsky, D., Magidson, V., Khodjakov, A., Mogilner, A., Kaverina, I.. (2012). Concerted effort of

centrosomal and Golgi-derived microtubules is required for proper Golgi complex assembly but not for maintenance. *Molecular Biology of the Cell*, 23(5), 820-833.

Vogelsang, E. G., Gallo, P. (1941). *Globidium besnoiti* (Marotel, 1912) y habronemosis cutanea en bovinos de Venezuela. *Revista de la Facultdad de Ciencias Veterinarias*, 3, 153-155.

Voloshin, O., Gocheva, Y., Gutnick, M., Movshovich, N., Bakhrat, A., Baranes-Bachar, K., Bar-Zvi, D., Parvari, R., Gheber, L., Raveh, D. (2010). Tubulin chaperone E binds microtubules and proteasomes and protects against misfolded protein stress. *Cellular and Molecular Life Sciences*, 67, 2025–2038.

von Schubert, C., Xue, G., Schmuckli-Maurer, J., Woods, K. L., Nigg, E. A., Dobbelaere, D. A. (2010). The transforming parasite *Theileria* co-opts host cell mitotic and central spindles to persist in continuously dividing cells. *PLoS Biology*, 8(9), e1000499.

Waap, H., Cardoso, R., Marcelino, E., Malta, J., Cortes, H., Leitão, A. (2011). A modified agglutination test for the diagnosis of *Besnoitia besnoiti* infection. *Veterinary Parasitology*, 178(3-4). 217-22.

Waap, H., Nunes, T., Cortes, H., Leitão, A., Vaz, Y. (2014). Prevalence and geographic distribution of *Besnoitia besnoiti* infection in cattle herds in Portugal. *Parasitology Research.*

Wagner, C. T., Lu, I. Y., Hoffman, M. H., Sun, W. Q., Trent, J. D., Connor, J. (2004). T-complex polypeptide-1 interacts with the erythrocyte cytoskeleton in response to elevated temperatures. *The Journal of Biological Chemistry*, 279, 16223-16228.

Walker, M. E., Hjort, E. E., Smith, S. S., Tripathi, A., Hornick, J. E., Hinchcliffe, E. H., Archer, W., Hager, K. M. (2008). *Toxoplasma gondii* actively remodels the microtubule network in host cells. *Microbes and Infection* 10, 1440 – 1449.

Wang, W., Ding, J., Allen, E., Zhu, P., Zhang, L., Vogel, H., Yang, Y. (2005). Gigaxonin interacts with tubulin folding cofactor B and controls its degradation through the ubiquitin-proteasome pathway. *Current Biology*, 15, 2050–2055.

Wang, Y., Weiss, L. M., Orlofsky, A. (2009). Intracellular parasitism with *Toxoplasma gondii* stimulates mammalian-target-of-rapamycin-dependent host cell growth despite impaired signalling to S6K1 and 4E-BP1. *Cellular Microbiology*, 11, 983–1000.

Wang, Y., Weiss, L. M., Orlofsky, A. (2010). Coordinate Control of Host Centrosome Position, Organelle Distribution, and Migratory Response by *Toxoplasma gondii* via Host mTORC2. *The Journal of Biological Chemistry*, 285, 15611–15618.

Watanabe, T., Noritake, J., Kaibuchi, K. (2005). Regulation of microtubules in cell migration. *Trends in Cell Biology*, 15, 76–83.

Wei, J. H., Seemann, J. (2010). Unraveling the Golgi ribbon. *Traffic*, 11, 1391–1400.

Weidner, J. M., Kanatani, S., Hernández-Castañeda, M. A., Fuks, J. M., Rethi, B., Wallin, R. P., Barragan, A. (2013). Rapid cytoskeleton remodelling in dendritic cells following invasion by *Toxoplasma gondii* coincides with the onset of a hypermigratory phenotype. *Cellular Microbiology*, 15(10), 1735-1752.

Willardson, B. M., Howlett, A. C. (2007). Function of phosducin-like proteins in G protein signalling and chaperone assisted folding. *Cell Signalling*, 19, 2417–2427.

Willison, K. R., Hynes, G., Davies, P., Goldsborough, A., Lewis, V. A. (1990). Expression of three t-complex genes, Tcp-1, Dl7khll7c3 and Dl7Leh66, in purified murine spermatogenic cell populations. *Genetics Reserach Cambridge*, 56, 193-201.

Wilson, B. S., Nuoffer, C., Meinkoth, J. L., McCaffery, M., Feramisco, J. R., Balch, W. E., Farquhar, M. G. (1994). A Rab1 mutant affecting guanine nucleotide exchange promotes disassembly of the Golgi apparatus. *The Journal of Cell Biology*, 125, 557–571.

Wittwer, C. T., Herrmann, M. G., Gundry, C. N., Elenitoba-Johnson, K. S. (2001). Real-time multiplex PCR assays. *Methods*, 25, 430–442.

Won, K. A., Schumacher, R. J., Farr, G. W., Horwich, A. L., Reed, S. I. (1998). Maturation of human cyclin E requires the function of eukaryotic chaperonin CCT. *Molecular and Cellular Biology*, 18, 7584–7589.

Woods, K. L., Theiler, R., Mühlemann, M., Segiser, A., Huber, S., Ansari, H. R., Pain, A., Dobbelaere, D. A. (2013). Recruitment of EB1, a master regulator of microtubule dynamics, to the surface of the *Theileria annulata* schizont. *PLoS Pathogens*, 9(5), e1003346.

Xiao, H., El Bissati, K., Verdier-Pinard, P., Burd, B., Zhang, H., Kim, K., Fiser, A., Angeletti, R. H., Weiss, L.M. (2010). Post-translational modifications to *Toxoplasma gondii* alpha- and beta-tubulins include novel C-terminal methylation. *Journal of Proteome Research*, 9, 359-372.

Xie, X., Palacios, R. (1994). Cloning and expression of a new mammalian chaperonin gene from a multipotent hematopoietic progenitor clone. *Blood*, 84, 2171–2174.

Xiong, H., Rivero, F., Euteneuer, U., Mondal, S., Mana-Capelli, S., Larochelle, D., Vogel, A., Gassen, B., Noegel, A. A. (2008). *Dictyostelium* Sun-1 connects the centrosome to chromatin and ensures genome stability. *Traffic*, 9, 708–724.

Yadav, S., Puri, S., Linstedt, A. D. (2009). A primary role for Golgi positioning in directed secretion, cell polarity, and wound healing. *Molecular Biology of the Cell*, 20, 1728–1736.

Yan, X., Habedanck, R. Nigg, E. A. (2006). A complex of two centrosomal proteins, CAP350 and FOP, cooperates with EB1 in microtubule anchoring. *Molecular Biology of the Cell*, 17, 634-644.

Yang, Z. Z., Tschopp, O., Baudry, A., Du Mmler, B., Hynx, D., Hemmings, B. A. (2004). Physiological functions of protein kinase B/Akt. *Biochemical Society Transactions*, 32, 350–354.

Yokota, S., Yanagi, H., Yura, T., Kubota, H. (1999). Cytosolic chaperonin is up-regulated during cell growth. *The Journal of Biological Chemistry*, 274(52), 37070–37078.

Yvon, A. M., Walker, J. W., Danowski, B., Fagerstrom, C., Khodjakov, A., Wadsworth, P. (2002). Centrosome reorientation in wound-edge cells is cell type specific. *Molecular Biology od the Cell*, 13, 1871–1880.

Zabala, J. C., Cowan, N. J. (1992) Tubulin dimer formation via the release of α- and β-tubulin monomers from multimolecular complexes. *Cell Motility and the Cytoskeleton*, 23, 222–230.

Zhang, D., Rogers, G. C., Buster, D. W., Sharp, D. J. (2007). Three microtubule severing enzymes contribute to the Pacman-flux machinery that moves chromosomes. *The Journal of Cell Biology*, 177, 231–242.

Zheng, Y., Wong, M. L., Alberts, B., Mitchison, T. (1995). Nucleation of microtubule assembly by a gamma-tubulin-containing ring complex. *Nature*, 378, 578-583.

Annex I: Sequence alignment for genes of *T. gondii* and *N. caninum*

(A)CCTα

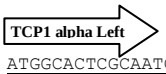


```
ToxoplasmagondiiTGME49_229990      ATGGCACTCGCAATCTTCGGCGACCGTCAGAGCGGGCAAGACGTCCGTACCGCCAATGCG
NeosporacaninumNCLIV_030660        ATGGCGCTCGCAATCTTCGGCGACCGTCAGAGCGGTCAGGACGTCCGTACCGCCAATGCT
                                   *****.****************************** **.********************

ToxoplasmagondiiTGME49_229990      GCGGCGGTGCAGTCGATCGCGAACATTCTGCGGTCGTCTCTCGGCCCCCAGGGGCTAGAC
NeosporacaninumNCLIV_030660        GCGGCGGTTCAGTCGATCGCGAACATTTTGCGGTCCTCTCTCGGACCCCAGGGTTTGGAC
                                   ******** ****************** ******* ********.********  *.***

ToxoplasmagondiiTGME49_229990      AAGATGCTCGTGGACGACATCGGAGACATGACGATTACGAACGATGGTGCGACGATTCTC
NeosporacaninumNCLIV_030660        AAAATGCTCGTGGACGACATTGGAGACATGACAATTACGAACGACGGCGCGACGATTCTC
                                   **.***************** ***********.*********** ** ************

ToxoplasmagondiiTGME49_229990      AAGCAACTCGAGGTGCAGCACCCTGCAGCGAAAGTTCTTGTTGAACTTTCCGATCTCCAG
NeosporacaninumNCLIV_030660        AAGCAGCTCGAAGTGCAACATCCTGCAGCGAAAGTCCTCGTGGAGCTCTCGGATCTGCAG
                                   *****.*****.*****.** ************** ** ** **.** ** ***** ***

ToxoplasmagondiiTGME49_229990      GACAAAGAGGTGGGCGACGGCACCACCTCCGTCGTCCTCCTCGCCGCCGAGTTCCTTCGA
NeosporacaninumNCLIV_030660        GACAAAGAAGTGGGAGACGGCACCACGTCCGTCGTTCTCCTTGCCGCCGAGTTTCTCCGG
                                   ********.*****.*********** ******** ***** ********** ** **.

ToxoplasmagondiiTGME49_229990      GTCGGAAATCAACTCGTGAAAGAGGGCGTTCACCCCACTGCTGTCATTGCAGGCTTCAAA
NeosporacaninumNCLIV_030660        GTCGGAAACCAACTGGTGAAGGAGGGTGTCCACCCCACGGCTGTCATTGCTGGCTTCAAA
                                   ******** ***** *****.***** ** ******** ***********:**********

ToxoplasmagondiiTGME49_229990      CTTGCAATGAAGGAAAGCGTTAAATTTATTCAAGAGCATTTGACATCTCGCGTTGATGCC
NeosporacaninumNCLIV_030660        CTCGCGATGAAGGAGAGCGTGAAGTATATTCAAGAACATCTGACGTCGCGAGTTGACGCG
                                   ** **.********.***** **.*:**********.*** ****.** **.***** **

ToxoplasmagondiiTGME49_229990      AACAACAGAGAGGTGCTCATGAACGTCGCAACAACGACCATCAGCTCGAAGCTCATCGGA
NeosporacaninumNCLIV_030660        AACAACAAGGAGGTTCTCCTGAACGTCGCAACAACGACGATCAGCTCCAAGCTCATTGGC
                                   *******..***** ***.******************** ******** ******** **.

ToxoplasmagondiiTGME49_229990      ACAGAGACAGCCCACTTCGCGGATCTTGTTGTTCGTGCTATTCTCTCCGTCAAGATGATC
NeosporacaninumNCLIV_030660        ACTGAAACAAACCACTTTGCAGATCTCGTTGTCCGTGCCATTCTCTCCGTCAAGATGATC
                                   **:**.***..****** **.***** ***** ***** ************************
```

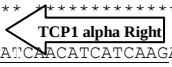


```
ToxoplasmagondiiTGME49_229990      ACCGAAAGAGGAGACGTCAAGTACCCTGTCAGCTCGATCAACATCATCAAGACCCACGGC
NeosporacaninumNCLIV_030660        ACCGAGCGAGGCGACGTGAAGTATCCCGTCAGCTCCATCAACATCATCAAGACCCACGGC
                                   *****..****.***** ***** ** ******** ************************

ToxoplasmagondiiTGME49_229990      AAATCGATGCGCGAATCGAGTCTCGTGGAAGGCTACGCACTGAAAGCGGGTCGCGCAGCA
NeosporacaninumNCLIV_030660        AAGTCGATGCGCGAGTCCACCCTCGTTGAAGGCTACGCCCTCAAAGCGGGTCGCGCCGCT
                                   **.***********.** *  ***** ***********.** ***************.**:

ToxoplasmagondiiTGME49_229990      CAAGGCATGCCCCAGTGCGTGAAGAACGCCAAGGTCGCCCTGCTCGACTTCAACCTTCGG
NeosporacaninumNCLIV_030660        CAAGGCATGCCCCAATGCGTGAAAAATGCTAGAGTCGCTCTCCTCGACTTCAATCTTCGT
                                   **************.********.** ** *..***** ** *********** *****

ToxoplasmagondiiTGME49_229990      CAGCATCGCATGCAACTCGGCGTCCAGATTCAGGTTGACAACCCCGAGGAACTGGAAAAG
NeosporacaninumNCLIV_030660        CAGCACCGAATGCAGTTAGGTGTGCAGATTCAGGTCGACAACCCTGAGGAGCTGGAGAAA
                                   ***** **.*****. *.** ** *********** ******** *****.*****.**.

ToxoplasmagondiiTGME49_229990      ATCCGGCAAAAAGAGAAGGACATCACGGCGGCGAAGATTCAGAAGATCCTTGCATCAGGA
NeosporacaninumNCLIV_030660        ATTCGGCAAAAGGAAAAGGACATCACAGCGGCGAAGATTCAAAAGATCCTCGCTTCAGGA
                                   ** ********.**.***********.***************.******** **:******

ToxoplasmagondiiTGME49_229990      GCAAACGTCATCTTGACAACCCAGGGCATCGACGATATGGCCATGAAGTACTTCGTCGAG
NeosporacaninumNCLIV_030660        GCGAACGTCATCCTGACCACGCAAGGAATCGACGATATGGCTATGAAGTATTTCGTTGAA
                                   **.********* ****.** **.**.*************** ******** ***** **.

ToxoplasmagondiiTGME49_229990      GCGGGGGCCATTGCCGTCCGCCGTGTTGACAGAAAAGACCTTCGCAGAATCGCCAAAATC
NeosporacaninumNCLIV_030660        GCTGGAGCCATTGCTGTTCGCCGTGTCGACAGAAAAGATCTCCGTCGAATTGCAAAAATT
                                   ** **.******** ** ******** *********** ** ** .**** **.*****

ToxoplasmagondiiTGME49_229990      ACAGAAGGCACTGTGGTGCTCACGATGGCTACTCTGGACGGAGACGAGAAGTTCGACGCT
NeosporacaninumNCLIV_030660        ACAGAGGGCACGGTGGTACTCACCATGGCGACTCTGGACGGAGACGAGAAGTTCGACGCT
                                   *****.***** *****.***** ***** ********************************

ToxoplasmagondiiTGME49_229990      TCCTGTCTTGGCACTTGCGAAGAAGTTTACGAGGAGCGCATTGGCGACTGGGATCACCTT
NeosporacaninumNCLIV_030660        TCCTGTCTGGGATCTTGCGAGGAAGTCTATGAGGAGCGTATCGGTGACTGGGACCACCTT
                                   ******** **.:********.***** ** ******** ** ** ******** ******

ToxoplasmagondiiTGME49_229990      ATGTTTAAAGGGTGCAAAGGTGGAAAGGCTGCGACAGTCATTCTTCGTGGAGCAAACGAG
NeosporacaninumNCLIV_030660        CTTTTCAAGGGCTGCAAAGGCGGAAAGGCTGCGACTGTCATTCTTCGGGGAGCTAACGAG
                                   .* ** **.** ******** **************:*********** *****:******

ToxoplasmagondiiTGME49_229990      TACATGCTGGACGAGGTCGACCGTTCTGTCCACGACGCCCTTTGCGCCGTATCTCGAGCT
NeosporacaninumNCLIV_030660        TACATGCTTGACGAAGTGGACCGGTCGGTTCACGACGCTCTCTGCGCGGTGTCTCGAGCT
                                   ******** *****.** ***** ** ** ******** ** ***** **.*********

ToxoplasmagondiiTGME49_229990      CTGGAGTACACGCACGTGTGTCCGGGCGGCGGCGCAGTGGAGACGTCGCTTTCTGTGTAT
```

```
NeosporacaninumNCLIV_030660       CTGGAGCATACGCATGTGTGCCCAGGTGGAGGCGCTGTCGAAACGTCGCTTTCTGTCTAC
                                  ****** * ***** ***** **.** **.*****:** **.************** **

ToxoplasmagondiiTGME49_229990     TTAGAGAACTTTGCCCGGACGCTTGGGTCCCGAGAGCAGCTAGCCATCGCAGCGTTTGCA
NeosporacaninumNCLIV_030660       CTGGAAAACTTTGCTCGCACTCTTGGGTCGCGGGAGCAGCTCGCGATTGCAGCGTTTGCC
                                   *.**.******** ** ** ******** **.********.** ** ***********.

ToxoplasmagondiiTGME49_229990     GAGGCTCTGCTGATCATTCCAAAGACCCTCGCGGTGAACGCCGCTCTCGATGCCACAGAG
NeosporacaninumNCLIV_030660       GAGTCTCTGCTGATCATTCCCAAGACGCTCGCCGTGAACGCAGCCCTCGACGCCACGGAG
                                  *** *****************.***** ***** ********.** ***** *****.***

ToxoplasmagondiiTGME49_229990     CTCGTCGCCAGGCTCCGCGCCGTGCATGCAAAGGCTCAGGGGCAGTTGCTTGACGCGGCT
NeosporacaninumNCLIV_030660       CTCGTGGCCCGTCTCCGCGCGGTGCATGCAAAGGCTCAGGGTCAGTTGCCGGACGCAGCT
                                  ***** ***.* ******** ********************** *******  *****.***

ToxoplasmagondiiTGME49_229990     GGGAACGGGGACGAGGAACTCAAGTGGCATGGCTTAGATCTAACTTCAGGGAAAACGAGG
NeosporacaninumNCLIV_030660       GGGAACGGGGACGACGAGCTCAAGTGGCATGGGCTCGATCTGGTCACAGGCAAGACGCGA
                                  ************** **.***************  * ******.. :***** **.***.*.
                                                                      PR2CCTatoxo
ToxoplasmagondiiTGME49_229990     AACAACATGGCTGCTGGAGTTATCGAGGCTGCTGTGACCAAGACGAAGGCACTGCGCTTT
NeosporacaninumNCLIV_030660       AACAACATGGCAGCCGGCGTCATTGAGGCGGCTGTGAGCAAAACGAAGGCCCTCCGCTTT
                                  ************:** **.** ** ***** ************.*********.** ******

ToxoplasmagondiiTGME49_229990     GCTACAGAAGCAGCCGTTACCATTCTACGGATCGATGACTTAATAAAAATCGCCCCCGAA
NeosporacaninumNCLIV_030660       GCTACGGAAGCTGCAGTTACCATTCTCCGTATTGACGACCTCATTAAAATTGCTCCGGAA
                                  *****.*****:** ********** ** ** ** *** *.**:***** ** ** ***
                                             CCTaReverse
ToxoplasmagondiiTGME49_229990     CCCGAACGGGGCCAACAGGATGACTAG
NeosporacaninumNCLIV_030660       CCGGAACGGGGACAGCCCGATGACTAG
                                  ** ********.**.*. *********
```

(B) TBCB

```
ToxoplasmagondiiTGME49_305060     ATGTCGGGCTTGTCTATCAACGGTGACGCCCAGGCTCGCCTGCGTCTCGGTC---AAGAT
NeosporacaninumNCLIV_001310       ATGGTGGACGCGGCTTTGGACAGTGACGCACAGGCTCGCCTGCTTCTCTGTCCACGGGAG
                                  ***  **.*  * **:* .**.*******.************* **** ***   ..**

ToxoplasmagondiiTGME49_305060     GACGCAGCTTACGCACGCCTAGATATCACACACAATTTGCACCCTGGACGCAGATGGATG
NeosporacaninumNCLIV_001310       AGCGCAGCTTACGCGCGCCTCGACGTCACACACAACCTCCATCCTGGGCGTAGGTGGATG
                                  ..************.*****.** .********** * ** *****.** **.******
                                                                      TBCB F
ToxoplasmagondiiTGME49_305060     GAGATTGTCTTTTCGTTGGATGCGCCTTTGACTTCGGTCAAAGACAAGCTGTACAGACAC
NeosporacaninumNCLIV_001310       GAAATTGTGTTTACGCTGGATGCGCCCTTGGCCTCCGTCAAAGACAAGCTGTACAGACAC
                                  **.***** ***:** ********** ***.* ** **********************
                                                                      TBCB Left
ToxoplasmagondiiTGME49_305060     ACCGGCAGCAACCCGAGCAACATCAAGGTTTTCCTCAAATTCACTCCAGAGGACCCTGGA
NeosporacaninumNCLIV_001310       ACGGGAAGCAGCCCGAGCAATATCCAGGTTTTCCTCAAATTCACGCCGGAGGACCCGGGA
                                  ** **.****.********* ***.******************* **.******** ***

ToxoplasmagondiiTGME49_305060     AGGCTTCTCCTCGACCCCACCCAAACGCTCAGAGCAGTCGGCTGTGTCGAAGGTTGCATT
NeosporacaninumNCLIV_001310       AGGCCTCTCCTCGACCCCGCGCAAACGCTCAGAGAAGCAGGCTGCGTAGAAGGCTGCATT
                                  **** *************.* *************.** .***** **.***** ******

ToxoplasmagondiiTGME49_305060     CTCCACGTGGTTGACGAGAGTGGGGAGGCTGGGGTGATCCCTTCTGG------------A
NeosporacaninumNCLIV_001310       CTCCACGTCGTCGACGACAGTGGGGAGCGAGTCGCCGTTCCTCCCTCTTCCGTGGGCGAA
                                  ******** ** ***** *********  :*  *  .* *** *             *

ToxoplasmagondiiTGME49_305060     GAGAGAACAGAGAACATGGAGGGGAAGTACGTCATGGACGATGAAACATACGACAAACGT
NeosporacaninumNCLIV_001310       AGCAGGGAAGAAAGTTTAGAGGGGAAGTATGTTATGGACGAAGAAACGTACGACCAACGT
                                  .. **...***.*. :*.************ ** ********:*****.******.*****

ToxoplasmagondiiTGME49_305060     GACGGCACCGCCAGGAAATTCCTCGCGCGTTTGCAGAAGCAGCAGCCGGACTTGTTTTCT
NeosporacaninumNCLIV_001310       GAAGGAACTGCCCGAAAGTTTCTCGCGCGCCTGCAAAAGGAACAGCCCGACTTGTTTGCC
                                  **.**.** ***.*.**.** ********  ****.*** *.***** ********* *

ToxoplasmagondiiTGME49_305060     AAGAAGGAAGAGAAGA------TCGAAGAAGATGAAGAGTCGTGGAAGAAACGACTGGAC
NeosporacaninumNCLIV_001310       AAGAAAAAGGAAGCGAAGGTCGAGGAGGAAGATGAAGAAACGTGGAAGCAACGATTGGAA
                                  *****..*.**...**      : **.***********.:********.***** ****.

ToxoplasmagondiiTGME49_305060     AGTGCCCGAACTACATTCGCCATCGGCACCCGCTGCAGACTCTCTGGCGACCGACGCGGG
NeosporacaninumNCLIV_001310       ACCGCGCGAACCACGTTCCCCATCGGCAGCCGTTGCAGGCTCTCTGGCGACCGCCGCGGG
                                  *  ** ***** **.*** ********* *** *****.**************.******
                                          TBCB Right                                  TBCB R
ToxoplasmagondiiTGME49_305060     GCTGTTGCCTATGTGGGTCCGCGTCCGTCAAAGTCCCTGCGACAAATTTGGATTGGCGTG
NeosporacaninumNCLIV_001310       GCGGTTGCTTATGTGGGACCGCGTCCGTCGAAGTCTCTTCGGCAAATCTGGATTGGCGTG
                                  ** ***** ********:************.***** ** **.***** ************

ToxoplasmagondiiTGME49_305060     GCTCTGGATGAACCCTTGGGGTGTACAGACGGTCGAGACGATCCAACGAAAAAAACTCCC
NeosporacaninumNCLIV_001310       GCTCTGGACGAACCCCTCGGCACGACAGACGGCCGAGATGGGACGTCGAAGAAGGCTGCC
                                  ******** ****** * ** :  ******** ***** *. .*.:****.**..** **

ToxoplasmagondiiTGME49_305060     G---CCTCGCAGAAGGTTCTTTTCGAGTGTAACGGAGATAACTACGGAGAGTTTGTAGAG
NeosporacaninumNCLIV_001310       GGCGCGCATCTGAAGCCTCTTTTTGAGTGTAATGGAGAGAAATATGGAGAGTTTGCAACG
                                  *   *  . *:****  ****** ******** ***** **.** ********** *..*

ToxoplasmagondiiTGME49_305060     CCGGACCAAGTAGAAGTTGGCGCCTTCCCGCCTATTGATCCATTTGATTTGCTGGACGAA
NeosporacaninumNCLIV_001310       CCGGACGAAGTGGAAGTGGGCGACTTCCCGCCCATAGACCCGTTTGATTTGCTCGACGAA
```

```
                                ****** ****.***** ****.********* **:** **.********** ******

ToxoplasmagondiiTGME49_305060   ATCTAA
NeosporacaninumNCLIV_001310     ATTTAG
                                ** **.
```

(C) TBCE

```
ToxoplasmagondiiTGME49_285220   ATGGAAGAAGCCGCGGCCTCCTTAGAGGCAGCCGGCGCTTGCGCCGAAAGCACCTTCTTG
NeosporacaninumNCLIV_014970     ----------------------------------------------------------ATGGCG
                                                                                           :*   *

ToxoplasmagondiiTGME49_285220   CATCGCCAAGCTACCTCTACGGGGTGTATCTACACCGGAAGTCACTCTGCCGTCTCGCCT
NeosporacaninumNCLIV_014970     GAACCCGCAACGGCAGTTGCGGCTTGTCCAGACACTGCAAACCCACCTCCCCTGTTGCCC
                                 *:* * .*.* .*.  *.***  ***. . **** * **. *.. ** ** * * ***

ToxoplasmagondiiTGME49_285220   CTGAGGTGTACGTACACCCCAGGTGACCGAGTAGCGGACCTGGACGGCCACCTCGGCACC
NeosporacaninumNCLIV_014970     TTGAGGTGTATGTACACCCCGGGCGACAGAGTAGCGGACCTCGACGGCCACTTGGGCACG
                                ********* *********.** ***.************** ********* * *****
                                TBCE Left
ToxoplasmagondiiTGME49_285220   GTCCGATACATGGGTCCTGTCGAGGGCTACTCCCGAAGAACCGCTTCTGCATCATATGA-
NeosporacaninumNCLIV_014970     GTCCGTTACATTGGTCCAGTCGACGGTTACTCCCGACGAGGCGCGTCCTTCTCGGGCGGT
                                *****:***** *****:***** ** ********* .** *** *  .**. . *.
                                                                  TBCE Forward
ToxoplasmagondiiTGME49_285220   --------GACTTCTTCCTCTTCTTCTTTGTGTGAAGACGCAGAGTTGTGGATAGGGATC
NeosporacaninumNCLIV_014970     GGCGCCTCAGATTCCTGCTCGTTGTCTTCCAGCGAAGACGCAGATTTGTGGATAGGCGTC
                                        ...*** * *** *  ****  :* *********** *********** .**

ToxoplasmagondiiTGME49_285220   GAGTGGGACGACGCTGGACGCGGGAAGCACGACGGGTCCTTGAATGGGAAAGTTTACTTC
NeosporacaninumNCLIV_014970     GAGTGGGACGAAGCGGAGCGCGGGAAGCACGACGGATCCCTCAACGGGAAAGTTTATTTC
                                ***********.** *..***************.*** * ** ********** ***

ToxoplasmagondiiTGME49_285220   TCTTGTGTGGGGTCGCTGAGGAAGAAACCGGCAGCCTC----------------------
NeosporacaninumNCLIV_014970     ACTTGCGTGGGAGCTTTATCGAGGTCGAAGACCGCCACCGCTGGGGGCACCGCCGCGTCA
                                :**** *****. *  *.: **.*:....*.*.***:*

ToxoplasmagondiiTGME49_285220   --------------------TGGCGCGGATGGAGAGCAGGCGGAGCGCGTCACGGCCGGT
NeosporacaninumNCLIV_014970     GCAGACGGGAGCAGCGCTGGAGACCCGAAAGAACAGAAATCGAAGCGATGCACGGCAGGC
                                                    :*.* **.*:*.* **.*. **.****.  ******.**

ToxoplasmagondiiTGME49_285220   TCTTTCGTCAAGAGACACAAATTGCTCGAACCGACAGACTTCAAAAGAGCCGTCCTCGAG
NeosporacaninumNCLIV_014970     TCCTTCGTCAAAAGACACAAACTCCTGGAGCCCAAAGACTTCAAGAGAGCTGTCATGGAG
                                ** ********.********* * ** **.** *.********** ***** ***.* ***
                                                                  TBCE Right
ToxoplasmagondiiTGME49_285220   AGATACACCGAAAAGCTCACGCAAGAACAAATAGACTTCATGCTCCTCGTCAACCCTCTC
NeosporacaninumNCLIV_014970     CGATACACCAGGAAACTCACGCAGGAGCAAATTGATTCCATGATCCTCGTCAATCATGTT
                                .********...**.********.**.*******.** *******.********** *.* *
                                                TBCE Reverse
ToxoplasmagondiiTGME49_285220   ACAAACAAGACGAAACCCGTGGAATTCGTCGGACGCAAGGAGGCAGAGGAACACTTTGCT
NeosporacaninumNCLIV_014970     ACAAATAAAACCAAGCCCGTCGAATTCGTCGGACGCAAGGAGGCAGAGGAGTACTTTGCT
                                ***** **.** **.***** ****************************. ********

ToxoplasmagondiiTGME49_285220   CGTCTGCATCTGTTGAACGCGATGAGTTTCACGAGTGTTTCTGCCATTCGTTACGCGGGT
NeosporacaninumNCLIV_014970     CGCCTCCACCTGCTGAACGCCATGAGCTTCACGAGCACCTCGGCGATCCGCACGGCGGGG
                                ** ** ** *** ******* ***** ******** .  ** ** ** ** :. *****

ToxoplasmagondiiTGME49_285220   TCGCCTCCTCACCTTCTCCTTCCAAATCTCCGACGTTTGTCGCTGGCAAACAGCTTGATC
NeosporacaninumNCLIV_014970     CCTCCTCCTCGTCTCGTGCTTCCAAATCTCCGCCTCTTGTCGCTTGCAAACAGCCTGATC
                                 * *******. **  * **************.*  ******** ********* *****

ToxoplasmagondiiTGME49_285220   ACGAACTGGGAGGAACTTCTGGGGATTTTGCGGTGCGTTCCTCGCCTCTCGTCGCTCTCT
NeosporacaninumNCLIV_014970     ACCGACTGGCAGGAGTTGCTGGCGATTCTTCGATGCGTCCCACGCCTTTCTTCGCTCTCT
                                ** .***** ****. * **** **** * **.***** **:***** ** *********

ToxoplasmagondiiTGME49_285220   CTCTGCGGCACACGACTCCAGGCGTCCACGCTGCCTTCCGGGGGGGTTCGCGTCGTCTGGA
NeosporacaninumNCLIV_014970     CTCTGCGGCACGCGGCTGCGAGCTTCTACCTTGCCTCCGTTTGTCTCTCGCGTTTCTCCT
                                ***********.**.** *..** ** **  ***** *    *  *        ***  :

ToxoplasmagondiiTGME49_285220   AAGGCAGA------------------------GCCCTGCGGACACACAGAGCGAGTAATT
NeosporacaninumNCLIV_014970     GAACCTGCGCAAGGAGAAAAGGGAGACGCCCACGCAGAACGCGCCGAGGAATGGACGATT
                                .*. *:*.                          *. .. *. .*...**. *.. .***

ToxoplasmagondiiTGME49_285220   CTTGAGGAGCTGAACGACCTGCAACTCGACGGAACATTTGTCACCTGGGAAGAGCTTCTC
NeosporacaninumNCLIV_014970     CTCGAGGAGCTAACGGAGCTTCAACTGGATCAGACCTTCGTTACCTGGGACGAGCTTCTC
                                ** ********.*. ** ** ***** **  ..**.** ** ********.*********

ToxoplasmagondiiTGME49_285220   GCCTTTGATGCTCTCGCGCCCAACCTGCAGCGTTTGTCCATTCGCGGAAACGACCTCTCT
NeosporacaninumNCLIV_014970     GCCTTTGACTCGCTCGCGCCCCACTTGCAGCGTCTTTCGATTCGTGGAAACGACTTCTCG
                                ********  * *********.** ******** * ** ***** ********* ****

ToxoplasmagondiiTGME49_285220   CCTTTTGAAAGAAACACTGCTTCTTCTCCGGACGACGTCTTACCCCCTTTTCCTCTCTTC
NeosporacaninumNCLIV_014970     CCTGCACTTCCACTGTTTGACCCC-------------------------------------
                                ***  : ::. *.: : **.  *

ToxoplasmagondiiTGME49_285220   GATCCCAGAGCTTCGCTGCCCGAGCGCAGGACAGAGATAG---------GAAAAGAAGAA
NeosporacaninumNCLIV_014970     ------CGAGCTGGGCTGCCAGCGCGGCGGGCGAACGCGGGCGTCAACGGGGAAGAAAGC
                                      .*****  ******.*.*** .**.*..* . .*        *..*****...
```

```
ToxoplasmagondiiTGME49_285220      ACCGCGTTGTCTCTGAAGGATGAACACGCGCCTTTACCGCCGAGAGAAGCGGTCCTGGAG
NeosporacaninumNCLIV_014970        CCGGCAGAAAC----------------------------------------------------
                                   .* **. :.:*

ToxoplasmagondiiTGME49_285220      AACCCCTCCTCTCGAATTTTCCATGGTCTCCGTTCTCTGGATGTCTCAGACAATCCCATT
NeosporacaninumNCLIV_014970        --------GGCCAGGGCCTTCCAAAATCTGGTATTTCTGGATGTCTCGGACAATCCTGTC
                                           * .*..  *****:..***   :* ************.******** .*

ToxoplasmagondiiTGME49_285220      CAGTCCTGGGCGGCGATTTTTGCCTGCATGCGGCACTTGCCGAGGCTAGAGTCTCTCTGC
NeosporacaninumNCLIV_014970        CACTCTTGGACCCCGCTGGTCGCCTGCATGCGCCACCTGCCGCGCCTGGAAACCATCTGT
                                   ** ** ***.*  **.*  * *********** *** *****.* **.**.:* .****

ToxoplasmagondiiTGME49_285220      GCCGTGAACGCTGAGTTGGGAGACTTCTCGGGTGCACGGACGCCTGACCTGGCTGCGTGC
NeosporacaninumNCLIV_014970        GCCGTCAACGCTAACCTGGGCGATTTCGCGGGTGTACAGACACCGCAGACAGACGAGCCA
                                   ***** ******.*  ****.** *** ****** **.***.**  * . .*. *.*  .

ToxoplasmagondiiTGME49_285220      G-----------------------------------------------------------
NeosporacaninumNCLIV_014970        GAAGTCTGTACACCCGAGAAATCGCCCTCCAGGACAGGCGCACCGCTCCAGGGAGGTGAA
                                   *

ToxoplasmagondiiTGME49_285220      ---GGGGTCGCGGTGTACGTA-------------CCGCCGAGCCCCGGGGCGCCGAGTCG
NeosporacaninumNCLIV_014970        GAGTCGGCAACGGATTCCGAACGATCTCGGGAATCCGCTGCACAGGACGGCCAACGGTCC
                                        ** ..***: *.**:*             **** *..*.  . *** .. .***

ToxoplasmagondiiTGME49_285220      ACCGCAACGGTTGAAAGCGCCGGAAATCAGACGGGAAACGGAGACTTTCGAGAGACATGT
NeosporacaninumNCLIV_014970        GGCTGTGAGTTGGAAATCGGCGCACGCGAAACGCGCGACGGCT-CTGCAGCGTGGGCTCT
                                   . *  :..* * **** ** ** *..  *.*** *..****.  **  .*.*:*. .* *

ToxoplasmagondiiTGME49_285220      GGAGTGGGGGACAGCGCGAAAGGGTATGCTTGTGTCGCAGATCGGCTGGAGAAAGAGGCA
NeosporacaninumNCLIV_014970        CTCTATGCGCCAGGACCGGAGGGCGAAGATTATCGAGCTGTGCCTGGAAGACAACTGCAT
                                     . : * * ...*. **.*.**  *:*.**.*  .**:*: *    .....** :* .:

ToxoplasmagondiiTGME49_285220      AGAGAAATGGGCGACT------------------GCTTGGCTGCTGCGTGGGCTCTCGCT
NeosporacaninumNCLIV_014970        CGAGAAATGGTACATCCGAGAGGGGCCGAACGGCCCCAGACTGCTCCTCAGGGTGTGTGT
                                   .********* . *                     * :*.***** *  .** * *   *

ToxoplasmagondiiTGME49_285220      CTGGACCGGAACCGGCGGGAGAAGATCCGCGAGCTGTGTGTTGAAGATAATTGCGTTGAC
NeosporacaninumNCLIV_014970        GAAGGCA-------GCGAG-TTCCGCCCTCGGAGAGAGAGCGAGTTTCCCTGTGCTTGCG
                                    :.*.*.       ***.*  :. . ** **.. :*:*:*  ..: : ..*    ***.

ToxoplasmagondiiTGME49_285220      CAATGGGAGACAATAACGGCTCTCGCTAGGCTGTTCCCCTCACTGCAGAGACTGATGATT
NeosporacaninumNCLIV_014970        TTCCAGGAGACGATAACGTCGCTCGCGCGTCTCTTTCCGTCTCTGGAAAGACTGATGCTG
                                    :. .******.****** * ***** .* ** ** ** **:*** *.*********.*

ToxoplasmagondiiTGME49_285220      CAAGGAAATCCT---CTTCTTCAACCTTGCGCAACTGCAAAGGTGACCGCCGTCTCTACA
NeosporacaninumNCLIV_014970        CAGGGGAACCCCCTGCTTCTTCAGCCGTGCTCGAACTCAAAGGCGGCGTCCGTCCCCACC
                                   **.**.** **    ********.** *** *.*.  ****** *.*  ***** * **.

ToxoplasmagondiiTGME49_285220      GGCTTCGGAGCCTCTTCTCCGCAGCGCCAGGTCGTGATTTCGCTTTTCCCTTGCCTGGAA
NeosporacaninumNCLIV_014970        GGCTTCGGCGCCTCGTCTCCACAACGCCAAGTGATGATTTCTCTGTTCCCGAGCCTGAAA
                                   ********.***** *****.**.*****.** .******* ** ***** :*****.**

ToxoplasmagondiiTGME49_285220      GTGCTGAGTGGCGGAACAATTTCTAAGGCGGACAGAGCAGCAGCTGAGAAGTACACGCTT
NeosporacaninumNCLIV_014970        GTTCTGAGCGGAGGAACAATCTCCAGGGCGGATCGATCGGCAGCGGAACGGTACACGCTG
                                   ** ***** **.******** ** *.****** .** *.***** **...*********

ToxoplasmagondiiTGME49_285220      TCCCTGCTCCATCGCATCAGGAGAACAGAGAACGAGAACTCGCTCCCCATTCCAGCTGGT
NeosporacaninumNCLIV_014970        TCTCTTTTGCACCGCATAAAACGCCAAGGCGA---AGTTTCCCTGCCGATCCCTCCTGGC
                                   ** **  * ** *****.*...*...**. .*   ..: ** ** ** ** **: ****

ToxoplasmagondiiTGME49_285220      CTCGTCGAGGCACTGCAGCTTCCTACCCCGGGAGAGGAGCACAATAATTCTGCGTTTGAT
NeosporacaninumNCLIV_014970        TTGGTGGCCGCGCTGCAGAGCCCCAACCAGGCGGCAGACAGAAATTCCTCAGCCTACGAG
                                    * ** *. **.******.  ** *.**.** .*..** ...***:. **:** *: **

ToxoplasmagondiiTGME49_285220      GAGCTGCTCGACCGTCTCACACAAATCCACGGGGACTTTTCTCTTGCAAC---CACCCAG
NeosporacaninumNCLIV_014970        GCGCTGCTCGATCGACTCACGGAGACACACGGAGACTTCTCTCTTGGCGAAACCGCGCAG
                                   *.********** **:*****. *.* .*****.***** ******* ...   *.* ***

ToxoplasmagondiiTGME49_285220      GGGGAAGGAGGCGCCGCCGTGCTCGCTTCCTCTCTGATTGGCATTCTCCTGCAACCGGAC
NeosporacaninumNCLIV_014970        GGAGAAGGCGGCGCGGTCGTCCTCGCTTCGTCGCTGGTAGACGTGCTGCTTCAGCCTGAC
                                   **.*****.***** * *** ******** ** ***.*:*.*.* ** ** **.** ***

ToxoplasmagondiiTGME49_285220      GCAGCGTCCATCTTCGATAAACCGGCAGTAAAAAAGCGAATCCCAAAATCAATGAGAGTC
NeosporacaninumNCLIV_014970        GCAGCAGTCATTTTCGACAAGCCTCCCGTGAAGAAGCGAGTTCCCAAGTCGATGCGAGTC
                                   *****.  *** ***** **.**  *.**.**.******.* **.**.**.***.*****

ToxoplasmagondiiTGME49_285220      AGAGATCTGAAGACACTATGCATGCGCCTGTTTGGACTTCCCGTTGCGCACATAGAACTT
NeosporacaninumNCLIV_014970        CGAGATCTCAAGACTCTGTGCATGCGGCTCTTCGGCCTTCCCGTCGCACATATCGACCTC
                                   .******* *****:**.******** ** ** **.******** **.** **.**.**

ToxoplasmagondiiTGME49_285220      CTTTACAACGACGGGAAAATGCCGGTCAGCACCCCGTTGGACGACGACGCCGCCTCTCTT
NeosporacaninumNCLIV_014970        CTGTACAACGACGGGAACATGCCTGTGAGCACCCCGCTGGATGACGATGCTTCGTCCCTG
                                   ** **************.***** ** ********* **** ***** **  * ** **

ToxoplasmagondiiTGME49_285220      GATTTCTTCGGAGTCGACACTGGATCTGTCGTCCGAGTCCAGGACAAAAACGACAGACGA
NeosporacaninumNCLIV_014970        GATTTCTTCGGAGTCGGAGCCGGATCGGTCGTTCGCGTGCAGGACAAGAACGACAAAAAG
                                   ****************...* ***** ***** **.** ********.*******.*...

ToxoplasmagondiiTGME49_285220      TCTGCCTGA---
NeosporacaninumNCLIV_014970        AGTGAAGTTTGA
                                   : **..  :
```

(D) α - tubulin


```
ToxoplasmagondiiTGME49_316400      ATGAGAGAGGTTATCAGCATCCACGTCGGCCAGGCCGGTATCCAAATCGGTAACGCCTGC
NeosporacaninumNCLIV_058890        ATGAGAGAGGTTATCAGCATCCACGTCGGCCAAGCCGGTATCCAAATCGGTAACGCCTGC
                                   **********************************.**************************

ToxoplasmagondiiTGME49_316400      TGGGAGCTCTTCTGCCTGGAACATGGTATCCAGCCGGATGGGCAGATGCCCTCTGACAAG
NeosporacaninumNCLIV_058890        TGGGAGCTCTTCTGCCTGGAGCATGGCATTCAGCCGGATGGGCAGATGCCCTCTGACAAG
                                   ********************.***** ** ********************************

ToxoplasmagondiiTGME49_316400      ACCATTGGAGGTGGTGACGACGCCTTCAACACCTTCTTTTCCGAGACAGGCGCTGGCAAG
NeosporacaninumNCLIV_058890        ACCATCGGTGGTGGTGACGACGCCTTCAACACCTTCTTCTCCGAGACTGGCGCTGGCAAG
                                   ***** **:****************************** ********:*************

ToxoplasmagondiiTGME49_316400      CACGTGCCCCGATGCGTCTTCTTGGATTTGGAGCCCACCGTCGTCGATGAGGTTCGCACC
NeosporacaninumNCLIV_058890        CATGTGCCCCGCTGCGTCTTCTTGGATTTGGAGCCCACTGTCGTGGACGAGGTCCGCACC
                                   ** ********.************************** ***** ** ***** ******

ToxoplasmagondiiTGME49_316400      GGCACTTACCGCCACCTGTTCCACCCGGAGCAGTTGATCAGCGGGAAAGAGGATGCTGCG
NeosporacaninumNCLIV_058890        GGCACTTACCGCCATCTGTTCCATCCGGAGCAGCTCATTAGCGGCAAGGAAGATGCGGCG
                                   ************** ******** ********* * ** ***** **.**.***** ***

ToxoplasmagondiiTGME49_316400      AACAACTTCGCGCGTGGTCACTACACCATCGGCAAGGAGATCGTCGACCTCTCCCTCGAC
NeosporacaninumNCLIV_058890        AACAACTTCGCTCGTGGTCACTACACCATCGGCAAGGAGATCGTCGACTTGTCTCTTGAC
                                   ************ ************************************ * ** ** ***

ToxoplasmagondiiTGME49_316400      CGTATCCGCAAGTTGGCTGACAACTGCACTGGTCTCCAGGGTTTCTTGATGTTCAACGCC
NeosporacaninumNCLIV_058890        CGTATTCGCAAGTTGGCGGACAACTGCACAGGTCTTCAGGGTTTCCTGATGTTCAACGCC
                                   ***** ************ ************:***** ********* **************

ToxoplasmagondiiTGME49_316400      GTCGGCGGTGGTACCGGTTCCGGTCTCGGTTGCCTCCTGCTCGAGCGCCTGTCTGTTGAC
NeosporacaninumNCLIV_058890        GTCGGTGGTGGTACCGGTTCCGGTCTCGGGTGCCTCCTCCTCGAGCGCCTGTCTGTTGAC
                                   ***** ********************** ******** **********************

ToxoplasmagondiiTGME49_316400      TACGGCAAGAAGTCGAAGCTGAACTTCTGCTCGTGGCCCTCGCCCCAGGTGTCGACCGCA
NeosporacaninumNCLIV_058890        TACGGCAAGAAGTCGAAGCTGAACTTCTGCTCGTGGCCCTCGCCCCAGGTCTCCACGGCA
                                   ************************************************** ** ** ***

ToxoplasmagondiiTGME49_316400      GTTGTGGAACCGTACAACTCCGTCCTTTCCACTCACTCTCTGTTGGAGCACACCGACGTG
NeosporacaninumNCLIV_058890        GTTGTCGAGCCGTACAACTCCGTCCTTTCCACCCACTCCCTTTTGGAGCACACCGACGTC
                                   ***** **.********************** ***** ** *****************

ToxoplasmagondiiTGME49_316400      GCCGTCATGCTCGACAACGAGGCCATCTACGACATCTGCCGCCGCAACCTGGACATCGAG
NeosporacaninumNCLIV_058890        GCCGTCATGCTTGACAACGAGGCCATCTACGACATCTGCCGCCGCAACCTCGACATCGAG
                                   ************ ****************************************** *********

ToxoplasmagondiiTGME49_316400      CGCCCGACCTACACCAACCTGAACAGACTGATTGCCCAGGTCATCTCCTCCCTGACCGCG
NeosporacaninumNCLIV_058890        CGCCCGACCTACACCAACCTGAACAGACTGATTGCGCAGGTCATTTCCTCTTTGACTGCG
                                   ************************************ ******** *****  **** ***

ToxoplasmagondiiTGME49_316400      TCTCTCCGTTTCGATGGTGCGCTCAACGTCGACGTGACTGAGTTCCAGACCAACTTGGTG
NeosporacaninumNCLIV_058890        TCTCTCCGTTTCGACGGCGCGCTCAACGTCGACGTTACTGAGTTCCAGACGAACTTGGTC
                                   ************** ** ***************** ************** ********

ToxoplasmagondiiTGME49_316400      CCCTACCCGCGCATTCACTTCATGCTCTCATCGTATGCGCCCATCATCAGCGCAGAGAAG
NeosporacaninumNCLIV_058890        CCCTACCCGCGCATCCACTTCATGCTTTCTTCCTATGCGCCCATCATCAGCGCAGAGAAG
                                   ************** ************ **:** ****************************

ToxoplasmagondiiTGME49_316400      GCGTACCACGAGCAGTTGTCTGTCGCTGAGATCACCAACTCGGCTTTCGAGCCCGCGAGC
NeosporacaninumNCLIV_058890        GCGTACCACGAGCAACTGTCTGTTGCCGAGATCACCAACTCGGCATTCGAGCCCGCAAGC
                                   **************. ******* ** *****************:************.***

ToxoplasmagondiiTGME49_316400      ATGATGGCCAAGTGTGATCCTCGTCACGGAAAGTACATGGCCTGCTGCTTGATGTACCGT
NeosporacaninumNCLIV_058890        ATGATGGCGAAGTGCGATCCGCGCCACGGAAAGTACATGGCCTGCTGCCTGATGTACCGT
                                   ******** ***** ***** ** ************************ ************

ToxoplasmagondiiTGME49_316400      GGTGATGTCGTCCCCAAGGATGTGAACGCAGCCGTTGCGACCATCAAGACCAAGAGAACC
NeosporacaninumNCLIV_058890        GGTGATGTCGTCCCCAAGGATGTGAACGCAGCCGTCGCTACCATCAAGACGAAGAGAACT
                                   ************************************ ** ************ ********

ToxoplasmagondiiTGME49_316400      ATCCAGTTCGTCGACTGGTGTCCCACCGGGTTCAAGTGCGGTATCAACTACCAGCCACCC
NeosporacaninumNCLIV_058890        ATCCAGTTCGTGGACTGGTGCCCCCACCGGTTTCAAGTGTGGTATCAACTACCAGCCCCCC
                                   ************ ******** ******** ******** *****************.***

ToxoplasmagondiiTGME49_316400      ACTGTGGTTCCTGGTGGTGACTTGGCCAAGGTCATGCGCGCCGTCTGCATGATCAGCAAC
NeosporacaninumNCLIV_058890        ACTGTGGTCCCTGGCGGTGATCTCGCAAAGGTCATGCGCGCTGTGTGCATGATCAGCAAC
                                   ******** ***** *****  * **.*************** ** ***************

ToxoplasmagondiiTGME49_316400      AGCACTGCCATCGCAGAAGTTTTCAGTCGCATGGACCACAAATTCGATCTCATGTACGCC
NeosporacaninumNCLIV_058890        AGCACTGCCATCGCGGAAGTTTTCAGCCGCATGGACCACAAGTTCGATCTTATGTATGCC
                                   **************.************ **************.******** ***** ***

ToxoplasmagondiiTGME49_316400      AAGAGGGCCTTCGTCCACTGGTATGTCGGTGAGGGTATGGAAGAAGGTGAATTCTCTGAG
NeosporacaninumNCLIV_058890        AAGAGGGCCTTCGTCCACTGGTACGTCGGTGAGGGTATGGAAGAAGGTGAATTCTCTGAG
                                   ********************** ************************************
```

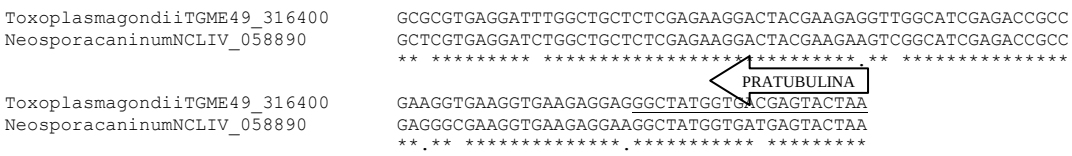

Fig. 54: Sequence alignment for genes of *T. gondii* ME49 and *N. caninum* LIV.

(A) gene CCTα (TGME49_229990 and NCLIV_030660 are accession numbers from EupathDB database); (B) gene TBCB, (TGME49_305060 and NCLIV_001310 are accession numbers from EupathDB database); (C) gene TBCE, (TGME49_285220 and NCLIV_014970 are accession numbers from EupathDB database); (D) gene α-tubulin, (TGME49_316400 and NCLIV_058890 are accession numbers from EupathDB database). Primers are underlined, and arrows contain primer name and direction of amplification.